

**Transition Metal Oxazoline Complexes:
Synthesis and Applications in
Asymmetric Catalysis**

**Thesis submitted for the Degree of
Doctor of Philosophy**

by

Shaun Anthony Garratt

**in the Department of Chemistry
at the
University of Leicester**

October 1998

UMI Number: U113935

All rights reserved

INFORMATION TO ALL USERS

The quality of this reproduction is dependent upon the quality of the copy submitted.

In the unlikely event that the author did not send a complete manuscript and there are missing pages, these will be noted. Also, if material had to be removed, a note will indicate the deletion.



UMI U113935

Published by ProQuest LLC 2014. Copyright in the Dissertation held by the Author.
Microform Edition © ProQuest LLC.

All rights reserved. This work is protected against
unauthorized copying under Title 17, United States Code.



ProQuest LLC
789 East Eisenhower Parkway
P.O. Box 1346
Ann Arbor, MI 48106-1346

**Title: Transition Metal Oxazoline Complexes:
Synthesis and Applications in Asymmetric Catalysis**

Author: Shaun Anthony Garratt

ABSTRACT

This thesis describes the synthesis and chemistry of “(arene)Ru” and “Cp*Rh” complexes of chiral oxazoline-containing ligands and their use as asymmetric Lewis-acid catalysts.

Chapter One introduces important aspects of asymmetric catalysis, then describes in more detail the use of chiral oxazoline ligands to induce high levels of stereocontrol in many important catalytic reactions.

Chapter Two initially introduces the area of chiral half-sandwich complexes, describing their chemistry and their use in asymmetric synthesis. The synthesis and characterisation of half-sandwich ruthenium and rhodium complexes of C₂-symmetric bis-oxazoline ligands is then described (these complexes are chiral at ligand only). The complex solution behaviour of the aqua species [M(OH₂)(N-N)(ring)]²⁺ was extensively investigated. In the latter part of the chapter, the synthesis of half-sandwich complexes of unsymmetrical oxazoline ligands is described. In this case, the complexes are chiral-at-metal and the relative diastereoselectivities of formation and configurational stabilities in solution are discussed in detail and were generally found to be very high. Numerous X-ray structures have been obtained and variable temperature and 2D NMR techniques have been employed to study the solution behaviour of the complexes.

Chapter Three describes the use of the half-sandwich complexes as asymmetric Lewis-acid catalysts. Complexes [Ru(OH₂)(N-N)(mes)](SbF₆)₂ (N-N = pymox, benbox) were found to be efficient and enantioselective catalysts for the Diels-Alder reaction of acrylic dienophiles with simple dienes. A selection of different catalysts and substrates were used, with varying results. Other Lewis-acid catalysed reactions (including the Hetero-Diels Alder and Mukaiyama Aldol) were studied, but with less success. The inverse electron-demand Hetero Diels-Alder reaction was identified as an area worthy of further study.

Statement

This thesis is based on work conducted by the author, in the Department of Chemistry of the University of Leicester, during the period between October 1995 and September 1998.

All the work described in the thesis is original unless otherwise stated in the text or in the references. This work is not being presented for any other degree.

Signed: SA Garratt

Date: 21/12/98

Shaun Anthony Garratt

ACKNOWLEDGEMENTS

I would like to thank my supervisor, Dr. D.L. Davies for all the help and guidance through out the last three years, and also Dr. D.R. Russell and especially Dr. J. Fawcett for the X-ray structure determinations. Thanks are also due to Dr. G.A. Griffith for Variable temperature and 2D NMR spectra and to Dr. G.A. Eaton for the mass spectra. Thanks also to K. Singh for the synthesis of various starting materials and for helpful discussions in the use of laboratory equipment.

My thanks are also extended to all the people who have helped enormously in the practical work over the three years, and to everyone working in the organometallic laboratory for numerous helpful discussions.

Acknowledgement is made to the University of Leicester for funding this research. Thanks to my family and friends for all their support and encouragement.

Abbreviations and Symbols

General and Physical

Å - Angstrom unit

br s - broad singlet

COSY - Correlated Spectroscopy

cm³ - cubic centimetres

d - doublet

dd - doublet of doublets

dt - doublet of triplets

δ - chemical shift

° - degrees

ES M/S - Electrospray Mass Spectroscopy

FAB M/S - Fast Atom Bombardment Mass Spectroscopy

g - gram

HOMO - Highest Occupied Molecular Orbital

h - hour

Hz - Hertz

K - Kelvin

LUMO - Lowest Unoccupied Molecular Orbital

m - multiplet

min - minute

mmol - millimole

μl - microlitre

μmol - micromole

NOESY - Nuclear Overhauser Enhancement Spectroscopy

NMR - Nuclear magnetic resonance

ppm - parts per million

RT - room temperature

s - singlet

t - triplet

Abbreviations and Symbols

Chemical

aa - anion of amino acid

acac - anion of pentane-2,4-dione

Bn - benzyl

benbox - 1,2-bis(oxazolinyl)-benzene

BINAP - 2,2' -Bis(diphenylphosphino)-1,1' -binaphthyl

bipy - 2,2' -bipyridine

bom - bis-oxazolinyl methane

Bu - n-Butyl

^tBu - t-butyl

Chiraphos - (2S,3S)-Bis-(diphenylphosphino)-butane

COD - cyclooctadiene

Cp - cyclopentadienyl

Cp* - pentamethylcyclopentadienyl

p-cymene - 4-isopropyl-toluene

DMAP - *N*-dimethyl-4-amino-pyridine

DMBD - 2,3-dimethyl-1,3-butadiene

dopa - 3,4-dihydroxy-phenylalaninato

dppe - 1,2-bis(diphenylphosphino)ethane

Et - ethyl

EtOH - ethanol

LDA - lithium diisopropylamide

Me - Methyl

MeCN - acetonitrile

MeOH - methanol

2-Me-py - 2-methyl-pyridine

4-Me-py - 4-methyl-pyridine

mes - mesitylene (1,3,5-trimethylbenzene)

Ms - methanesulphonyl

NOBA - *o*-nitro-benzyl alcohol

OAc - acetate

OTf - triflate

Ph - phenyl

pic - picolinate

ⁱPr - isopropyl

ⁱPr-animox - (4S)-2-(2-aminophenyl)-4-isopropylloxazoline

ⁱPr-bop - 2,2'-bis-[(4S)-isopropyl-oxazolanyl]-propane

ⁱPr-box - 2,2'-bis-(4S)-isopropyl-oxazoline

ⁱPr-NTs-animox - (4S)-2-[2-[(tolylsulphonyl)amino]phenyl]-4-isopropylloxazoline

(R)-Prophos - (R)-(+)-1,2-bis(diphenylphosphino)propane

ⁱPr-phenmox - (4S)-2-(2-hydroxyphenyl)-4-isopropylloxazoline

py - pyridine

pybox - 2,6-bis-oxazolanyl-pyridine

pymox - 2-oxazolanyl-pyridine

THF - tetrahydrofuran

Ts - toluenesulphonyl

TsDPEN - (1R,2R)-*N*-(*p*-tolylsulphonyl)-1,2-diphenylethylenediamine

List of Contents

		Page Number
Chapter One	General Introduction	
(1.1)	The Importance of Asymmetric Catalysis	1
(1.2)	Oxazoline Ligands in Asymmetric Catalysis	5
Chapter Two	Synthesis of Chiral Half-Sandwich Oxazoline Complexes	
(2.1)	Introduction	19
(2.2)	Results and Discussion	
	(2.2.1) Complexes of C ₂ -symmetric Bis-Oxazolines	37
	(2.2.2) Half-Sandwich Complexes of Unsymmetrical Oxazoline Ligands	52
(2.3)	Experimental	95
Chapter Three	Chiral Half-Sandwich Complexes as Lewis-acid catalysts	
(3.1)	Introduction	142
(3.2)	Results and Discussion	151
(3.3)	Experimental	172
	Conclusions and Further Work	174
	References	176

Chapter One:
General
Introduction

Chapter One - General Introduction

(1.1) - The Importance of Asymmetric Catalysis

Over the last twenty years, the synthesis of chiral products has assumed an ever-increasing importance.¹ In 1983, only 11% of chiral pharmaceuticals were produced in single-enantiomer form. By the turn of the century, however, this percentage will have risen to over 80% obtained optically pure, many via asymmetric catalysis. All natural amino acids in proteins are L-configured about their chiral centres, whilst all sugars in DNA have D-configurations and as a result, drugs designed to interact with living systems are often chiral themselves. In many cases, different enantiomers of a chiral drug will interact differently with the target. One enantiomer may have a specific interaction with a cell receptor, whilst the other will either be inactive or even produce an unwanted toxic effect through some alternative interaction, as in the well-documented case of thalidomide, for which the (R)-isomer can ease morning-sickness, whilst the (S)-isomer is teratogenic.

In the past, many drugs were marketed as racemates, but since 1992, the US Food and Drugs Administration (FDA) and the European committee for Proprietary Medicinal Products have required manufacturers to individually characterise and research each enantiomer of all drugs proposed to be marketed as a mixture. Since then, it has become commercially unviable to produce new drugs as racemates, unless both enantiomers are shown to have a beneficial effect. There is now, therefore, much emphasis on the use of chiral technology for the synthesis of single-isomer pharmaceuticals. There are three methods of introducing chirality into a synthesis:

i) The Chirality Pool - where the desired chiral centres are already present in the starting materials, usually naturally occurring. Any subsequent synthetic steps will not interfere with the chiral centres. Ideally, the desired product can be extracted directly from a natural source. Important examples include the anticancer drug taxol (extracted from the Pacific yew tree) and penicillins. In addition, chiral building blocks such as amino acids and sugars are naturally occurring.

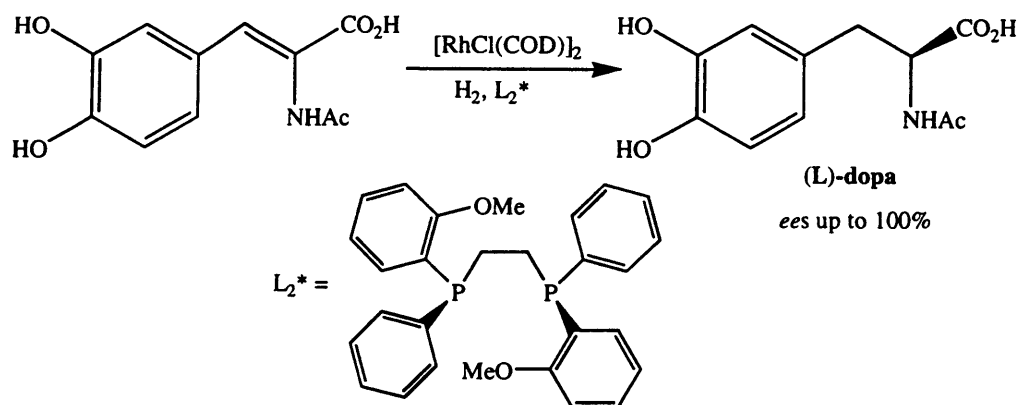
ii) Resolution Methods - where a racemic mixture is separated by chemical or physical methods into the pair of enantiomers. Classically, this is done by forming diastereomeric salts with a chiral acid or base, which are separable by crystallisation (the anti-inflammatory drug (S)-Naproxen is resolved in this way²). Alternatively,

racemates can be resolved by physical methods such as chromatography on a chiral stationary phase. Whilst resolution methods have been developed substantially, many chiral products cannot be obtained in this way and in cases where only one enantiomer of the mixture is required, forming 50% of the other isomer is wasteful. A more direct method of synthesising the required isomer would then be desirable.

iii) Asymmetric synthesis - where an achiral substrate is converted directly into the desired isomer of the product, in favourable cases with little or none of the unwanted isomer. This can be done stoichiometrically, with a chiral auxiliary or by asymmetric catalysis. In a stoichiometric method, a chiral centre in the substrate directly induces an asymmetric reaction at a prochiral group (such as an alkene), usually leading to diastereomeric products. While high diastereoselectivity can be observed, there is, by definition, no amplification in chirality, since only one chiral product is formed from each chiral starting molecule. The use of a chiral auxiliary potentially gives a more efficient synthetic route. In this case, a chiral group (*e.g.* (L)-menthyl) is reacted with the substrate molecule and is used to induce an asymmetric reaction, then removed from the final product (*e.g.* by hydrolysis). The reaction will again be stoichiometric, but the chiral auxiliary can often be recycled for further use. By far the most efficient method of synthesising chiral molecules is asymmetric catalysis, in which many chiral product molecules can be obtained using only a few molecules of a chiral ligand, usually with a metal catalyst. High levels of chiral amplification are thus achieved and in many reactions, only one enantiomer is obtained, eliminating the need for resolution.

In nature catalytic reactions are performed by enzymes, which are usually highly efficient and selective. For example, cytochrome P₄₅₀S (heme-containing electron-transfer enzymes) can catalyse the oxidation of a variety of alkenes to alcohols, whilst reductase enzymes are also used as asymmetric catalysts in industry. Chemists strived for decades to emulate the activity and selectivity of enzymes, using synthetic catalysts. It was not until the late 1970s that catalytic systems to rival enzymes were developed. The most successful early catalysts were combinations of Rh(I) with chiral diphosphines, which catalyse the asymmetric reduction of various substituted alkenes.³ This catalytic system has been most successful for the hydrogenation of various N-acylaminoacrylic acids to the corresponding amino-acid

derivatives, which was developed into an industrial process by Monsanto, in the synthesis of the anti-Parkinson's drug (L)-dopa (**Scheme 1.1**).⁴



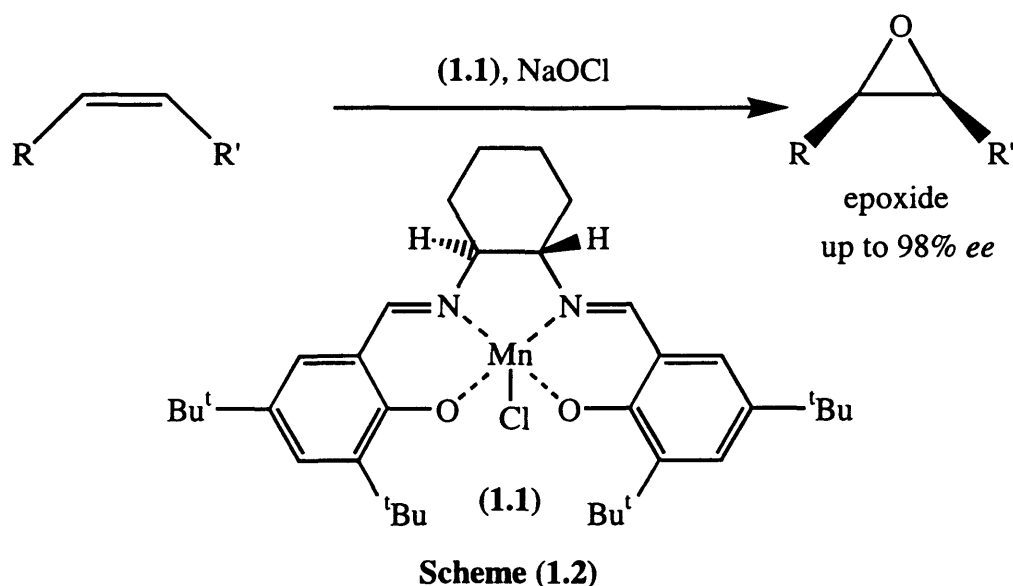
Scheme (1.1)

Whilst chiral phosphines have proved excellent ligands for catalytic reductions, their susceptibility towards oxidation and reaction with species such as diazo-compounds makes them rather unsuitable for use in, for example, catalytic epoxidation or cyclopropanation. These reactions often require less electron-rich metal complexes, where 'hard'-ligands such as N- and O-donors are preferred. There has recently been much interest in the use of chiral N-donor ligands in asymmetric catalysis, notably in oxidations, cyclopropanations, aziridinations, ketone reductions, allylic substitutions, nucleophilic additions and Lewis-acid catalysed cycloadditions and the area has been well reviewed.⁵

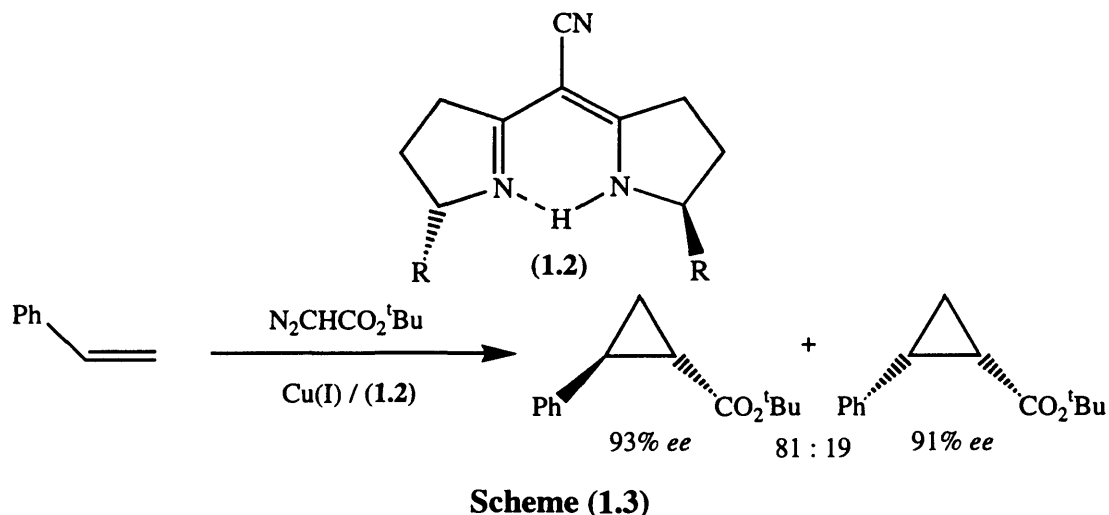
Many nitrogen-donor ligands are derived enantiopure from 'chiral pool' sources (*e.g.* amino acids) and are therefore less expensive and often rather easier to synthesise than many chiral phosphines, which often require resolution of enantiomers. Some of the earliest asymmetric catalysts using N-donor ligands were Mn(III)- and Fe(III)-porphyrins used for the asymmetric epoxidation of alkenes.^{6, 7} By placing bulky groups such as binaphthyl or amino-acids on the periphery of the porphyrin, high *ees* (up to 90%) can be obtained, by directing approach of an alkene to the metal-oxo centre. The difficulty of synthesis of chiral porphyrins, however, has limited their applications in asymmetric synthesis.

A more important series of catalysts for asymmetric epoxidation of *cis*-alkenes are Jacobsen's and Katsuki's "Mn(salen)" complexes.^{8, 9} The salen ligands derive from a condensation of substituted salicylaldehydes with chiral diamines, giving a ligand environment somewhat similar to that in porphyrins, but rather more flexible,

which may explain the high enantioselectivity obtained with this system. The Mn(III) centre of (1.1) will accept an oxygen from a co-oxidant such as PhI=O or NaOCl to give an oxo-species [Mn(V)=O], with the oxo-group oriented perpendicular to the plane of the salen ligand. Complex (1.1) will epoxidise *cis*-disubstituted alkenes (Scheme 1.2), with *ees* up to 98%¹⁰ and catalysts of this type are now used on an industrial scale.



Another class of ligands inspired by enzyme catalysts are C_2 -symmetric semicorrins,¹¹ which are similar in structure to corrinoid metal complexes found in living systems. Chiral semicorrins (1.2) were first reported by Pfaltz in 1986, as ligands for the asymmetric cyclopropanation of alkenes with diazoacetates, using copper catalysts (Scheme 1.3).¹²

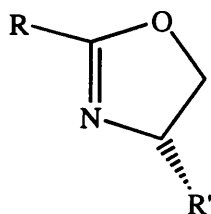


Cyclopropanes are crucial in pyrethroid insecticides and cilastatin and had previously been formed asymmetrically using copper catalysts with chiral Schiff base ligands.¹³

At the time of reporting, the copper/semicorrin catalysts were probably the best for asymmetric cyclopropanation, with considerably better enantioselectivities and *cis/trans* selectivities than had been achieved previously, but a further improvement in selectivity was to be found using C₂-symmetric bis-oxazolines as chiral ligands, which have a similar structure to semicorrins. The use of these ligands has subsequently been extended to a whole variety of asymmetric reactions, high enantioselectivity being achieved in many cases, as described below.

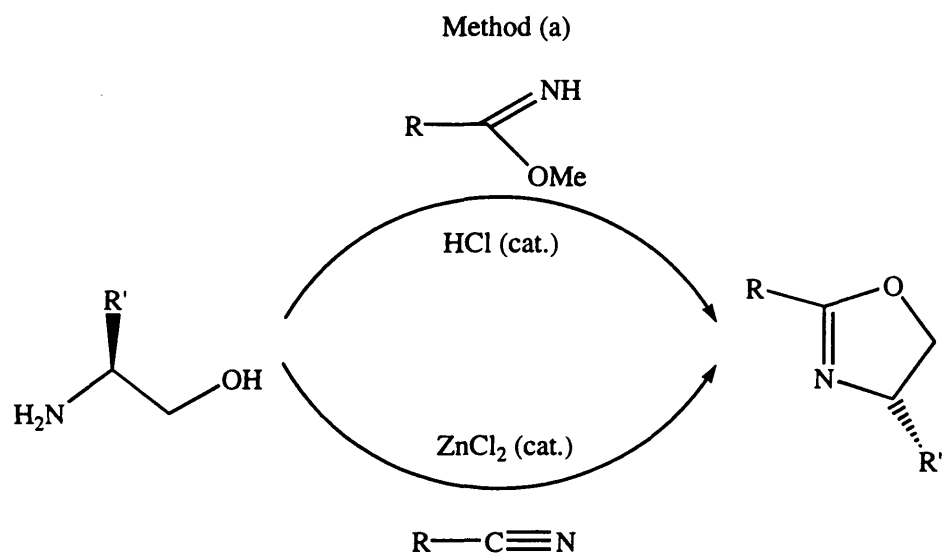
(1.2) - Oxazoline Ligands in Asymmetric Synthesis

Chiral oxazolines (1.3) are now the ligands of choice for a wide variety of asymmetric catalytic reactions, with high enantioselectivity being observed for cyclopropanations, aziridinations, allylic substitutions, cycloadditions and other reactions.^{11, 14, 15} The fact that the chiral centre is situated next to the nitrogen atom is significant; when the oxazoline ring coordinates to a metal centre via the nitrogen, the large groups (*e.g.* isopropyl, phenyl) attached to this carbon will then be close to the active site in any catalytic reaction proceeding at the metal. Thus, the substituents should have a significant effect on the enantioselectivity of reactions at that metal centre.

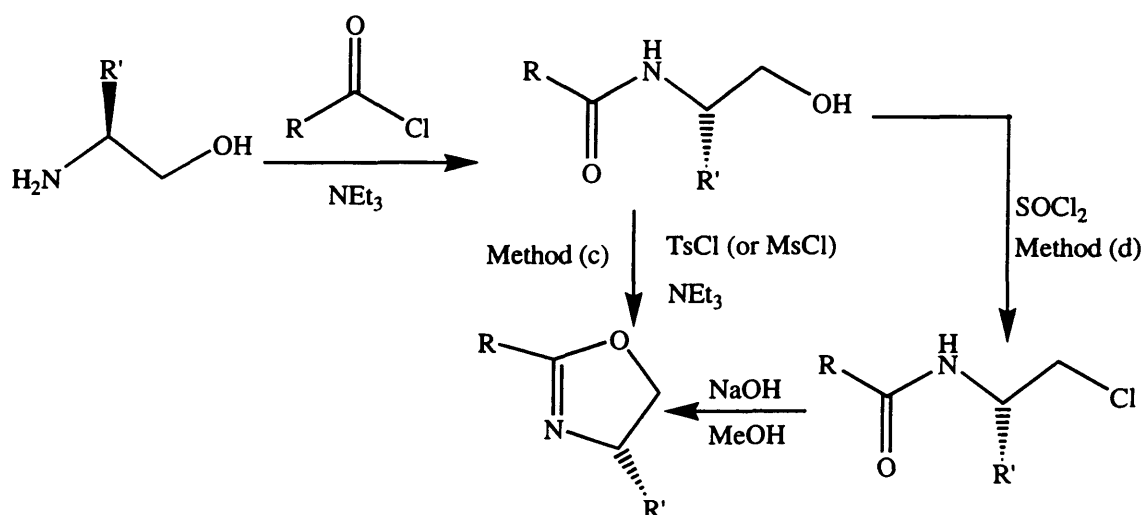


(1.3)

Oxazolines are inexpensively and conveniently synthesised by reaction of chiral amino alcohols (obtained by reduction of amino-acids¹⁶) with a suitable carbonyl or nitrile pre-cursor, **Schemes (1.4 - 1.5)**. The use of amino-acids as the source of chirality gives a wide choice of possible groups R' allowing variation of steric properties in the final oxazoline ligand and, importantly, results in enantiopure ligands, with no separation of enantiomers (as is often the case with chiral phosphine ligands).



Scheme (1.4)

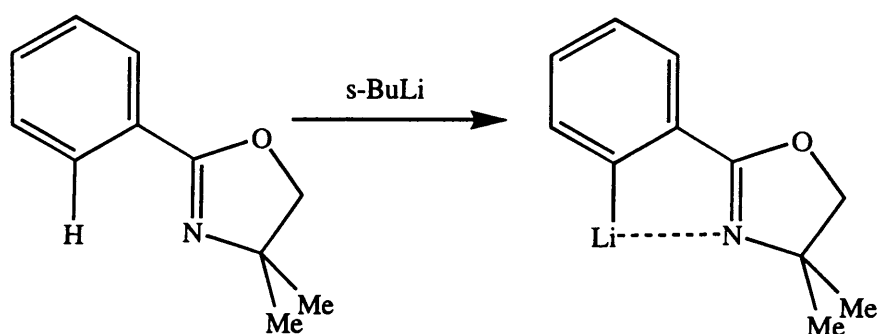


Scheme (1.5)

Method (a) has been used for many years in the synthesis of oxazolines. The imidate precursors $\{\text{RC}(\text{OMe})=\text{NH}\}$ are synthesised from the corresponding nitrile by treatment with NaOMe in MeOH .¹⁷ This method works well with electron-withdrawing groups R (e.g. pyridine), moderate to high yields of oxazoline being obtained. In some cases, the HCl -salt of the imidate $\{\text{RC}(\text{OEt})=\text{NH}_2\text{Cl}\}$ is more accessible, by treatment of RCN with $\text{HCl}_{(\text{g})}$ in EtOH .¹⁸ With 1,2-dicyanobenzene, method (a) fails and a high yield route to oxazolines derived from this nitrile is method (b), a one-pot synthesis involving refluxing amino alcohol, nitrile and ZnCl_2 catalyst in chlorobenzene.¹⁹ This method works well when $\text{R} = \text{aryl}$ or pyridinyl , but less well when $\text{R} = \text{alkyl}$ (NCCH_2CN gives no bis-oxazoline product at all). Despite having more steps, methods (c) and (d) often give the highest yields of oxazoline

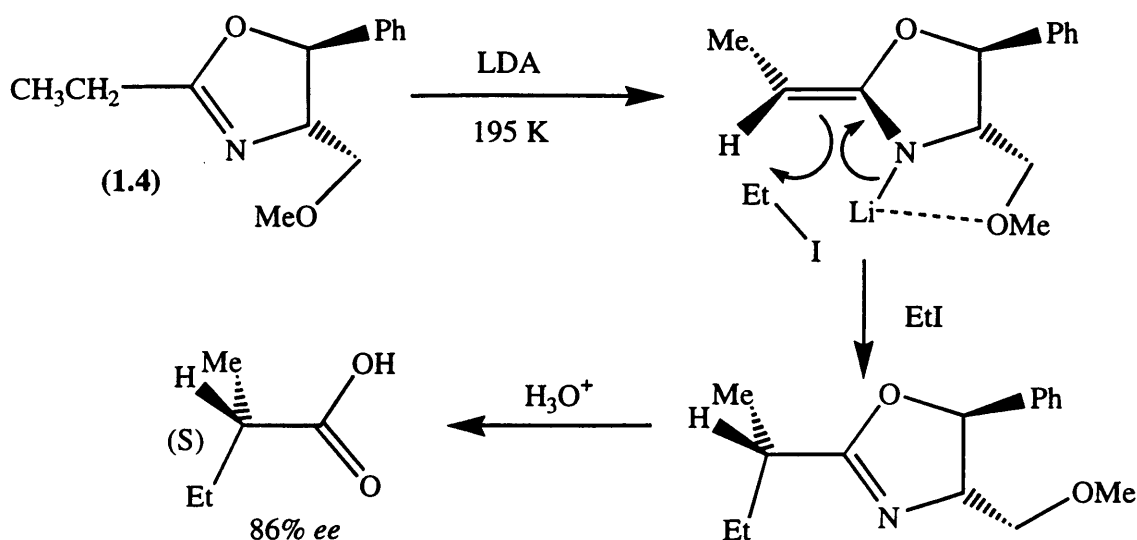
ligand.^{20, 21} Initially, the acyl chloride precursors (RCOCl) react with the amino alcohols to give a stable hydroxy-amide species. The terminal OH group must then be converted into a leaving group (Cl or, better, OTs), to allow base-induced cyclisation to occur, giving the required oxazoline. These methods work particularly well for C₂-symmetric bis-oxazolines such as bop and pybox (see below).

The use of oxazolines as ligands for asymmetric catalysis is a fairly recent practice; previously, they had been extensively used in stoichiometric lithiations. Oxazoline rings are highly effective at directing ortho-lithiation in aryl-species (Scheme 1.6).²²

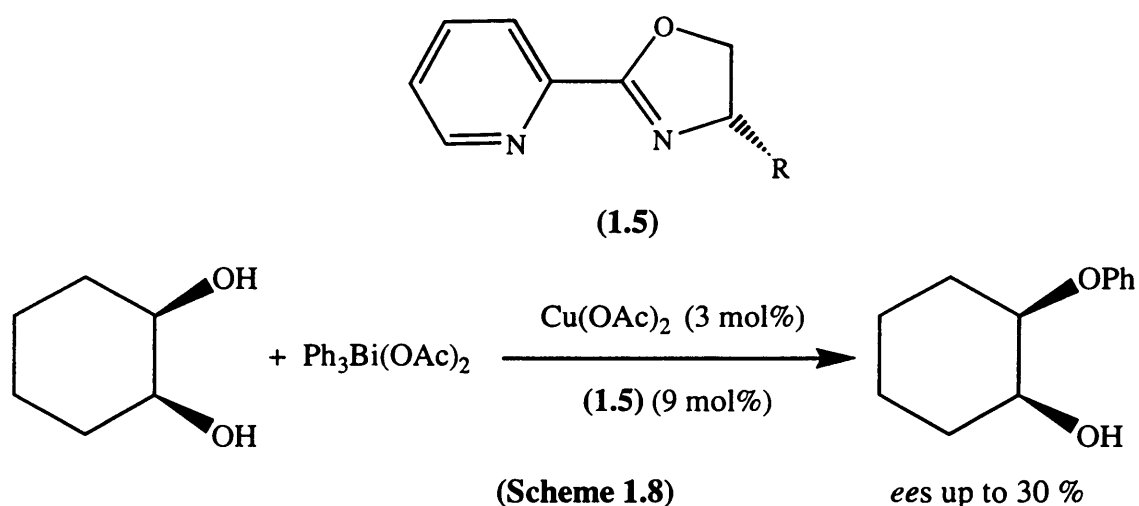


Scheme (1.6)

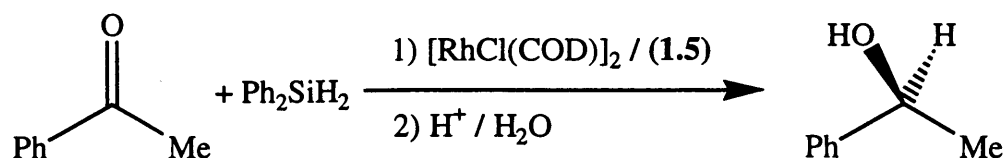
It was realised in the mid 1970s that the ability of oxazolines to promote lithiations could be made an asymmetric process, for example in the synthesis of dialkyl acetic acids, using oxazolines as chiral auxiliaries. The α -CH₂-group of (1.4) is activated towards deprotonation by LDA (Scheme 1.7); addition of EtI to the resultant enolate gives preferentially the (*S*)-isomer of the product,²³ which is hydrolysed to give the desired dialkylacetic acid, with regeneration of the O-methylated amino alcohol. A series of such reactions has been extensively reviewed by Meyers.²⁴



Although chiral oxazolines had been used in stoichiometric synthesis for some time, it was not until the late 1980s that their potential utility as ligands for asymmetric catalysis was recognised. The first examples of chiral oxazoline-containing ligands used in asymmetric catalysis were mono-oxazolanyl pyridines (pymox - **1.5**). These unsymmetrical bidentate ligands were first used by Brunner in 1986, for the mono-phenylation of *meso*-diols with $\text{Ph}_3\text{Bi}(\text{OAc})_2$, using a combination of $\text{Cu}(\text{OAc})_2$ and pymox ligands as catalyst (**Scheme 1.8**), *ees* of up to 30% being obtained $\{\text{R} = \text{CH}(\text{Me})(\text{Et})\}$.²⁵

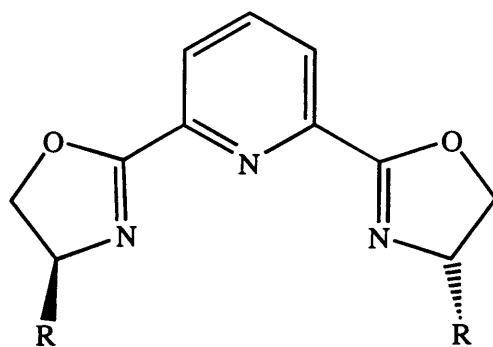


Subsequently, in 1989, Brunner used pymox ligands for the $\text{Rh}(\text{I})$ -catalysed asymmetric hydrosilylation of ketones, to give chiral alcohols (**Scheme 1.9**).²⁶ Enantiomeric excesses of up to 83% were obtained ($\text{R} = \text{'Bu}$), which were superior to those obtained using diphosphines up to that time.



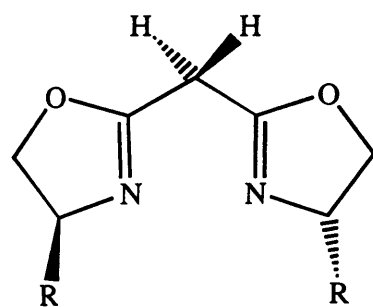
Scheme (1.9)

As a logical progression of Brunner's results, above, Nishiyama *et al.* first introduced C_2 -symmetry to this class of ligands, with the synthesis of bis-oxazolinyl-pyridines (pybox - **1.6**), which reacted with $RhCl_3$ to give complexes $[RhCl_3(pybox)]$. On treatment with $AgBF_4$ these complexes were also found to be catalysts for asymmetric hydrosilylation, enantiomeric excesses of >90% being observed.^{27, 28} More recently, Nishiyama has shown that ruthenium (II) complexes of pybox will act as asymmetric cyclopropanation catalysts.²⁹

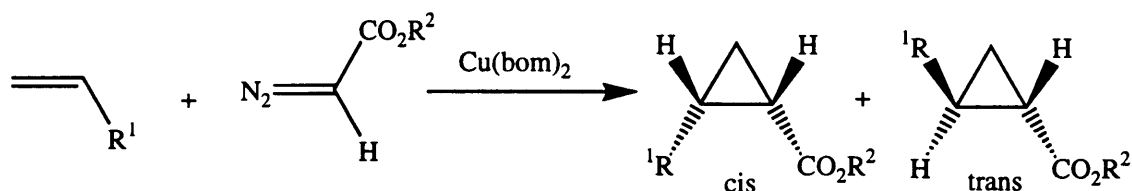


(1.6 - pybox)

Recognising the improved enantioselectivity possible with C_2 -symmetric ligands (both with the pybox ligands and with the semicorrins discussed earlier), a number of groups devised bidentate bis-oxazoline ligands for use in asymmetric catalysis; the first were bis-oxazolinyl methanes (bom - **1.7**), synthesised by Masamune *et al.* in 1990.³⁰ The bridging methylene group is readily deprotonated and neutral copper(II) complexes were found to be active catalysts for the asymmetric cyclopropanation of alkenes with diazoacetates; enantiomeric excesses of up to 99% were obtained (**Scheme 1.10**). Shortly after these results were published, a number of groups reported syntheses of, and catalysis with, derivatives of the bis-oxazolinyl methane ligands.

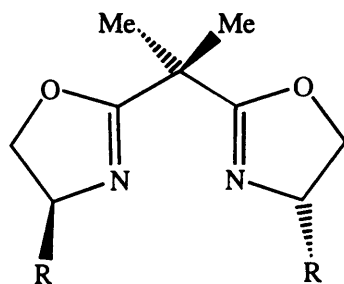


(1.7- bom)

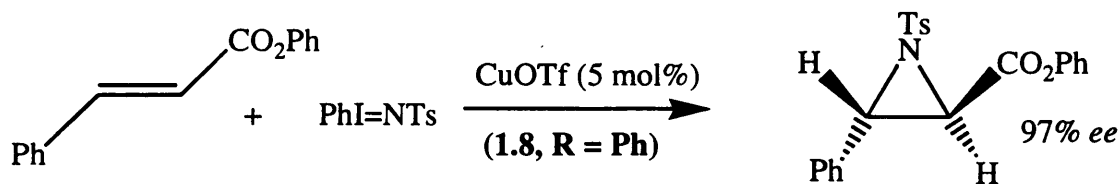


Scheme (1.10)

Replacing the bridging methylene group with a CMe₂ group gives bis-oxazolonyl propanes (bop - **1.8**), which generally provide higher *cis/trans* ratios and enantio-selectivity, in cyclopropanations, than the corresponding bom ligands.^{13, 31} The gem-dimethyl group of the bop ligands prevents enolisation, giving a more catalytically active complex. The bop ligands have also found application in the asymmetric aziridination of alkenes, catalysed by CuOTf, using PhI=NTs as the nitrene source (Scheme 1.11), high enantioselectivity (*ees* up to 97%) being obtained with *trans*-disubstituted alkenes.³² In this reaction, the intermediate is assumed to be a species “Cu=NTs”, analogous to a carbene.



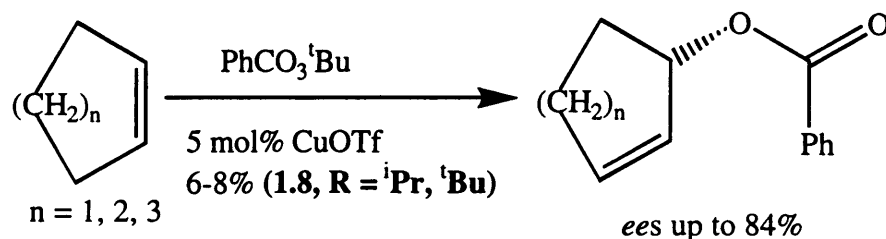
(1.8- bop)



Scheme (1.11)

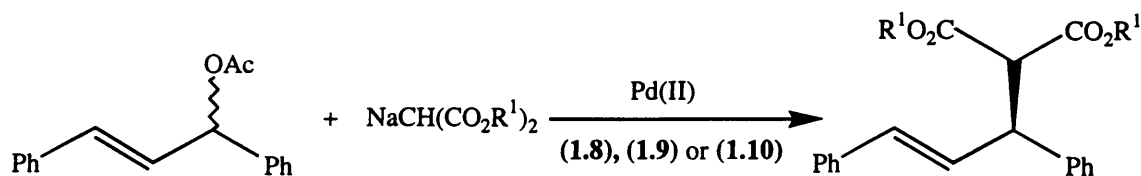
Pfaltz has shown that combinations of bop ligands (**1.8**) with CuOTf will act as catalysts for the allylic oxidation of cyclic alkenes with PhCO₃^tBu (Scheme 1.12),

ees of up to 84% being obtained.³³ The mechanism is thought to involve addition of an allyl radical to the Cu/oxazoline catalysts, followed by transfer of the carboxylate to the copper-bound allyl system.

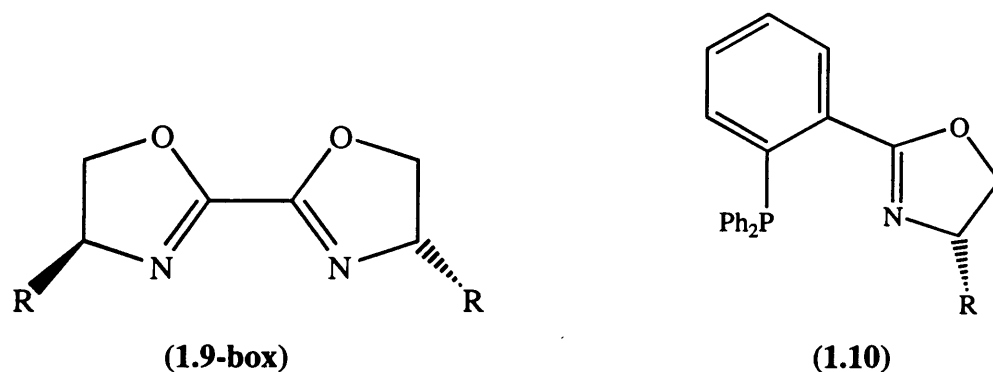


Scheme (1.12)

Allylic alkylation is a reaction that can be catalysed by Pd(II) complexes of either phosphines or N-donor ligands. In this reaction, an allylic acetate coordinates to the palladium to give a symmetrical allyl species; as in (Scheme 1.13). Attack of a nucleophile (e.g. malonate) occurs selectively at one end of the allyl. With C₂-symmetric 2,2-bis-oxazolines (box) ligands (1.9), ees of up to 77% were obtained for this reaction,³⁴ comparable to the enantioselectivity observed with diphosphines at that time. With ligands (1.8), the ee is further improved (with bn-bop, up to 88% ee is obtained for the reactions shown in Scheme (1.13)).³⁵



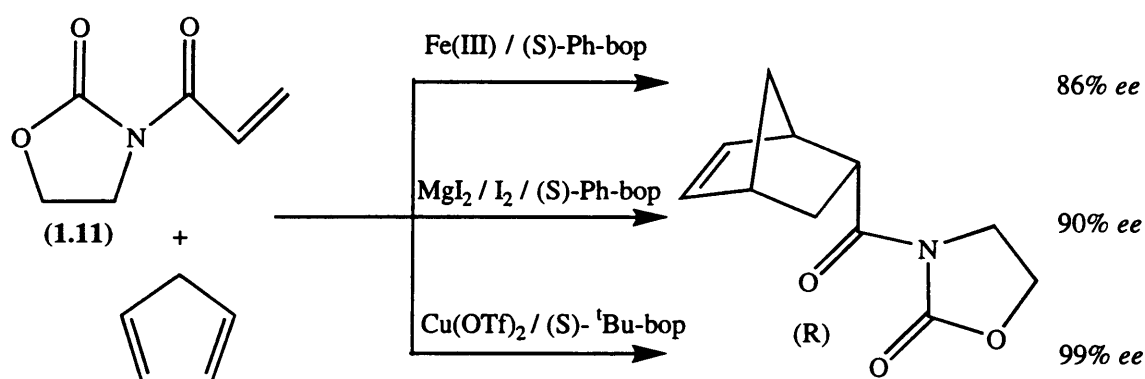
Scheme (1.13)



Replacing one oxazoline ring with a diphenylphosphine unit (producing a phosphino-oxazoline - 1.10), gives a much better ligand for catalytic allylic alkylation, which can control selectivity by electronic effects; the termini of the intermediate allyl species can be differentiated electronically, due to the differing trans effects of phosphorous and nitrogen. Good rates and very high enantioselectivity (ees up to 99%) are

observed, demonstrating that C_2 -symmetry is not essential for obtaining high selectivity with oxazoline ligands.³⁶

The potential of oxazoline ligands for use in asymmetric Lewis-acid catalysis was soon recognised. Combinations of Mg(II),³⁷ Fe(III)³⁸ and Cu(II)³⁹ with chiral bop ligands (**1.8**) resulted in extremely efficient asymmetric Diels-Alder catalysts; for example, catalysed reactions of cyclopentadiene with bidentate oxazolidinone dienophiles (**1.11**) proceed with excellent *exolendo* selectivity and with *ees* up to 99% (Scheme 1.14).



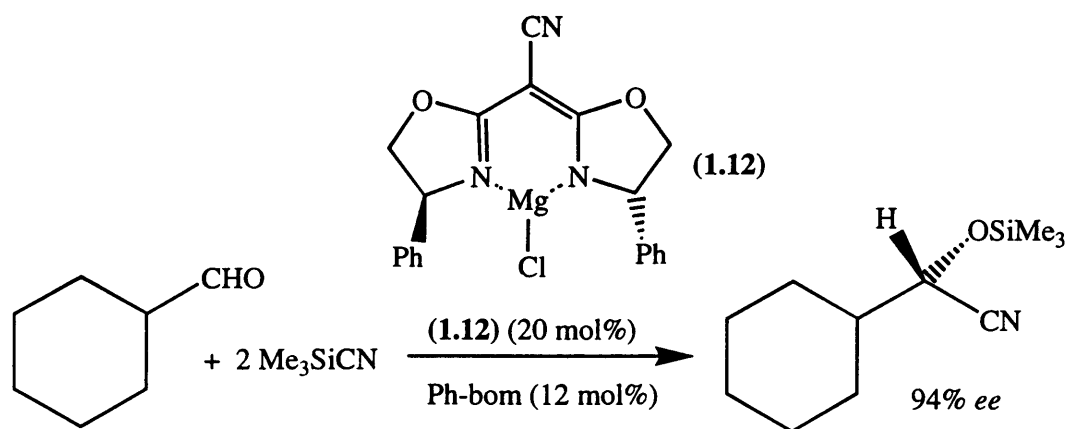
Scheme (1.14)

In each case, the *endo* product is formed almost exclusively and the (R)-enantiomer is formed preferentially. As the catalysts are formed *in situ*, the nature of the actual active species has been open to some question. With iron, the catalyst is thought to be octahedral in character, with the bidentate dienophile occupying an axial and an equatorial site, whilst with magnesium, a tetrahedral catalytic geometry is postulated. With copper, however, the geometry of the active catalyst is more uncertain. Evans has suggested that the catalyst adopts a square-planar geometry, which would be consistent with many results obtained with the Cu/bop system; however, several anomalous results remain to be explained. In particular, the reaction of cyclopentadiene with (**1.11**) catalysed by Cu(OTf)₂ and (S)-Ph-bop gives the (S) enantiomer of product in 30% *ee*, which is the opposite enantiomer to that obtained with Cu(II) / (S)-^tBu-bop,³⁹ which suggests different geometries in the various copper reactions.

Impressive results have also been obtained for asymmetric hetero-Diels Alder and ene reactions with Cu/bop catalysts.^{40, 41} With the bidentate bop ligands, two-point binding dienophiles such as (**1.11**), are often necessary to obtain the highest enantioselectivity. The catalyst formed from Cu(II) and pybox ligands, presumably

$[\text{Cu}(\text{pybox})]^{2+}$, will effectively catalyse the asymmetric reaction of monodentate acrylic dienophiles with cyclopentadiene, with good *exo:endo* selectivity and high *ees* (up to 96%).⁴² The catalyst is still formed *in situ*, but results are consistent with a square planar geometry. With the Cu/pybox system, the rate of catalysis is highly dependent on the choice of anion; for example, with SbF_6^- the reaction of methacrolein with cyclopentadiene at -20°C took 8 hours to go to completion, whilst with TfO^- , the reaction time was 120 hours and with BF_4^- the rate was even slower. These results illustrate that totally non-coordinating anions are necessary to obtain optimum activity.

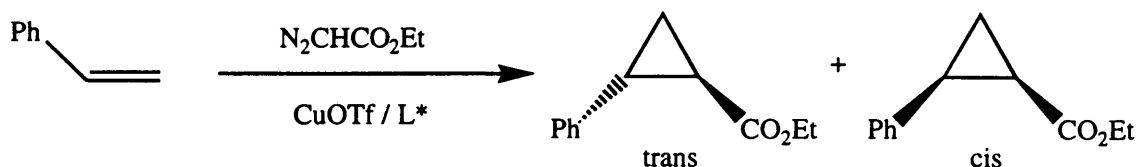
Another important Lewis-acid catalysed reaction that uses bis-oxazoline ligands is the addition of Me_3SiCN to aldehydes, giving cyanohydrins. Corey has used a $\text{Mg}(\text{II})$ complex of a monoanionic bom-derivative (**1.12**) as a catalyst for this reaction, enantiomeric excesses of up to 94% being obtained, with cyclohexyl-carbaldehyde (**Scheme 1.15**).⁴³ The mechanism is thought to involve Lewis-acid activation of the carbonyl group towards attack by CN^- , followed by addition of the TMS group. A Ph-bom co-catalyst is required to stabilise the intermediates.



Scheme (1.15)

The size of the chelate ring formed when bis-oxazolines such as (**1.8**) and (**1.9**) coordinate to a metal centre can have a significant impact on the enantioselectivity of many catalytic reactions. Andersson *et al.* have recently investigated the effects of chelate ring size, and flexibility, on the CuOTf -catalysed cyclopropanation of styrene, with ethyl diazoacetate, using a selection of bis-oxazoline ligands (**Scheme 1.16** and **Table 1.11**).⁴⁴ A general increase in enantioselectivity was obtained, as the chelate ring size increased. With ^iPr -box (five-membered ring), only 3% *ee* was obtained, but with the bom and bop ligands (six-membered chelate ring), considerably improved

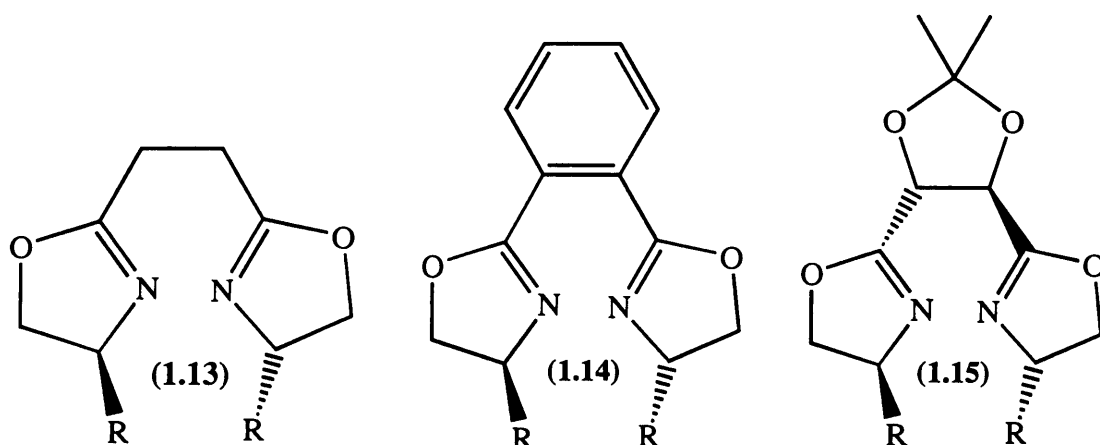
selectivity was found (up to 49% *ee*). With the ligand 1,2-bis-oxazolinyl ethane (**1.13**), the enantioselectivity increased still further, presumably because the isopropyl groups were closer to the carbene intermediate. By placing a rigid 1,3-dioxolane backbone between the two oxazoline rings (giving **1.15**), the *ee* of cyclopropane produced was increased to 84%.



Scheme (1.16)

Table (1.1): Effect of chelate ring size on cyclopropane *ee*

Ligand, L* (R = ^t Pr)	Chelate Ring size	<i>ee</i> of trans cyclopropane / %
box (1.9)	5-membered	3
bom (1.7)	6-membered	36
bop (1.8)	6-membered	49
(1.13)	7-membered	59
(1.14)	7-membered	8
(1.15)	7-membered	84



Interestingly, the *ee* of the cyclopropane obtained with CuOTf and 1,2-bis-oxazolinyl benzene (benbox - **1.14**) was very low (8%); this is presumably because the oxazoline rings of (**1.14**) are forced to rotate out of the plane of the benzene ring in order to coordinate to the copper. Such an effect was observed for zinc complexes of benbox,

by Bolm *et al.* (Figure 1.1),¹⁹ the complexes undergoing a rapid equilibration between the two possible conformations shown. As a result of the oxazoline rings rotating out of the plane of the benzene ring, one of the R-substituents is brought closer to the metal, whilst the other is moved further away than would be expected, based on a planar arrangement.

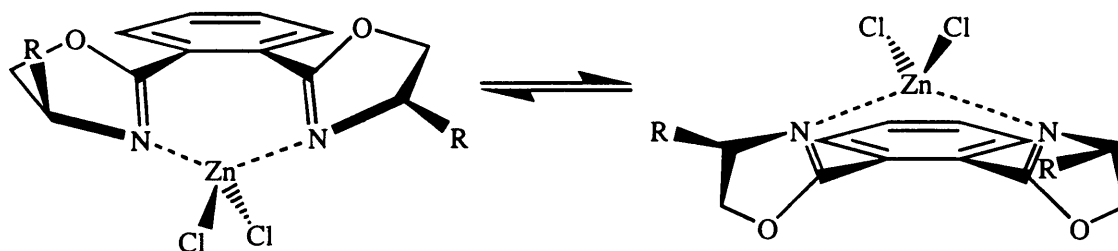
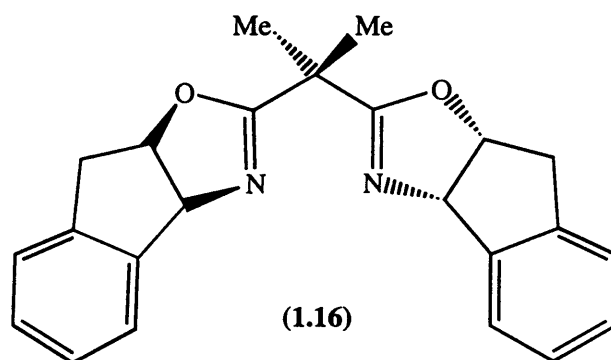


Figure (1.1)

The effect of chelate ring size on the $\text{Cu}(\text{OTf})_2$ / bis-oxazoline catalysed Diels-Alder reaction of oxazolidinone (1.11) with cyclopentadiene was investigated by Takacs *et al.*, who found that higher enantioselectivities (76% *ee*) were obtained with ^tBu-bop (six-membered chelate ring) than with ligands (1.13) (51% *ee* - seven-membered ring), in contrast to the results for cyclopropanation (Table 1.1).⁴⁵

Another factor that can affect the selectivity in catalysis with oxazoline ligands is their rigidity, as shown for ligand (1.15) in Table (1.1). Some substituents, such as phenyl, are capable of rotation, which is found to reduce the enantioselectivity of catalytic reactions with the ligand, relative to substituents such as ⁱPr and ^tBu. Recently, Davies has shown that rigid bis-oxazolines, such as the bop ligand (1.16), derived from amino-indanol, give dramatically higher enantioselectivity than their Ph-bop analogues for the $\text{Cu}(\text{OTf})_2$ -catalysed Diels-Alder reaction of (1.11) with cyclopentadiene.⁴⁶ With (1.16), 82.5 % *ee* of the (S) adduct was obtained (at -50°C), whilst with Ph-bop, only 30 % *ee* was obtained. By placing an extra methylene group between the oxazoline rings and the phenyl substituents, the latter are prevented from rotating, which would occur with Ph-bop.



Until recently, only C_2 -symmetric bis-oxazoline ligands had been shown to give high enantioselectivity in Lewis-acid catalysis, using metal salts. However, a recent paper by Fujisawa and co-workers demonstrates that unsymmetrical oxazoline ligands are capable of inducing high levels of enantiocontrol in the Diels-Alder reaction.⁴⁷ Magnesium complexes of unsymmetrical mono-oxazoline ligands, like that shown in **Figure (1.2)**, were found to be asymmetric catalysts for the Diels-Alder reaction of oxazolidinones (**1.11**) with cyclopentadiene; *ees* of up to 91% were obtained. It was concluded from ^1H NMR studies that the conformation of the catalyst shown in (**Figure 1.2**) was energetically preferred to that with the tolyl group in a 'cis' orientation with the phenyl substituent on the oxazoline. Thus, the catalyst adopted a pseudo- C_2 -symmetric orientation.

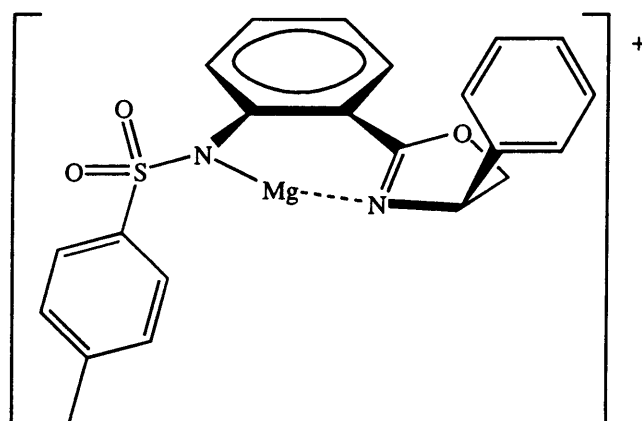
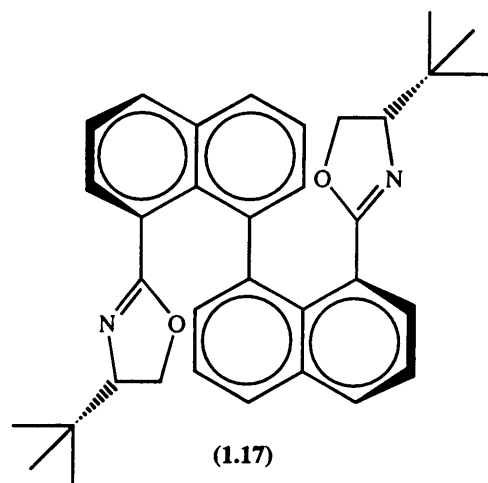


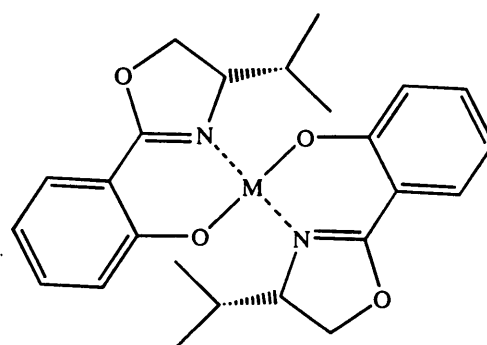
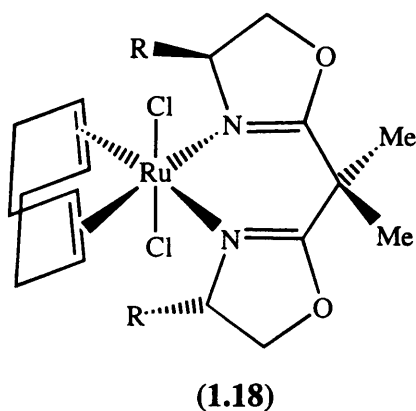
Figure (1.2)

It has recently been recognised that incorporating oxazoline rings into larger ring systems, particularly those with a chiral axis, can potentially lead to high levels of enantioselectivity. Several groups have reported binaphthyl-oxazoline ligands, such as (**1.17**), which have chiral centres on the oxazoline rings and a chiral axis.^{48, 49} Ligand (**1.17**) will coordinate in a bidentate fashion to CuOTf , the complex acting as a

catalyst for the asymmetric cyclopropanation of styrene with ethyl diazoacetate. Up to 90 % *ee* of the *cis*-cyclopropane was produced.⁴⁹

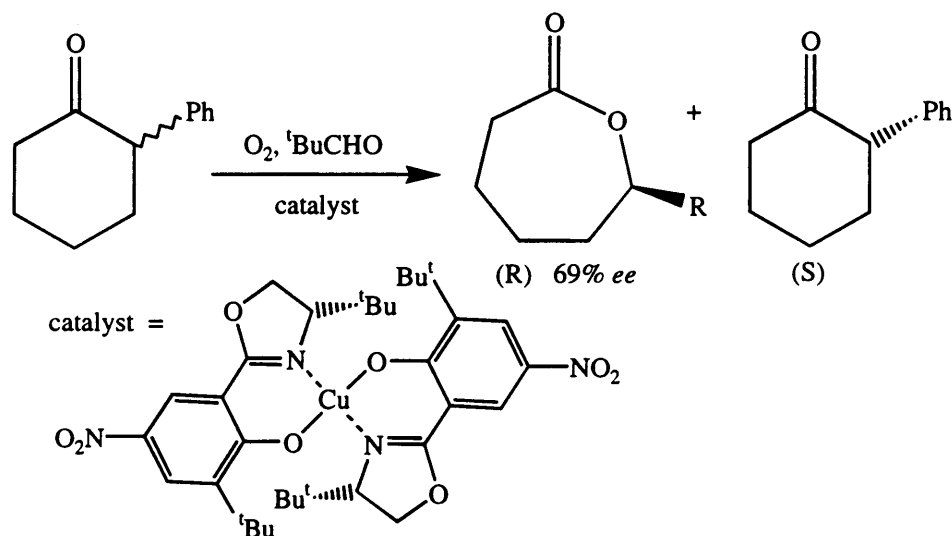


For a large number of asymmetric catalytic reactions using oxazoline ligands, the catalytically-active species is formed *in situ*, particularly with reactions involving copper. Examples where a fully characterised, pre-formed oxazoline complex has been used in catalysis are still somewhat rare; these include the rhodium complexes of pymox and pybox described previously. Several groups have set out to synthesise well-defined complexes of oxazoline ligands, with a view to their use in asymmetric catalysis. The complex $[\text{RuCl}_2(\text{COD})(^i\text{Pr-bop})]$ (1.18) was synthesised by Woodward *et al* as a pre-cursor for an asymmetric epoxidation catalyst, but did not prove to be an efficient asymmetric catalytic system.⁵⁰ A series of complexes (Figure 1.3) of the unsymmetrical mono-oxazolanyl ligand phenmox were formed by Bolm *et al*, as possible analogues of metal-salen complexes.⁵¹



Copper complexes of the type shown in Figure (1.3) were found to be catalysts for the asymmetric Baeyer-Villiger oxidation of racemic cyclic ketones to

lactones, under Mukaiyama oxidation conditions (in which molecular oxygen acts as oxidising agent with ^tBuCHO as oxygen acceptor) - **Scheme (1.17)**.⁵²



Scheme (1.17)

This process, which had only previously been performed catalytically with the aid of enzymes, was found to proceed with an element of kinetic resolution; the unreacted ketone was enriched in the (S)-enantiomer. The ^tBu- and nitro-groups on the arene resulted in a more catalytically active complex, with higher yields of lactone obtained, than in the unsubstituted complex.

As outlined in this section, it is clear that oxazoline ligands have been used with great success in asymmetric catalysis. Many catalysts, however, are still formed *in situ*, so understanding of enantioselectivity at a molecular level is not always straightforward (*e.g.* the Cu(II) / *bop* catalysed Diels-Alder reactions discussed earlier). To obtain such understanding, the use of a well-defined, structurally stable metal complex would be desirable. On this basis, the use of half-sandwich ruthenium and rhodium complexes of oxazoline ligands offers great potential. These complexes would be suitable for reactions in which only one coordination site is required by the substrate, such as Lewis-acid catalysed processes. The synthesis of such complexes is described in Chapter Two and their use in asymmetric Lewis-acid catalysis is described in Chapter Three.

**Chapter Two:
Synthesis of Chiral
Half-Sandwich
Oxazoline Complexes**

Chapter Two : Synthesis of Chiral Half-Sandwich

Oxazoline complexes

(2.1) - Introduction

The defining characteristic of a half-sandwich complex is the presence of a ring, either an arene or a cyclopentadienyl, π -bound to a metal centre, such that three positions of the metal's coordination sphere are filled. There are then one to four sites available for coordination of other ligands, making half-sandwich complexes potentially useful synthetic templates. The main focus here will be on pseudo-octahedral complexes, with three additional ligands L_1 - L_3 (Figure 2.1).

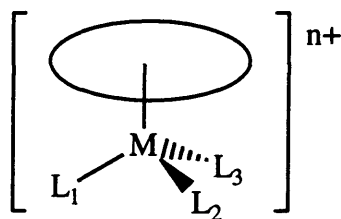


Figure (2.1)

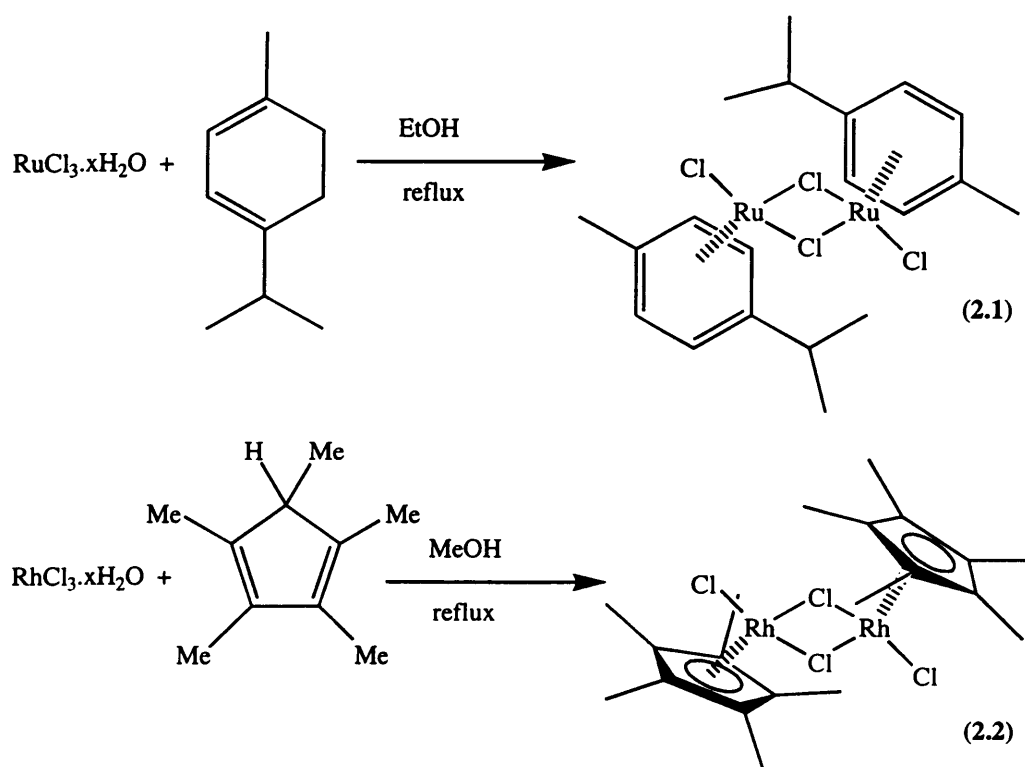
 = arene or cyclopentadienyl

An early example of a half-sandwich arene complex was $\text{Cr}(\text{CO})_3(\text{C}_6\text{H}_6)$.⁵³ Derivatives of this compound are useful in synthesis, as the arene ring is activated towards attack by nucleophiles, relative to uncoordinated benzene, due to significant σ -donation of electrons from the arene to chromium.⁵⁴ Aside from those of chromium, the arene complexes that have attracted most attention are those of ruthenium. The first example of a half-sandwich ruthenium complex was $[\text{RuCl}_2(\text{PBU}_3)(\text{C}_6\text{H}_6)]$,⁵⁵ synthesised in 1967 by Winkaus and Singer by treatment of a species of composition $[\text{RuCl}_2(\text{C}_6\text{H}_6)]_n$ with PBU_3 ; a large number of similar compounds are now known.

The half-sandwich ruthenium complexes that have been studied most are cyclopentadienyl-containing species such as $[\text{RuCl}(\text{CO})_2\text{Cp}]$ and $[\text{RuCl}(\text{PPh}_3)_2\text{Cp}]$.⁵⁶ The latter will undergo ligand substitution reactions, particularly with chelating diphosphines, to give $[\text{RuCl}(\text{P-P})\text{Cp}]$;⁵⁷ with chiral phosphine ligands, such complexes are useful in asymmetric synthesis, which will be discussed shortly. Replacement of CO or PPh_3 by nitrogen-donor ligands, however, is difficult.

Analogous rhodium(III) species such as $[\text{RhCl}(\text{PPh}_3)_2\text{Cp}]^+$ are known, but the majority of half-sandwich rhodium complexes feature the bulky and robust pentamethylcyclopentadienyl (Cp^*) ligand.⁵⁸

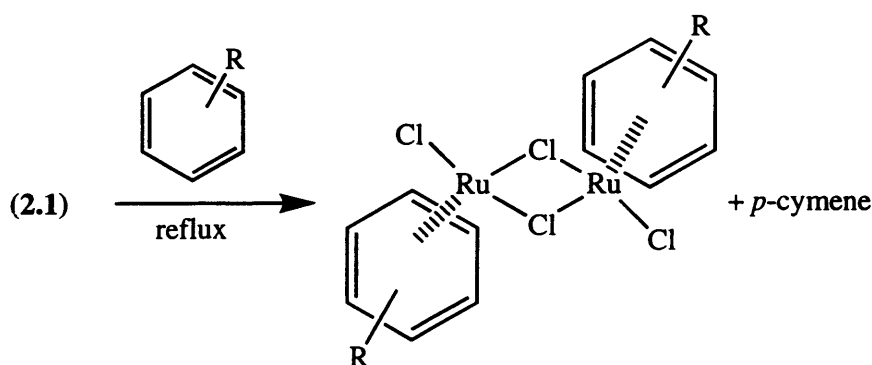
The fragments “ $\text{Cp}^*\text{Rh(III)}$ ” and “ $(\text{arene})\text{Ru(II)}$ ” are both useful in organometallic chemistry and synthesis. The precursors for many complexes containing these fragments are the chloro-bridged dimeric species $[\text{RuCl}_2(p\text{-cymene})]_2$ (**2.1**)⁵⁹ and $[\text{RhCl}_2\text{Cp}^*]$ (**2.2**),⁶⁰ which are synthesised from commercially available $\text{RuCl}_3 \cdot x\text{H}_2\text{O}$ and $\text{RhCl}_3 \cdot x\text{H}_2\text{O}$ respectively (**Scheme 2.1**). The iridium analogue $[\text{IrCl}_2\text{Cp}^*]_2$ is synthesised in the same way.⁶⁰ In the synthesis of (**2.1**), the ruthenium is reduced from Ru(III) to Ru(II) , accompanied by oxidation of the α -phellendrene (a mixture of para-disubstituted cyclohexadienes) to give the arene *p*-cymene. The rhodium of (**2.2**), however, remains in the +3 oxidation state. Both complexes have stable 18-electron configurations and contain two bridging chloride ligands, the $[\text{M}-\text{Cl}]_2$ centre shown by X-ray diffraction to have a two-fold axis of symmetry.⁶¹



Scheme (2.1)

A series of analogous dimeric species $[\text{RuCl}_2(\text{arene})]_2$ can also be obtained. $[\text{RuCl}_2(\text{C}_6\text{H}_6)]_2$ is synthesised, analogously to (**2.1**) by reaction of $\text{RuCl}_3 \cdot x\text{H}_2\text{O}$ with cyclohexadiene, whilst some other arene-containing dimers can be obtained by arene exchange reactions of (**2.1**).⁶² Thus, $[\text{RuCl}_2(\text{C}_6\text{Me}_6)]_2$ is synthesised by heating (**2.1**)

with hexamethylbenzene in a melt,⁵⁹ whilst other dimers, such as $[\text{RuCl}_2(\text{mes})]_2$, $[\text{RuCl}_2(1,4\text{-Me}_2\text{C}_6\text{H}_4)]_2$ and $[\text{RuCl}_2(1,2,4,5\text{-Me}_4\text{C}_6\text{H}_4)]_2$ are obtained by refluxing (2.1) in neat arene (Scheme 2.2). The arene exchange reactions are effective with high-boiling or solid arenes, as high temperatures are required in order to displace the *p*-cymene.⁶² Synthesis of dimers containing more substituted arenes by the route used to make (2.1) is often impractical, as the cyclohexadiene derivatives are not readily available. Exchange of the Cp* ligand in half-sandwich rhodium complexes has not been reported.



Scheme (2.2)

The dimers $[\text{RuCl}_2(\text{arene})]_2$ and $[\text{MCl}_2\text{Cp}^*]_2$ ($\text{M} = \text{Rh}, \text{Ir}$) undergo many analogous reactions.^{58, 63, 64} Treatment with two-electron donor ligands L ($\text{L} = \text{py}, \text{PPh}_3, \text{dmsO}, \text{CO}, \text{amines}$) gives half-sandwich complexes $[\text{MCl}_2(\text{L})(\text{ring})]$ (Figure 2.2), also known as ‘piano-stool’ complexes. The dimers can also react with two monodentate ligands L to give cations $[\text{MCl}(\text{L})_2(\text{ring})]^+$, or with a bidentate ligand L–L ($\text{L-L} = \text{bipyridyls}, \text{diamines}, \text{diphosphines}$) in polar solvents. Two different types of complex are possible with bidentate ligands; usually the ligand will act as a chelate, giving complexes $[\text{MCl}(\text{L-L})(\text{ring})]^+$, but complexes of type $[\text{M}_2\text{Cl}_4(\text{ring})_2(\mu\text{-L-L})]$ ($\text{L-L} = \text{diamines}, \text{diphosphines}$) (Scheme 2.3) are also possible. Anionic bidentate ligands (*e.g.* the anions of 2,4-pentane-dione and pyranones) react, with $[\text{MCl}_2(\text{ring})]_2$ to give neutral complexes $[\text{MCl}(\text{L-L})(\text{ring})]$.^{65, 66}

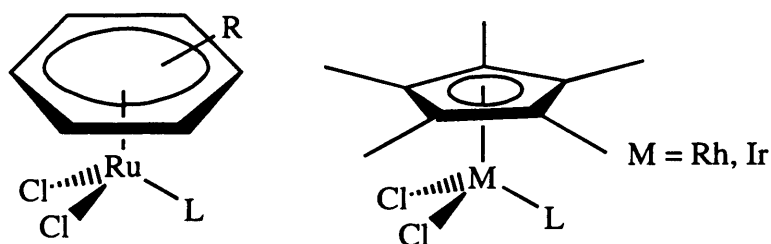
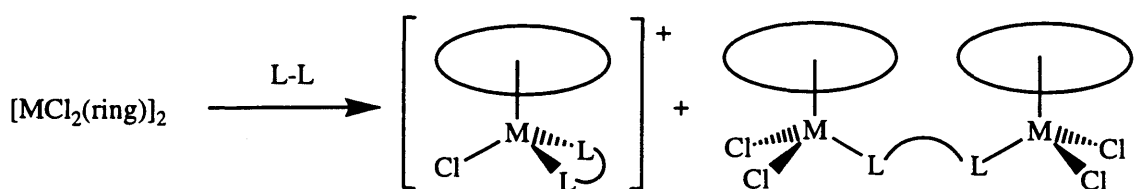


Figure (2.2)



Scheme (2.3)

The ever-increasing need for chiral products has led to great interest in the use of chiral half-sandwich complexes in asymmetric synthesis, both stoichiometric and catalytic. In the simplest examples of chiral half-sandwich complexes, only one element of chirality is present, the three main types of which are:

- (1) a chiral metal centre,
- (2) a chiral centre on one of the ligands

or (3) chirality arising due to coordination of a prochiral ligand such as a disubstituted arene or unsymmetrical alkene.

The particular emphasis in this section will be on chiral complexes of types (1) and (2). A general example of a chiral-at-metal complex is shown in **Figure (2.3)**.

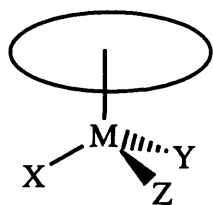
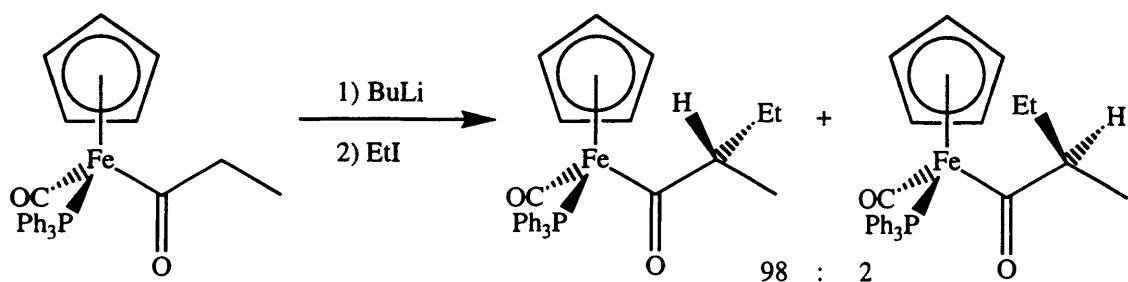


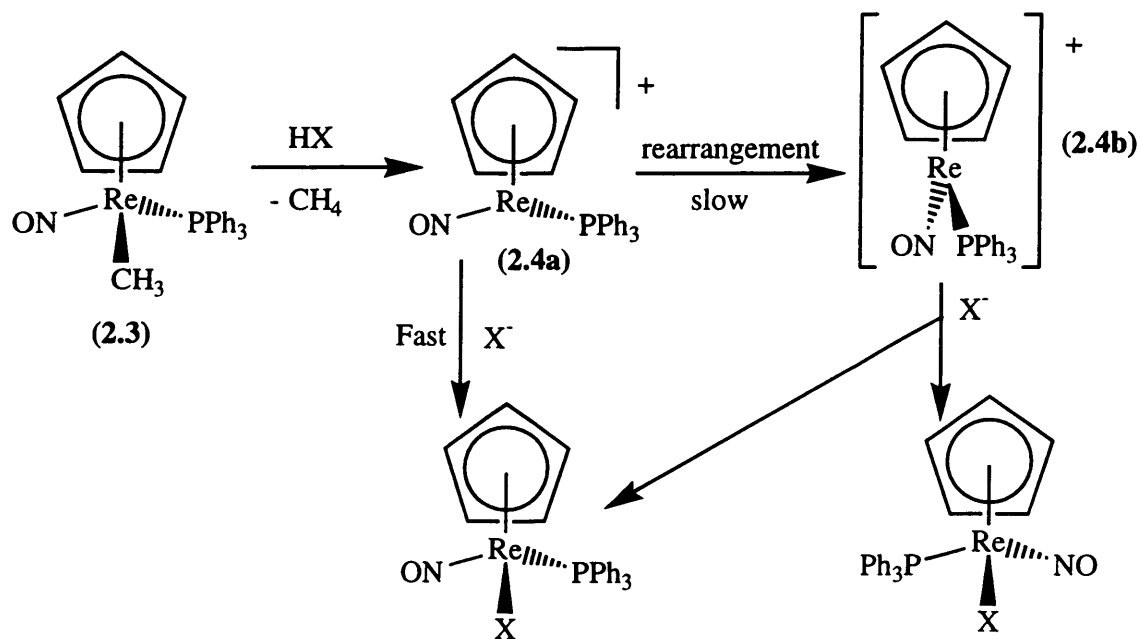
Figure (2.3)

The pseudo-tetrahedral structure, shown in **Figure (2.3)**, is analogous to four-coordinate carbon compounds and, thus, if ligands X, Y and Z are all different, then the metal centre is chiral and two enantiomers are possible. Similarly, if ligands Y and Z form an unsymmetrical chelate, then a chiral centre is also present at the metal. Examples of such chelating ligands are picolinate and glycinate, which form complexes as racemates.^{67, 68} Utilisation of purely chiral-at-metal complexes in asymmetric synthesis requires enantiopure complexes to be used. The separation of enantiomers is often achieved by crystallisation of diastereomeric salts, often giving enantiopure complexes. Some particularly impressive examples have involved “Fe-Cp” reagents. Davies *et al.* have shown that addition of ethyl iodide to the lithium enolate of $[\text{Fe}(\text{COEt})(\text{CO})(\text{PPh}_3)\text{Cp}]$ occurs preferentially from the opposite face to the bulky PPh_3 ligand, giving diastereomeric products, in a ratio of 98:2 (**Scheme 2.4**).⁶⁹



Scheme(2.4)

Another highly effective chiral auxiliary for stoichiometric asymmetric synthesis is the fragment “[Re(NO)(PPh₃)Cp]⁺”. Enantiomeric rhenium complexes containing this fragment have been studied extensively, notably by Gladysz and co-workers. Enantiopure complexes [Re(NO)(PPh₃)LCp]ⁿ⁺ are often easily resolved, by separation of diastereomeric salts (*e.g.* when L = CO, diastereomeric “amido” complexes are made by reaction with chiral amines, which are then crystallised and the amine removed by hydrolysis).⁷⁰ The essentially enantiopure compounds will then undergo many subsequent reactions without racemisation.

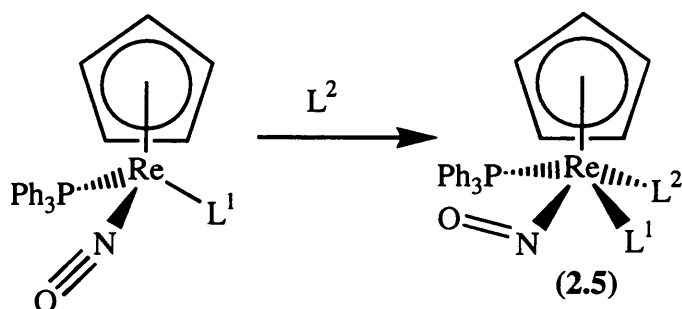


Scheme (2.5)

The high stereochemical rigidity of this system is demonstrated by the reaction of [Re(CH₃)(NO)(PPh₃)Cp] (**2.3**) with electrophiles HX (X = Cl, Br, I, OTs, OTf), yielding complexes [ReX(NO)(PPh₃)Cp] with ≥ 99% retention of configuration at rhenium observed in most cases.⁷¹ These reactions were thought to occur via the unsaturated chiral pyramidal intermediate [Re(NO)(PPh₃)Cp]⁺ (**2.4a**), formed after the elimination of CH₄ from (**2.3**) (Scheme 2.5).⁷² To account for the high

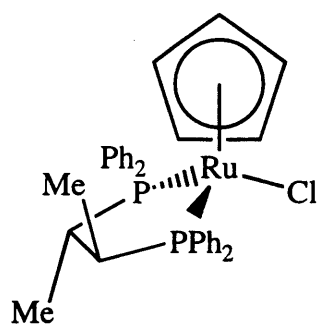
stereoselectivity, the inversion barrier to conversion of (2.4a) to the planar species (2.4b) must be sufficiently high that the rate of addition of X^- to (2.4a) is much faster than that of rearrangement. Clearly, addition of X^- to (2.4b) would result in racemic products.

Hoffmann *et al.* have recently calculated that the inversion barriers for interconversion of pyramidal and planar $16e^-$ half-sandwich species (such as 2.4a / 2.4b) are fairly low in most cases.⁷³ Pyramidal geometries are particularly favoured for systems containing ligands which combine strong π -acceptor and σ -donor properties (e.g. CS), resulting in inversion barriers of 10 - 15 kcal mol⁻¹. For the rhenium system (2.4a / 2.4b), the barrier was calculated to be only 0.7 kcal mol⁻¹, which made the high selectivity of the system surprising. Gladysz has recently suggested an alternative mechanism for substitutions with [Re(PPh₃)(NO)LCp] in which substitution is *associative* in character, an intermediate (2.5) being formed, which is stabilised by bending of the nitrosyl ligand (which acts as an electron-sink, with two electrons filling its π^* -orbital), **Scheme (2.6)**.⁷⁴

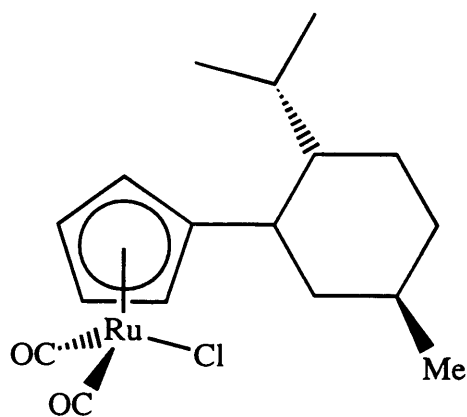


Scheme (2.6)

The second type of optically-active half-sandwich complex has chirality only on the ligands, not at the metal centre. This occurs when a chiral monodentate ligand or C_2 -symmetric bidentate ligand coordinates to the metal (as in 2.6⁷⁵), or when the polyhapto ligand itself has a chiral auxiliary attached, such as the menthyl group in (2.7).⁷⁶

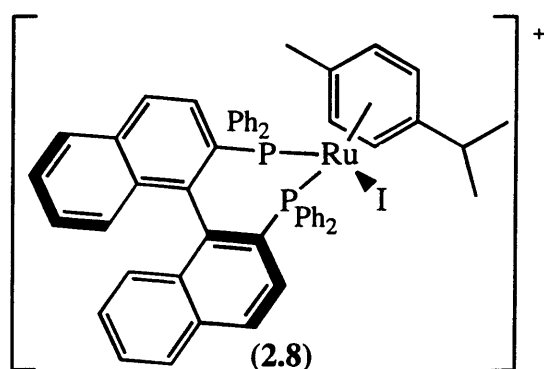
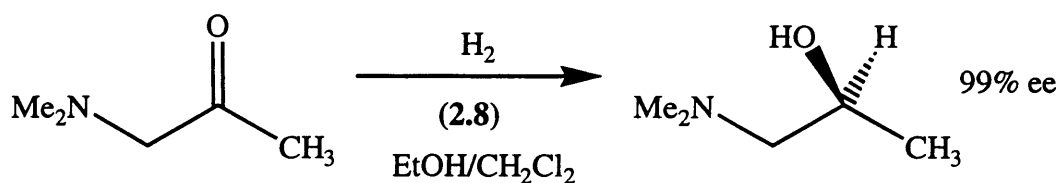


(2.6)



(2.7)

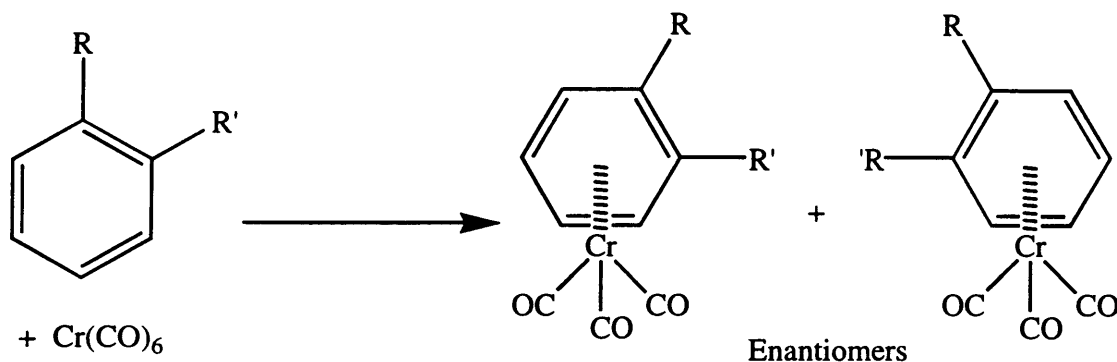
There have been relatively few reports of this type of half-sandwich complex as chiral auxiliaries in asymmetric catalysis (although there have been many mechanistic studies). Complexes $[\text{Ru}(\text{BINAP})(p\text{-cymene})]^+$ (2.8) are precursors for asymmetric hydrogenation catalysts (Scheme 2.7).⁷⁷ A variety of substituted alkenes and ketones could be hydrogenated, with *ees* > 95%, under relatively mild conditions (30 - 40°C). Under the reaction conditions, however, the arene ligand was easily removed and the active catalyst was thought to be a less coordinatively saturated species, so this catalyst cannot truly be referred to as 'half-sandwich'.



Scheme (2.7)

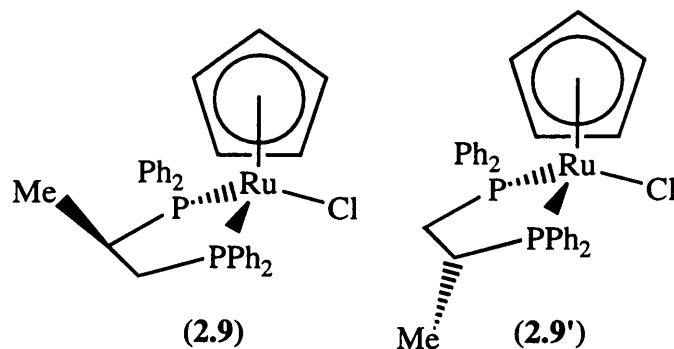
The third type of chiral half-sandwich complex is that formed by coordination of a pro-chiral ligand, usually an unsaturated species such as an alkene or a disubstituted polyhapto ring, to an achiral metal centre. Important examples in asymmetric synthesis of this type of complex are $\text{Cr}(\text{CO})_3(\text{arene})$ (arene = 1,2-

disubstituted), formed by treatment of $\text{Cr}(\text{CO})_6$ with the arene (**Scheme 2.8**). Racemates are obtained, which in some cases can be separated by crystallisation of diastereomeric derivatives and/or chiral HPLC, but these methods are not easily performed on an industrial scale.⁷⁸⁻⁸⁰

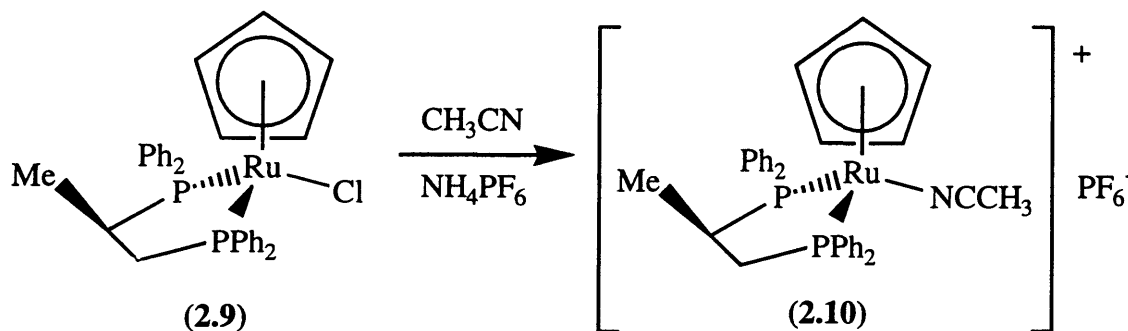


Scheme (2.8)

The chiral half-sandwich complexes discussed thus far have contained only one element of chirality and are formed as racemates. If, however, there are two elements of chirality in a complex, then there is the potential to form diastereomers. The main focus in this section will be on complexes with chirality at both metal centre and ligand, an area of great interest for asymmetric synthesis. Diastereomeric half-sandwich complexes are ideal substrates for the study of mechanisms of ligand exchange; indeed, many cyclopentadienyl ruthenium complexes have been synthesised primarily for this purpose. Detailed studies have been made of whether reactions are associative or dissociative in nature and of the stereochemical changes at the metal centre involved in reactions of these species. Diastereomeric complexes $[\text{RuCl}\{(\text{R})\text{-Prophos}\}\text{Cp}]$ (**2.9/2.9'**) feature in many such studies.⁸¹



Ligand substitution reactions of (2.9/2.9') generally proceed with retention of configuration at the metal centre. For example, treatment of (2.9) or (2.9') with NaOMe/MeOH leads to the corresponding hydride complexes [RuH{(R)-Prophos}Cp] with complete retention of configuration.⁸² Similarly, reaction of (2.9) with CH₃CN and NH₄PF₆ leads stereospecifically to the cationic complex [Ru(NCCH₃){(R)-Prophos}Cp]PF₆ (2.10) (Scheme 2.9).⁸³ A corresponding reaction occurs with (2.9').



Scheme (2.9)

Analogous diastereomeric complexes [RhCl{(R)-Prophos}Cp*]Cl (2.11/2.11'), studied by Carmona and co-workers, were formed by reaction of [RhCl₂Cp*]₂ with (R)-Prophos, an isomer ratio of 77:23 being obtained.⁸⁴ The configuration at the metal centre was found to be stable at room temperature in d₄-MeOH, even after 30 days, but epimerisation occurred at reflux temperature. Thus, a 96:4 mixture of diastereomers was obtained after refluxing the 77:23 mixture of (2.11/2.11') for 7 days in methanol. Epimerisation was not observed on refluxing in chloroform. Excess chloride ions were found to accelerate the epimerisation, suggesting that an associative mechanism was operating. Generally, for complexes [MCl(P-P)(ring)]ⁿ⁺ (P-P = unsymmetrical, chiral phosphine), there is little inherent diastereoselectivity in the synthesis of the complexes, but once formed, the configuration at metal is reasonably stable. In many cases, replacement of the chloride ligand occurs with diastereospecific retention of configuration at the metal.⁸¹

As described above, many detailed mechanistic studies of the reactions of diastereomeric half-sandwich complexes have employed chiral phosphine ligands. There has recently been considerable interest in the use nitrogen and oxygen donor ligands in such studies. Furthermore, such ligands are often more readily available and/or synthesised than many phosphine ligands, making their complexes potentially very useful in asymmetric synthesis (See Chapter One). One of the cheapest and most

readily available sources of chirality is from amino acids ($\text{H}_2\text{NCH(R)CO}_2\text{H}$). These ligands can bind by both the amine and carboxyl termini, depending on the pH, to a wide variety of metals. At neutral pH, amino acids exist in the 'zwitterionic' form with positive charge on nitrogen and negative on oxygen, but at high pH (≈ 9) both the nitrogen and oxygen are available for coordination. Complexes $[\text{MCl}(\text{amino-acidate})(\text{ring})]$ (Figure 2.4) have attracted much interest, due to their potential use in asymmetric synthesis.⁸⁵ Naturally-occurring amino-acids have (S)-configurations at their C chiral centre, so their half-sandwich complexes will potentially exist as pairs of diastereomers, with configurations ($S_{\text{M}}S_{\text{C}}$) and ($R_{\text{M}}S_{\text{C}}$), based on a ligand priority ring > Cl > O > N.^{86, 87}

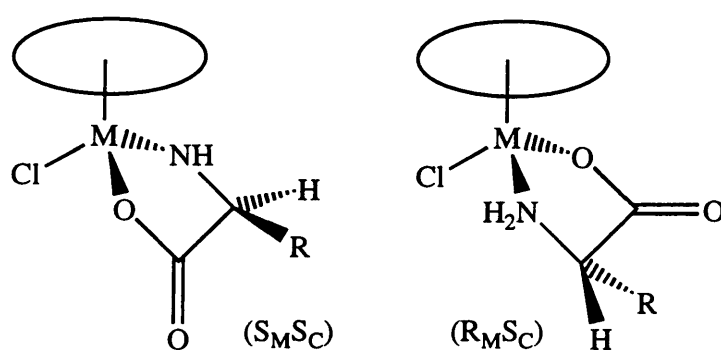


Figure (2.4)

There are 20 naturally occurring amino acids, giving a wide variety of possible side-chains R. Arene-ruthenium and Cp^*Rh complexes of amino acids are of particular interest here, initial work with ruthenium being carried out by Dersnah and Baird.⁶⁸ Beck⁸⁸ and Sheldrick⁸⁹ have subsequently extended the area to rhodium and iridium. Complexes $[\text{RuCl}(\text{aa})(\text{arene})]$ and $[\text{RhCl}(\text{aa})\text{Cp}^*]$ were synthesised by treatment of the appropriate chloro-bridged dimer (e.g. 2.1 and 2.2) with two equivalents of amino acid in the presence of base (e.g. NaOMe in MeOH/ H_2O).⁸⁸ All complexes were synthesised as mixtures of diastereomers, typically in ratios of 60:40 to 50:50, except in unusual cases (e.g. where aaH = proline⁸⁸). The reason for the low diastereoselectivities observed in syntheses of these complexes appears to be that neither possible orientation of the substituent R is particularly sterically hindered, as shown in X-ray structure determinations (so there is little steric or energetic difference between the two isomers). X-ray structures also show that, in many cases, the pairs of diastereomers co-crystallise, typically as 50:50 mixtures.^{67, 90}

Isomer ratios of crystallised amino-acidate complexes can be confirmed by use of ^1H NMR. Diastereomer exchange in solution is thought to be slow, at least on the NMR timescale, for complexes $[\text{MCl}(\text{aa})(\text{ring})]$, particularly in less-polar solvents, such as CDCl_3 .^{67, 91} Diastereomer mixtures do not change their composition after several days in solution, which leads to the conclusion either that equilibrium is reached quickly or the configuration at the metal is stable. Epimerisation at the metal centre does occur, however, in polar solvents such as water and methanol. In D_2O , complexes $[\text{RuCl}(\text{aa})(\text{arene})]$ undergo partial substitution of D_2O for Cl^- , giving the equilibria shown in **Figure (2.5)**.^{68, 88} Thus, in the ^1H NMR spectra in D_2O , signals due to four species are observed- two diastereomers of both the chloro-bound and aqua complexes. At room temperature, all signals are sharp, indicating slow diastereomer exchange on the NMR timescale. At higher temperatures, broadening of the resonances attributed to the aqua complexes is observed, implying that rapid interconversion of diastereomers is occurring, resulting in inversion of configuration at ruthenium.

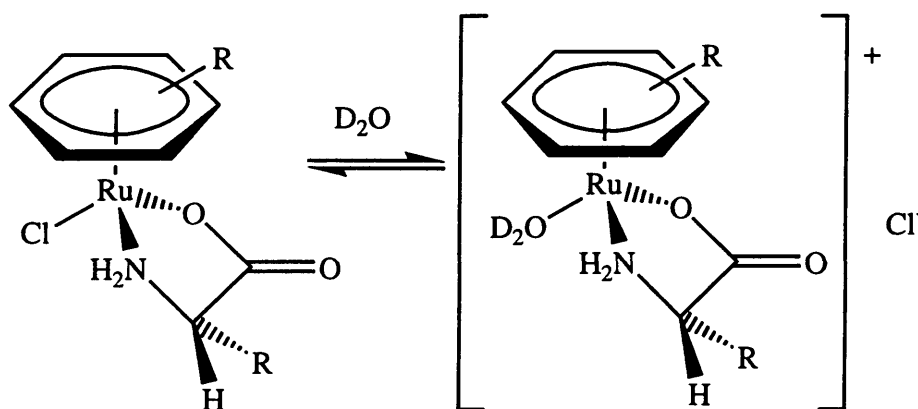
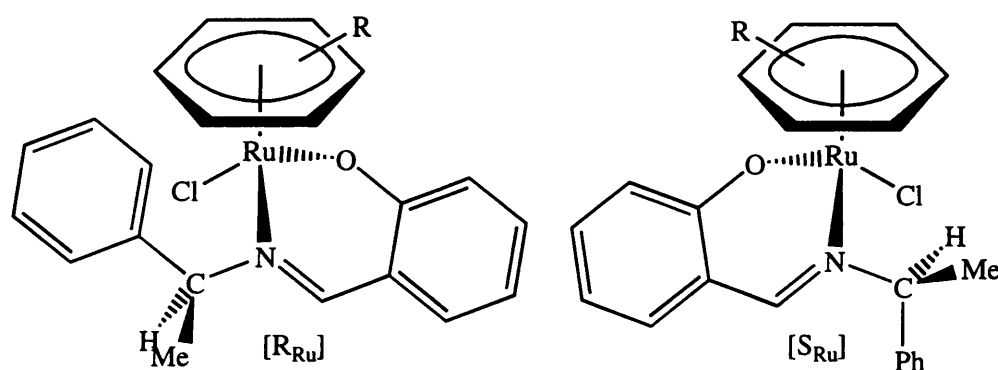


Figure (2.5)

Rapid epimerisation at the metal centre is also found in the complexes formed by chloride abstraction from $[\text{MCl}(\text{aa})\text{Cp}^*]$ ($\text{M} = \text{Rh}, \text{Ir}$) by AgBF_4 .⁹² ^1H NMR spectra in $\text{d}_4\text{-MeOH}$ contain only one set of signals, which broaden when the spectra are obtained at -90°C , indicating that two rapidly interconverting diastereomers are present. Epimerisation was thought to be due to dissociation of a labile MeOH ligand, but more recently, trimeric species have been postulated.⁹³

Chiral Schiff-base ligands have been used to great effect in asymmetric catalysis, most notably in Jacobsen's and Katsuki's epoxidation catalysts (see Chapter 1).^{9, 10} They are readily synthesised by condensation of a carbonyl group and a chiral

amine, giving an imine that can act as a donor atom to a metal. There has recently been much interest in arene-ruthenium complexes of Schiff-base ligands, both from their catalytic potential and as a means of investigating the stereochemistry of reactions of chiral half-sandwich compounds. If chiral-at-metal complexes are to be used in asymmetric synthesis, the configuration at the metal centre should be stable under reaction conditions; any epimerisation might lead to a reduction in the enantioselectivity of the reaction. Thus, thorough investigation of epimerisation at chiral metal complexes is very important, and arene-ruthenium Schiff-base complexes have been used for this purpose. Complexes $[\text{RuCl}(\text{L-L}^1)(\text{arene})]$ {where L-L^1 = the anion of (*S*)-*N*-(1-phenylethyl)-salicylalimine} and many derivatives have been synthesised by the groups of Brunner,^{94, 95} and Mandal and Chakravarty.^{96, 97} The diastereomeric complexes (**2.12/2.12'**) and (**2.13/2.13'**) (**Figure 2.6**) were obtained by reaction of the dimers $[\text{RuCl}_2(\text{arene})]_2$ with $\text{Na}^+[\text{L-L}^1]^-$.



Arene = C ₆ H ₆ :	(2.12)	86:14	(2.12')
= <i>p</i> -cymene:	(2.13)	85:15	(2.13')

Figure (2.6)

Complexes (**2.12/2.12'**) and (**2.13/2.13'**) were formed with almost identical diastereomer ratios (as shown in **Figure 2.6**) and, despite initial reports to the contrary,^{96, 97} behave similarly in solution. Crystallisation of the crude mixture of isomers (**2.12/2.12'**) gives only (**2.12**), shown by X-ray diffraction studies to have an (R_{Ru}) configuration.⁹⁴ Two independent crystals gave exactly the same unit-cell dimensions and each crystal in the sample had a uniform shape, so it was concluded that there was no (S_{Ru}) isomer present. Dissolution of the crystals at -80°C immediately gave an 86:14 mixture of isomers, as shown by ^1H NMR, indicating that epimerisation of the ruthenium configuration is rapid, even at low temperature. The

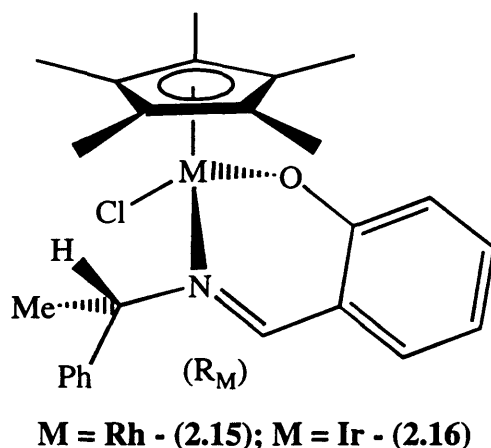
isomer ratio obtained was identical to that initially formed in the crude product, suggesting that the equilibrium position had been reached. Such rapid equilibration was also observed for complexes (**2.13/2.13'**), which were incorrectly reported to be configurationally stable in solution, even at 70°C.^{96, 97} The problems arose because the equilibrium position was reached quickly, in the short time between making up the NMR sample at room temperature and actually running it. No further change in isomer ratio was observed, which was wrongly interpreted as being because the ruthenium configuration was stable. In fact, for many complexes of this type, several half-lives will have passed in the time it takes to run an NMR spectrum and exchange of isomers is thus slow on the NMR timescale ($k < 10^{-1} \text{ s}^{-1}$) but relatively fast on a chemical timescale ($k > 10^{-3} \text{ s}^{-1}$).

There are several important steric and electronic effects that lead to the (R_{Ru}) isomer being thermodynamically favoured in complexes (**2.12/2.13**), which also apply in other Schiff-base complexes, where the ligand is derived from (*S*)-*N*-(1-phenylethyl)-amine. Firstly, X-ray structures indicate that there is an attractive interaction caused by the face-on orientation of the phenyl ring to the η^6 -arene ligand. This orientation is known as the ' β -phenyl effect' and is presumed to be retained in solution, since distinct 'high-field' shifts of the ^1H NMR signals due to the η^6 -arene ligand are observed (due to the magnetic anisotropy of the phenyl substituent). This effect is seen in many arene-ruthenium Schiff-base complexes of this type. This orientation of the phenyl group is only favoured in the major (*R*) isomers (as shown by X-ray structures), as the hydrogen substituent at the carbon chiral centre will then be oriented towards the chloride ligand. If the phenyl substituent in the (*S*) isomer was oriented towards the arene ligand, then the methyl substituent (at the carbon chiral centre) would be oriented towards the chloride, which would be sterically disfavoured (clearly, this is a more important factor than any stabilisation due to a β -phenyl effect).

A number of substitution complexes $[\text{RuL}^*(\text{L-L}^1)(\text{arene})]^+$ ($\text{L}^* = 2\text{-Me-py}, 4\text{-Me-py}, \text{PPh}_3$) have been synthesised, by treatment of isomer mixtures of (**2.12**) or (**2.13**) with ligand L^* , in the presence of Ag^+ (to remove the chloride ligand).⁹⁴ Many of these derivatives undergo rapid epimerisation at the metal centre, in the same way as (**2.12/2.13**). An example is the complex $[\text{Ru}(4\text{-Me-py})(\text{L-L}^1)(\text{C}_6\text{H}_6)]\text{PF}_6$ (**2.14**), which exists as a 67:33 mixture of diastereomers in d_6 -acetone at room temperature,

as shown by ^1H NMR. Crystallisation of the sample gave a single isomer {shown by X-ray diffraction to be the equivalent isomer to (2.14)} in 90% yield, indicating that substantial epimerisation at the metal centre had occurred. The crystallised (2.14) was dissolved at -80°C and the ^1H NMR spectrum obtained; this confirmed that only one isomer was present and indicated that epimerisation was not rapid at -80°C , unlike in (2.12). It was concluded that as the configuration at ruthenium in (2.14) was unstable under the conditions of synthesis, it could not be determined whether the complex was formed with inversion or retention of configuration.

More recently, Parr has reported that the analogous complexes $\text{MCl}(\text{L-L}^1)\text{Cp}^*$ { $\text{M} = \text{Rh}, \text{Ir}$; $\text{L-L}^1 = (\text{S})\text{-N-(1-phenylethyl)salicylaldiminato}$ - 2.15/2.16} are formed as only the (R) diastereomers (the configuration determined from X-ray diffraction).⁹⁸



No evidence for the (S) isomers was found in the ^1H NMR spectra of either the crude or crystallised samples. However, as the reported NMR data were obtained at room temperature, there is a possibility that what is observed is, in fact, a time-averaged spectrum, due to rapid epimerisation in solution. One would expect this process to be faster for (2.15/2.16) than for the ruthenium analogues (2.12/2.13),⁹⁴ for which epimerisation was rapid, even at -80°C and the equilibrium position was reached quickly.

Having established that epimerisation at the metal centre is rapid for complexes (2.12 - 2.14), with an anionic N,O-donor ligand,^{94, 95} Brunner *et al.* investigated analogous compounds with anionic N,N-donor Schiff-base ligands; *e.g.* $[\text{RuCl}(\text{L-L}^2)(\text{C}_6\text{H}_6)]$ (2.17/2.17') ($\text{L-L}^2 =$ the anion of (S)-N-(1-phenylethyl)pyrrolle-carbaldimine),⁹⁹ (Figure 2.7).

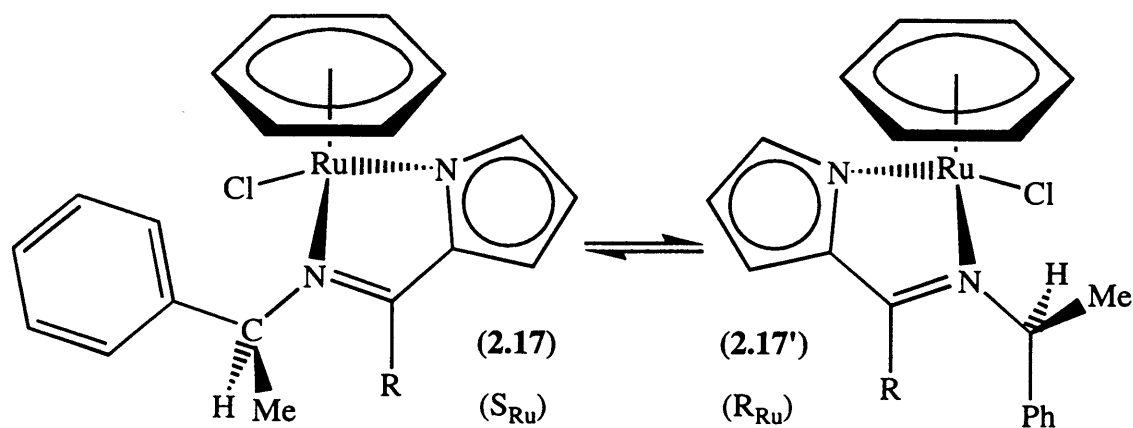


Figure (2.7)

The room temperature ^1H NMR spectrum of the crude product showed the ratio (2.17):(2.17') to be 68:32, which didn't change over time, suggesting that it corresponds to the equilibrium ratio. Crystallisation of the mixture gave only (2.17) (in yields higher than those expected based on the equilibrium isomer ratio), as determined by X-ray diffraction and ^1H NMR spectra at -25°C . The X-ray structure of (2.17) shared several features with those of (2.12/2.13); a ' β -phenyl effect' was again observed between the phenyl substituent and the benzene ligand, whilst the C-H bond of the phenyl-ethyl substituent is oriented towards the chloride, minimising steric hindrance. On warming the ^1H NMR sample of (2.17) from -25°C , signals due to the minor isomer began to appear at temperatures above 0°C and at room temperature, the equilibrium isomer ratio (68:32) was established. The half-life for the approach to the equilibrium (2.17) \rightleftharpoons (2.17') was determined as $\tau = 9.2 \pm 0.1$ min (27°C) in CDCl_3 , so although epimerisation at the metal centre in (2.17/2.17') does occur, it is considerably slower than in the analogous salicylaldimine complexes (2.12/2.13), where exchange was rapid, even at -80°C .⁹⁴

In this series of analogous arene-ruthenium Schiff-base complexes, the configuration at metal becomes more kinetically stable, switching from anionic N,O-donors to anionic N,N-donor ligands. It would be logical, then, for similar complexes containing *neutral* N,N-donor ligands to be even more configurationally stable, since these would be cationic, rather than neutral compounds and loss of the chloride ligand from a cation should be less favoured. Such complexes $[\text{RuCl}(\text{L-L}^3)(\text{mes})]\text{BF}_4$ {2.18/2.18' and 2.19/2.19', L-L^3 = the Schiff-bases formed by reaction of (S)-1-phenylethylamine with either pyridine-2-carboxaldehyde or 2-acetyl pyridine} were

formed as mixtures of diastereomers (**Figure 2.8**) by reaction of L-L³ with [RuCl₂(mes)]₂ in the presence of NaBF₄.¹⁰⁰

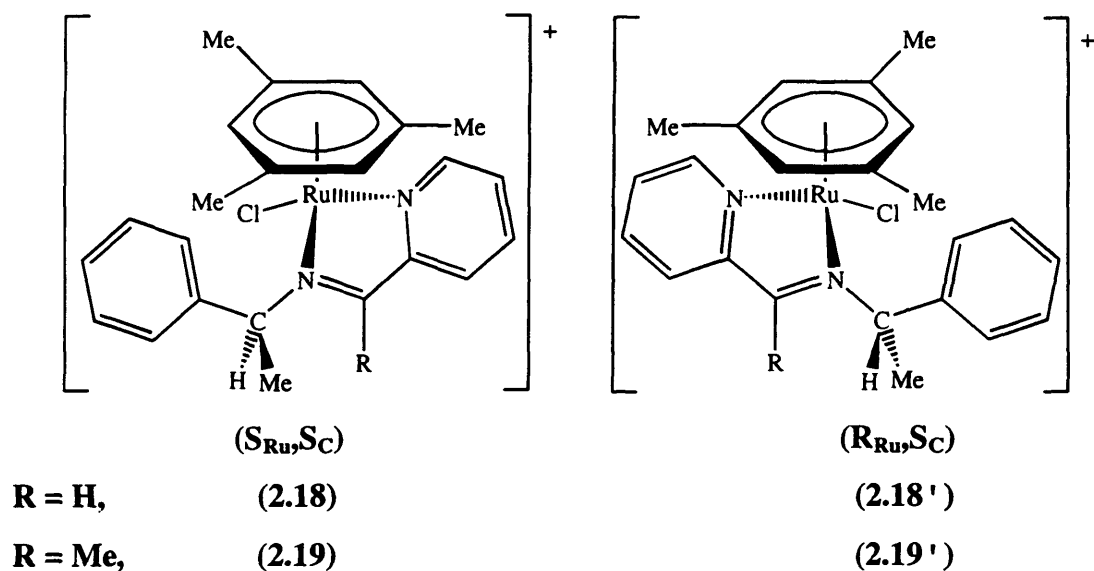


Figure (2.8)

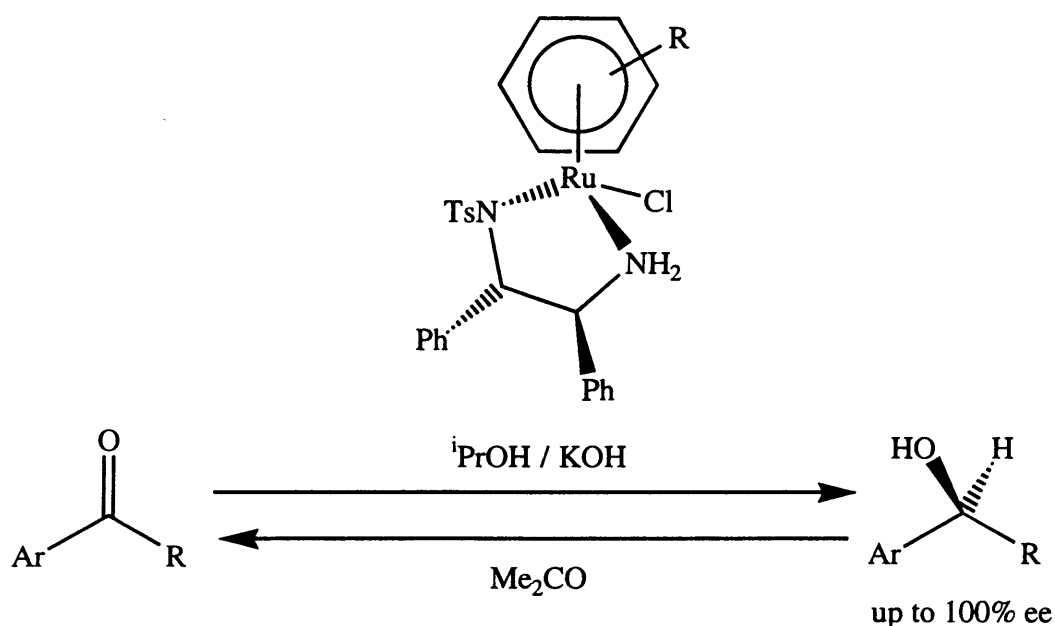
On formation, the diastereomer ratio (**2.18**):(**2.18'**) was found to be 2.7:1, whilst the ratio (**2.19**):(**2.19'**) was 2:1 (both determined by integration of ¹H NMR signals). In both cases, the major isomer could be crystallised, enabling study by X-ray diffraction. The solid-state structures of (**2.18**) and (**2.19**) are somewhat different to those of the analogous complexes (**2.12**, **2.13** and **2.17**); for (**2.18**) and (**2.19**), no β-phenyl effect is found, perhaps because the arene is mesitylene, for which the methyl substituents might inhibit the β-phenyl interaction. For both structures, the C-Me bond (at the C chiral centre) is the substituent that is oriented most towards the chloride. This may be because there is less steric hindrance between the methyl and the chloride for a five-membered chelate ring than in the six-membered ring found in complexes of salicylaldiminato ligands.^{94, 95} This factor might explain the inherently lower diastereoselectivity in the formation of (**2.17** - **2.19**) than that in (**2.12/2.13**).

On dissolution of the crystallised samples of (**2.18**) and (**2.19**) in CDCl₃, a small amount (< 5%) of the minor isomer was observed by ¹H NMR; the ratio of isomers was then essentially unchanged, even after 2-3 days. The ¹H NMR spectra of the mother liquors, in CDCl₃, showed a very different isomer ratio, enriched in the more soluble isomer. Again, the ratio did not change significantly after several days, which suggests that for complexes (**2.18**) and (**2.19**), interconversion of diastereomers is relatively slow, even on a chemical timescale, in CDCl₃.

When crystals of (**2.18**) were dissolved in D₂O, signals due to four species were observed in the ¹H NMR spectrum. These were assigned to diastereomeric pairs of chloro- and D₂O-coordinated complexes, similar to those observed in amino-acidate complexes discussed earlier. When excess NaCl was added to the spectrum, the signals due to the D₂O-coordinated complex disappeared. The ratio of diastereomers (**2.18**):(**2.18'**) changed slowly over time, the equilibrium ratio (1.2:1) only being obtained after many days. It seems likely that epimerisation at the metal centre occurs via exchange in the labile aqua complexes, as observed for amino-acidate complexes.^{68, 88}

To summarise, for arene-ruthenium Schiff-base complexes, it is clear that moving from anionic N,O and N,N donors to neutral N,N-donor ligands, epimerisation at the metal centre becomes less rapid. The inherent diastereoselectivity of forming some of the complexes is not great, however, which might limit their application in asymmetric synthesis. The most diastereoselective complexes were found to be those with salicylaldimine, but these suffer the potential problem of rapid epimerisation in solution. To obtain the best results in asymmetric synthesis with diastereomeric chiral-at-metal complexes, it would be desirable to form a single isomer, which did not epimerise in solution. Significant asymmetric induction might then be obtained in catalytic (or stoichiometric) reactions using this complex. To obtain a more configurationally stable complex, a neutral N,N'-donor set and an overall charge on the complex might be important.

The most impressive examples of using chiral half-sandwich complexes in asymmetric catalysis are Noyori's transfer hydrogenation catalysts, which use N-donor ligands and promote the reaction of an unsymmetrical ketone (or imine) with a hydrogen source, such as 2-propanol, to give secondary alkenes (or amines) with very high enantioselectivity (*ees* of up to 100% being obtained).¹⁰¹ The precursors for the active catalysts are complexes of the type [RuCl(TsDPEN)(arene)] (**Scheme 2.10**). Only the (S)-isomer is found by X-ray diffraction and NMR.¹⁰² The transfer hydrogenation reaction is reversible and Noyori's catalysts exploit this fact, in some cases, to selectively convert the minor enantiomer of alcohol product back to starting ketone, thus giving very high yields and *ees* (a kinetic resolution effect).



Scheme (2.10)

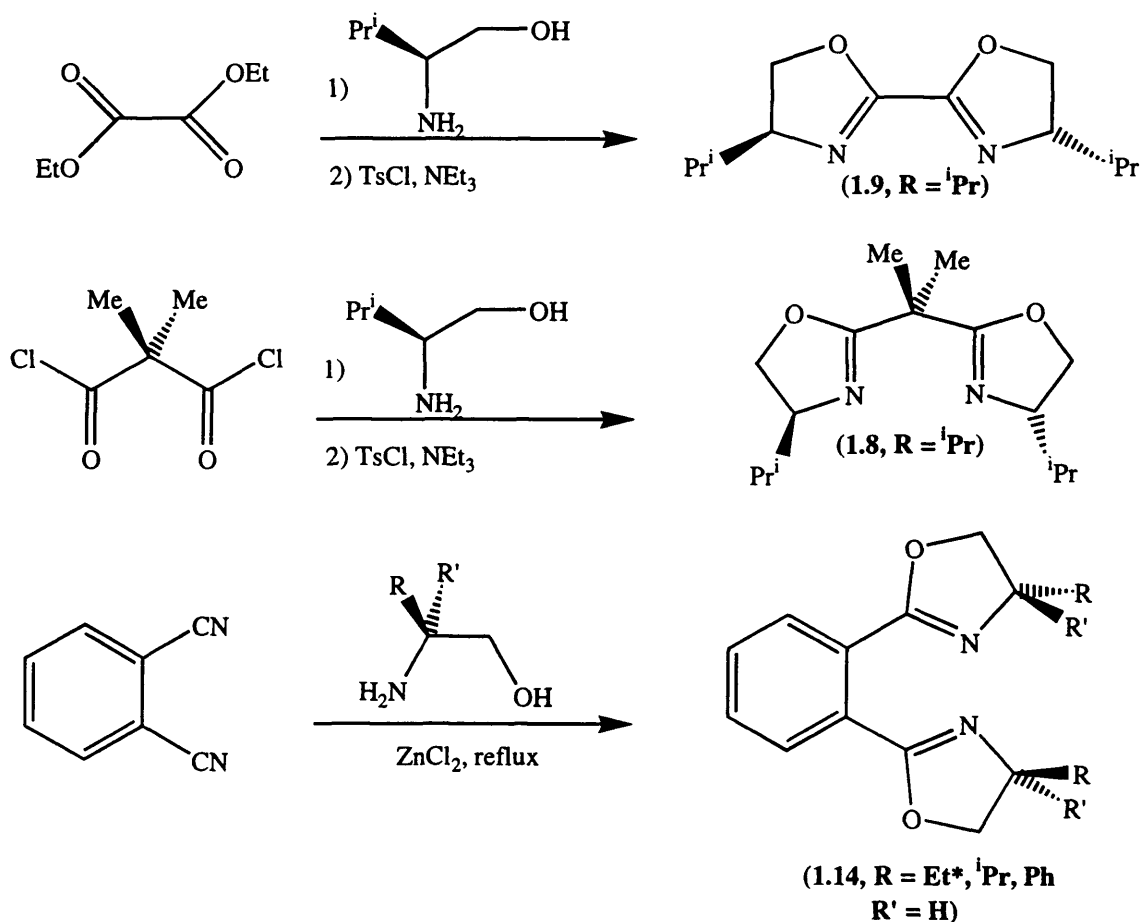
Noyori's catalysts illustrate that highly asymmetric catalytic systems can be obtained with chiral half-sandwich complexes and also that nitrogen-donor ligands can give good results in these systems. As explained in Chapter One, oxazoline ligands have been used to great effect in numerous asymmetric catalytic reactions, but in most cases, the active catalyst has been formed *in situ* and has not been characterised. The incorporation of oxazoline ligands in half-sandwich complexes should allow for easy characterisation and give a rigid environment for use in asymmetric catalysis. Some of the oxazoline ligands discussed in Chapter One are analogous (in terms of donor type and ring size) to the Schiff-base ligands discussed earlier in this section (notably the unsymmetrical pymox and phenmox ligands), so comparisons of the behaviour of corresponding oxazoline complexes to those described in this introduction will be relevant.

Shortly after the commencement of this work, there was one publication reporting the synthesis of arene-ruthenium oxazoline complexes, in which the C_2 -symmetric ligand (R)-Ph-bop was used as a chiral auxiliary to study diastereoselective exchange of N-H groups of amines coordinated to a ruthenium centre.¹⁰³ The synthesis and behaviour of $[\text{RuCl}\{(\text{R})\text{-Ph-bop}\}(\text{arene})]\text{BF}_4$ and its derivatives will be discussed in more detail in the Results and Discussion section, to follow.

(2.2) - Results And Discussion

(2.2.1) - Complexes of C₂-symmetric Bis-Oxazolines

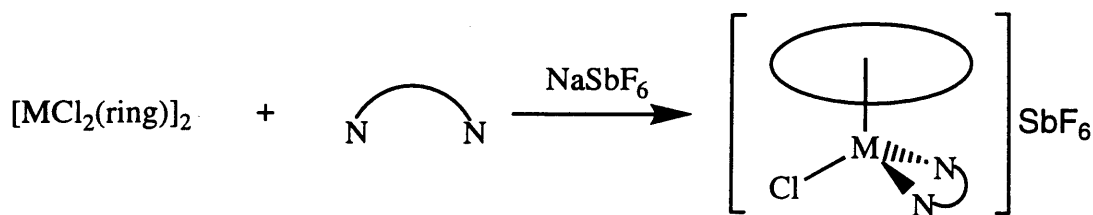
The ligands ⁱPr-box (1.9, R = ⁱPr), ⁱPr-bop (1.8, R = ⁱPr) and 1,2-benbox (1.14, R = Et, ⁱPr, Ph) were synthesised according to literature procedures (Scheme 2.11), or modifications thereof. Thus, ⁱPr-box was synthesised from diethyl oxalate and (L)-valinol, by the method of Pfaltz,³⁴ whilst ⁱPr-bop was prepared according to the method of Denmark (method (c) - see Chapter 1).²¹ Benbox ligands were synthesised by the method of Bolm (the ZnCl₂-catalysed reaction of amino alcohol with dicyanobenzene).¹⁹ The new ligand (1.14, R' = Et) was prepared in 89% yield.



Scheme (2.11)

* For R = Et, the configuration was (R), i.e. R = H, R' = Et

Complexes [MCl(N-N)(ring)]SbF₆ (M = Ru, Rh, Ir; N-N = bop, box, benbox; ring = arene, Cp*; X = SbF₆, PF₆: 2.20-2.29, see Table 2.1) were synthesised in high yield by treatment of [MCl₂(ring)]₂ with two equivalents of bis-oxazoline ligand (N-N) and NaSbF₆ in refluxing methanol (Scheme 2.12). The presence of the large anion SbF₆⁻ allowed for ready crystallisation of the half-sandwich complexes.



Scheme (2.12)

(2.20 - 2.29)

Table (2.1) - Complexes [MCl(N-N)(ring)]SbF₆

Code Number	M	ring	N-N
2.20	Ru	mes	ⁱ Pr-box
2.21	Rh	Cp*	ⁱ Pr-box
2.22	Ru	mes	ⁱ Pr-bop
2.23	Rh	Cp*	ⁱ Pr-bop
2.24	Ir	Cp*	ⁱ Pr-bop
2.25	Ru	C ₆ H ₆	ⁱ Pr-benbox
2.26	Ru	<i>p</i> -cy	benbox, R = Et, ⁱ Pr
2.27	Ru	mes	benbox, R = Et, ⁱ Pr, Ph
2.28	Rh	Cp*	benbox, R = Et, ⁱ Pr, Ph
2.29	Ir	Cp*	ⁱ Pr-benbox

Complexes (2.20 - 2.29) were characterised by ¹H NMR, mass spectrometry, elemental analysis (Tables 2A.2 - 2A.4, see Experimental) and, where possible, X-ray diffraction. The complexes are chiral-at-ligand only, not at metal, so only one half-sandwich structure is possible for each species. The free bis-oxazoline ligands are C₂-symmetric, but on formation of (2.20 - 2.29), the symmetry is destroyed and the ¹H NMR spectra become more complex as a result. The spectra of ⁱPr-box complexes (2.20) and (2.21) were obtained in CDCl₃ (Table 2A.2). On complexation, each oxazoline ring proton becomes inequivalent, signals being observed in the range 5.15-4.26 ppm, a 'downfield' shift of up to 1 ppm, compared to free ligand {for which, multiplets are observed at δ 4.44 (2H) and 4.10 (4H)}. The CHMe₂ protons also become inequivalent {δ 2.14 and 2.54 for 2.20 and 2.13 and 2.38 for 2.21} and are similarly deshielded, relative to free ligand (2H multiplet observed at δ 1.84). For each complex, four 3H doublets are observed for the CHMe₂ groups in the range δ 1.10 - 0.74. Singlets due to the mesitylene ring of (2.20) are observed at δ 2.32

($C_6H_3Me_3$) and 5.67 ($C_6H_3Me_3$) whilst the Cp^* group of (2.21) gives rise to a 15H singlet at δ 1.78.

Crystals of the rhodium complex (2.21) were obtained (suitable for X-ray diffraction) by crystallisation from CH_2Cl_2 /ether. The structure of the cation is shown in **Figure (2.9)** and selected bond distances and angles are given in **Table (2.2)**.

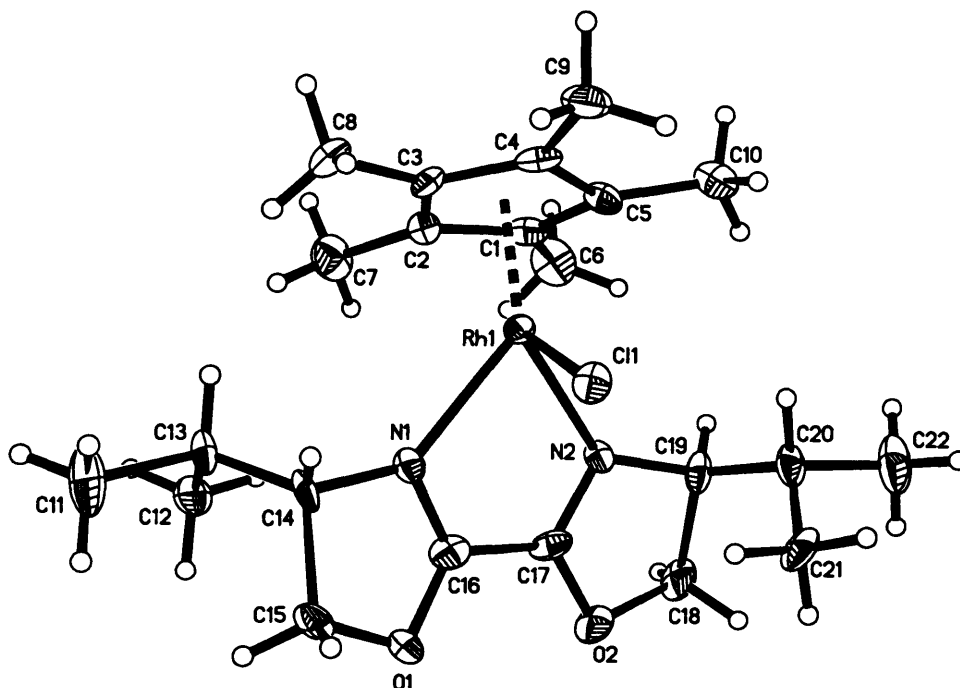


Figure (2.9): X-ray structure of the cation of (2.21)

Table (2.2) - Selected Bond Distances (Å) and Angles (°) of (2.21)

Rh–N(1)	2.178(11)	N(2)–Rh–N(1)	75.3(4)
Rh–N(2)	2.115(10)	N(1)–Rh–Cl	82.2(3)
Rh–Cl	2.388(4)	N(2)–Rh–Cl	88.2(3)

Complex (2.21) adopts the expected pseudo-octahedral structure, with only the N(1)–Rh–N(2) chelate angle {75.3(4)°} being significantly lower than the 90° expected for an octahedron. The Rh–N(2) distance of {2.115(10)Å} is slightly shorter than the Rh–N(1) bond length {2.178(11)Å}, possibly because the isopropyl group on C(14) interacts with the Cp^* ring preventing closer approach of N(1) to the rhodium centre.

Unsurprisingly, the 1Pr -bop complexes (2.22 - 2.24) have similar spectroscopic characteristics to the analogous (2.20) and (2.21). Crystals of the rhodium complex (2.23) were obtained that were suitable for X-ray crystallography. The molecular

structure of the cation is shown in **Figure (2.10)** and selected bond distances and angles are given in **Table (2.3)**.

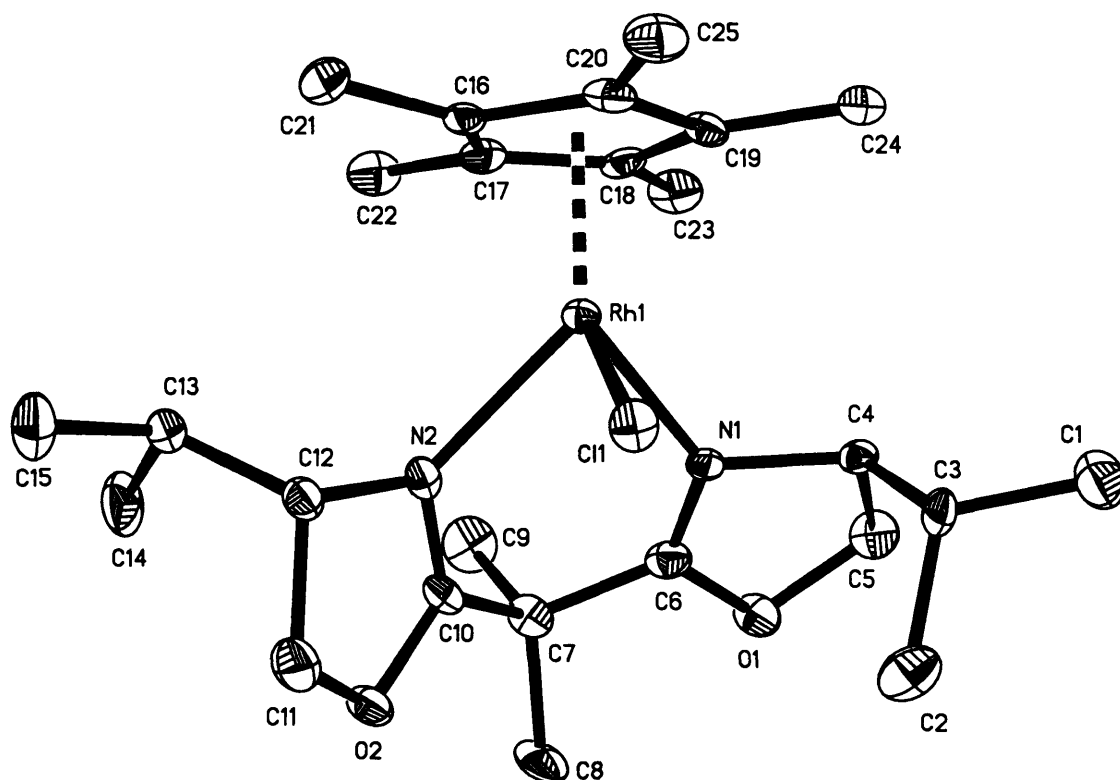


Figure (2.10): X-ray structure of the cation of (2.23)

Table (2.3) - Selected Bond Distances (Å) and Angles (°) of (2.23)

Rh–N(1)	2.117(6)	N(2)–Rh–N(1)	84.0(2)
Rh–N(2)	2.157(6)	N(1)–Rh–Cl	90.2(2)
Rh–Cl	2.406(2)	N(2)–Rh–Cl	82.1(2)

As with the structure of **(2.21)**, **(2.23)** adopts a pseudo-octahedral geometry. The Rh–N(1) distance is again slightly shorter than the Rh–N(2) bond length, but not quite as much as for **(2.21)**. The N(2)–Rh–N(1) chelate bite angle of 84.0(2)° is larger than that for the box analogue **(2.21)** {75.3(4)°}, which is expected because of the larger chelate ring (six-membered rather than five-membered in **2.21**).

The ¹H NMR spectra (**Table 2A.2**) of **(2.22 - 2.24)** were obtained in CDCl₃, and exhibit many common features with the spectra of **(2.20)** and **(2.21)**. Again, the signals due to the oxazolinyl ring and CHMe₂ protons (*i.e.* those closest to the metal centre) are observed at higher frequency than those of the free ⁱPr-bop ligand. The OCH and NCH signals generally give rise to complex multiplets, in the range δ 4.70 -

4.18 (compared to those of the free ligand: δ 4.23 and 4.00). The signals assigned to CMe_2 backbone are found in the range δ 1.66 - 1.38, as pairs of 3H singlets (in the free ligand a 6H singlet is observed at δ 1.51), whilst four 3H doublets are found for the $CHMe_2$ groups in the range δ 1.04 - 0.55, for each complex.

Benbox complexes (2.25 - 2.29) were characterised in the same way as (2.20 - 2.24). Crystals of $[RuCl(Et\text{-benbox})(p\text{-cy})]PF_6$ (2.26a, R = Et) were obtained that were suitable for X-ray crystallography (it should be noted that the configurations at the carbon chiral centres are (R) for this ligand, rather than (S), which is usually the case). The X-ray structure of the cation is shown in Figure (2.11) and selected bond distances and angles are shown in Table (2.4).

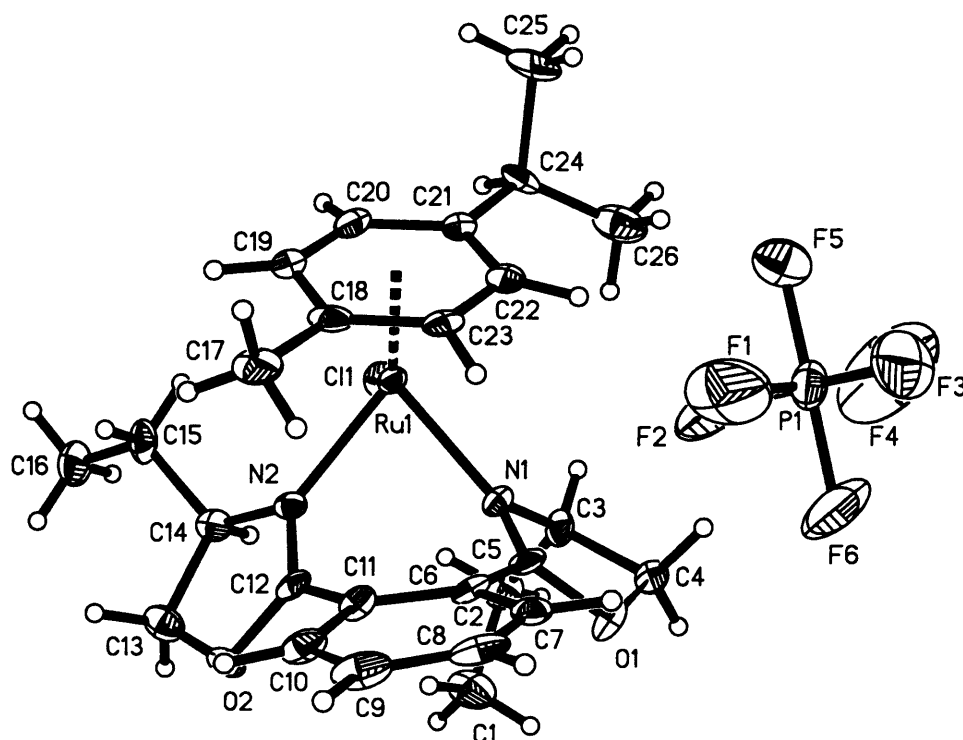


Figure (2.11): X-ray structure of complex (2.26a, R = Et)

Table 2.4 : Selected bond lengths (Å) and angles (°) of complex (2.26a, R = Et)

Ru(1)–N(1)	2.127(8)	Ru(1)–N(2)	2.119(9)
Ru(1)–Cl(1)	2.403(3)	N(1)–Ru(1)–N(2)	80.2(4)
N(1)–Ru(1)–Cl(1)	88.1(2)	N(2)–Ru(1)–Cl(1)	88.6(3)

The most striking feature of the structure is that the oxazoline rings must rotate out of the plane of the benzene ring in order to coordinate to the metal centre, which results in a larger N(1)–Ru(1)–N(2) bite angle {80.2(4)°} than if the ligand were

planar. The angles of rotation out of the plane are 45.2° (for the oxazoline ring with Et oriented towards arene) and 48.3° (for the oxazoline ring with Et oriented towards chloride). As a consequence, one ethyl substituent is brought nearer to the chloride ligand than would be expected (if the ligand was planar), whilst the other ethyl is correspondingly further away from the arene ligand. The resultant Ru–N bond distances {2.127(8) and 2.119(9)} are statistically the same, unlike the M–N distances in the structures of (2.21) and (2.23), in which steric interactions between an isopropyl substituent and the Cp* ligand appear to influence a Rh–N bond distance.

Crystals of the analogous complex $[\text{RhCl}(\text{Et-Benbox})\text{Cp}^*]\text{PF}_6$ (2.28a, R = Et) were obtained, that were again suitable for X-ray crystallography. The X-ray structure of the cation of (2.28a, R = Et) is shown in Figure (2.12) and selected bond lengths and angles are shown in Table (2.5).

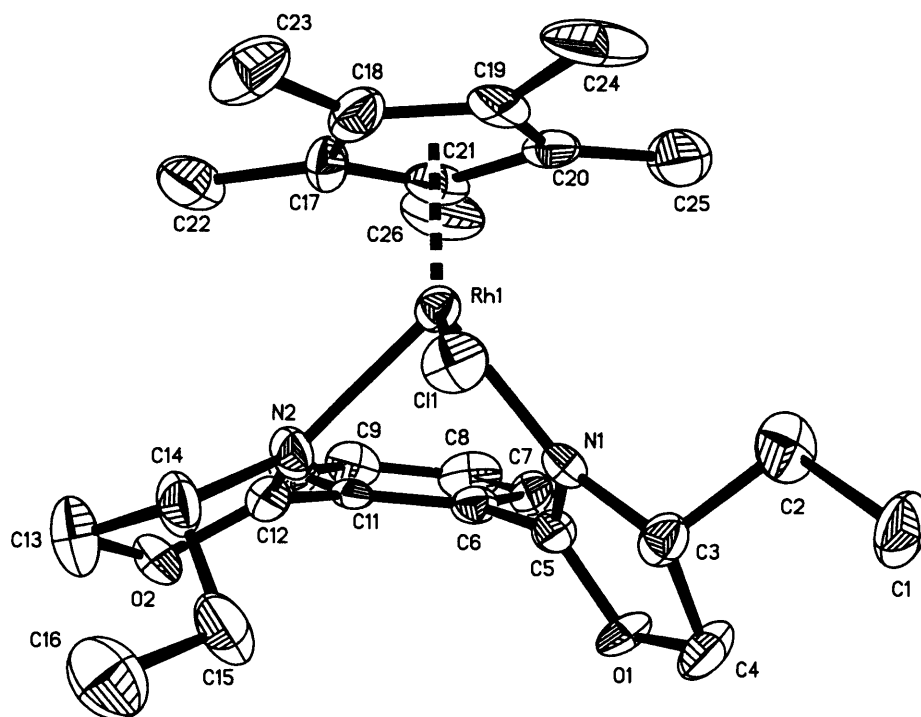


Figure (2.12): X-ray structure of the cation of (2.28a, R = Et)

Table (2.5) : Selected Bond lengths (Å) and angles ($^\circ$) of (2.28a, R = Et)

Rh–N(1)	2.111(13)	N(2)–Rh–N(1)	83.0(5)
Rh–N(2)	2.102(14)	N(1)–Rh–Cl	89.4(3)
Rh–Cl	2.409(4)	N(2)–Rh–Cl	91.2(4)

The complex, again, adopts a pseudo-octahedral structure, with both the N(1)–Rh–Cl (89.4°) and the N(2)–Rh–Cl (91.2°) angles being very close to the 90° expected for an octahedral complex. As for the analogous ruthenium complex (**2.26a**, R = Et), the oxazoline rings of benbox are tilted out of the plane of the benzene ring when chelated to the rhodium, such that the N(2)–Rh–N(1) chelate angle is 83.0(5)°, very similar to that of the analogous ⁱPr-bop complex (**2.23**), which has a six-membered chelate ring.

Complexes (**2.25 - 2.29**), containing chiral benbox ligands, were characterised by ¹H NMR in CDCl₃ (**Table 2A.3**). In general, the signals due to OCH, NCH (δ 4 -5) and benzene backbone (δ 7.6 - 8.2) protons of the benbox ligand (*i.e.* those closest to the metal centre) are moved to higher frequency, by up to 0.5 ppm compared to free ligand, on coordination. The effect of coordination upon signals due to the R-substituents varies with each complex. Where R = ⁱPr, four doublets are observed for the CHMe₂ groups and as found for complexes (**2.20 - 2.24**), one of the doublets is shifted upfield by *ca.* 0.5 ppm (to δ 0.47) compared to free ligand. In contrast, the CHMe₂ protons (δ 2 - 3) are deshielded on coordination, signals moving to higher frequency by up to 1 ppm.

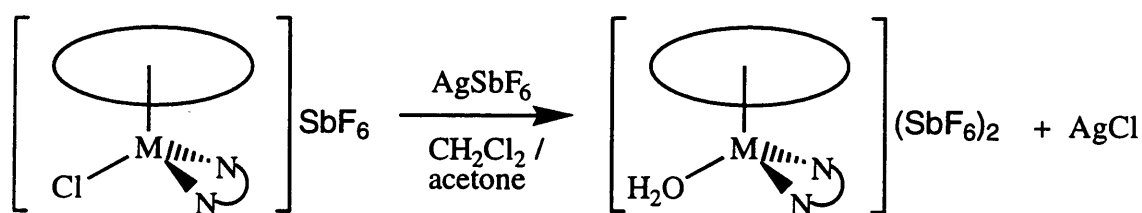
The ¹H NMR signals for the η⁵ or η⁶ ligands are sensitive to the substituents R. Thus, for the rhodium and iridium complexes (**2.28-2.29**) when R = alkyl, the Cp* singlet appears at *ca.* δ 1.3, but when R = Ph, the singlets are found at δ 1.0. Similar effects are seen in the arene-ruthenium complexes (**2.25 - 2.27**), *e.g.* the aryl signals for (**2.27**, R = ⁱPr) are observed at δ 1.95 and 4.8 whilst those for (**2.27**, R = Ph) are found at δ 1.7 and 4.1. A difference in chemical shift of up to 0.7 ppm is unlikely to be due to the relative electron donor properties of phenyls and alkyls. The fact that the arene ligands are *more* shielded in the Ph-benbox complexes suggests that a ring current effect is operating; presumably the protons on the arene ligand are brought close to one of the phenyl substituents on the benbox ligand, and are hence shielded by the aromatic ring current (a β-phenyl-effect).

Comparing the chemical shifts of the mesitylene signals of (**2.27**, R = ⁱPr) {δ 1.9 (C₆H₃Me₃) and 4.8 (C₆H₃Me₃)} with those of the analogous bop complex (**2.23**) (δ 2.3 and 5.75) and the box complex (**2.20**) (δ 2.32 and 5.67), a substantial difference is found. A difference in shift of up to 1 ppm between corresponding signals is most unlikely to be due to the relative electron donor properties of the benbox, box and bop

ligands. Indeed, comparison of the X-ray crystal structures of (2.21), (2.23, **R** = *i*Pr) and (2.28, **R** = Et) shows that all of the Ru - N bond distances are of the order of 2.10 Å, which means that the difference in bond strength is minimal. The cause of the differences in chemical shift between the various complexes is most likely another ring current effect, this time between the benzene ring backbone of benbox and the arene. The protons on the π -bound ring are presumably close enough to the benzene ring of the ligand to be shielded by the π -aromatic cloud. For confirmation, a 2D NOESY experiment was performed on a sample of (2.27, **R** = *i*Pr) and, indeed, nOes are observed between the two mesitylene signals and all three multiplets ($2 \times 1\text{H}$ and $1 \times 2\text{H}$) assigned to the benzene backbone protons. Interestingly, the experiment also shows that the two highest frequency doublets at δ 1.12 and 0.97 are due to the CHMe_2 methyls oriented towards the η^6 -arene, which indicates that the lowest frequency *MeCHMe*' signal (δ 0.47) is not due to a methyl group shielded by a ring current from the mesitylene ring. Smaller, but still significant, differences in chemical shift are observed between the Cp* signals of (2.28 / 2.29, **R** = *i*Pr) (δ 1.3) and those of (2.21) (δ 1.78) and (2.23 / 2.24) (δ 1.7).

Complexes (2.20 - 2.29) were also characterised by mass spectrometry, using Fast Atom Bombardment (FAB) and Electrospray (ES) techniques (Table 2A.4). In all cases, the major ion pattern was due to the molecular ion $[\text{MCl}(\text{N-N})(\text{ring})]^+$, with minor ion patterns also observed due to loss of HCl from the molecular ion and loss of the bis-oxazoline ligand to give $[\text{MCl}(\text{ring})]^+$, the latter particularly being the case with the rhodium and iridium complexes. Of the three bis-oxazolines used, the box ligand was more readily lost in both FAB and ES spectrometry, but whether this has any bearing on the relative stability of the complexes is unclear.

To activate (2.20 - 2.29) for use in asymmetric catalysis it is necessary to remove the strongly-bound chloride ligand. This was done by treatment with AgSbF_6 in CH_2Cl_2 / acetone to give a precipitate of AgCl and the aqua complexes $[\text{M}(\text{OH}_2)(\text{N-N})(\text{ring})](\text{SbF}_6)_2$ (2.30 - 2.37), as shown in Scheme (2.13) and Table (2.6).



Scheme (2.13) (2.30 - 2.37, see Table 2.6)

Table (2.6) - Complexes $[M(OH_2)(N-N)(ring)](SbF_6)_2$

Code Number	M	ring	N-N
2.30	Ru	mes	ⁱ Pr-box
2.31	Rh	Cp*	ⁱ Pr-box
2.32	Ru	mes	ⁱ Pr-bop
2.33	Rh	Cp*	ⁱ Pr-bop
2.34	Ru	C ₆ H ₆	ⁱ Pr-benbox
2.35	Ru	<i>p</i> -cy	ⁱ Pr-benbox
2.36	Ru	mes	benbox, R = Et, ⁱ Pr
2.37	Rh	Cp*	ⁱ Pr-benbox

The water ligand of (2.30 - 2.37) is obtained from the acetone solvent used in the syntheses of the complexes. Complexes (2.30 - 2.37) were characterised by mass spectrometry/elemental microanalysis (Table 2D.13), X-ray diffraction and, particularly, ¹H NMR (Tables 2D.2 - 2D.5) which was used to study the exchange phenomena found in many of the complexes. The ⁱPr-box complexes (2.30) and (2.31) behave rather differently in solution, as shown by ¹H NMR in d₆-acetone. The general appearance of the spectrum of (2.30) is much like that of the precursor (2.20), with the exception that some of the resonances are brought to higher frequency due to the formation of a dication (in particular, the oxazoline ring and CHMe₂ protons). The initial spectrum of (2.30) showed signals due to two ⁱPr-box containing species, in a 6:4 ratio. Only one 9H singlet was observed due to C₆H₃Me₃ protons, but two singlets were found for C₆H₃Me₃. The major set of box resonances were all somewhat broadened, whilst the peaks due to the minor species were all sharp. Addition of small aliquots of H₂O to the sample increased the proportion of the minor species and after eleven equivalents of water (based upon NMR integration) had been added, only this species could be observed. Thus, the minor set of signals can be assigned to the aqua complex (2.30), whilst the broad set of resonances is presumably due to a d₆-acetone

coordinated complex, which indicates that a large excess of a carbonyl ligand might be needed in order to displace water in this type of complex. At all stages, signals due to free water in solution (*ca.* δ 3) and coordinated water (*ca.* δ 7) could be observed as sharp singlets, which indicates that water exchange is slow, at least on the NMR timescale. Exchange of acetone, however, is clearly more rapid at room temperature. The coordinated water gives rise to a 2H singlet at δ 7.15 in the final water-containing NMR spectrum of (2.30), whereas in the initial spectra, two singlets in a 7:2 ratio were observed, at δ 6.94 and 6.97 (*i.e.* in the range for coordinated water), the minor signal disappearing on addition of excess H₂O. The identity of this second singlet will be discussed shortly.

The room temperature ¹H NMR spectrum of the rhodium complex (2.31) indicates that, in contrast to (2.30), exchange of coordinated and free water in this rhodium complex is rapid on the NMR timescale. No coordinated water signal is observed, whilst only a very broad resonance is seen for free water in solution. The rapid water exchange also allows time-averaging of the signals due to the box ligand to occur; thus only two 6H doublets are observed for the CHMe₂ groups, whilst a broad 2H multiplet is found for the CHMe₂ protons. At lower temperatures, all of the box signals begin to resolve into their expected multiplicities. At 273 K, most signals are close to coalescence and by 223 K, the expected sharp set of resonances is observed, with four 3H doublets and two 1H multiplets found for the CHMe₂ groups. Free water is now observed as a sharp singlet at δ 3.87, whilst the coordinated water region of the spectrum contains two singlets (δ 7.00 and 7.04) in an 11:2 ratio, analogous to those observed for (2.30).

The variable temperature NMR spectra above can be explained by an interconversion between species A and B, as shown in Figure (2.13), via a 16 electron intermediate (formed due to loss of water). Although A and B are structurally identical, each individual proton of the bis-oxazoline ligand will be in a different environment in each of A and B. Thus, if the interconversion is fast, time-averaging of ¹H NMR signals is expected. It should be noted that the interconversion described below relies on *aqua* exchange (*i.e.* loss of H₂O as a whole). Another type of process involving water ligands is *proton* exchange, in which the oxygen atom of water remains bound to the metal centre. The latter process may be faster than *aqua*

exchange and probably explains some of the broadness of the coordinated and free water signals in the NMR spectra of the half-sandwich complexes.

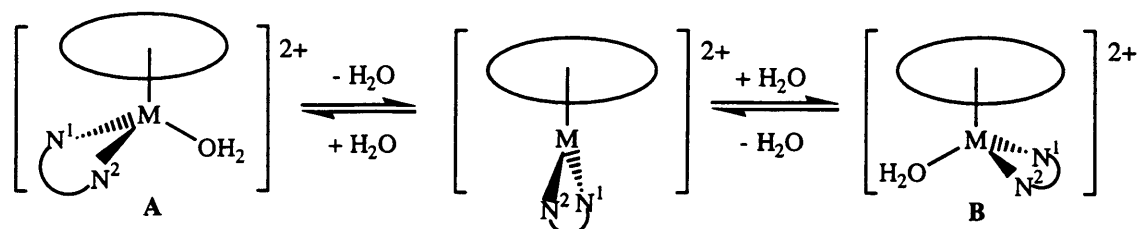


Figure (2.13)

This exchange process also occurs in the analogous ¹Pr-bop complexes (2.32 / 2.33). For the rhodium complex (2.33), the ¹H NMR spectrum in d₆-acetone (at 300 K) indicates that the exchange is very fast, as the signals due to the bop ligand are consistent with a C₂-symmetric system, *e.g.* two 6H doublets are found for the CHMe₂ groups and a 6H singlet for the CMe₂ group. A very broad resonance is found at δ 3.5 - 3.9, due to time-averaging of exchanging coordinated and free water signals. As the temperature is lowered, the signals slowly resolve to give the expected number of peaks, but even at 213 K, the resonances are still reasonably broad, indicating that the exchange process A ⇌ B is considerably faster for (2.33) than for (2.31).

Exchange of the ruthenium analogue (2.32) is also rapid at 300 K, but slower than for (2.33), as many of the bop signals are close to coalescence point. At 233 K, all of the ¹H NMR signals of (2.32) are well resolved, those due to the bop ligand being much like the precursor (2.22), with the exception that the majority of the signals are more deshielded, due to formation of a dication. Free water is observed as a broad singlet at δ 3.61 with singlets due to coordinated water at δ 7.06 and 7.10 (1.5 equivalents, ratio 7:3). No second set of complex signals is observed, unlike in (2.30), which indicates that coordination of acetone is less favoured with the bop complexes. Similar fluxional behaviour has been observed for the analogous complex [Ru(OH₂)(Ph-bop)(C₆H₆)](BF₄)₂ (2.38), reported by Kurosawa *et al.*¹⁰³ the exchange processes being frozen out at 223K, with free and coordinated water signals observed by ¹H NMR at δ 6.60 and 3.57, respectively (*i.e.* consistent with the chemical shifts reported here).

Recrystallisation of samples of (2.32) from acetone/ether gave crystals that were suitable for an X-ray structure determination. The structure of the cation is shown in Figure (2.14) with selected bond distances and angles given in Table (2.7).

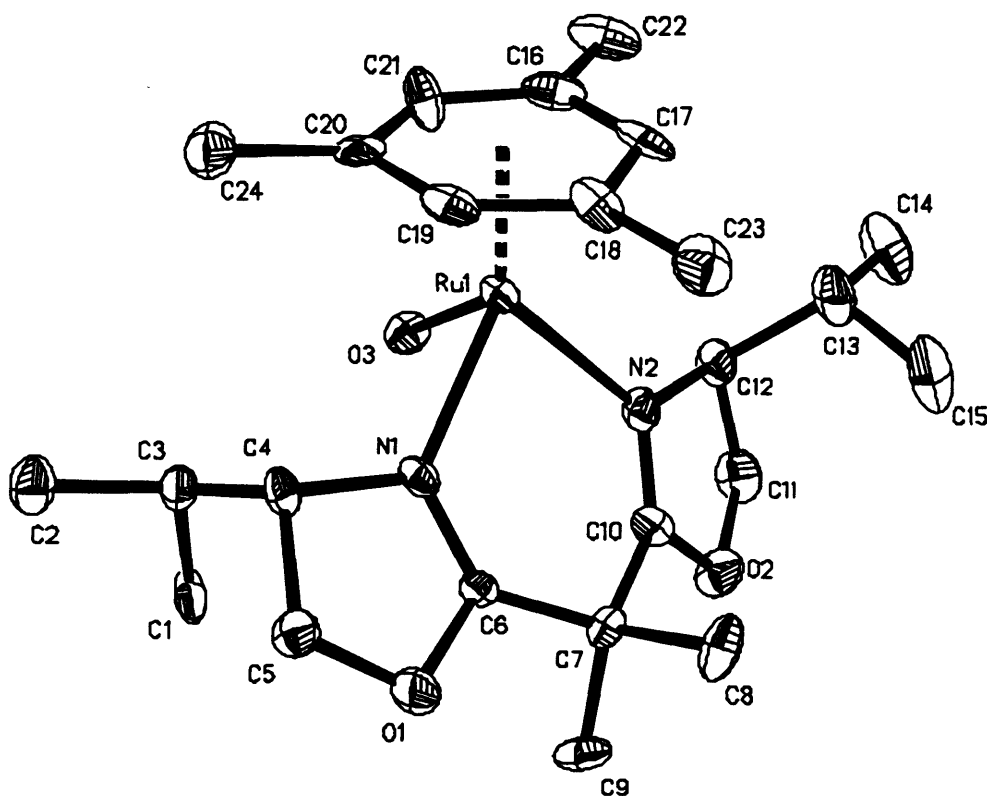


Figure (2.14): X-ray structure of the cation of (2.32)

Table (2.7) - Selected Bond Distances (Å) and Angles (°) of (2.32)

Ru(1)–N(1)	2.135(11)	N(1)–Ru(1)–N(2)	83.5(5)
Ru(1)–N(2)	2.153(12)	N(1)–Ru(1)–O(3)	85.1(4)
Ru(1)–O(3)	2.160(10)	N(2)–Ru(1)–O(3)	81.1(4)

The bond distances and angles reported in **Table (2.7)** resemble those for the X-ray structure of the known ruthenium analogue **(2.38)**.¹⁰³ The Ru–O(3) bond distances of **(2.32)** and **(2.38)** are statistically the same, and similar N(1)–M–N(2) chelate angles are found in each complex {N(1)–Ru–N(2) for **(2.38)** was 82.6(4)° vs. 83.5(5)° for **(2.32)**}. The Ru–N(1) and Ru–N(2) bond distances {2.135(11)° and 2.153(12)° respectively} are statistically the same, unlike the Rh–N distances of the ¹Pr-bop complex **(2.23)**, above {2.117(6)° and 2.157(6)°}.

The benbox complexes **(2.34 - 2.37)** were characterised by ¹H NMR in d₆-acetone (**Tables 2D.4 - 2D.5**). No ligand exchange process of the type A⇌B is observed with either ruthenium or rhodium complexes. In the spectrum of the rhodium complex **(2.37)** at 300K, sharp signals are observed for the Cp* ligand (δ 1.45) and all benbox protons, the latter giving rise to the expected number of signals

(e.g. four doublets found between δ 0.57 and 1.18 due to the $CHMe_2$ groups). At this temperature, however, a very broad resonance is found for exchanging free and coordinated water (ca. δ 3.5), but on cooling, both water signals begin to resolve. At 223K, sharp singlets are seen at δ 7.5 (coordinated water) and δ 3.9 (free water). The variable temperature results indicate that while exchange of water (either proton or aqua) is rapid on the NMR timescale for (2.37), the change in ligand orientation that leads to time-averaging of spectra in (2.31 - 2.33) is slow, probably due to the coordination geometry of the benbox ligand, shown in the X-ray structures. The oxazoline rings are forced to rotate significantly out of the plane of the benzene backbone in order to coordinate to the metal centre and this may make the interconversion $A \rightleftharpoons B$ energetically disfavoured (as the benzene ring would have to rotate *through* the plane of the oxazoline rings to allow the interconversion to occur, which would result in a planar ligand arrangement at some point; this would give an unfavourably small chelate angle with the metal).

The ruthenium complexes (2.34 - 2.36) behave much like their box analogue (2.30), as exchange of free and coordinated water is slow on the NMR timescale and, like (2.37), no time-averaging of signals is observed by 1H NMR. In addition, spectra in d_6 -acetone contain two sets of complex-containing signals. For (2.34), two singlets were observed due to $\eta^6-C_6H_6$ ligands, at δ 6.02 and 6.10 in a ratio 5:3, the sample containing two equivalents of free water. Addition of an extra seven equivalents of water to the sample increased the ratio of $\eta^6-C_6H_6$ signals to 10:1, which indicates that the major species is the desired aqua complex, whilst the minor species is assigned as an acetone-coordinated complex. Coordinated water gave rise to singlets at δ 7.56 and 7.63 (ratio 10:1) in the initial spectrum, with free water seen as a singlet at δ 3.14. On addition of excess water, the high frequency coordinated water signal disappeared.

The slow exchange of water found with (2.34) facilitates investigation of the minor singlet observed in the coordinated water region, found in the 1H NMR spectra of all complexes (2.30 - 2.37). This extra singlet is always observed to the high frequency side of the main coordinated water signal, in a region of the spectrum quite separate from any other ligand peaks. Addition of a large excess of H_2O to (2.34) results in the disappearance of the minor signal, whilst a D_2O shake results in the loss of both singlets, implying that both were due to coordinated water and that D_2O was

then the ligand at the sixth coordination site. Addition of aliquots of D₂O to a sample of (2.34) in d₆-acetone resulted in an increase in the proportion of the high frequency singlet, relative to its neighbour. Thus, when five equivalents of D₂O had been added to a sample already containing five equivalents of H₂O (relative to moles of complex), two singlets were observed in a 1:1 ratio at δ 7.76 and 7.84 (overall integration: 1 proton). These results are consistent with the high frequency signal being due to coordinated HOD, formed due to proton exchange between coordinated H₂O and free D₂O in solution.

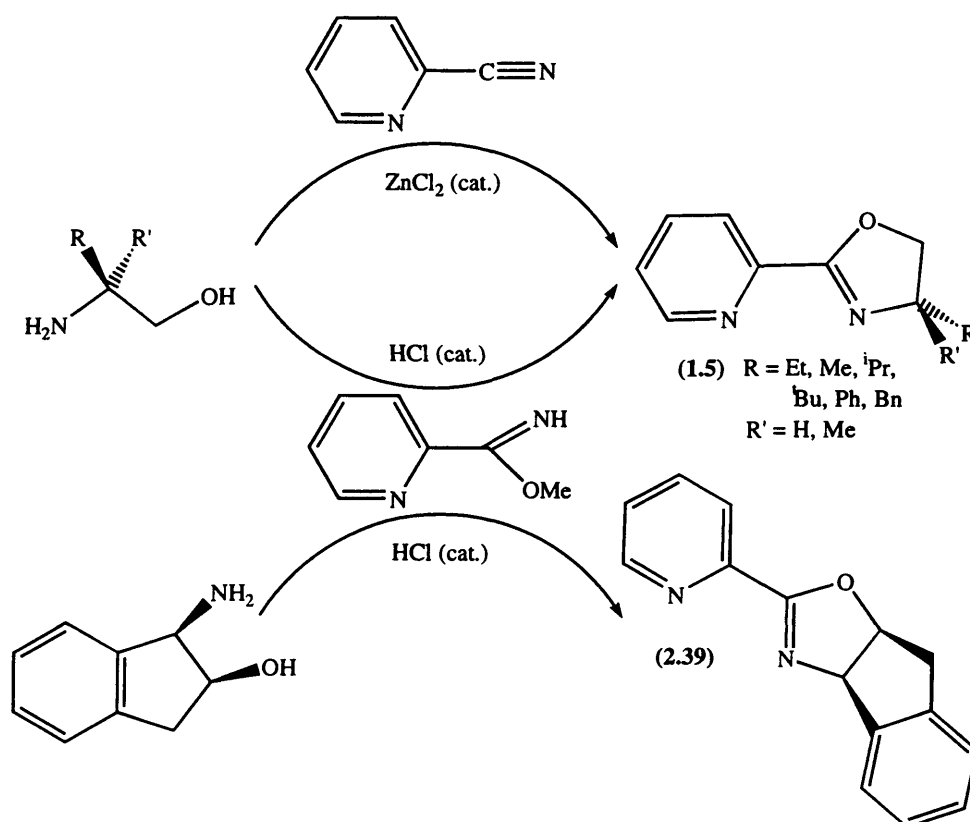
Transition metal aqua complexes are expected to be slightly acidic, so proton exchange is anticipated. For example, the pK_a of the cation [Ru(OH₂)(bipy)(C₆H₆)]²⁺ is 6.9, whilst that of the analogous [Rh(OH₂)(bipy)Cp*]²⁺ is 8.2.¹⁰⁴ Kurosawa has shown that treatment of the aqua complex (2.38) with bases such as NHEt₂ or NEt₃ results in deprotonation of the water ligand, giving the hydroxyl-species [Ru(OH)(Ph-bop)(C₆H₆)]⁺.¹⁰³ In contrast, treatment of (2.38) with less basic amines NH₂R leads to species [Ru(NH₂R)(Ph-bop)(C₆H₆)]⁺ (R = H, Me, Bu). The N-hydrogens of the amine complexes undergo exchange with deuterium in CD₃OD solution, analogously with the proton exchange observed with aqua ligands. Considering these observations, formation of HOD-coordinated complexes is therefore not surprising. The observation of the HOD signal to *high* frequency of the H₂O signal is unexpected, since deuterium isotope shifts should, in theory, be to *lower* frequency. There are, however, a number of examples where isotope shifts are to high frequency, for a variety of different nuclei (*e.g.* ¹H, ¹⁸O, ¹⁹F).^{105, 106} Hydrogen-bonding can have a significant effect on deuterium isotope shifts. In certain carbohydrate systems, for which extensive H-bonding systems operate, both low frequency deuterium shifts (O–H[⋯]O–D situation) and high frequency shifts (H–O[⋯]D situation) are observed by ¹H NMR, after selectively deuterating various OH substituents.¹⁰⁷ High-frequency deuterium shifts are also observed in the ¹⁹F NMR spectra of fluorinated compounds such as acetyl fluoride-d₃ (CD₃COF), in the order of 0.05 - 0.1ppm.¹⁰⁸ These results indicate that deuterium isotope shifts do not have to be to low frequency and support the proposition that the minor signals observed in the coordinated water region of the ¹H NMR spectra of (2.30 - 2.37) are due to HOD ligands. Hydrogen-bonding might be an important factor in determining the relative shifts of HOD and H₂O ligands; Kurosawa has suggested that several solvating acetone molecules will be strongly held in the

vacinity of the aqua ligand of (2.38) (in d_6 -acetone solution) and these could provide a mechanism for H-bonding.¹⁰³ Alternatively, D_2O or an SbF_6 anion might H-bond to the aqua ligands.

To summarise, the solution behaviour of the half-sandwich aqua complexes described above varies somewhat, depending on metal and ligand type. In all cases, exchange of water was, as expected, faster with rhodium than with ruthenium, aqua exchange allowing the box complex (2.31) and the bop complex (2.33) to undergo a ligand exchange process in solution. In a detailed study, Merbach has reported a series of rate constants (k_{ex}) for water exchange in various “(arene)Ru” and “Cp*Rh” aqua complexes.¹⁰⁴ In all cases, the values for rhodium complexes were several orders of magnitude higher than those for the corresponding ruthenium complexes. For example, $k_{ex} = 1.59 \times 10^3 \text{ s}^{-1}$ for water exchange in $[Rh(OH_2)(bipy)Cp^*]^{2+}$, whilst for $[Ru(OH_2)(bipy)(p\text{-cymene})]^{2+}$, $k_{ex} = 8.5 \times 10^{-2} \text{ s}^{-1}$ (these complexes are clearly analogous to the oxazoline complexes described here, for which similar rate constants might be expected). Interestingly, though, the introduction of bipyridyl to the complexes above leads to a considerable reduction in the rates of water exchange, relative to $[M(OH_2)_3(\text{ring})]^{2+}$ ($k_{ex} = 1.6 \times 10^5 \text{ s}^{-1}$ when $M = Rh$, ring = Cp* and 11.5 s^{-1} when $M = Ru$, ring = *p*-cymene).

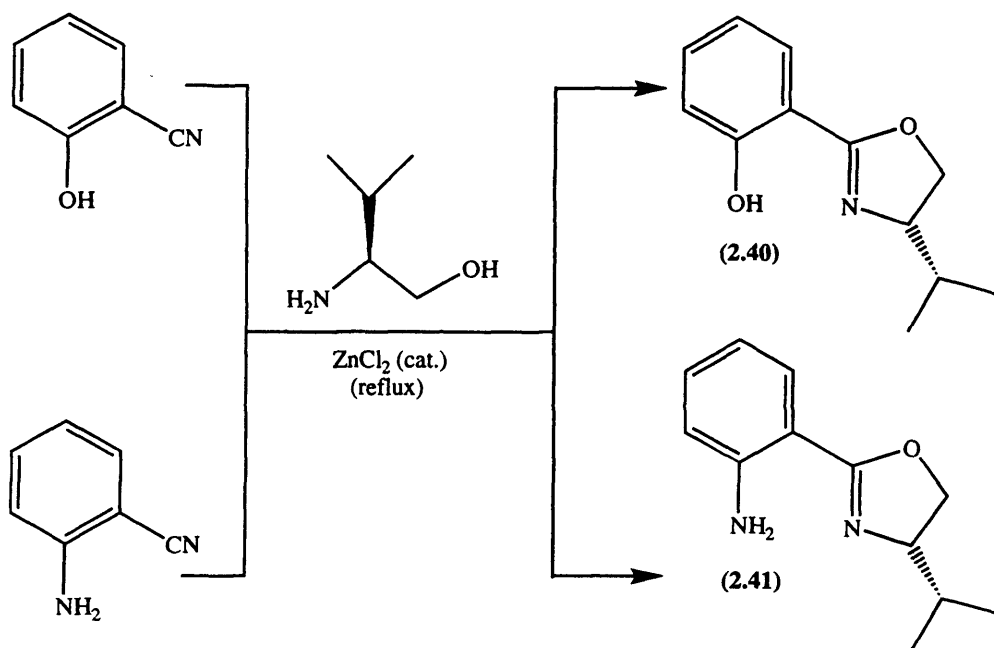
(2.2.2) - Half-Sandwich Complexes of Unsymmetrical Oxazoline Ligands

The ligands R,R'-pymox (**1.5**) were made by literature methods, either the imidate-based route devised by Brunner²⁶ or the ZnCl₂-catalysed preparation from 2-cyanopyridine, used by Bolm.¹⁹ The latter method is more convenient in some cases (e.g. R = ⁱPr), but the imidate method is more generally applicable, often giving higher yields (based on amino-alcohol, of which the ZnCl₂-method requires excess). The new ligand indanyl-pymox (**2.39**) was synthesised from 1-amino-2-indanol in 79% yield, according to Scheme (2.14).

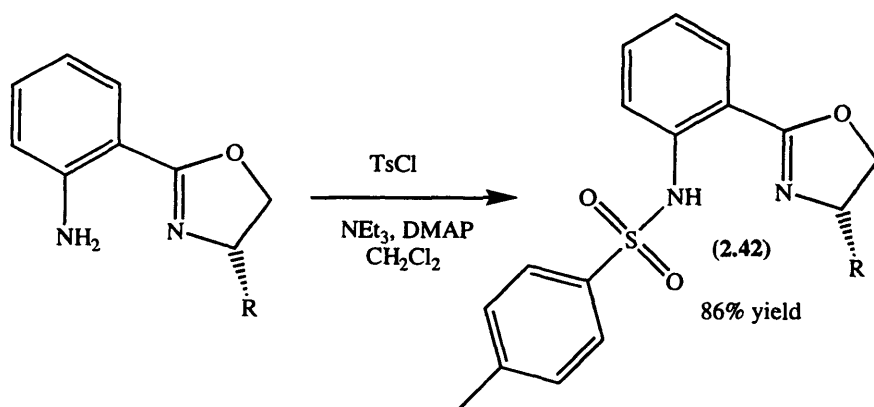


Scheme (2.14)

The ligands ⁱPr-phenmox (**2.40**) and ⁱPr-animox (**2.41**) were synthesised from L-valinol, and 2-hydroxy-benzonitrile or anthranilonitrile, respectively, according to the ZnCl₂-method of Bolm (Scheme 2.15).¹⁹ The ligand (**2.41**) was previously unreported and was synthesised in 60% yield. The new ligand ⁱPr-NTs-animox (**2.42**) was made by reaction of (**2.41**) with TsCl, catalysed by DMAP (Scheme 2.16), according to the method of Fujisawa.⁴⁷

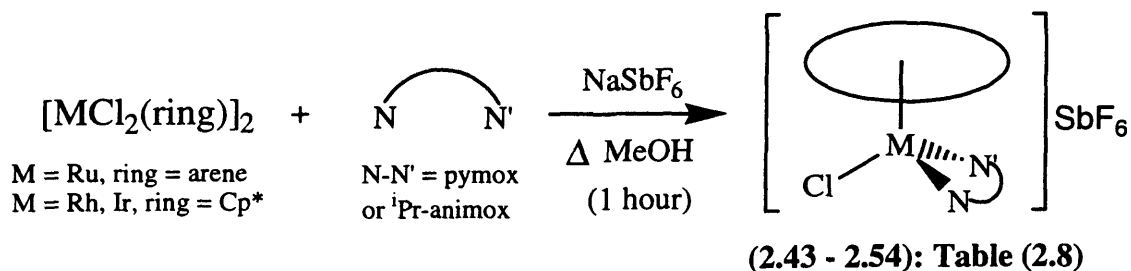


Scheme (2.15)



Scheme (2.16)

Half-sandwich complexes [MCl(N-N)(ring)]SbF₆ (2.43 - 2.54) containing the unsymmetrical oxazoline-containing ligands pymox (1.5/2.39) and ⁱPr-animox (2.41) were synthesised in high yield (78 - 96%) from the dimeric compounds [MCl₂(ring)]₂ (M = Ru, ring = arene; M = Rh or Ir, ring = Cp*), by treatment of the dimer with two equivalents of both ligand and NaSbF₆, in refluxing MeOH (Scheme 2.17).



Scheme (2.17)

Table (2.8): Complexes [MCl(N-N')(ring)]SbF₆

Code Number	M	ring	N-N'
2.43	Ru	C ₆ H ₆	pymox (R = ⁱ Pr, ^t Bu)
2.44	Ru	p-cymene	pymox (R = ⁱ Pr, ^t Bu)
2.45	Ru	mes	pymox (R = Et, ⁱ Pr, ^t Bu, Ph, Bn)
2.46	Ru	mes	Me ₂ -pymox
2.47	Ru	mes	Indanyl-pymox
2.48	Ru	C ₆ Me ₆	ⁱ Pr-pymox
2.49	Rh	Cp*	pymox (R = Et, ⁱ Pr, ^t Bu, Ph, Bn)
2.50	Rh	Cp*	Me ₂ -pymox
2.51	Rh	Cp*	Indanyl-pymox
2.52	Ir	Cp*	ⁱ Pr-pymox
2.53	Ru	mes	ⁱ Pr-animox
2.54	Rh	Cp*	ⁱ Pr-animox

Complexes (2.43 - 2.54) were characterised by ¹H NMR, mass spectrometry and microanalysis (Tables 2B.2 - 2B.9; see Experimental) and by X-ray diffraction where possible. In all of the complexes (2.43 - 2.54), the metal centre is chiral because of the unsymmetrical oxazoline ligands. For (2.46) and (2.50) (containing the achiral Me₂-pymox ligand), racemates are thus expected; however, for the remaining complexes the oxazoline ligand itself is chiral, so a mixture of diastereomers can theoretically be obtained, Figure (2.15).

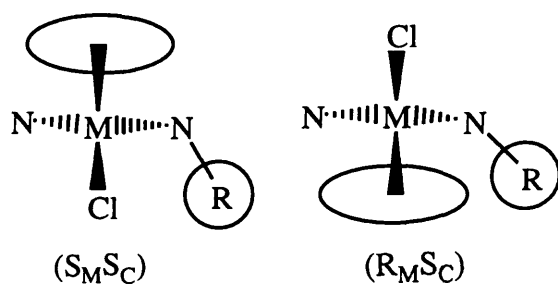


Figure (2.15)

In both isomers, the configuration about the carbon chiral centre of the oxazoline ligand is (S) so the (S_MS_C) and (R_MS_C) isomers correspond to switching the positions of the ring and chloride ligands. The diastereoselectivity of formation, *i.e.* the ratio of the two isomers, will thus depend on the sizes of the ring and R-substituents. If both

are large, the steric interactions between them in the ($R_M S_C$) isomer are expected to be significant; thus the ($S_M S_C$) isomer, in which the R-substituent points at the chloride, would be energetically preferred. For all complexes, the ratios of diastereomers formed were determined by 1H NMR (obtained initially of the crude reaction mixture, before recrystallisation), with X-ray crystallography and nOe experiments, used to confirm the configuration at the metal centre. The characterisation of the animox complexes (2.53 - 2.54) will follow shortly, but the discussion will begin with the complexes of pymox (2.43 - 2.52).

Pymox complexes (2.44) and (2.48) are soluble in $CDCl_3$ whilst (2.43, 2.45-2.52) are insoluble in $CDCl_3$ but are sparingly soluble in CD_2Cl_2 . The 1H NMR spectra (Tables 2B.2 - 2B.7) of the complexed ligands are significantly different from those of the free ligands. The signals due to the pyridine and oxazoline ring protons of the ruthenium complexes (2.43 - 2.48) are mostly shifted downfield (by 0.2 - 0.7 ppm), due to the ligand donating electron density to the metal, whilst for the rhodium and iridium complexes (2.49 - 2.52), the high frequency shift (0.1-0.3 ppm) is not as great. For the ruthenium complexes, singlets are observed at ca. δ 6 due to C_6H_6 in (2.43) and at δ 2.25 - 2.0 ($C_6H_3Me_3$) and δ 5.5 - 5.1 ($C_6H_3Me_3$) for complexes (2.45 - 2.47), whilst complexes (2.44) show the expected signals for the *p*-cymene, with inequivalent methyls of the iPr -group (ca. δ 1.0) and four doublets at δ 5.9 - 5.4 for Ar-H, as expected for a chiral complex. The 15H singlets due to the Cp* groups of complexes (2.49 - 2.52) are observed at δ 1.77 - 1.45. The spectra of the rhodium and iridium complexes of iPr -pymox (2.49 and 2.52) are essentially identical, apart from a slightly better separation of the OCH protons in the iridium complex. Where diastereomers are present, a second set of signals is observed.

The 1H NMR spectra of the Me_2 -pymox complexes (2.46 / 2.50) (in CD_2Cl_2) each show two singlets for the CMe_2 groups (δ 1.75 - 1.42) and two 1H doublets for the OCH_2 group (δ 4.66 - 4.44). This indicates that exchange of enantiomers is slow, at least on the NMR timescale (if exchange was faster than the NMR timescale, a time-averaged spectrum, with a 6H singlet for the CMe_2 group and a 2H singlet for the OCH_2 group, would result). Thus, if the enantiomeric pymox complexes (which are equal in energy) are not interconverting on the NMR timescale, then epimerisation of

the diastereomeric pymox complexes is expected to be slow (although the barrier to interconversion is not *necessarily* greater for the latter).

Signals due to pairs of diastereomers can readily be distinguished by ^1H NMR, particularly those due to arenes and the py-6-H. The relative integration of the two species gives the diastereomer ratio. The rhodium and iridium complexes (**2.49**, **2.51** - **2.54**) were all formed highly diastereoselectively; no trace of a minor isomer was observed by ^1H NMR, at any stage. It would appear that the steric hindrance which would result from orienting the R-substituents towards the Cp* ring is great enough to prevent this isomer being formed in the case of the chloride complexes.

With the ruthenium-pymox complexes, the diastereoselectivity depends on the size of the R-substituents and the arene ring, as expected. For example, the C_6H_6 and *p*-cymene complexes (**2.43/2.44**, $\text{R} = \text{}^i\text{Pr}$) were both formed as 50:50 mixtures of diastereomers, whilst with the bulkier arenes mesitylene and C_6Me_6 , the complexes (**2.45/2.48**, $\text{R} = \text{}^i\text{Pr}$) were formed highly diastereoselectively, no minor isomer being observed by ^1H NMR. Increasing the size of the R-substituent also increases the diastereoselectivity; thus, the C_6H_6 , *p*-cymene and mesitylene complexes (**2.43/2.44/2.45**, $\text{R} = \text{}^t\text{Bu}$) were all formed as apparently one isomer. All other ruthenium/pymox complexes were formed highly diastereoselectively, except for (**2.45**, $\text{R} = \text{Ph}$), which was obtained as a mixture of isomers (ratio 5:2) which gave the major isomer exclusively on crystallisation; this complex will be discussed in more detail shortly. For complexes giving 50:50 mixtures of diastereomers, attempts to separate them by crystallisation failed.

A crystal of complex (**2.45**, $\text{R} = \text{}^i\text{Pr}$) was obtained that was suitable for X-ray crystallography. The structure of the cation is shown in **Figure (2.16)**, with selected bond lengths and angles given in **Table (2.9)**. The complex adopts the expected pseudo-octahedral structure, with the pymox ligand coordinated such that the isopropyl group is pointing towards the Cl, instead of towards the mesitylene ring, thus minimising unfavourable steric interactions. The configuration at the ruthenium centre is (S), based on the priority arene > Cl > N_{ox} > N_{py} (the configuration at the chiral carbon in the ligand is also (S), as (S)-valinol was used in its synthesis).^{86, 87} The Ru–N(1) (oxazoline) and Ru–N(2) (pyridine) bond lengths are the same, suggesting that the oxazoline and pyridine rings have similar electron-donating properties.

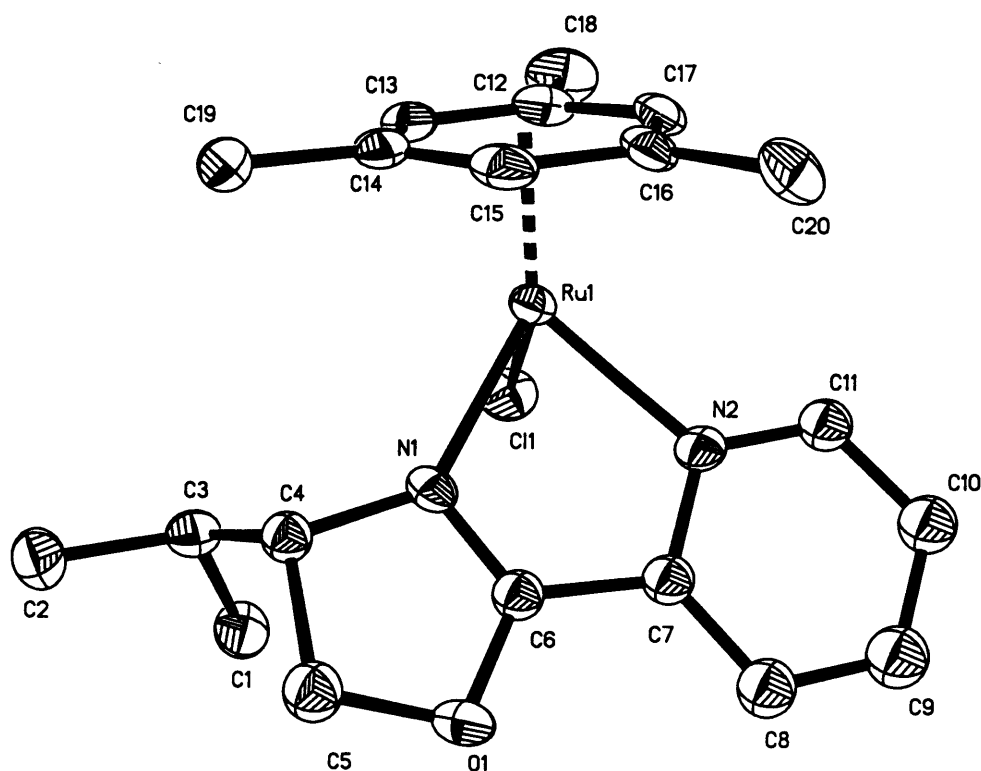


Figure (2.16): X-ray Structure of the cation (2.45, R = ⁱPr)

Table (2.9) - Selected Bond Distances (Å) and Bond Angles (°) of (2.45, R = ⁱPr)

Ru–N(1)	2.118(4)	N(2)–C(7)	1.351(7)
Ru–N(2)	2.117(4)	C(7)–C(6)	1.449(8)
Ru–Cl (1)	2.402(2)	C(6)–N(1)	1.280(7)
N(2)–Ru–N(1)	76.4(2)		

As signals due to only one isomer of (2.45, R = ⁱPr) were observed by ¹H NMR, it is assumed that the solid-state structure is retained in solution. Attempts to verify this by nOe experiments failed due to unfortunate overlap of NMR signals (in particular, the pymox NCH signal overlaps with an OCH peak, whilst the CHMe₂ signal is completely masked by the C₆H₃Me₃ singlet). Confirmation that a solid-state structure is retained in solution was found for the rhodium analogue (2.49, R = ⁱPr). The X-ray structure of the cation for this complex is shown in **Figure (2.17)**, whilst selected bond distances and an angle are given in **Table (2.10)**.

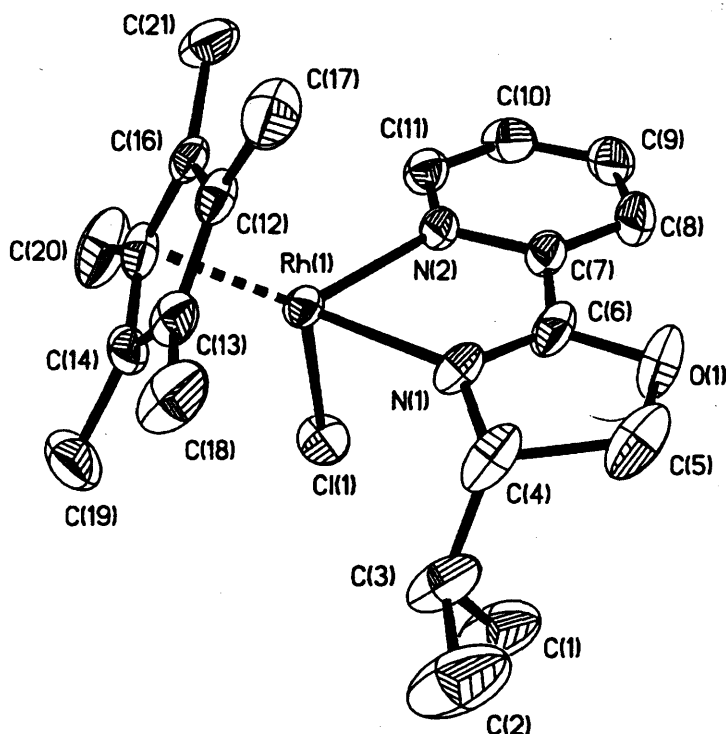


Figure (2.17): X-ray Structure of the cation of (2.49, R = *i*Pr)

Table (2.10): Selected bond distances (Å) and angles (°) of (2.49, R = *i*Pr)

Rh(1)–N(1)	2.109(4)	Rh(1)–Cl(1)	2.407(1)
Rh(1)–N(2)	2.142(4)	N(1)–Rh(1)–N(2)	76.0(2)

The structure is analogous to the arene-ruthenium complex above, with the isopropyl group pointing towards the chloride, rather than towards the Cp*, minimising unfavourable steric interactions. Interestingly, the Rh–N(1) (ox) bond distance is shorter than the Rh–N(2) (py) distance (unlike in the ruthenium complex), due to a lengthening of the latter distance {2.142(4) Å}.

To confirm that the solid-state structure of (2.49, R = *i*Pr) is retained in solution, a series of nOe experiments were performed (in CD₂Cl₂ at 400 MHz). Based on the crystal structure, the most likely nOe will be between the NCH proton and the methyls of the Cp*; if the other diastereomer was present, one might expect to see nOes between the isopropyl group and the Cp*. The experiments were carried out by irradiating separately at each signal below δ 5 in the ¹H NMR spectrum. Irradiation at the NCH gives a large nOe (relative integration 1.0) to the CHMe₂, which is bound to the adjacent carbon, and a smaller nOe (int. 0.12) to the Cp* methyls. Other nOes from the NCH are to one OCH (int. 0.3) and to a CHMe (int. 0.17). Irradiation at the

$CH(Me)_2$ or at $CH(Me)_2$ fails to give an nOe to the Cp^* (only through-bond interaction is observed). Irradiation at the Cp^* gives a weak nOe to the NCH proton, which provides quite good evidence that the NCH proton is closer to the ring than the isopropyl group and therefore that the solid-state structure is retained in solution. By analogy, the same situation is presumed for the ruthenium complex (**2.45**, $R = iPr$).

Crystals of the benzyl-pymox complex (**2.49**, $R = Bn$) were obtained that were suitable for X-ray crystallography; the structure of the cation of (**2.49**, $R = Bn$) is shown in **Figure (2.18)**, with selected bond distances and an angle in **Table (2.11)**. The structure is much like that of the iPr -pymox analogue, as all important bond distances and angles are statistically the same. The configuration at the rhodium centre is again (*S*), with the phenyl ring of the benzyl substituent oriented away from both the chloride ligand and the Cp^* ring.

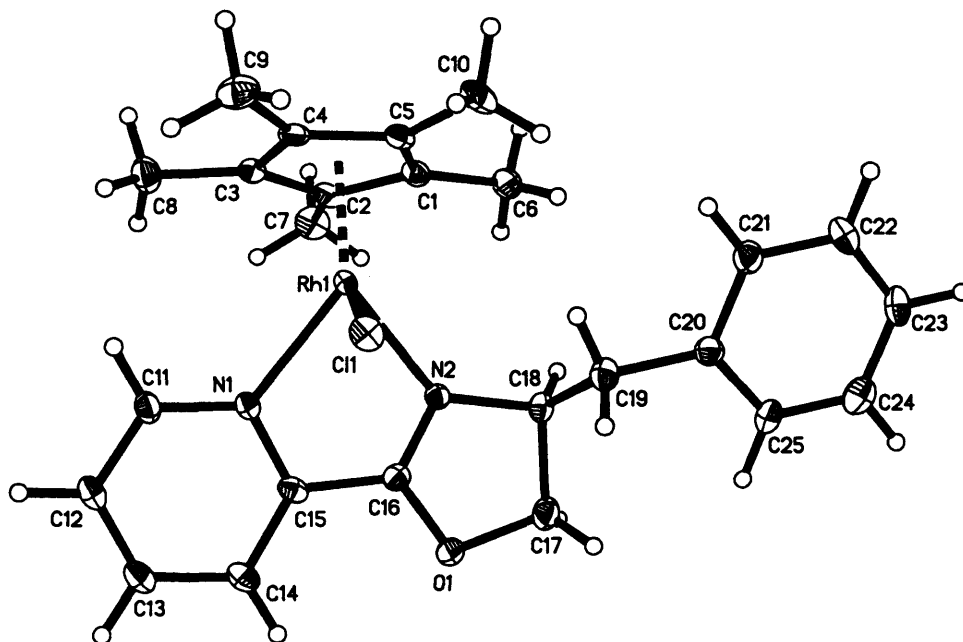


Figure (2.18): Crystal Structure of the cation of (2.49, $R = Bn$)

Table (2.11): Selected bond distances (Å) and angles (°) of (2.49, $R = Bn$)

Rh(1)–N(1)	2.138(3)	Rh(1)–Cl(1)	2.4025(12)
Rh(1)–N(2)	2.115(4)	N(1)–Rh(1)–N(2)	76.4(2)

The three structures shown above confirm that in the isomers formed exclusively for many half-sandwich oxazoline complexes, the *R*-substituent is oriented away from the bulky η -ring. As stated earlier, the Ph-pymox complex (**2.45**, $R = Ph$) was formed as a 5:2 mixture of diastereomers, as shown by 1H NMR of the

crude mixture, in which two sets of signals could be seen for each of $C_6H_3Me_3$, $C_6H_3Me_3$ and the pymox ligand. Recrystallisation of the mixture of isomers from CH_2Cl_2 /ether gave the major isomer exclusively, as shown by 1H NMR, which only contained one set of signals. Even after one week in solution, no trace of the minor isomer was observed. Evaporation of the mother liquors from the crystallisation yielded a sample of (**2.45**, **R = Ph**) heavily enriched in the minor isomer, again as shown by 1H NMR; the ratio did not change over several days. These observations lead to the conclusion that the ruthenium centre in (**2.45**, **R = Ph**), and presumably in the other pymox complexes, is configurationally stable at room temperature. The 5:2 ratio of isomers is presumably due to the inherent steric factors involved in forming the complex and may represent the equilibrium position in refluxing methanol, but not at room temperature; if the latter were true, one would expect the 5:2 ratio to be re-established on dissolving the crystallised product to obtain the NMR spectrum.

Unfortunately, the crystallised sample of (**2.45**, **R = Ph**) was not suitable for X-ray crystallography. To resolve this problem, the complex $[RuCl(Ph-pymox)(mes)]BPh_4$ (**2.45a**, **R = Ph**) was made by the same route, but with $NaBPh_4$ replacing $NaSbF_6$. This salt, as expected, behaved identically to the SbF_6 analogue; a mixture of isomers was obtained initially, with the major isomer crystallising exclusively and being configurationally stable in solution. Crystals of (**2.45a**, **R = Ph**) were obtained that were suitable for X-ray crystallography; the structure of the cation is shown in **Figure (2.19)** with selected bond distances and an angle given in **Table (2.12)**. The structure confirms that the major isomer of (**2.45a**, **R = Ph**), has the pymox ligand coordinated such that the phenyl substituent is oriented towards the chloride ligand rather than towards the mesitylene ring. The configuration at the ruthenium centre is thus (S), as in the analogous (**2.45**, **R = ⁱPr**). The Ru–N bond distances are again the same, while the N(1)–Ru(1)–N(2) bond angle is identical to that in (**2.45**, **R = ⁱPr**).

Table (2.12): Selected bond distances (Å) and angles (°) of (2.45a**, **R = Ph**)**

Ru(1)–N(1)	2.104(5)	N(1)–C(14)	1.335 (8)
Ru(1)–N(2)	2.105(5)	C(14)–C(15)	1.454(8)
Ru(1)–Cl(1)	2.403(2)	C(15)–N(2)	1.285(7)
N(1)–Ru(1)–N(2)	76.4(2)		

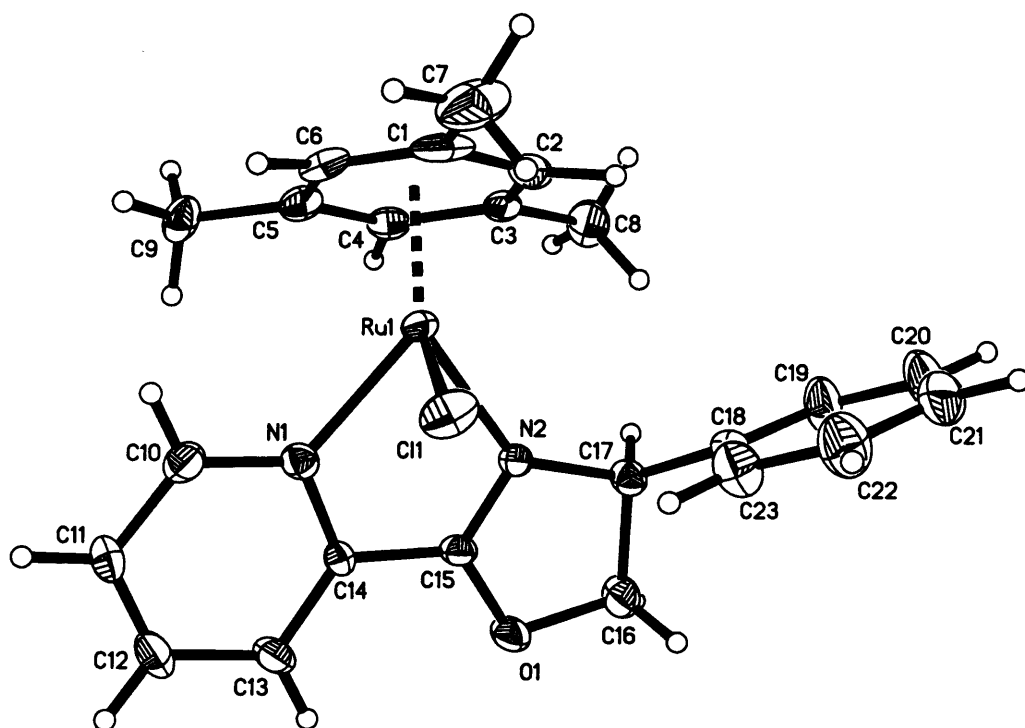


Figure (2.19): X-ray structure of the cation of (2.45a, R = Ph)

It is unclear why (2.45, R = Ph) is formed as a mixture of diastereomers, when all other complexes (2.45) are formed diastereospecifically. Sterically, one would expect phenyl to be no smaller than ethyl. One possible explanation is that the phenyl substituent in the minor isomer has an attractive π - π -interaction with the mesitylene ring, a ' β -phenyl effect' of the type observed in many arene-ruthenium Schiff-base complexes,^{94, 99} thus making this isomer more energetically favourable. In complexes (2.14 - 2.17), this effect was characterised by a 'ring current effect' in the ^1H NMR spectrum, *i.e.* a shift to lower frequency of the η^6 -arene signal of the isomer having this π - π interaction, relative to that of the other isomer. In the spectrum of (2.45, R = Ph), no such ring current effect is observed, the signals due to $\text{C}_6\text{H}_3\text{Me}_3$ being found at δ 5.08 (major isomer) and δ 5.25 (minor isomer). The signals are reasonably separated; however, that due to the minor isomer is at higher, rather than lower frequency, which suggests that there is no ' β -phenyl effect' in the minor isomer of (2.45, R = Ph).

A more likely explanation for the presence of two isomers in the Ph-pymox complex is that the phenyl substituent is bulky in only *two* directions, unlike alkyl groups. In the minor isomer, by simple rotating the ox-Ph bond, such that the phenyl

ring is oriented pseudo-parallel to the mesitylene ring, some of the strain between the two might be relieved; thus, the (R) isomer would be more favoured than in other complexes (2.45). The effects of fixing the substituent in a particular conformation can be examined in the indanyl-pymox complex (2.47), in which a methylene group links the phenyl ring to the OCH of the oxazoline ring (note: in this ligand, the configuration at the NCH chiral centre is (R), unlike in most of the other complexes). Only one isomer of (2.47) was observed by ^1H NMR, and crystals were obtained that were suitable for X-ray crystallography. The structure of the cation is shown in Figure (2.20), with selected bond distances and angles given in Table (2.13).

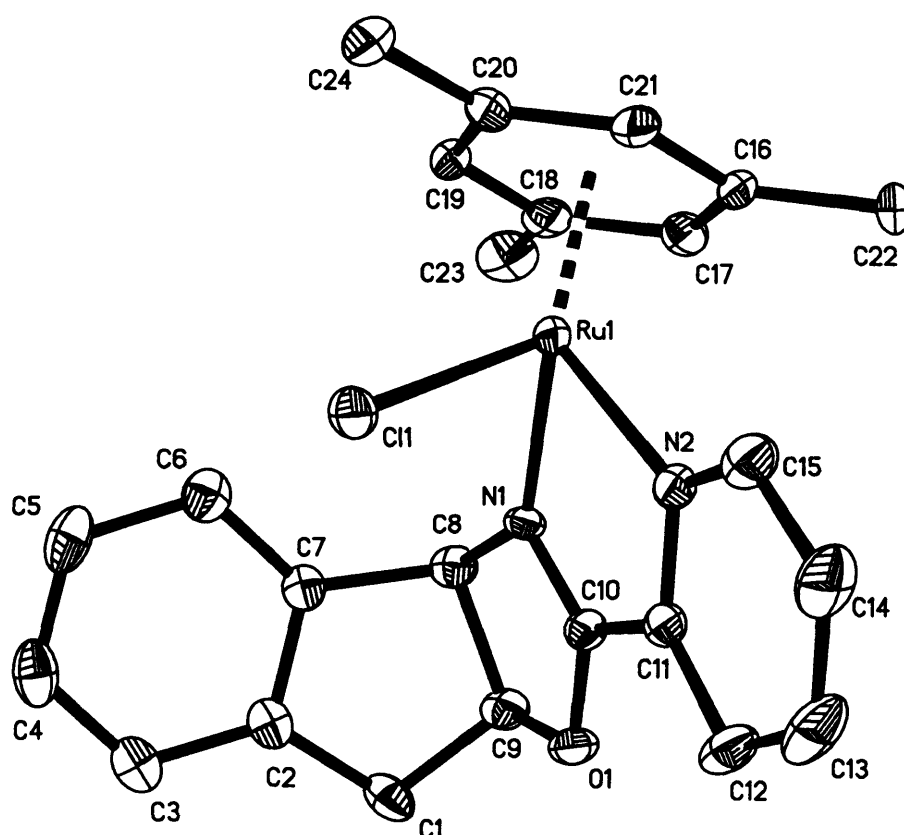


Figure (2.20): X-ray Structure of the cation of (2.47)

Table (2.13): Selected bond distances and an angle of (2.47)

Ru(1)–N(1)	2.103(5)	N(1)–C(11)	1.346 (8)
Ru(1)–N(2)	2.126(5)	C(11)–C(10)	1.435(9)
Ru(1)–Cl(1)	2.393(2)	C(10)–N(1)	1.285(8)
N(1)–Ru(1)–N(2)	76.5(2)		

In (2.47), the pymox ligand is coordinated such that the phenyl-group is oriented in the same direction as the chloride, perpendicular to the plane of the mesitylene ring

(quite different to the orientation of the phenyl ring in the structure of the phenyl-pymox complex). The configuration of the ruthenium centre is (R), while the indanyl-pymox has an (R)-configuration at the NCH chiral centre and is (S)-configured at the OCH centre (note: the configuration at the metal centre is again the same as that at the NCH chiral centre). Most of the important bond distances and the N(ox)–Ru–N(py) chelate angle are statistically the same as those of (2.45, R = Ph). An exception is the Ru–N(2) (py) distance 2.126(5) Å, which is slightly longer than that in the phenyl pymox analogue. It is clear that preventing rotation of the phenyl substituent prevents formation of two isomers; steric hindrance in the (S)-isomer of (2.47) would presumably be too severe.

Thus for the complexes (2.43 - 2.52), containing unsymmetrical pymox ligands, the three main points are:

- i) Interconversion of enantiomeric Me₂-pymox complexes (2.46) and (2.50) is not observed on the NMR timescale.
- ii) With a bulky η-ring and/or a large R-substituent, complexes (2.43-5, 2.47-9, 2.51-2) are formed highly diastereoselectively.
- iii) With (2.45, R = Ph), diastereomers are formed, but the major isomer could be selectively crystallised and was apparently configurationally stable. No epimerisation could be observed for any of the diastereomeric compounds.

These points are particularly important, as the diastereoselectivity and configurational stability of the diastereomeric pymox complexes compare favourably with those of many known diastereomeric half-sandwich complexes of ruthenium and rhodium. The most direct comparison is with the arene-ruthenium Schiff-base complexes discussed earlier (2.12-4, 2.17-9), which were all formed as mixtures of diastereomers, the highest equilibrium diastereomer ratio being 86:14.^{94, 95, 99} This inherently lower diastereoselectivity can be attributed to the freedom of rotation of the N_(imine)–CH(Me)(Ph) bond in the Schiff base ligands (all derived from (S)-1-phenylethylamine). Although certain orientations of the imine substituent may be favoured in some cases, the resultant difference in energy between the two isomers is insufficient to give one diastereospecifically. With (2.44 - 2.52), however, the R-substituents on the oxazoline rings are fixed in their orientation; thus, they are either oriented towards the η-ring or towards the chloride ligand. The steric strain involved

when the more bulky R-substituents and η -rings clash presumably disfavours the formation of those isomers.

The Schiff-base complexes (**2.12-4**, **2.17-9**) were all found to epimerise in solution, at various rates, depending on donor-atom type, overall charge and solvent. For (**2.18/2.19**), with pyridine-containing Schiff-base ligands, diastereomer exchange was found to be relatively slow, even on a chemical timescale, in CDCl_3 and was still slow on the NMR timescale in D_2O .¹⁰⁰ In contrast, the pymox complex (**2.46**, $\text{R} = \text{Ph}$) does not appear to epimerise at all, in any solvent. The chloride ligands of (**2.44 - 2.52**) are not displaced by treatment with D_2O , unlike in the Schiff-base complexes (**2.18/2.19**) or amino-acidate complexes, where this provided a route for epimerisation in those systems.^{67, 68, 100}

The animox complexes (**2.53**) and (**2.54**) were both formed as mixtures of diastereomers (**Figure 2.21**), as shown by ^1H NMR spectroscopy (**Table 2B.8**). The ruthenium complex (**2.53**) gave an 8.5:1 mixture, whilst with the rhodium complex (**2.54**), the ratio was 15:1. Recrystallisation of samples of (**2.53-4**) from various solvent mixtures failed to give either X-ray quality crystals or a different ratio of isomers.

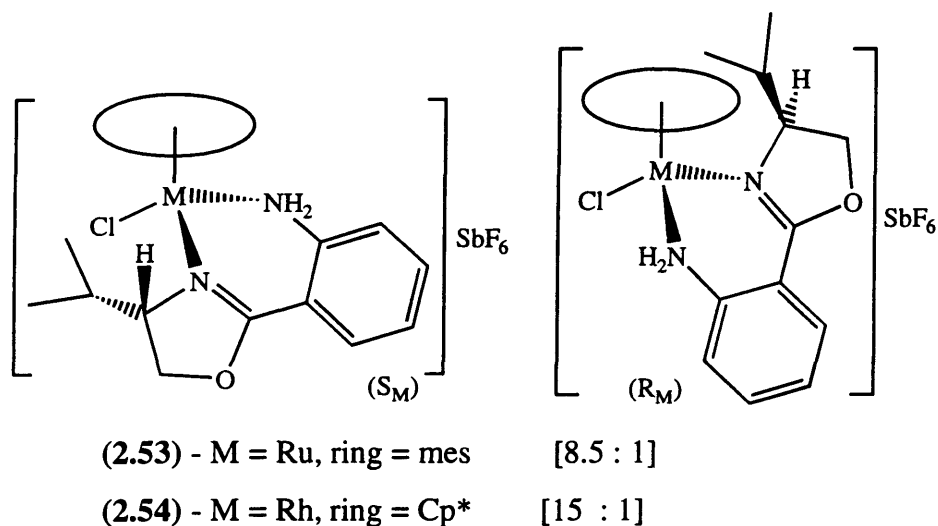


Figure (2.21)

In general, the ^1H NMR signals (in CD_2Cl_2) for the animox ligand are, as expected, moved to higher frequency upon coordination to the metal centres of (**2.53-4**), as found with pymox and C_2 -symmetric oxazoline complexes; in particular, the oxazoline ring signals appear between δ 4.63 and 4.31 (compared to δ 4.32 and 4.11 in the free ligand) and the CHMe_2 signals, which appear as multiplets at δ 2.8 (for the

major isomers - a downfield shift of 1 ppm). The aniline ring signals are similarly shifted to higher frequency, though assignment of signals for each isomer is difficult due to overlap. Signals due to the CHMe_2 groups of the major isomers of (2.53-4) (δ 0.88 - 0.51) are observed at *lower* frequency than those of the free ligand (δ 1.03 and 0.94), whilst the corresponding signals for the minor isomers are found to be essentially unchanged on coordination.

For the ruthenium complex (2.53), ^1H NMR signals, in CD_2Cl_2 , are observed at δ 2.08 and 1.99 ($\text{C}_6\text{H}_3\text{Me}_3$ for the major and minor isomers, respectively), and at δ 4.82 ($\text{C}_6\text{H}_3\text{Me}_3$ for both isomers). In d_6 -acetone, the signals due to the $\text{C}_6\text{H}_3\text{Me}_3$ protons in each isomer of (2.53) can be readily distinguished, at δ 5.10 and 5.17 (major and minor, respectively). These signals appear at rather lower frequency than those for the pymox analogue (2.45, $\text{R} = \text{Pr}$) (δ 2.25 and 5.33), possibly because the pyridine ring, is a better π -acceptor than the aniline. The Cp^* signal of (2.54) (δ 1.42) is similarly at lower frequency than for the pymox analogue (2.49, $\text{R} = \text{Pr}$) (δ 1.73).

The diastereotopic NH_2Ar protons of the animox ligand give rise to two signals for each isomer of the complex, instead of the broad 2H singlet found for the free ligand (at δ 6.14). In d_6 -acetone, two distinct sets of broad doublets can be seen, at *ca.* δ 5.7 and 7.2 (major isomer) and at δ 6.0 and 6.9 (minor isomer). For the rhodium complex (2.54), a pair of broad doublets is observed at δ 4.9 and 5.4. The chemical shifts of the NH signals vary slightly (up to 0.1 ppm difference) with the amount of water present in the NMR sample, presumably due to H-bonding effects and/or exchange of NH with water protons; accordingly, the line-width also varies slightly.

As fixed ratios of diastereomers were found for complexes (2.53-4), the possibility exists that they represented the equilibrium positions in each case. Thus, these ratios might have been rapidly established, due to exchange being slow on the NMR timescale, but fast on a chemical timescale. To investigate this, and to identify the structure of the major isomer, a phase-sensitive NOESY experiment was performed, on a sample of the ruthenium complex (2.53) in d_6 -acetone. In the ^1H NMR spectrum of the sample used, some signals are slightly broad (particularly those of the minor isomer), indicating that chemical exchange is occurring. Accordingly, in

the NOESY spectrum, both chemical exchange and through-space interactions (nOes) are found, the latter all in the major isomer (Figure 2.22).

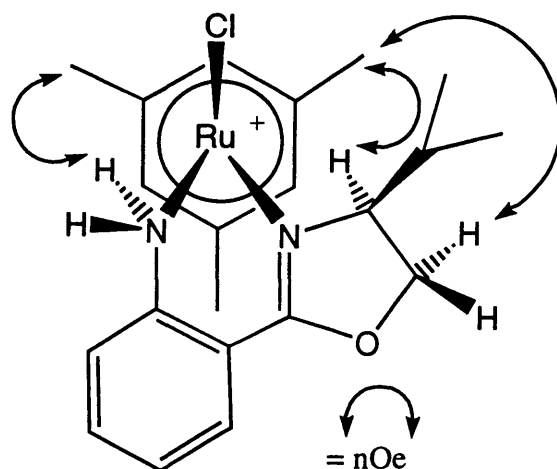


Figure (2.22)

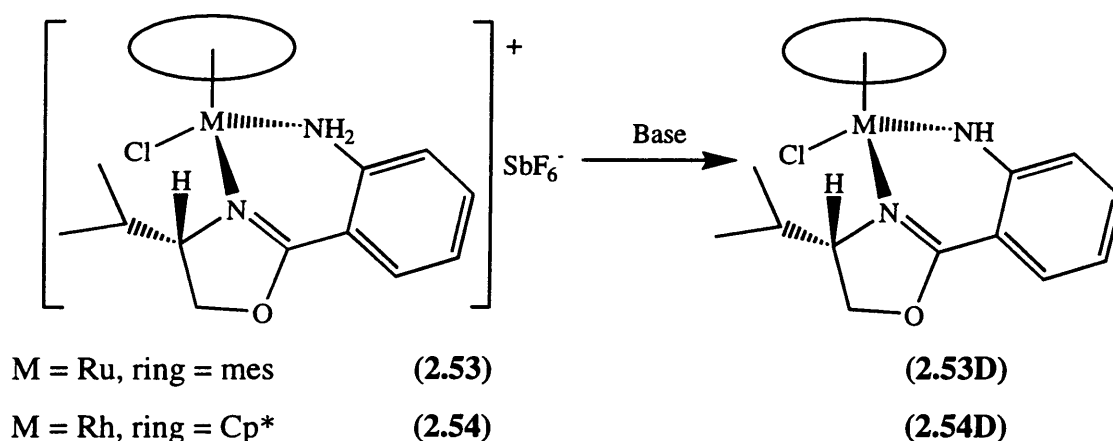
Strong nOes are observed from the NCH and an OCH to the $C_6H_3Me_3$ group, whilst no nOes are seen between the $CHMe_2$ and the mesitylene ring, indicating that the iPr -group is oriented towards the chloride, rather than towards the η^6 -arene. The configuration at ruthenium in the major isomer is thus (S), as found for the corresponding pymox complexes. An nOe is also seen from the high frequency NH signal to the mesitylene ring, thus confirming that they are close in space.

Correlations due to chemical exchange are found for most signals in the spectrum. The diastereotopic NH protons, in each isomer, are undergoing exchange with free water in solution, at considerably different rates, since the correlation intensities for the lowest frequency signals (of each isomer) are much stronger than those for the higher frequency signals. This apparent difference in exchange rate is expected, since the higher frequency signals are due to NH protons oriented towards the mesitylene ring, which will be a more sterically hindered site for the approach of water molecules. Similar behaviour of diastereotopic amine protons has been reported by Kurosawa, who showed that the NH protons in complexes $[Ru(NH_2R)(Ph-bop)(C_6H_6)](BF_4)_2$ underwent exchange with deuterium in CD_3OD solution at very different rates.¹⁰³ It was deduced that the hydrogens undergoing the slowest exchange were in the more sterically hindered positions.

In addition to chemical exchange of the NH_2 -group, strong chemical exchange correlations are seen (in the NOESY spectrum of 2.53) between the animox ligand signals of the major and minor isomers, indicating that epimerisation is occurring in

solution, at a rate comparable with the NMR timescale. The correlations are particularly apparent for the ^1Pr -resonances, presumably because there is a reasonable difference in chemical shift between signals due to ^1Pr in each diastereomer. These results indicate that the animox complexes *are* capable of epimerisation in solution and that the isomer ratios observed for (2.53/2.54) correspond to the equilibrium ratios.

The NH_2 -protons of both (2.53) and (2.54) are fairly acidic, one proton being readily lost by treatment with bases such as triethylamine and di-*tert*-butylpyridine, presumably giving neutral complexes (2.53D/2.54D), as shown in Scheme (2.18). This deprotonation is accompanied by a dramatic colour change- from yellow to very intense purple (presumably due to a charge-transfer band).

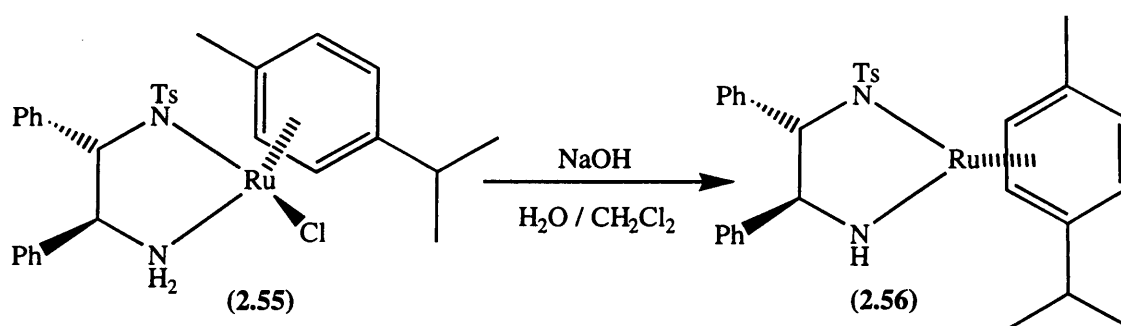


Scheme (2.18)

Attempts to isolate a pure sample of (2.53D) or (2.54D) were unsuccessful, as the protonated precursors were found to crystallise selectively from solution; however, the neutral complexes can be observed by ^1H NMR (Table 2B.8). Addition of aliquots of NEt_3 to a sample of (2.53) in CD_2Cl_2 results in a broadening of the NH signals, with a new set of ligand and arene signals appearing. With less than one equivalent of NEt_3 added, signals due to the oxazoline ring and $\text{C}_6\text{H}_3\text{Me}_3$ protons are somewhat broad, presumably due to the cationic and neutral species interconverting via proton exchange, which would also explain the broadness of the NH signals themselves. After one equivalent of NEt_3 has been added, the signals due to the oxazoline and arene ring become sharp and are significantly more downfield than in the precursor (2.53), the NCH and OCH protons are observed as complex multiplets in the range δ 5.00 - 4.65, with the $\text{C}_6\text{H}_3\text{Me}_3$ signal being found at δ 5.55 (a downfield shift of 0.73

ppm). A very broad resonance is observed at δ 10.8, which is presumably due to the remaining *NH* proton, corresponding to a downfield shift of > 5 ppm from those of (2.53), which could be due to a hydrogen-bonding effect. The reason for the arene and oxazoline ring signals appearing at *higher* frequency than in (2.53) is unclear; the neutral complex formed should be more electron-rich than the cationic precursor, so the chemical shifts would be expected at *lower* frequency. Similar spectra are obtained with the rhodium analogue (2.54D). The appearance of only one set of complex signals suggests that epimerisation might occur rapidly on the NMR timescale for (2.53D/2.54D), as two isomers are observed for the protonated precursor complexes (2.53/2.54).

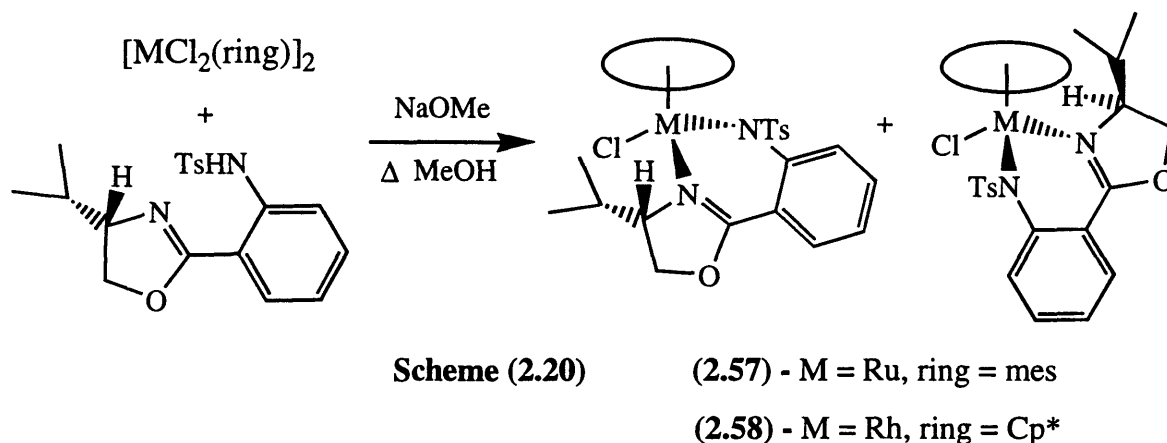
A similar deprotonation of a coordinated amine was reported by Noyori,¹⁰² who showed that the complex $[\text{RuCl}(\text{TsDPEN})(p\text{-cymene})]$ (2.55) can be converted to the 16-electron complex (2.56), by treatment with NaOH (like 2.53D and 2.54D, 2.56 gives rise to an intense purple colour). Complex (2.56) is an active catalyst for asymmetric transfer hydrogenation. It should be noted, however, that the process occurring to give (2.56) is a dehydrohalogenation (*i.e.* the chloride is also lost). It is conceivable that such a process might be occurring with (2.53D/2.54D); however, loss of a chloride from either of the latter would give monocations (rather than a neutral species such as 2.56, which would be less willing to react with free chloride). In addition, complexes (2.53D/2.54D) are considerably more soluble than their precursor salts, which suggests that they are neutral.



Scheme (2.19)

To summarise, it is apparent that chemical exchange processes in the animox complexes occur readily at room temperature. Proton exchange of the *NH* protons occurs at different rates, whilst epimerisation is also observed in d_6 -acetone at room temperature. The deprotonated complexes (2.53D/2.54D) are easily formed under basic conditions, but are not readily isolable, due to re-protonation.

Replacing one NH proton of ⁱPr-animox with an electron-withdrawing, less basic, tosyl group should discourage reprotonation, hence the isolation of neutral half-sandwich complexes is expected to be easier. Complexes [MCl(ⁱPr-NTs-animox)(ring)] (M = Ru, ring = mes: **2.57**; M = Rh, ring = Cp*: **2.58**) were prepared by treatment of the appropriate dimer [MCl₂(ring)]₂ with two equivalents of ⁱPr-NTs-animox and NaOMe (to deprotonate the ligand) in refluxing methanol (Scheme 2.20).



Complexes (**2.57**) and (**2.58**) were both formed as mixtures of diastereomers, as shown by ¹H NMR (Table 2C.3). The ruthenium complex (**2.57**) was formed as a 7.5:1 mixture of isomers, whilst the rhodium complex (**2.58**) gave a 13:8 mixture. Neither complex could be crystallised, due to their very high solubility in many common solvents, so assignment of the configurations at the metal centre has relied on NMR techniques. ¹H NMR signals due to the mesitylene ring for (**2.57**) are observed at δ 2.02 and 4.91 (major isomer) and at δ 2.11 and 4.80 (minor isomer), whilst for (**2.58**), the Cp* signal for both isomers is found at δ 1.48. All of these shifts are very close to the corresponding values in the analogous animox complexes, probably because the electron-donating ability of NH₂Ar and TsArN⁻ are similar.

In both isomers, deshielding of the aniline ring, CHMe₂ and NCH protons is observed on coordination (by up to 0.3 ppm), as found for the animox analogues. The signals due to the oxazoline ligand are rather different for the pairs of isomers, with some very large differences in chemical shift observed for certain signals. For example, in the major isomers of (**2.57/2.58**), the CHMe₂ signals are observed in the range δ 0.97 - 0.87 (very similar to those of the free ligand: δ 1.06 and 0.95). In the minor isomers, however, these signals are observed at lower frequency, with one

signal very close to 0 ppm (δ 0.08 for **2.57** and δ 0.18 for **2.58**). These low frequency signals might be due to a ring-current effect from the tosyl group.

To confirm this, and hence to deduce the structures of each isomer, a phase-sensitive NOESY experiment was performed, on the rhodium complex (**2.58**), in CDCl_3 . Correlations were observed due to through-space interactions (nOes) and chemical exchange of diastereomers. The most important structure-determining nOes are shown in (Figure 2.23). In the major isomer, nOes are seen from the Cp^* signal to those of the CHMe_2 and one MeCHMe' group, with none seen from the NCH proton to the Cp^* . This clearly indicates that the major isomer has the ^iPr -group oriented towards the Cp^* ring. For the minor isomer, nOes are found between the low frequency MeCHMe' signal and both of the tosyl Ar-H doublets (thus confirming the ring-current hypothesis) and between the NCH signal and the Cp^* ring. Thus, in the minor isomer, the ^iPr is oriented away from the Cp^* , such that it is closer to the tosyl group. The sulphur atom in the tosyl group is tetrahedrally substituted, which will allow the tosyl group to orient itself away from the Cp^* , in both isomers, presumably. Thus, when the ^iPr -group is also oriented away from the Cp^* , it is close enough to the tosyl group to experience shielding due to the π -aromatic cloud, in an interaction “beneath” the M-Cl bond. In the major isomer, a weak nOe is seen between the NCH proton and the Ts-2/6-H doublet, indicating a similar interaction.

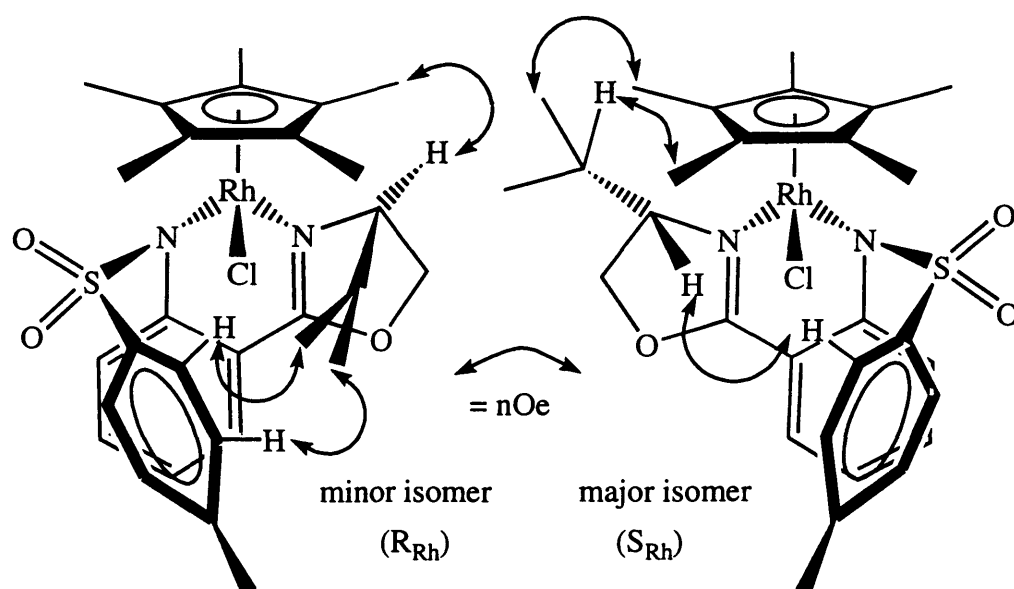
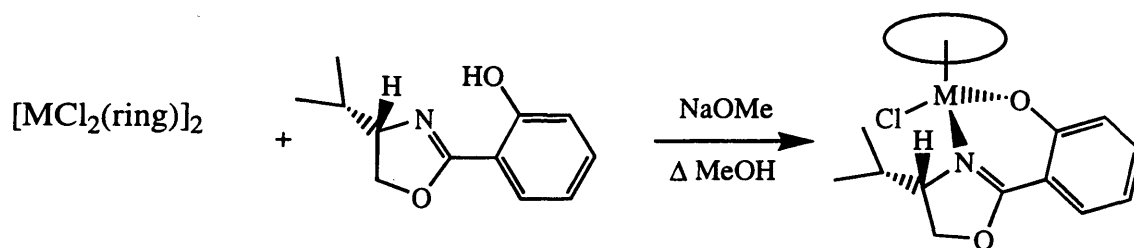


Figure (2.23)

From the nOe data, the configuration at rhodium is (S) in the major isomer and (R) in the minor isomer, based on the priority: Cp* > Cl > N(Ts) > N(ox).^{86, 87} As the spectra of (2.58) and the ruthenium analogue (2.57) are very similar (with the minor isomer in each case having a low frequency *MeCHMe'* signal), it is assumed that the latter also has an (S)-configuration at the metal in the major isomer (*i.e.* ⁱPr → mes). To account for the observed diastereoselectivity, there must be greater steric hindrance when the isopropyl group is oriented towards the tosyl group (in the minor isomers) than when it points towards the η-ring (major isomers), assuming that the tosyl group adopts the conformation shown above. If this is true, the fact that the rhodium complex (2.58) was formed less diastereoselectively than (2.57) is reasonable; for complexes of pymox and animox, the diastereomer with the ⁱPr-group oriented *away* from the η-ring was formed more selectively with rhodium than with ruthenium, presumably because Cp* is more bulky than many of the arene ligands.

As with the animox complexes (2.53/2.54), mixtures of diastereomers were obtained for (2.57/2.58), the ratios not changing over time. The NOESY spectrum shows chemical exchange correlations between all corresponding signals for the pairs of isomers. Thus, exchange of diastereomers occurs at a slow rate on the 1D NMR timescale, but is fast on a chemical timescale and can be seen in the 2D experiment. The 13:8 mixture of diastereomers used in the NOESY experiment thus represents the equilibrium position, as no change in ratio is seen, even after a week in solution. Neither NTs-animox complex could be crystallised, only oils precipitating which showed the equilibrium ratio of isomers. To study epimerisation in this system further, it would be useful to selectively crystallise one isomer, then dissolve it up at low temperature to run the ¹H NMR.

As with the NTs-animox ligand, ⁱPr-phenmox must be deprotonated in order to form analogous, neutral half-sandwich complexes [MCl(ⁱPr-phenmox)(ring)] (M = Ru, ring = *p*-cymene, mes; M = Rh, Ir, ring = Cp* - 2.59 - 2.62), by the same method used to synthesise (2.57/2.58), as shown in Scheme (2.21).



Scheme (2.21)

(2.59): M = Ru, ring = *p*-cy

(2.60): M = Ru, ring = mes

(2.61): M = Rh, ring = Cp*

(2.62): M = Ir, ring = Cp*

Complexes (2.59 - 2.62) were all formed as single diastereomers, as shown by ^1H NMR (Table 2C.4, see Experimental). A crystal of (2.60) (obtained by A. Davenport) was analysed by X-ray diffraction; the structure is shown in Figure (2.24), with selected bond distances and the chelate angle given in Table (2.14).

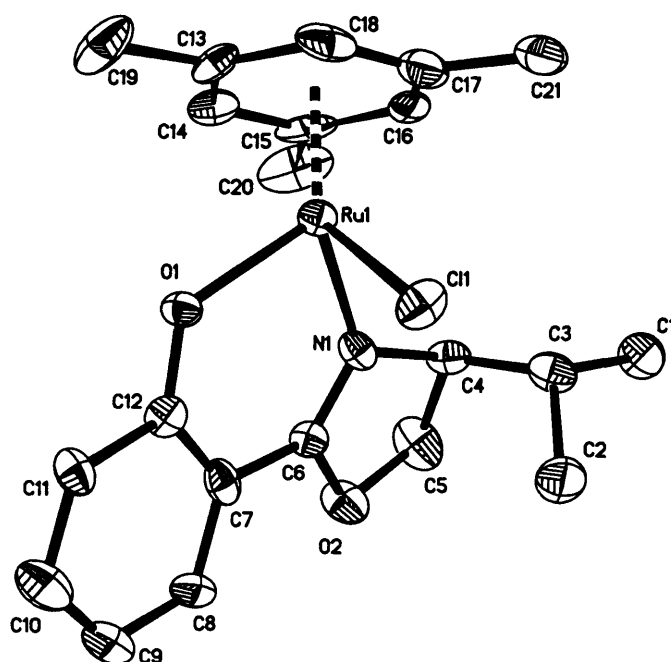


Figure (2.24): X-ray Structure of (2.60)

Table (2.14): Selected Bond Distances (Å) and Angles (°) for (2.60)

Ru(1)—O(1)	2.062(7)	O(1)—C(12)	1.299(13)
Ru(1)—N(1)	2.075(10)	C(12)—C(7)	1.41(2)
Ru(1)—Cl(1)	2.427(3)	C(7)—C(6)	1.44(2)
N(1)—C(6)	1.295(14)	O(1)—Ru—N(1)	87.2(3)

Complex (**2.60**) adopts the expected pseudo-octahedral structure, with the phenmox ligand coordinated such that the ⁱPr-substituent is oriented towards the chloride rather than towards the mesitylene ring. The configuration at the metal centre is thus (R), based on the priority arene > Cl > O > N {the configuration at the chiral centre of the phenmox ligand is (S)}. Although the configuration at ruthenium in (**2.60**) (R_{Ru}) is *formally* different from that in the analogous pymox complex (**2.45**, $R = {}^iPr$) (S_{Ru}), the spatial arrangement of ligands is the same, with the phenoxy ring replacing pyridine. Most of the bond distances and angles, about the metal centre, are the same as those of the analogous salicylaldimine complex (**2.14**), notably the Ru(1)–O(1) and Ru(1)–Cl(1) distances. The Ru–N(ox) distance {2.075(10) Å} is slightly shorter than that in the analogous pymox complex (**2.45**, $R = {}^iPr$) {2.118(4) Å}, whilst the Ru–Cl distance for (**2.60**) {2.427(3) Å} is slightly longer than that of the pymox complex {2.402(2) Å}. The chelate angle {87.2(3)°} is significantly larger than that of (**2.45**, $R = {}^iPr$) {76.4(2)°}, as expected, with a six-membered chelate ring.

In the ¹H NMR spectra of (**2.59** - **2.62**), the signals due to the phenoxy ring of the phenmox ligand are all moved to lower frequency, by up to 0.5 ppm, compared to free phenmox-H ligand, partly due to the deprotonation of the OH group. The signals due to the NCH and CHMe₂ protons are essentially unchanged from the free ligand (ca. δ 4.3 and 0.9 respectively). The largest change in chemical shift upon coordination is found for the CHMe₂ protons, which are deshielded by almost 1 ppm, from δ 1.8 to δ 2.75 (the reason for this is not clear). Signals due to Cp* are found at δ 1.5 for (**2.61**) and (**2.62**), whilst mesitylene signals (of **2.60**) are observed at δ 2.22 and 4.9. All the arene and Cp* ring signals are observed at lower frequency than those of the analogous ⁱPr-pymox complexes {presumably because (**2.59** - **2.62**) are neutral compounds}, but at very similar shifts to the corresponding animox and NTs-animox complexes.

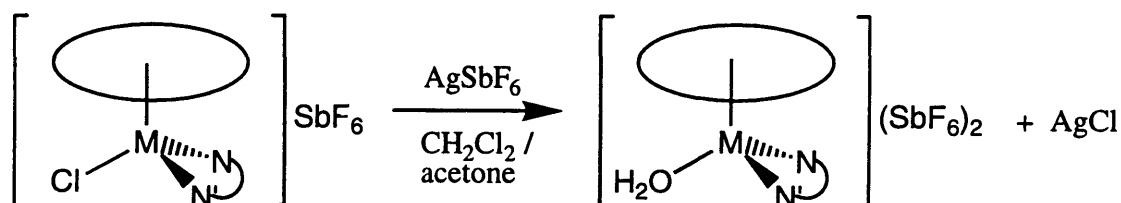
The high diastereoselectivity observed in the formation of (**2.60** - **2.62**) is analogous to that with ⁱPr-pymox. However, for the *p*-cymene complex (**2.59**), the formation of only one isomer is slightly surprising, as the analogous ⁱPr-pymox complex (**2.44**, $R = {}^iPr$) was obtained as a 1:1 mixture of isomers. Possibly, the isomer where the ⁱPr group is closer to the ring is even more sterically disfavoured for phenmox, because the chelate ring is six-membered, rather than five-membered as is

the case for pymox. An alternative explanation for the apparent high selectivity is that ligand exchange occurs at a rate much faster than the NMR timescale; in this case, a time-averaged spectrum would be observed. This is unlikely, however, as the spectra of **(2.60)** at 233K still did not show any trace of a second isomer.

The formation of complexes **(2.59/2.60)** is clearly much more diastereoselective than for the analogous ruthenium salicylaldimine compounds **(2.12/2.13)**,^{94, 95} presumably because the isomers of the latter are relatively close in energy. No epimerisation was observed with the phenmox complexes, unlike with the ruthenium/Schiff-base complexes, for which epimerisation was rapid even at -80°C. Recently, it has been shown that the complex [RuCl(Ph-phenmox)(mes)],¹⁰⁹ is formed as a mixture of diastereomers and undergoes epimerisation at a rate comparable with the NMR timescale, in dichloromethane solution at room temperature, such that signals due to each isomer are broad. This result indicates that complexes [MCl(phenmox)(ring)] are labile in solution (such that the chloride ligand can be lost), but with ⁱPr-phenmox, the thermodynamic equilibrium ratio is so heavily over to the (R)-isomer that epimerisation is not seen. It has been observed that arene-ruthenium amino-acidate and Schiff-base complexes can undergo epimerisation in polar solvents such as MeOH and water, equilibria between aqua- and chloro-complexes existing in D₂O.^{67, 68, 100} Diastereomer exchange for the labile aqua complexes was found to be more rapid than that in the chloride complexes. No displacement of chloride ligand was observed when **(2.60)** was dissolved in d₄-MeOH, even when a large excess of D₂O was added.

To summarise, the half-sandwich complexes of pymox and animox **(2.43-2.54)** and NTs-animox and phenmox **(2.57-2.62)** are formed with high diastereoselectivity (particularly with bulky substituents), much higher than that found for most analogous amino-acidate and Schiff-base complexes. The NTs-animox complexes were the least diastereoselective, overall, the tosyl substituent appearing to hinder, rather than aid, the formation of one isomer. For this ligand, the major isomers have the isopropyl-substituent oriented towards the η-ring, which is not found with any other ligand class discussed here. The pymox complexes were shown to be configurationally stable in solution, whilst epimerisation in the animox and NTs-animox was found to be slow on the 1D NMR timescale, but observable by 2D NMR techniques.

In order to use the half-sandwich oxazoline complexes as catalysts, it is necessary to remove the chloride ligand, which is particularly strongly bound in the pymox and animox complexes. Aqua complexes $[M(OH_2)(N-N')(ring)](SbF_6)_2$ (**2.63** - **2.73**) were synthesised from the chloride precursors using $AgSbF_6$ in CH_2Cl_2 /acetone (7:1) (Scheme (2.22), traces of water in the acetone providing the aqua ligand.



Scheme (2.22) {2.63 - 2.73, see Table (2.15)}

Table (2.15): Complexes $[M(OH_2)(N-N')(ring)](SbF_6)_2$

Code Number	M	ring	N-N'
2.63	Ru	C_6H_6	pymox (R = ⁱ Pr, ^t Bu)
2.64	Ru	<i>p</i> -cymene	pymox (R = ⁱ Pr, ^t Bu)
2.65	Ru	mes	pymox {R = Et, ⁱ Pr, ^t Bu, Ph, Bn}
2.66	Ru	mes	Me ₂ -pymox
2.67	Ru	mes	Indanyl-pymox
2.68	Ru	C_6Me_6	ⁱ Pr-pymox
2.69	Rh	Cp*	pymox {R = Et, ⁱ Pr, ^t Bu, Ph, Bn}
2.70	Rh	Cp*	Me ₂ -pymox
2.71	Rh	Cp*	Indanyl-pymox
2.72	Ir	Cp*	ⁱ Pr-pymox
2.73	Ru	mes	ⁱ Pr-animox

Pure complexes could be isolated by filtration of the crude reaction mixture through celite, to remove the $AgCl$ by-product; however, many of the dications were somewhat hygroscopic and recrystallisations typically gave oily products. When solid products were precipitated, they were only powder-like and consequently, no X-ray crystal structures of complexes (**2.63** - **2.73**) could be obtained. As a result, the characterisation of (**2.63** - **2.73**) has relied on NMR, mass spectrometry and analysis (Tables 2D.6 - 2D.14, see Experimental). The H_2O ligands of (**2.63** - **2.73**) are

expected to be easily lost in solution, as was found for aqua complexes of the bis-oxazoline ligands, discussed earlier (Section 2.2.1). As a result, epimerisation is more likely than with the corresponding chloride precursors. There are possible complications of competing acetone or methanol coordination in solution (found for ruthenium complexes **2.30**, **2.34-6**) as well as the potential to form diastereomers in most cases; thus, the NMR spectra may be more complex. Complexes (**2.63 - 2.73**) are all insoluble in CHCl_3 and H_2O , sparingly soluble in CH_2Cl_2 , but are very soluble in polar solvents such as acetone and MeOH. The ^1H NMR spectra were, therefore, obtained in d_6 -acetone and/or d_4 -MeOH, but to allow comparison of spectra with those of the precursors, the ruthenium complexes (**2.64 - 2.66**) were also dissolved in an ~ 10:1 mixture of CD_2Cl_2 / d_6 -acetone.

Initially, the complexes (**2.66**) and (**2.70**), containing the achiral Me_2 -pymox ligand, were studied; the complexes should exist as racemates, the two enantiomers of each being indistinguishable by ^1H NMR. For these compounds, the effects of water exchange and competing solvent coordination could be investigated, without the added complication of having two possible diastereomers. For the ruthenium complex (**2.66**), only one set of signals is observed in the ^1H NMR spectrum in the CD_2Cl_2 / acetone mixture. The spectrum is very similar to that of the chloride precursor, except that the arene and pymox ligand signals are shifted to higher frequency by up to 0.35 ppm (py-6-H); two singlets are observed for the CMe_2 group and two doublets found for the OCH_2 group. A slightly broad 2H singlet at δ 5.5 is assigned to coordinated H_2O , with a broad singlet at δ 1.8 being due to free water in solution; the observation of separate signals for free and coordinated water indicates that exchange of water is slow on the NMR timescale.

In d_6 -acetone, the ^1H NMR spectrum of (**2.66**) shows a mixture of two similar species, the ratio of which depends on the amount of free water in solution. With one equivalent of free water, the ratio was 7:5 (based upon the relative integration of the arene and py-6-H signals), whilst with two equivalents of water, the ratio was 5:1. The signals due to the major species match very closely those of the complex in the CD_2Cl_2 / acetone mixture and the presence of a singlet (relative integration 2H) at δ 6.5 clearly identifies water as the ligand at the sixth coordination site in the major species. A singlet at δ 2.9 is observed due to free water, so exchange of water is again slow on the NMR timescale. For the minor species, sharp signals due to the arene and

pyridine ring signals are observed, but very broad resonances at δ 1.8 (CMe_2) and 4.9 (OCH_2) clearly indicate that epimerisation at the metal is occurring at a rate comparable to the NMR timescale. Cooling the sample to 253K, the broad signal at δ 1.8 resolved into two 3H singlets (δ 1.75 and 2.15) and the broad peak at δ 4.9 resolved into two 1H doublets (δ 4.89 and 4.96). Addition of 3 equivalents of H_2O to the solutions of (2.66) in d_6 -acetone gave a ratio of $> 15:1$ and addition of a further equivalent of water leads to the disappearance of the minor set of peaks. This indicates that the minor species is an acetone-coordinated complex (like those found for the box and benbox complexes described earlier), with epimerisation at the metal being considerably faster with acetone coordinated than with water.

In the 1H NMR spectrum of the analogous rhodium complex (2.70), at room temperature, only one singlet is found for the CMe_2 group with another singlet found for the OCH_2 group, which indicates that fast epimerisation, on the NMR timescale, is occurring the metal centre. A very broad resonance at δ 3.9 is due to exchanging coordinated and free water. On cooling the sample to 223K, the signal due to the CMe_2 group resolved into two sharp 3H singlets (at δ 1.61 and 1.93) and the singlet due to the OCH_2 group resolved into two 1H doublets (at δ 4.65 and 4.9), whilst sharp singlets at δ 6.7 and 3.9 were due to coordinated and free water respectively. Presumably, dissociative loss of water from (2.70), giving a 16-electron intermediate, allows interconversion of enantiomers to occur at a fast rate on the NMR timescale (Figure 2.25).

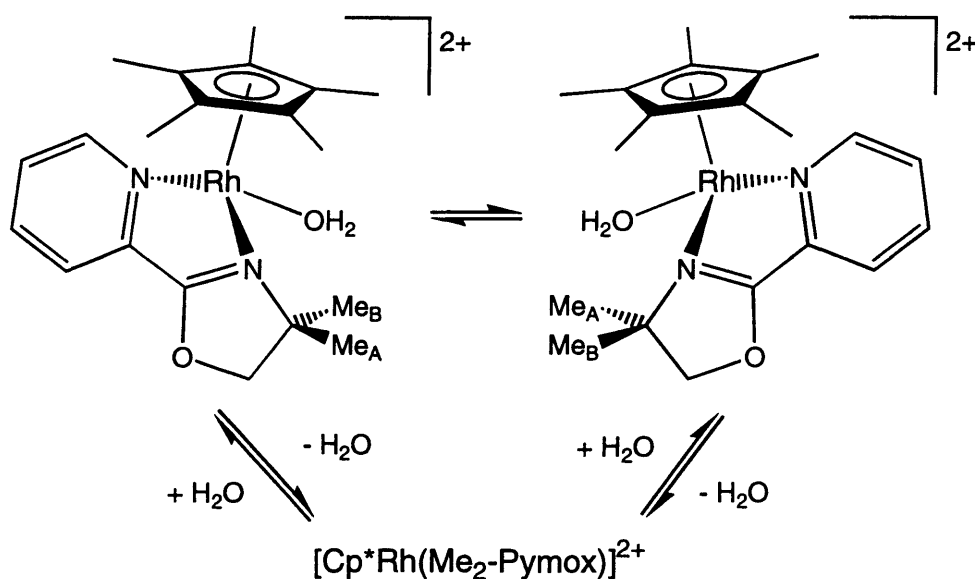


Figure (2.25)

It is likely that a similar process occurs in solution for all complexes $[\text{Rh}(\text{OH}_2)(\text{pymox})\text{Cp}^*]^{2+}$, but with chiral pymox ligands, the two species interconverting are diastereomeric, not enantiomeric, and therefore do not necessarily exist in a 1:1 ratio. The equilibrium should favour the less sterically hindered isomer. The results with the Me_2 -pymox complexes indicate that epimerisation of the diastereomeric ruthenium aqua-complexes should be considerably slower than for the corresponding rhodium complexes.

The ^1H NMR spectra of the ruthenium complexes (**2.64/2.65**) in the mixed $\text{CD}_2\text{Cl}_2/d_6$ -acetone solvent reveal that each complex is formed as a single diastereomer. Interestingly, the complex (**2.65**, $\text{R} = \text{Ph}$) only shows one diastereomer in the ^1H NMR spectrum, synthesised either from the crystallised major isomer or the 5:2 mixture of both diastereomers of (**2.45**, $\text{R} = \text{Ph}$). The signals due to the pymox ligands are further deshielded compared to the chloride precursors (by 0.1 - 0.4 ppm), due to formation of a dication, as are the *Ar-H* signals of the arene ligands (0.2 - 0.6 ppm shifts observed). All spectra contain a slightly broad 2H singlet in the range δ 5.8 - 5.0, which is assigned as the coordinated H_2O signal, with free water observed at ca. δ 1.8. Again, the observation of two different signals for free and coordinated H_2O demonstrates that water exchange is relatively slow on the NMR timescale.

The ^1H NMR spectra of (**2.63-2.65**) and (**2.67**) in pure d_6 -acetone are again more complicated than those in the mixed solvent. Coordinated H_2O is observed as a singlet at ca. δ 6.6 (the signal disappearing after a D_2O shake), with free water at ca. δ 3, again suggesting slow water exchange on the NMR timescale. There are also second, minor sets of signals due to the pymox and arene protons. Since the same phenomenon is found for the Me_2 -pymox, box and benbox analogues (none of which are diastereomeric), the minor signals can be assigned to acetone-coordinated complexes, rather than to minor diastereomers. This was confirmed by addition of small quantities of H_2O to the samples, leading to the disappearance of the minor species, as expected, due to displacement of acetone by water. For example, in the spectrum of the mesitylene complex (**2.65**, $\text{R} = {}^i\text{Pr}$) (containing 0.8 equivalents of free water), the ratio of water:acetone coordinated is 15:7, whilst with 1.4 equivalents of water it is 15:4. With four equivalents of free water the ratio has risen to > 12:1, which provides good evidence that the minor species is an acetone-coordinated complex, and that water is by far the preferred ligand of the two.

The only ruthenium aqua-compounds that appear as mixtures of diastereomers are the benzene-complex (**2.63**, **R = ⁱPr**) and the *p*-cymene complex (**2.64**, **R = ⁱPr**). The complexes are poorly soluble in CD₂Cl₂ and the ¹H NMR spectra were only obtained in d₆-acetone. In the initial spectrum of (**2.63**, **R = ⁱPr**) (containing one equivalent of free water), four signals were observed due to η⁶-C₆H₆ groups (δ 6.48, 6.54, 6.59 and 6.64) in a ratio 1:9:1.3:11.4. Addition of excess H₂O to the sample dramatically reduced the integration of the two higher frequency signals, which are thus assigned to diastereomeric acetone-coordinated complexes. The ratio of the two remaining singlets remained unchanged throughout and the equilibrium ratio of isomers for the aqua-complex is deduced as 9:1. In addition, singlets due to coordinated H₂O in the diastereomers can be observed, again in a 9:1 ratio. This isomer ratio is considerably higher than that found for the chloro-bound precursor (1:1). Similar features are observed in the NMR spectra of (**2.64**, **R = ⁱPr**), with the diastereomer ratio again deduced as 9:1. The observation of diastereomers of ruthenium water complexes at room temperature indicates that exchange of water and epimerisation are slow on the NMR timescale.

Rhodium and iridium complexes (**2.69**) and (**2.71/2.72**) were characterised by ¹H NMR spectroscopy (**Tables 2D.10-2D.11**), in d₆-acetone, since the complexes are virtually insoluble in CD₂Cl₂. In each case, a single diastereomer is observed at room temperature, with no evidence of acetone-coordination. Signals due to the pymox ligands are generally shifted to higher frequency than those in the monocationic precursors, as were the Cp* signals (ca. δ 2). Very broad humps (or no signal at all) are observed for water, indicating that aqua, or proton, exchange of free and coordinated water is rapid on the NMR timescale. An exception is the indanyl-pymox complex (**2.71**), for which slightly broad singlets are observed at δ 6.1 and 3.1, due to coordinated and free water respectively. The observation of these relatively well-resolved signals indicates that water exchange (either aqua or proton) is hindered by the bulky indanyl substituent.

To freeze out the water signals for complexes (**2.69**, **R = ⁱPr**) and (**2.72**), the ¹H NMR spectra (at 400 MHz) were run at various temperatures down to 223K. For the rhodium complex (**2.69**, **R = ⁱPr**), the coordinated water signal is initially observed as a broad hump at δ 6.5, with free water seen at δ 3, then at 223K, sharp singlets are

observed at δ 6.75 (coordinated water) and δ 3.6 (free water). In addition, as the temperature is lowered, signals for a second rhodium species appear. At 273K, the Py-6-H proton gives a broad singlet (δ 9.52), but at 223K it has resolved into two doublets (δ 9.5 and 9.71, ratio 15:1). There are also extra signals for other peaks in the spectrum, which suggests either that there are two diastereomers present or that some acetone coordination occurs. For the iridium complex, only one set of complex signals are observed at 223K, with the coordinated water signal seen at ca. δ 8.2. Even if two diastereomers of (**2.69**, $R = ^iPr$) are present in solution, the energy difference between them must be large enough to shift the equilibrium ratio heavily in favour of one isomer, presumably that with the isopropyl oriented towards the water ligand, rather than at the Cp* ring (**Figure 2.26**).

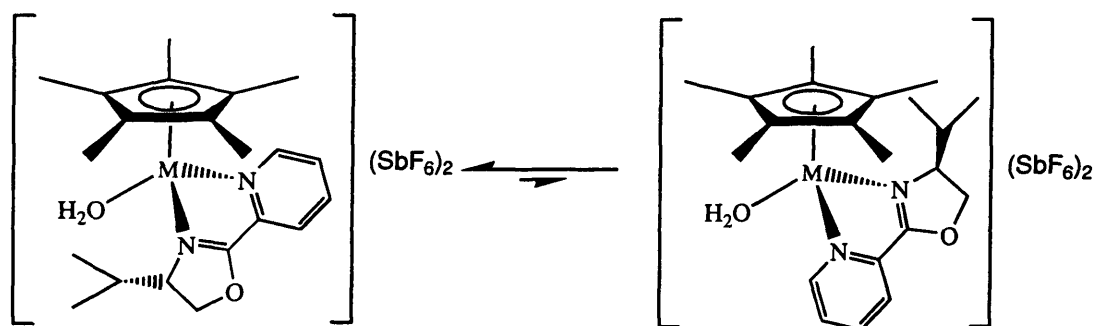


Figure (2.26)

As with bis-oxazoline complexes (**2.30 - 2.37**), the 1H NMR spectra of the pymox-containing aqua-complexes (**2.63 - 2.72**) in d_6 -acetone feature an extra signal in the δ 6-7 region, which appears to be due to coordinated HOD. For both ruthenium complexes (at room temperature) and rhodium complexes (at low temperature), this minor signal is observed at slightly *higher* frequency (up to 0.1 ppm) than for the major coordinated H_2O signal. As observed earlier, addition of excess H_2O leads to the disappearance of the higher frequency signal, whilst with excess D_2O , both singlets disappear. Addition of *small* quantities of D_2O (*i.e.* several equivalents) to the NMR sample results in a proportional increase in the higher frequency water signal, with an overall decrease in the integration of the pair of singlets, with respect to the other complex signals. The same effect is observed with complexes of the chiral pymox ligands and of the achiral Me_2 -pymox, so can not be attributed to diastereomeric complexes. As described in section (2.2.1), high field deuterium

isotope shifts have been observed before, often in systems where hydrogen-bonding occurs.¹⁰⁵

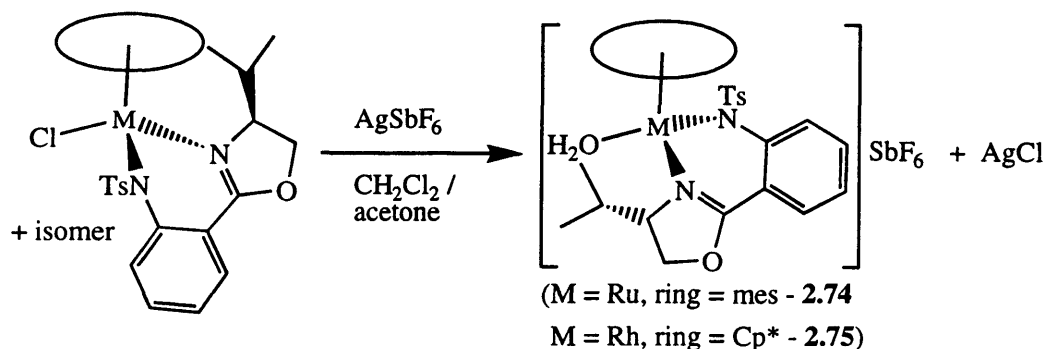
The electrospray mass spectra of complexes (2.63-2.68) in MeOH/water contain several ion patterns, none of which contain an aqua ligand (Tables 2D.14). A typical example is (2.65, R = ⁱPr), for which the major ion is at m/z 649, attributed to $[\{\text{Ru}(\text{}^i\text{Pr-pymox})(\text{mes})\}\text{SbF}_6]^+$. A minor pattern (15%) at m/z 429 is due to $[\text{Ru}(\text{OH})(\text{}^i\text{Pr-pymox})(\text{mes})]^+$, whilst another ion pattern at m/z 411 (50%) is due to $[\{\text{Ru}(\text{}^i\text{Pr-pymox})(\text{mes})\}\text{-H}]^+$. The dication appears to hold on to one counter-ion in the mass spectrometer, probably through ion-pairing. Electrospray mass spectroscopy of complexes (2.69 - 2.72) gives similar results; in MeOH / water solution, the major ions observed are due to $[\{\text{M}(\text{pymox})\text{Cp}^*\}\text{+SbF}_6]^+$. No doubly-charged ions were observed (with or without coordinated water, which is apparently too weakly held).

If complexes (2.63 - 2.72) were to be used as Lewis acid catalysts, it was important to establish whether they could coordinate potential substrates. This was tested with methacrolein ($\text{CH}_2=\text{C}(\text{Me})\text{CHO}$), a typical Diels-Alder dienophile. Addition of methacrolein to a suspension of (2.65, R = ⁱPr) in dichloromethane led to rapid formation of a yellow solution. When observed by ¹H NMR in CD₂Cl₂, the addition of methacrolein led to a gradual formation of a second ruthenium complex. In addition to the four signals observed for the excess free methacrolein, minor peaks were also observed, shifted somewhat downfield, due to coordinated methacrolein (most obvious were two multiplets at δ 6.5 and 6.6 due to the vinylic protons). With six equivalents of dienophile, the ratio of water : methacrolein coordinated was ~ 1:1, so it is likely that under catalytic conditions (with 20-100 equivalents of dienophile), the methacrolein-coordinated species would dominate.

The complex $[\text{Ru}(\text{OH}_2)(\text{}^i\text{Pr-animox})(\text{mes})](\text{SbF}_6)_2$ (2.73) was prepared analogously to the pymox-containing aqua cations, but its solution chemistry is rather more complex. Equilibria between protonated/deprotonated and water/solvent coordinated species exist, which are not easy to fully characterise. As the complex proved to be a poor catalyst for the Diels-Alder reaction (see Chapter Three), a thorough investigation of the solution chemistry of (2.73) was not attempted.

Aqua complexes $[\text{M}(\text{OH}_2)(\text{}^i\text{Pr-NTs-animox})(\text{ring})]\text{SbF}_6$ (M = Ru, ring = mes - 2.74; M = Rh, ring = Cp* - 2.75) were synthesised from (2.57) and (2.58) respectively, by treatment with AgSbF₆, in 7:1 CH₂Cl₂ / acetone (Scheme 2.23). As

described previously, the AgCl by-product was filtered out and the products were crystallised from acetone / ether, giving thin yellow needles.



Scheme (2.23)

The complexes (2.74) and (2.75) were characterised by ^1H NMR (Table 2D.12), mass spectroscopy and elemental analysis (Table 2D.14). The ^1H NMR spectrum of the ruthenium complex (2.74) in d_6 -acetone, at 295 K, indicates that exchange of both diastereomers and water are fast on the NMR timescale. At this temperature, only the signals due to the mesitylene ring (δ 2.27 and 5.68) are sharp; all signals due to the NTs-animox ligand are extremely broad, with the multiplicities unresolved. No coordinated water signal is seen, with free water in solution observed as a broad resonance at δ 2.9. On cooling the sample to 253 K, coordinated water is observed as a singlet at δ 6.85, with free water seen at δ 3.3. Interestingly, only one set of signals due to the complex is seen; *i.e.* only one diastereomer is present. Doublets due to the ^1Pr -groups are found at δ 0.66 and 1.00, somewhat lower frequency than for the major isomer of the corresponding chloride complex and no doublets are observed near δ 0, as were found in (2.57). The oxazoline ring (δ 4.8 - 5.0) and $\text{C}_6\text{H}_3\text{Me}_3$ signals are significantly deshielded from the neutral precursor complex. It is unclear why the spectrum is so broad at room temperature; probably, diastereomer interconversion is occurring, but the ratio is clearly very high at 253K. It is possible that the signals due to the minor isomer have not yet resolved at the low temperature and as they are present in such a low amount, they are not readily seen. The isomer ratio may also change with temperature.

The ^1H NMR spectrum of the rhodium complex (2.75) (in d_6 -acetone at room temperature) shows only one isomer, with all NTs-animox and Cp^* signals well resolved. No signal is found due to coordinated water at room temperature, but on cooling the sample to 213 K, a broad singlet is observed at δ 6.79. No trace of a

second diastereomer is observed, even at this low temperature. No discernible change in line-width is observed. The presence of independent signals for free and coordinated water indicates that water exchange and as a consequence, epimerisation at the metal, is not occurring on the NMR timescale. Most of the signals due to NTs-animox are within 0.1 ppm of those for the ruthenium analogue (**2.74**) (at 253K), which suggests that if epimerisation is occurring, the thermodynamic equilibrium ratio is heavily in favour of one isomer. To assign the configuration at the metal centre of (**2.75**), a NOESY experiment was run, at room temperature; some of the important structure-elucidating nOes are shown in **Figure (2.27)**.

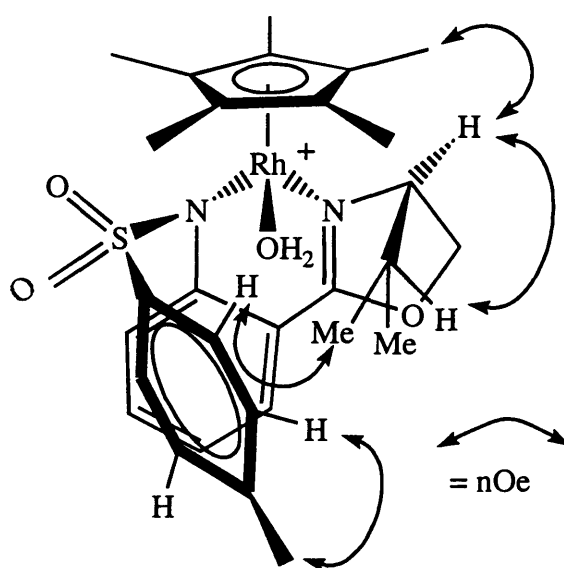


Figure (2.27)

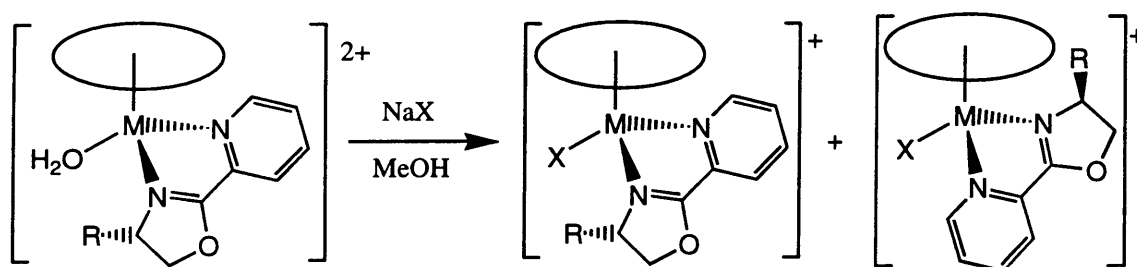
The most important nOes are those between the NCH signal (δ 4.88) and that for the Cp* ring (δ 1.68) and between the lowest frequency CHMe₂ signal (δ 0.73) and the C-2/6-H doublet of the tosyl ring (δ 7.56). No nOes are seen from the ⁱPr-group to the Cp* ring, which supports the theory that the equilibrium isomer ratio is very high. These results indicate that in (**2.75**), the ⁱPr is oriented away from the bulky Cp* ring, such that one MeCHMe' group is close to the tosyl group, which is presumably oriented below the H₂O ligand, as shown. The configuration at rhodium is thus (R), based on the priority: arene > OH₂ > N(Ts) > N(ox).^{86, 87} As the resolved NMR spectra of (**2.74**) and (**2.75**) are so similar, it is assumed that the former is also (R)-configured at the metal.

There is a considerable difference in diastereoselectivity between complexes [MCl(NTs-animox)(ring)] and [M(OH₂)(NTs-animox)(ring)]SbF₆, the major isomers

in the former having the ⁱPr-group oriented *towards* the η-ring; whilst in the latter, only one isomer is observed for rhodium and ruthenium, that with the ⁱPr-group oriented *away* from the η-ring. The reasons for the large differences are unclear, since for both chloride and aqua complexes, the thermodynamic equilibrium ratio has been obtained in each case.

As demonstrated in this section, the diastereoselectivity of pymox complexes with bulky η-rings and/or large R-substituents is very high; even when exchange of water ligands occurs, the resultant equilibrium ratios are still high. In the concluding part of this chapter, the focus of the work will be on pymox complexes with larger halides or N-donor ligands at the sixth coordination site of the metal, the diastereoselectivity and configurational stability being of interest. By increasing the size of the halide ligand from chloride to iodide, the diastereoselectivity of formation of the pymox complexes is expected to change, since there will be a greater steric interaction between the R-substituent and the halide in the (R_M) isomers.

Halide complexes [MX(R-Pymox)(ring)]SbF₆ (M = Ru, Rh; X = Br, I; ring = mes, Cp*; R = ⁱPr, Ph - **2.76-2.79** - see **Table 2.16**) were synthesised by treatment of the appropriate aqua complex with KBr or NaI in methanol, at room temperature. The reactions were instantaneous, an immediate colour change being observed, giving the desired bromide and iodide complexes quantitatively (**Scheme 2.24**).



Scheme (2.24) (R_M) (2.76 - 2.79) (S_M)

Table (2.16): Complexes [MX(R-pymox)(ring)]SbF₆

Code	M	X	R	ring
2.76	Ru	Br	ⁱ Pr or Ph	mes
2.77	Ru	I	ⁱ Pr or Ph	mes
2.78	Rh	Br	ⁱ Pr	Cp*
2.79	Rh	I	ⁱ Pr	Cp*

All complexes were characterised by ^1H NMR, mass spectroscopy and microanalysis (Tables 2E.2 - 2E.5) and in one case, X-ray crystallography. NMR spectra were obtained of both crude and recrystallised products, in order to establish the diastereomer ratios. The ^1H NMR spectrum (in d_6 -acetone) of the crude solid of the bromide complex (**2.76**, $\text{R} = \text{}^i\text{Pr}$) showed two distinct sets of arene and pymox signals in a ratio of 55:45. The resonances due to the minor isomer very closely resemble those due to the chloride analogue (**2.45**, $\text{R} = \text{}^i\text{Pr}$), most corresponding chemical shifts within 0.3 ppm; *e.g.* the signals due to CHMe_2 groups are found at δ 1.07 and 0.83 for the chloride complex, whilst those due to the minor bromide isomer are observed at δ 1.09 and 0.83. The signals due to the major isomer, however, are quite different; the CHMe_2 signals being observed at δ 1.06 and 1.22. The minor isomer is thus assigned an (R_{Ru}) configuration (*i.e.* the isopropyl is oriented towards the bromide) with the major isomer having an (S_{Ru}) configuration. Recrystallisation of the sample from acetone/ether gave a microcrystalline solid, which showed a 1:1 mixture of diastereomers, as determined by NMR, the isomer ratio not changing after several days at room temperature. It is clear that replacing chloride with bromide has a large effect on the diastereoselectivity in these pymox complexes, due to their relative steric influences.

The iodide complex (**2.77**, $\text{R} = \text{}^i\text{Pr}$) was prepared in methanol with two equivalents of NaI, and the crude ^1H NMR spectrum was obtained in CD_2Cl_2 . This shows a 13:2 mixture of isomers, the chemical shifts very similar to those of the bromide analogue, with the minor set of signals closely resembling those for the single isomer of the chloride analogue (**2.45**, $\text{R} = \text{}^i\text{Pr}$). The sample was recrystallised from CH_2Cl_2 /ether, which gave crystals suitable for an X-ray structure determination. The structure of the cation of (**2.77**, $\text{R} = \text{}^i\text{Pr}$) is shown in Figure (2.28) and selected bond distances and angles are given in Table (2.17). In the crystallised isomer of (**2.77**, $\text{R} = \text{}^i\text{Pr}$), the isopropyl-group is oriented away from the sterically large iodide ligand, such that the configuration at the metal centre is (*S*) {based on the priority $\text{I} > \text{arene} > \text{N}(\text{ox}) > \text{N}(\text{py})$ }. The Ru–N bond distances and the N–Ru–N chelate angle are statistically the same as those of the chloride analogue, but the Ru–I bond distance {2.702(2) Å} is significantly longer than the Ru–Cl distance of (**2.45**, $\text{R} = \text{}^i\text{Pr}$) {2.402(2) Å}, as expected.

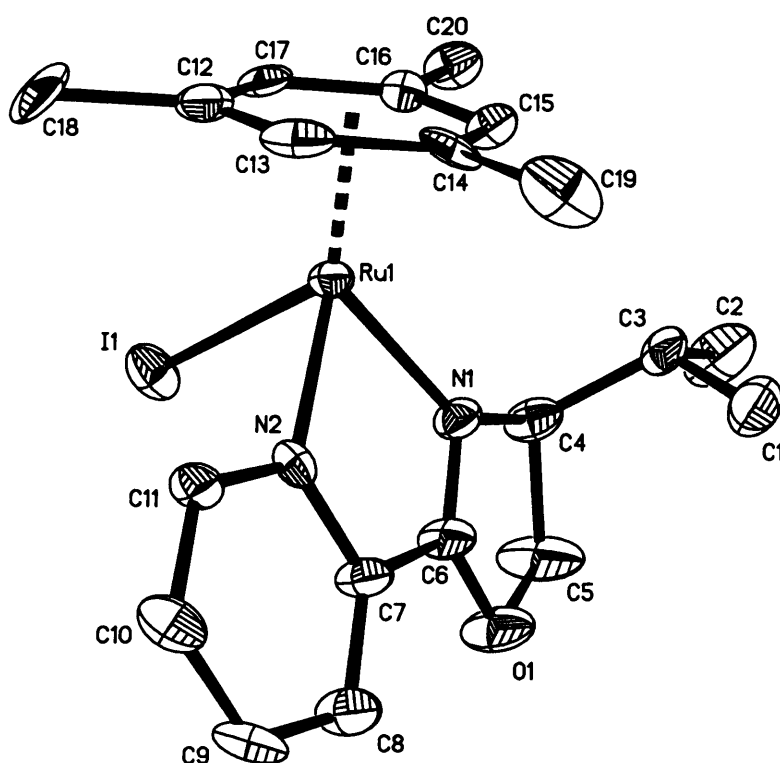


Figure (2.28)

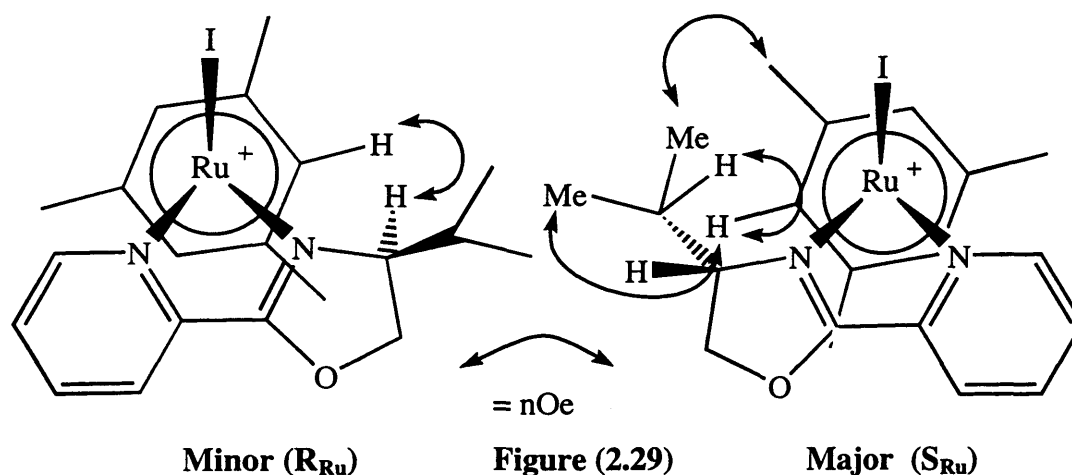
Table (2.18): Selected bond distances (Å) and an angle (°) of (2.77, R = *i*Pr)

Ru(1)–N(1)	2.109(11)	Ru(1)–N(2)	2.110(11)
Ru(1)–I(1)	2.702(2)	N(1)–Ru(1)–N(2)	76.3(5)

The ^1H NMR spectrum, in CD_2Cl_2 , of the crystals of (2.77, R = *i*Pr) shows the same 13:2 ratio of isomers obtained in the crude mixture, which means either that this was an equilibrium ratio of exchanging isomers or the crystals were a statistical (13:2) mixture of both isomers (insufficient sample remained to separate out crystals with different morphologies, and hence run the NMR spectra). When the complex was prepared using only *one* equivalent of NaI, a crude isomer ratio of 6:4 was found in both CD_2Cl_2 and d_6 -acetone. Crystallisation of this sample gave a 16:9 ratio, with the mother liquors enriched in the more soluble isomer, as shown by NMR. These ratios remained constant over several days, indicating that exchange of isomers of (2.77, R = *i*Pr) is slow, even on a chemical timescale.

As a means of investigating possible epimerisation in (2.77, R = *i*Pr), and of confirming the structures of each isomer, a phase-sensitive NOESY experiment was run on a 6:4 mixture of isomers, in d_6 -acetone (in this experiment, correlations due to

chemical exchange of isomers are distinguished from genuine nOes). No cross-peaks due to chemical exchange were found, but several useful nOes were observed (**Figure 2.29**). For the major isomer, nOes were observed between the highest frequency MeCHMe' signal and that due to the $\text{C}_6\text{H}_3\text{Me}_3$ ring, and from the $\text{C}_6\text{H}_3\text{Me}_3$ signal to both the lower frequency MeCHMe' resonance and that due to CHMe_2 . For the minor isomer, an nOe was observed between the NCH signal and that of $\text{C}_6\text{H}_3\text{Me}_3$, whilst no nOe was found between the mesitylene ring and the isopropyl-group. These results confirm that in the minor isomer, the isopropyl-group is oriented towards the iodide (R_{Ru}), whilst in the major isomer it is oriented towards the mesitylene ring, as found in the X-ray structure (S_{Ru}).



To further investigate the diastereoselectivity and configurational stability of the halide complexes, the formation of the iodide complex (**2.77**, $\text{R} = {}^i\text{Pr}$) was monitored by ${}^1\text{H}$ NMR, by addition of one equivalent of NaI to the aqua-complex (**2.65**, $\text{R} = {}^i\text{Pr}$), in $\text{d}_4\text{-MeOH}$. After five minutes, 85% conversion to iodide was observed and after twenty minutes the reaction was complete. At each stage of the reaction, the ratio of isomers formed ($\text{S}_{\text{Ru}}:\text{R}_{\text{Ru}}$) was 9:2; this was unchanged even after one hour. Overnight, extensive precipitation occurred; the ${}^1\text{H}$ NMR of the crystals in $\text{d}_4\text{-MeOH}$ showed a 4:1 mixture of isomers (*i.e.* much like the initial ratio), which changed very slowly over one week to 6:4. The mother liquor was also enriched in the minor isomer, which indicates that exchange of isomers occurs very slowly for (**2.77**, $\text{R} = {}^i\text{Pr}$) in methanol.

A similar experiment was performed with *two* equivalents of NaI added to a solution of the aqua complex in $\text{d}_4\text{-MeOH}$. By ${}^1\text{H}$ NMR, the (S):(R) isomer ratio was 7:2, changing over 15 minutes to 2.4:1, accompanied by precipitation of $\sim 75\%$ of the

expected (**2.77**, **R = ⁱPr**). The ¹H NMR spectrum of the crystals in CD₂Cl₂ shows only signals due to the major (S)-isomer (*i.e.* ⁱPr oriented towards mesitylene). No trace of the minor isomer was found, even after several days at room temperature. Precipitation of much of the (S)-isomer from the crude mixture presumably occurred before the initial NMR spectrum was obtained, thus giving a misleading picture of the initial diastereomer ratio, which might have been up to 12:1. These results are consistent with S_N2-type attack of iodide on the aqua complex, *i.e.* giving *inversion* of configuration at the metal. Slow epimerisation then occurs in methanol, to give more of the minor (R)-isomer (*i.e.* ⁱPr oriented towards iodide), but as the ratio never reaches 50:50, the (S) isomer is presumably the thermodynamically, as well as kinetically, favoured product.

The crude isomer ratio of the bromide complex (**2.76**, **R = Ph**) was 78:22, as deduced from ¹H NMR, in which two distinct sets of complex signals can be observed. The chemical shifts due to protons in each diastereomer are very close to those of the chloride analogue (**2.45**, **R = Ph**), signals due to corresponding isomers within 0.1 ppm in most cases, though with the major and minor being reversed for the bromide. Thus, in the bromide complex, the phenyl group in the major isomer is oriented towards the mesitylene ring. Crystallisation of the mixture from CH₂Cl₂/ether gave only the major isomer, as shown by ¹H NMR, no trace of the minor isomer being observed, even after several days. Evaporation of the mother liquor yields a sample enriched in the minor isomer, which indicates that, as with the chloride analogue, the configuration at ruthenium is stable at room temperature. The (S)-isomer, *i.e.* with phenyl oriented towards mesitylene, is clearly more favoured than in the corresponding ⁱPr-pymox complex (as found for the corresponding chloride complexes).

The complex [RuI(Ph-pymox)(mes)]SbF₆ (**2.77**, **R = Ph**), like the ⁱPr-pymox analogue, was found to be more configurationally labile than the corresponding chloride and bromide complexes. After preparation from the aqua complex (**2.65**, **R = Ph**) in MeOH, the ¹H NMR spectrum of the crude iodide (in CD₂Cl₂) shows a 2:1 mixture of diastereomers. By comparison of the spectra of the chloride and bromide analogues, the major product is deduced as the (S)-isomer (with phenyl oriented towards the mesitylene). Recrystallisation of the mixture (from CH₂Cl₂/ether) was unsuccessful and the whole mixture was evaporated (after several weeks in solution).

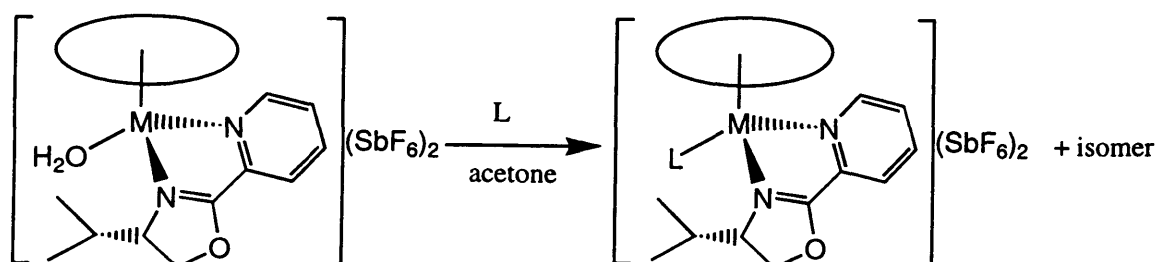
The ^1H NMR spectrum of the residue (containing all of the crude sample) shows a 6:7 mixture of diastereomers, with the major product now the (R)-isomer. This is indicative of slow epimerisation in solution, giving the (R)-isomer, as found with (2.77, R = ^iPr). In this case, the thermodynamic product appears to be that with the substituent oriented towards the iodide, rather than the mesitylene.

The rhodium complexes $[\text{RhX}(^i\text{Pr-pymox})\text{Cp}^*]\text{SbF}_6$ (X = Br - 2.78; X = I - 2.79) were both formed highly diastereoselectivity, as shown by ^1H NMR (Tables 2E.2 - 2E.3). For the bromide complex, only one isomer was observed, whilst the iodide was formed as > 97% one isomer. For both complexes, the NMR spectra are similar to those of the chloride analogue, with most corresponding pymox signals within 0.1 ppm, which implies that the favoured isomer in each case has the ^iPr -group oriented towards the halide. The main difference in chemical shift, in each case, is found for the Cp* signal (δ 1.73 for 2.49, R = ^iPr and δ 1.95 for 2.79). To confirm the structure of the major isomer of the iodide complex (2.79), a NOESY spectrum was run. This shows correlations only in the major isomer, the most important being an nOe between the NCH signal and that due to the Cp* ring. Accordingly, no nOes are seen between the ^iPr -group and the Cp*, which indicates that the former is oriented towards the iodide, and hence the major isomer has the same structural arrangement as the chloride analogue {although the configuration at rhodium will formally be (R), rather than the (S) found for 2.45}. The same situation is presumed for the bromide complex (2.78).

The variation of diastereoselectivity with size of halide is clearly different for rhodium complexes (2.78/2.79) than for the ruthenium analogues. For rhodium, the thermodynamic products have the isopropyl-substituent oriented towards the halide, in each case, rather than towards the Cp*, possibly because of greater steric hindrance between the ^iPr and the Cp* group. With ruthenium, the isomers with substituent oriented towards the arene are more favoured with the larger halides.

A series of substitution complexes $[\text{ML}(^i\text{Pr-pymox})(\text{ring})](\text{SbF}_6)_2$ (2.80 - 2.84; M = Ru, ring = mes; M = Rh, ring = Cp*; L = MeCN, 4-Me-py, 2-Me-py) were synthesised by treatment of the aqua complexes (2.65, R = ^iPr) or (2.69, R = ^iPr) with ligand L in acetone (Scheme 2.25). All of substitution complexes (2.80 - 2.84) were prepared in an NMR tube, such that the rates of reaction and any changes in diastereomer ratios with time could be accurately assessed by ^1H NMR (Tables 2E.4 -

2E.5, see experimental). Some reactions were repeated on a preparative scale and the complexes were then also characterised by microanalysis and mass spectrometry (Table 2E.6).



Scheme (2.25) (2.80) - M = Ru, ring = mes, L = MeCN
 (2.81) - M = Rh, ring = Cp*, L = MeCN
 (2.82) - M = Ru, ring = mes, L = 4-Me-py
 (2.83) - M = Rh, ring = Cp*, L = 4-Me-py
 (2.84) - M = Ru, ring = mes, L = 2-Me-py

The acetonitrile complex (2.80) was synthesised by addition of one equivalent of MeCN to a solution of the aqua complex (2.45, R = ⁱPr) in CD₂Cl₂/d₆-acetone (10:1), leading to a rapid replacement of the aqua ligand by MeCN. The coordinated water signal (ca. δ 5.4) is no longer present and a new 3H singlet is observed at δ 2.30, assigned to the MeCN ligand. Most of the other complex signals remain essentially unchanged, the main difference being a 0.15 ppm high field shift of the py-6-H signal. As with the aqua precursor, only one diastereomer of (2.80) is observed, assumed to have the ⁱPr-group oriented towards the nitrile, which should be no more sterically demanding than a water ligand, due to the linear nature of N≡C-Me. Acetonitrile is found to be a fairly strong ligand, compared to water. The FAB mass spectrum shows an ion pattern (~ 20%) due to [{Ru(NCMe)(ⁱPr-pymox)(mes)} + SbF₆]⁺ (water ligands are not seen in FAB M/S of the aqua complexes). The nitrile is also not displaced by addition of excess methacrolein to a solution of (2.80) in CD₂Cl₂, as shown by ¹H NMR, which indicates that (2.80) will not be a useful catalyst for the Diels-Alder reaction (nitriles are often employed as weak ligands in catalytically active transition metal complexes¹¹⁰).

The complex [Rh(NCMe)(ⁱPr-pymox)Cp*](SbF₆)₂ (2.81) was found to be more labile than its ruthenium analogue. It was prepared by addition of 1.5 equivalents of MeCN to the aqua complex (2.69, R = ⁱPr), in d₆-acetone. The room

temperature ^1H NMR spectrum, obtained immediately on addition, showed two rather broad sets of pymox-containing signals, in an $\sim 3:2$ ratio. Singlets are observed at δ 2.1 and 2.4, which are assigned to free and coordinated MeCN, respectively. On cooling to 233 K, both sets of signals are well resolved, the ratio confirmed as 3:2. The chemical shifts of the minor signals are consistent with those of the aqua-complex (**2.69**, $\text{R} = \text{}^i\text{Pr}$), with a singlet (2H w.r.t. minor species) observed at δ 6.95. A singlet is observed at δ 2.45 (3H w.r.t. major set of signals), which indicates that the major species present is the desired (**2.81**). Addition of a further 1.5 equivalents of MeCN to the solution at 233 K (containing 5 equivalents of H_2O) increases the proportion of the major species, such that the ratio is 5:1, confirming the major product is the acetonitrile complex. It is apparent that MeCN is a somewhat stronger ligand than water, but an excess is required to drive the equilibrium completely over to (**2.81**). At room temperature, exchange of water and nitrile is rapid on the NMR timescale, the process frozen out at low temperature. Both the aqua and MeCN complexes, however, appear to be highly diastereoselective, only one isomer of each being observed by ^1H NMR.

The synthesis of $[\text{Ru}(4\text{-Me-py})(\text{}^i\text{Pr-pymox})(\text{mes})](\text{SbF}_6)_2$ (**2.82**) was monitored by ^1H NMR (Table 2E.4). To a solution of (**2.65**, $\text{R} = \text{}^i\text{Pr}$) in d_6 -acetone was added 1.5 equivalents of 4-Me-py, the NMR spectrum being recorded immediately. Thus, after 7 mins, 53% conversion to (**2.82**) was observed, the reaction then proceeding smoothly, such that the yield was $> 97\%$ after 45 mins. In all spectra, signals due to two isomers of (**2.82**) can be observed, in a ratio of 2:1 in each case (the ratio remains the same after several days in solution). Recrystallisation of the sample by addition of diethyl ether to an acetone solution gave (after several weeks) a 13:9 mixture of isomers. Evaporation of the mother liquor afforded a 7:11 mixture of diastereomers (*i.e.* the ratio had reversed), indicating that epimerisation of (**2.82**) occurs very slowly, even on a chemical timescale.

Signals due to each isomer of (**2.82**) can readily be distinguished; in particular, a significant difference is found for the isopropyl groups. In the major isomer, signals due to CHMe_2 are observed as doublets at δ 1.28 and 1.01, whilst the corresponding signals in the minor isomer are seen at δ 1.14 and 0.28. The methyl giving the low frequency doublet is presumably shielded by the aromatic ring current of the 4-Me-py

ligand, indicating that the minor isomer has the isopropyl group oriented towards the 4-Me-py, rather than towards the mesitylene ring. This was confirmed by a 2D phase-sensitive NOESY experiment in d_6 -acetone, using a 13:9 mixture of isomers. Structure-confirming nOes are observed in both isomers (Figure 2.30). In the minor isomer, nOes are found between the low frequency *MeCHMe'* signal and both 2H doublets of the 4-methyl pyridine, providing good evidence that a ring-current is operating. In the major isomer, nOes are observed between the ^1Pr -group and the mesitylene ring, indicating a close interaction. Thus, the major isomer can be assigned an (R)-configuration at the metal centre {based on the priority: arene > N(ox) > N(py-ox) > N(4-Me-py)} and the minor an (S)-configuration. No correlations due to chemical exchange were observed, confirming that epimerisation is very slow on the NMR timescale.

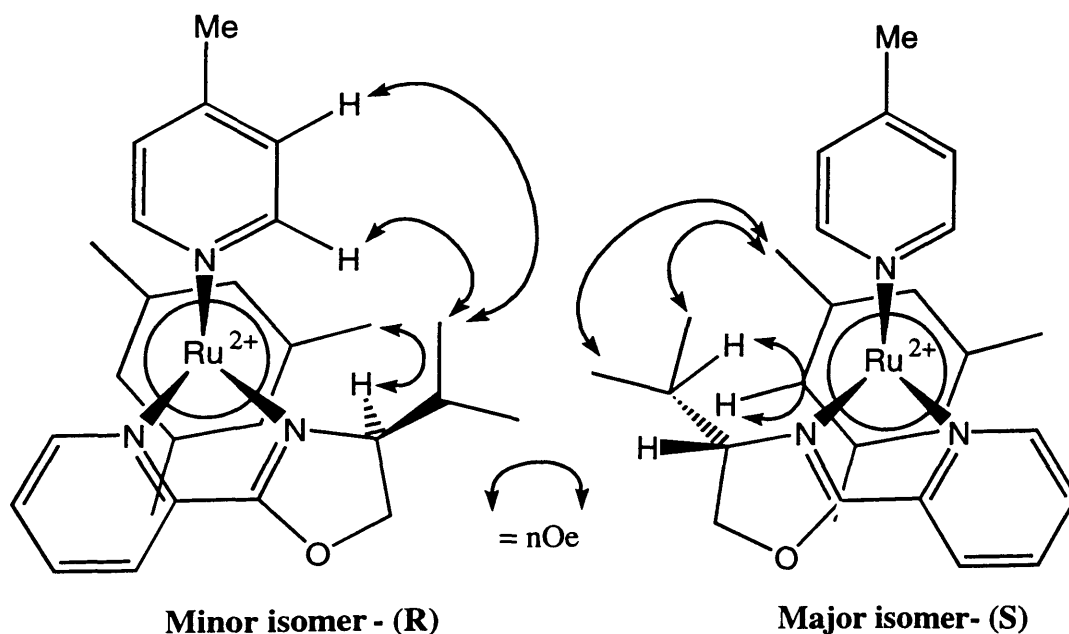


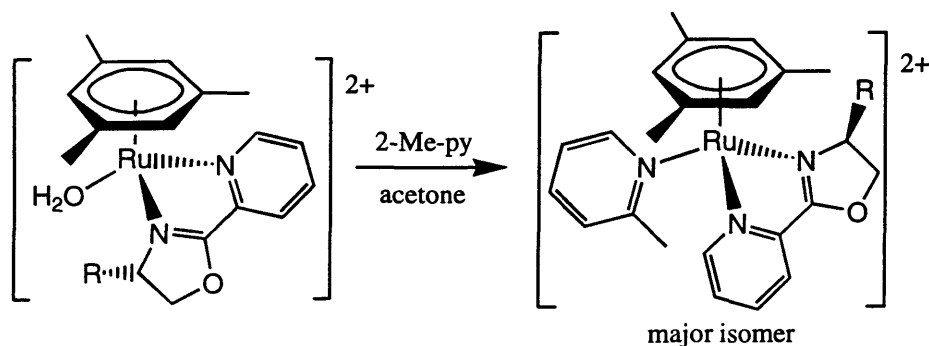
Figure (2.30)

The rhodium/4-Me-py complex (**2.83**) was prepared in the same way as the ruthenium analogue, with 1.5 equivalents of 4-Me-py added to a solution of (**2.69**, $\mathbf{R} = ^1\text{Pr}$) in d_6 -acetone. As expected, the reaction was considerably faster for rhodium than for ruthenium, complete reaction observed after five minutes. At this stage, ^1H NMR signals due to two diastereomers were observed, in a ratio 3:1, changing to 4:1 after 20 minutes. The ratio was then constant for several days, indicating that the equilibrium position had been reached. The chemical shifts due to the major isomer are very similar to those of the minor isomer of the ruthenium analogue (**2.82**),

indicating that the major isomer of (**2.83**) is that with the ⁱPr-group oriented towards the 4-Me-py, rather than towards the Cp*. Accordingly, signals due to CHMe₂, in the major isomer, are observed at δ 1.17 and 0.47 (the latter consistent with a ring current effect from the 4-Me-py ligand).

Steric factors presumably result in a greater preference for the (S)-isomer (ⁱPr → 4-Me-py) of the rhodium complex (**2.83**) than for the corresponding isomer of the ruthenium analogue. As with the rhodium-iodide and bromides, there may be greater steric hindrance between the ⁱPr-group and the Cp* than in the corresponding arene-ruthenium complex.

The complex [Ru(2-Me-py)(ⁱPr-pymox)(mes)](SbF₆)₂ (**2.84**) was synthesised by addition of one equivalent of 2-Me-py to a solution of the aqua complex (**2.65**, R = ⁱPr) in d₆-acetone (Scheme 2.26), the reaction monitored by ¹H NMR. The reaction was considerably slower than that with 4-Me-py, presumably due to the greater steric hindrance of the methyl group close to the pyridine nitrogen. Hence, only 20% conversion was observed after 15 mins, rising slowly to 53% after 140 mins.



Scheme (2.26)

At all times, ¹H NMR signals due to the aqua complex and two diastereomers of (**2.84**) are observed. After 15 mins, the isomer ratio was 5:2, but the proportion of the major isomer subsequently increased, such that the ratio was 7:1 after 140 mins. At this point, the reaction appeared to have reached an equilibrium between water and 2-Me-py coordinated (note: 1.5 equivalents of free water were observed in solution). Subsequent addition of two extra equivalents of 2-Me-py to the solution gave a 3:1 mixture of coordinated 2-Me-py / H₂O, the isomer ratio increasing to 9:1. Many of the NMR signals for the two diastereomers are rather similar. The main differences are found with the mesitylene, py-6-H and CHMe₂ signals, the latter observed at δ 0.93 and 1.28 for the major isomer and at δ 0.56 and 1.15 for the minor. By analogy with

the 4-Me-py complex (**2.82**), the isomer with the low frequency *MeCHMe*' doublet is that where the ⁱPr is oriented towards (and experiencing a ring-current effect from) the monodentate ligand, whilst the pair of *CHMe*₂ groups giving doublets centred about δ 1 are those oriented towards the η -ring. Thus, one would predict that the major isomer of (**2.84**) has the ⁱPr-group oriented towards the mesitylene, rather than towards the 2-Me-py. This is expected, since steric clashes between the ⁱPr and the methyl substituent on the py ligand are likely to be severe. Both possible sites for the ⁱPr will be hindered, which would explain the lower affinity of the ruthenium system for 2-Me-py, compared to 4-Me-py. Recrystallisation of the 3:1 mixture of (**2.65/2.84**) from acetone/ether gave a 10:3 mixture of the same products, as shown by NMR, but this time none of the minor isomer of (**2.84**) was observed, indicating that the major isomer is the thermodynamically favoured product.

To summarise the substitution chemistry of the pymox complexes described above, there are three main conclusions:

1. Increasing the size of the ligand at the sixth coordination site can dramatically alter the observed diastereoselectivity; the isomer where the substituent is oriented *towards* the η -ring becomes more favoured with the more bulky ligands (particularly with ruthenium).
2. With rhodium, the isomer with substituent oriented *away* from the η -ring is the thermodynamic product in each case. With ruthenium, the thermodynamic preference depends on the size of the ligand.
3. With ruthenium, substitution of bromide or iodide for water appears to proceed by an S_N2 mechanism, giving predominantly inversion of configuration at the metal.

(2.3) - Experimental

All reactions were carried out under an atmosphere of nitrogen, except for some purely organic reactions, or unless stated otherwise. Reactions were worked up in air. Degassed solvents were used for the reactions and were dried from the appropriate drying agents:

- a) Dichloromethane from calcium hydride
- b) Diethyl ether from sodium / benzophenone
- c) Chloroform from calcium sulphate
- d) Acetone from calcium sulphate
- e) Methanol from sodium
- f) Hexane from sodium / benzophenone

^1H and ^{13}C NMR spectra were obtained using Bruker 250, 300 and 400 MHz spectrometers, with CDCl_3 , CD_2Cl_2 , d_6 -acetone or d_4 -MeOH as solvent, as indicated in the text. Chemical shifts were recorded in ppm (on δ scale for ^1H NMR, with tetramethylsilane or protonated form of NMR solvent as internal reference). FAB mass spectra were obtained on a Kratos concept mass spectrometer using an NOBA matrix. Electrospray mass spectra were obtained using the solvents MeOH, MeOH/water or THF. Microanalyses were performed by Butterworth laboratories Ltd.

Preparation of Chiral Oxazoline Ligands

The ligands ^iPr -box,³⁴ ^iPr -bop,²¹ R-benbox (R = ^iPr and Ph),¹⁹ R,R'-pymox (R, R' = Me, Et, ^iPr , ^tBu , Ph or Bn)^{19, 26} and ^iPr -phenmox¹⁹ were prepared by literature methods, or by modifications thereof. Other ligands were prepared using methods based on those in the literature, as described below. The amino alcohols (R)-2-amino-1-butanol, (1R,2S)-1-amino-2-indanol and 2-amino-2-methyl-1-propanol were purchased from Aldrich. Other amino alcohols $\text{H}_2\text{NCHRCH}_2\text{OH}$ (R = ^iPr , ^tBu , Ph or Bn) were obtained by NaBH_4/I_2 reduction of the corresponding amino acid, according to the method of Meyers.¹⁶ Pyridine-carboxyimide was prepared from cyanopyridine, according to the literature procedure.¹⁷ All other reagents were obtained from Aldrich and Lancaster synthesis.¹⁹

Preparation of Et-benbox (1.14, R = Et)

Using the general method of Bolm,¹⁹ a solution of 1,2-dicyanobenzene (1.28 g, 10 mmol) and (R)-2-amino-1-butanol (2.8 cm³, 30 mmol) in chlorobenzene (30 cm³) was added to anhydrous ZnCl₂ (70 mg, 0.5 mmol) and the solution was refluxed for one day, then evaporated. The crude residue was dissolved in CH₂Cl₂ (30 cm³) and the solution was extracted with three 20 cm³ portions of water. The aqueous layers were extracted with CH₂Cl₂ (30 cm³) and the combined organic layers were dried over MgSO₄. The solution was concentrated, leaving a pale-green coloured oil, that was pure by ¹H NMR. Yield = 2.42 g (89%).

¹H NMR: δ 1.04 (t, 6H, *J* 7 Hz, CH₂Me), 1.62 (m, 2H, CH₂Me), 1.78 (m, 2H, CH₂Me), 3.87 (t, 2H, *J* 10 Hz, OCH), 4.20 (m, 2H, NCH), 4.41 (t, 2H, *J* 10 Hz, OCH), 7.46 (m, 2H, Ar-H), 7.72 (m, 2H, Ar-H). FAB mass spectrometry: *m/z* 273 (MH⁺).

Preparation of Indanyl-pymox (2.39)

A mixture of pyridine-carboxyimide (273 mg, 2.0 mmol), (1R,2S)-1-amino-2-indanol (300 mg, 2.0 mmol), concentrated HCl_(aq) (1 drop) and CHCl₃ (1 cm³) was stirred overnight at 60°C. The resulting yellow paste was purged with N₂, to remove any remaining MeOH and ammonia (by-products of the reaction) and then evaporated in vacuo. The crude product was chromatographed on silica, with CH₂Cl₂/MeOH (95:5) as eluents. Evaporation of the fore-run gave an oily product; washing with hexane afforded an off-white solid, Yield = 376 mg (79%).

¹H NMR: δ 3.50 (m, 2H, CH₂Ar), 5.58 (ddd, *J* 10.5, 8, 2.5 Hz, OCH), 5.81 (d, 1H, *J* 8 Hz, NCH), 7.27 (m, 3H, Ar-H), 7.35 (ddd, 1H, *J* 8, 5, 1 Hz, py-5-H), 7.59 (dd, 1H, *J* 5.5, 3.5 Hz, Ar-H), 7.73 (dt, 1H, *J* 2, 8 Hz, py-4-H), 8.04 (d, 1H, *J* 8 Hz, py-3-H), 8.68 (dd, 1H, *J* 5, 1 Hz, py-6-H). FAB mass spectrometry: *m/z* 237 (MH⁺)

Preparation of ⁱPr-animox (2.41)

Using the general method of Fujisawa,⁴⁷ a solution of 2-amino-benzonitrile (0.827 g, 7 mmol) and (S)-valinol (2.107 g, 21 mmol) in chlorobenzene (21 cm³) was added to anhydrous ZnCl₂ (60 mg, 0.5 mmol) and the solution was refluxed for five days, then evaporated. The crude residue was dissolved in CH₂Cl₂ (30 cm³) and the solution extracted with three 20 cm³ portions of water. The aqueous layers were extracted with CH₂Cl₂ (30 cm³) and the combined organic layers dried over MgSO₄.

The solution was evaporated and the crude residue chromatographed on silica, with diethyl ether/petroleum ether (1:1) as eluent. Evaporation of the fore-run afforded the title compound as a white solid. Yield = 859 mg (60 %). $^1\text{H NMR}$: δ 0.94 (d, 3H, J 7 Hz, CHMe_2), 1.03 (d, 3H, J 7 Hz, CHMe_2), 1.79 (octet, 1H, J 7 Hz, CHMe_2), 4.01 (t, 1H, J 7.5 Hz, OCH), 4.11 (m, 1H, NCH), 4.32 (dd, 1H, J 9, 7.5 Hz, OCH), 6.14 (br s, 2H, NH_2), 6.67 (m, 2H, Ar-H), 7.20 (m, 1H, Ar-H), 7.67 (dd, 1H, J 8, 1 Hz, Ar-6-H). FAB mass spectrometry: m/z 206 (MH^+)

Preparation of ^iPr -NTs-animox (2.42)

A solution of ^iPr -animox (300 mg, 1.47 mmol), toluene-sulphonyl chloride (421 mg, 2.21 mmol), NEt_3 (742 mg, 7.35 mmol) and DMAP (9 mg, 0.074 mmol) in CH_2Cl_2 (10 cm^3) was stirred for 2 days at room temperature. Water (10 cm^3) was added and the organic layer separated. The aqueous layer was washed with CH_2Cl_2 (10 cm^3) and the combined organic layers combined and evaporated to give a yellow oil. The crude product was chromatographed on silica, with CH_2Cl_2 as eluent. Evaporation of the fore-run afforded the desired ligand as a white solid. Yield = 454 mg (86 %).

$^1\text{H NMR}$: δ 0.95 (d, 3H, J 7 Hz, CHMe_2), 1.06 (d, 3H, J 7 Hz, CHMe_2), 1.80 (octet, 1H, J 7 Hz, CHMe_2), 2.33 (s, 3H, Ar-Me), 4.05 (t, 1H, J 8 Hz, OCH), 4.15 (m, 1H, NCH), 4.37 (dd, 1H, J 10, 8 Hz, OCH), 6.99 (dt, 1H, J 1, 8 Hz, Ar-H), 7.20 (d, 2H, J 8 Hz, Ts-H), 7.34 (m, 1H, Ar-H), 7.70 (m, 2H, Ar-H), 7.75 (d, 2H, J 8 Hz, Ts-H), 12.57 (s, 1H, NHTs). FAB mass spectrometry: m/z 359 (MH^+).

Preparation of half-sandwich complexes

The complexes $[\text{RuCl}_2(\text{arene})]_2$ (arene = C_6H_6 , *p*-cymene, mesitylene, C_6Me_6)⁵⁹,⁶² and $[\text{MCl}_2\text{Cp}^*]_2$ (M = Rh, Ir)⁶⁰ were prepared by literature methods. NaSbF_6 was obtained from Fluorochem, NaOMe from Aldrich and AgSbF_6 obtained from Lancaster.

General synthesis A: $[\text{MCl}(\text{bis-oxazoline})(\text{ring})]\text{SbF}_6$ (2.20 - 2.29)

A solution of bis-oxazoline ligand (2 equivalents) and NaSbF_6 (2 equivalents) in MeOH (10 cm^3) was added to $[\text{MCl}_2(\text{ring})]_2$ (1 equivalent) and the resulting suspension was heated to reflux for two hours. A yellow/brown coloured solution was obtained, which was then evaporated and the crude residue dissolved in CH_2Cl_2 . Filtration

through celite (to remove NaCl and any black decomposition product), giving a red/orange coloured solution, followed by evaporation afforded the crude complex. Recrystallisation from CH₂Cl₂/ether gave a product pure by NMR. Quantities of reagents used and yields obtained are given in **Table (2A.1)**, with ¹H NMR data given in **Tables (2A.2 - 2A.3)** and Mass spectrometry and Elemental microanalysis in **Table (2A.4)**.

General synthesis B: [MCl(N-N)(ring)]SbF₆ (2.43 - 2.54)

A solution of ligand N-N (N-N = pymox or animox) (2 equivalents) and NaSbF₆ (2 equivalents) in MeOH (10 cm³) was added to [MCl₂(ring)]₂ (1 equivalent) and the resulting suspension was heated to reflux for one hour. An orange/brown coloured solution was obtained, which was then evaporated and the crude residue dissolved in CH₂Cl₂. Filtration through celite (to remove NaCl and any black decomposition product), giving a red/orange coloured solution, followed by evaporation afforded the crude complex. Recrystallisation from CH₂Cl₂/ether gave a product pure by NMR. Quantities of reagents used and yields obtained are given in **Table (2B.1)**, with ¹H NMR data given in **Tables (2B.2 - 2B.8)** and Mass spectrometry and Elemental microanalysis in **Table (2B.9)**.

General synthesis C: [MCl(N-Y)(ring)] (2.57 - 2.62)

A solution of ligand N-Y (N-Y = NTs-animox or phenmox) (2 equivalents) and NaOMe (2 equivalents) in MeOH (10 cm³) was added to [MCl₂(ring)]₂ (M = Ru, ring = arene; M = Rh, Ir, ring = Cp*) (1 equivalent) and the resulting suspension was heated to reflux for one hour, giving a red/brown coloured solution, which was then evaporated. The crude residue was dissolved in CH₂Cl₂ and the solution was filtered through celite, to give a red coloured solution, which was evaporated to afford the crude product. Recrystallisation from CH₂Cl₂/ether gave a product pure by NMR. Quantities of reagents used and yields obtained, along with Mass spectrometry data, are given in **Table (2C.1)**. ¹H NMR data are given in **Tables (2C.3 - 2C.4)** with elemental microanalysis results in **Table (2C.2)**.

General Synthesis D: $[M(OH_2)(N-N)(ring)](SbF_6)_n$ (2.30-2.37, 2.63-2.75)

To a solution of $AgSbF_6$ (1 equivalent) in acetone (0.5 cm^3) was added a solution of $[MCl(N-N)(ring)]SbF_6$ or $[MCl(^iPr-NTs-animox)(ring)]$ ($M = Ru$, ring = arene; $M = Rh$, Ir, ring = Cp^* ; N-N = box, bop, benbox, pymox or animox) (one equivalent) in CH_2Cl_2 (4 cm^3), giving a yellow/orange coloured solution and an immediate precipitate of $AgCl$. The solution was stirred for 30 mins at room temperature (protected from light), then was filtered through celite to remove $AgCl$. Evaporation, followed by washing with CH_2Cl_2 afforded the aqua complexes as orange oils. In some cases (particularly with N-N = box, bop, benbox and NTs-animox), the products could be recrystallised from acetone/ether, affording a crop of fine needles. Quantities of reagents used and yields obtained are given in Table (2D.1), with 1H NMR data given in Tables (2D.2 - 2D.12) and Mass spectrometry data and Elemental microanalysis results given in Tables (2D.13 - 2D.14).

Preparation of substitution complexes $[ML(^iPr-pymox)(ring)](SbF_6)_2$ (2.80 - 2.84)

a) Preparative scale: To a solution of $[M(OH_2)(^iPr-pymox)(ring)](SbF_6)_2$ (2.65 - $M = Ru$, ring = mes; 2.69 - $M = Rh$, ring = Cp^*) (0.09 mmol) in acetone (3 cm^3) was added ligand L (L = MeCN or 4-Me-py) (0.133 mmol). The mixture was stirred for 1 hour at room temperature, then evaporated. Recrystallisation from CH_2Cl_2 /ether gave a product pure by NMR. A 91% yield of complex (2.82) was obtained by this method, whilst the yield of (2.83) was 98%.

b) NMR tube reactions: To a solution of $[M(OH_2)(^iPr-pymox)(ring)](SbF_6)_2$ (2.65 - $M = Ru$, ring = mes; 2.69 - $M = Rh$, ring = Cp^*) (0.02 mmol) in d_6 -acetone (0.5 cm^3) was added ligand L (L = MeCN, 4-Me-py or 2-Me-py) (0.02, 0.03 or 0.04 mmol) via syringe. The 1H NMR spectrum was obtained immediately, then at appropriate intervals thereafter. Conversion to product and diastereomer ratios were assessed by measurement of NMR integrals, the results given in section (2.2.2).

1H NMR spectroscopic data for complexes (2.80 - 2.84) are given in Tables (2E.4 - 2E.5), with mass spectrometry data and elemental analysis results given in Table (2E.6).

Note: In the tables of 1H NMR spectra to follow, assignments of π -ring signals are as follows: $\eta^6-C_6H_6$ - s, 6H; mes - ca. δ 2.5 - 2 (s, 9H, $C_6H_3Me_3$) and ca. δ 6 - 5 (s, 3H, $C_6H_3Me_3$); C_6Me_6 - s, 18H; Cp^* - s, 15H

Table (2A.1): Preparative details and yields obtained for complexes [MCl(N-N)(ring)]SbF₆ (N-N = box, bop, benbox)

Cation	Complex Code	Quantity of dimer (mg / mmol)	Quantity of ligand N-N (mg / mmol)	Quantity of NaSbF ₆ (mg / mmol)	Final Yield (mg / %)
[RuCl(¹ Pr-box)(mes)] ⁺	(2.20)	80 / 0.137	68 / 0.31	75 / 0.29	184 / 94
[RhCl(¹ Pr-box)Cp*] ⁺	(2.21)	76 / 0.113	56 / 0.25	61 / 0.24	146 / 88
[RuCl(¹ Pr-bop)(mes)] ⁺	(2.22)	80 / 0.137	74 / 0.28	72 / 0.28	150 / 72
[RhCl(¹ Pr-bop)Cp*] ⁺	(2.23)	80 / 0.129	90 / 0.34	68 / 0.26	159 / 80
[IrCl(¹ Pr-bop)Cp*] ⁺	(2.24)	80 / 0.11	70 / 0.26	59 / 0.23	149 / 74
[RuCl(¹ Pr-benbox)(C ₆ H ₆)] ⁺	(2.25)	60 / 0.12	75 / 0.25	63 / 0.24	138 / 77
[RuCl(Et-benbox)(<i>p</i> -cy)] ⁺	(2.26, R = Et)	80 / 0.13	76 / 0.28	72 / 0.28	161 / 79
[RuCl(¹ Pr-benbox)(<i>p</i> -cy)] ⁺	(2.26, R = ¹ Pr)	80 / 0.131	84 / 0.28	72 / 0.28	164 / 78
[RuCl(Et-benbox)(mes)] ⁺	(2.27, R = Et)	80 / 0.137	76 / 0.28	72 / 0.28	168 / 80
[RuCl(¹ Pr-benbox)(mes)] ⁺	(2.27, R = ¹ Pr)	80 / 0.137	90 / 0.30	72 / 0.28	196 / 90
[RuCl(Ph-benbox)(mes)] ⁺	(2.27, R = Ph)	70 / 0.12	92 / 0.25	65 / 0.25	178 / 86
[RhCl(Et-benbox)Cp*] ⁺	(2.28, R = Et)	80 / 0.129	71 / 0.26	68 / 0.26	155 / 77
[RhCl(¹ Pr-benbox)Cp*] ⁺	(2.28, R = ¹ Pr)	70 / 0.11	72 / 0.24	59 / 0.23	150 / 82
[RhCl(Ph-benbox)Cp*] ⁺	(2.28, R = Ph)	60 / 0.10	79 / 0.21	55 / 0.21	147 / 84
[IrCl(¹ Pr-benbox)Cp*] ⁺	(2.29)	80 / 0.10	66 / 0.22	57 / 0.26	138 / 77

Table (2A.2): ^1H NMR data for complexes $[\text{MCl}(\text{N-N})(\text{ring})\text{SbF}_6]$ ($\text{N-N} = {}^1\text{Pr-box}$ or ${}^1\text{Pr-bop}$) in CDCl_3 (δ / ppm)

Cation (code)	π -Ring	CHMe_2 group	CMe_2 signals	Oxazoline ring
$[\text{RuCl}({}^1\text{Pr-box})(\text{mes})]^+$ (2.20)	2.32, 5.67	0.74, 1.03, 1.04, 1.10 ($4 \times \text{d}$, 3H, J 7 Hz, CHMe_2), 2.14 (m, 1H, CHMe_2), 2.54 (m, 1H, CHMe_2)	—	4.26 (m, 1H, NCH), 4.66 (dd, 1H, J 10 Hz, OCH), 4.81 (m, 2H, OCH), 4.95 (m, 1H, NCH), 5.15 (t, 1H, J 9 Hz, OCH)
$\text{RhCl}({}^1\text{Pr-box})\text{Cp}^*]^+$ (2.21)	1.78	0.83 (d, 3H, J 7 Hz, CHMe_2), 1.02 (m, 9H, CHMe_2), 2.13 (m, 1H, CHMe_2), 2.38 (m, 1H, CHMe_2)	—	4.35 (m, 1H, NCH), 4.65 (t, 1H, J 9 Hz, OCH), 4.74 (m, 3H, 2 OCH + NCH), 5.03 (t, 1H, J 9 Hz, OCH)
$[\text{RuCl}({}^1\text{Pr-bop})(\text{mes})]^+$ (2.22)	2.25, 5.71	0.55, 0.92, 0.95, 1.04 ($4 \times \text{d}$, 3H, J 7 Hz, CHMe_2); 2.47 (m, 2H, CHMe_2)	1.38 (s, 3H), 1.61 (s, 3H)	4.18 (t, 1H, J 9 Hz, OCH), 4.37 (m, 1H, NCH), 4.45 (dd, 1H, J 9, 1 Hz, OCH), 4.48 (m, 1H, NCH), 4.67 (m, 2H, NCH + OCH)
$[\text{RhCl}({}^1\text{Pr-bop})\text{Cp}^*]^+$ (2.23)	1.68	0.60, 0.88, 0.93, 1.00 ($4 \times \text{d}$, 3H, J 7 Hz, CHMe_2), 2.23 (m, 1H, CHMe_2), 2.23 (m, 1H, CHMe_2)	1.47 (s, 3H), 1.66 (s, 3H)	4.25 (t, 1H, J 9 Hz, OCH), 4.52 (m, 5H, 3 OCH, 2 NCH)
$[\text{IrCl}({}^1\text{Pr-bop})\text{Cp}^*]^+$ (2.24)	1.67	0.60, 0.88, 0.93, 1.00 ($4 \times \text{d}$, 3H, J 7 Hz, CHMe_2); 2.21 (m, 1H, CHMe_2), 2.51 (m, 1H, CHMe_2)	1.51 (s, 3H), 1.61 (s, 3H)	4.33 (t, 1H, J 9 Hz, OCH), 4.37 (m, 1H, NCH), 4.55 (m, 3H, 2 OCH + NCH), 4.70 (t, 1H, J 9 Hz, OCH)

Table (2A.3): ^1H NMR data for complexes $[\text{MCl}(\text{R-benbox})(\text{ring})]\text{SbF}_6$ in CDCl_3 (δ / ppm)

Cation (code)	π -Arene ring	Benzene ring	Oxazoline ring	Substituent
$[\text{RuCl}(\text{}^i\text{Pr-benbox})(\text{C}_6\text{H}_6)]^+$ (2.25)	5.68 (s, 6H, C_6H_6)	8.03 (m, 3H), 8.25 (m, 1H)	4.42 (m, 1H, OCH), 4.58 (t, 1H, J 9 Hz, OCH), 4.71 (m, 1H, NCH), 4.90 (m, 3H, 2 OCH + NCH)	0.53, 0.84, 0.96, 1.16 ($4 \times$ d, 3H, J 7 Hz, CHMe_2), 2.59 (m, 1H, CHMe_2), 2.76 (m, 1H, CHMe_2)
$[\text{RuCl}(\text{Et-benbox})(p\text{-cy})]^+$ (2.26, R = Et)	1.26 and 1.29 (d, 3H, J 7 Hz, CHMe_2), 1.64 (s, 3H, ArMe), 2.76 (sept, 1H, J 7 Hz, CHMe_2), 4.35 and 5.18 ($2 \times$ d, 1H, J 7 Hz, ArH), 5.54 (m, 2H, ArH)	7.87 (m, 3H), 8.20 (m, 1H)	4.10 (m, 1H, NCH), 4.44 (m, 1H, NCH), 4.51 (m, 2H, OCH), 4.67 (dd, 1H, J 9, 8 Hz, OCH), 4.84 (dd, 1H, J 9.5, 8 Hz, OCH)	0.71 and 0.98 ($2 \times$ t, 3H, J 7 Hz, CH_2Me), 1.49 (m, 2H, CH_2Me), 1.74 (m, 1H, CH_2Me), 2.42 (m, 1H, CH_2Me)
$[\text{RuCl}(\text{}^i\text{Pr-benbox})(p\text{-cy})]^+$ (2.26, R = ^iPr)	1.30 and 1.35 (d, 3H, J 7 Hz, CHMe_2), 1.27 (s, 3H, ArMe), 3.02 (sept, 1H, J 7 Hz, CHMe_2); 4.20, 5.19, 5.40 and 5.83 ($4 \times$ d, 1H, J 7 Hz, ArH)	7.80 (m, 3H), 8.29 (m, 1H)	4.34 (t, 1H, J 9 Hz, OCH), 4.57 (m, 2H, NCH + OCH), 4.78 (m, 1H, NCH), 4.91 (m, 2H, $2 \times$ OCH)	0.44, 0.82, 1.00 and 1.12 ($4 \times$ d, 3H, J 7 Hz, CHMe_2); 2.47 and 2.67 ($2 \times$ m, 1H, CHMe_2)

Table (2A.3) cont. (δ / ppm)

Cation (Code)	π -ring	Benzene ring	Oxazoline ring	Substituent
[RuCl(Et-benbox)(mes)] ⁺ (2.27, R = Et)	1.96, 4.55	7.82 (m, 2H), 7.94 (m, 3H)	4.25 (t, 1H, <i>J</i> 9 Hz, OCH), 4.43 (m, 1H, NCH), 4.58 (m, 2H, OCH), 4.60 (m, 1H, OCH), 4.73 (m, 1H, NCH)	0.75 and 0.99 (2 \times t, 3H, <i>J</i> 7 Hz, CH ₂ Me), 1.56 (m, 2H, CH ₂ Me), 1.84 (m, 1H, CH ₂ Me), 2.40 (m, 1H, CH ₂ Me)
[RuCl(ⁱ Pr-benbox)(mes)] ⁺ (2.27, R = ⁱ Pr)	1.95, 4.77	7.82 (m, 2H), 7.93 (m, 1H), 8.22 (d, <i>J</i> 8 Hz, 1H)	4.25 (m, 1H, NCH), 4.34 (dd, 1H, <i>J</i> 9, 4 Hz, OCH), 4.68 (m, 3H, 2 OCH, NCH), 4.84 (t, 1H, <i>J</i> 9 Hz, OCH)	0.47, 0.86, 0.97 and 1.13 (4 \times d, 3H, <i>J</i> 7 Hz, CHMe ₂), 2.42 (m, 1H, CHMe ₂), 2.75 (m, 1H, CHMe ₂)
[RuCl(Ph-benbox)(mes)] ⁺ (2.27, R = Ph)	1.74, 4.07	7.97 (m, 2H), 8.17 (d, 1H), 8.29 (d, <i>J</i> 8 Hz, 1H)	4.55 (dd, 1H, OCH), 4.71 (t, 1H, <i>J</i> 9 Hz, OCH), 5.06 (m, 2H, OCH + NCH), 5.43 (m, 2H, OCH + NCH)	6.84 (m, 2H, PhH), 7.27 (m, 4H, PhH), 7.52 (m, 4H, PhH)

Table (2A.3) cont. (δ / ppm)

Cation (Code)	π -ring	Benzene ring	Oxazoline ring	Substituent
[RhCl(Et-benbox)Cp*] ⁺ (2.28, R = Et)	1.29	7.84 (m, 2H), 8.04 (m, 1H), 8.16 (m, 1H)	4.12 (tt, 1H, <i>J</i> 5, 8.5 Hz, NCH), 4.6 (m, 5H, 3 × OCH + 2 × OCH)	0.77 and 0.96 (2 × t, 3H, <i>J</i> 7 Hz, CH ₂ Me), 1.60 (m, 2H, CH ₂ Me), 1.95 and 2.30 (2 × m, 1H, CH ₂ Me)
[RhCl(ⁱ Pr-benbox)Cp*] ⁺ (2.28, R = ⁱ Pr)	1.28	7.78 (m, 1H), 7.85 (m, 2H), 8.19 (m, 1H)	4.14 (dt, 1H, <i>J</i> 7.5, 3 Hz, NCH), 4.28 (dd, 1H, <i>J</i> 12, 9.5 Hz, OCH), 4.61 (m, 3H, 3 × OCH), 4.92 (ddd, 1H, <i>J</i> 11, 7, 2 Hz, NCH)	0.50, 0.86, 0.97 and 1.13 (4 × d, 3H, <i>J</i> 7Hz, CHMe ₂), 2.42 and 2.75 (2 × m, 1H, CHMe ₂)
[RhCl(Ph-benbox)Cp*] ⁺ (2.28, R = Ph)	0.98	7.99 (dt, 1H, <i>J</i> 1, 8 Hz), 7.93 (dt, 1H, <i>J</i> 1, 8 Hz), 8.18 (dd, 1H, <i>J</i> 8, 1 Hz), 8.29 (dd, 1H, <i>J</i> 8, 1 Hz)	4.53 (dd, 1H, <i>J</i> 9, 2 Hz, OCH), 4.68 (t, 1H, <i>J</i> 10 Hz, OCH), 4.85 (dd, 1H, <i>J</i> 9, 6 Hz, OCH), 5.07 (t, 1H, <i>J</i> 9 Hz, OCH), 5.38 (dd, 1H, <i>J</i> 9, 2 Hz, NCH), 5.55 (dd, 1H, <i>J</i> 11, 6 Hz, NCH)	6.93 (m, 2H, PhH), 7.54-7.27 (m, 8H, Ph)
[IrCl(ⁱ Pr-benbox)Cp*] ⁺ (2.29)	1.27	7.77 (m, 1H), 7.86 (m, 2H), 8.18 (m, 1H)	4.13 (m, 1H, NCH), 4.40 (dd, 1H, <i>J</i> 10, 9 Hz, OCH), 4.66 (m, 3H, 3 × OCH), 5.09 (ddd, 1H, <i>J</i> 10, 6, 2 Hz, NCH)	0.61, 0.90, 0.98 and 0.99 (4 × d, 3H, <i>J</i> 7Hz, CHMe ₂), 2.12 and 3.01 (m, 1H, CHMe ₂)

Table (2B.1): Preparative details and yields obtained for complexes [MCl(N-N)(ring)]SbF₆ (N-N = pymox, animox) (2.43 - 2.54)

Compound	Code	Quantity of dimer (mg / mmol)	Quantity of ligand N-N (mg / mmol)	Quantity of NaSbF ₆ (mg / mmol)	Final Yield (mg / %)
[RuCl(^t Pr-pymox)(C ₆ H ₆)] ⁺	2.43, R = ^t Pr	50 / 0.10	40 / 0.21	53 / 0.205	106 / 83
[RuCl(^t Bu-pymox)(C ₆ H ₆)] ⁺	2.43, R = ^t Bu	60 / 0.12	55 / 0.246	63 / 0.243	130 / 83
[RuCl(^t Pr-pymox)(<i>p</i> -cy)] ⁺	2.44, R = ^t Pr	65 / 0.106	41 / 0.22	51 / 0.22	123 / 83
[RuCl(^t Bu-pymox)(<i>p</i> -cy)] ⁺	2.44, R = ^t Bu	70 / 0.114	50 / 0.23	60 / 0.232	136 / 84
[RuCl(Et-pymox)(mes)] ⁺	2.45, R = Et	80 / 0.137	53 / 0.30	75 / 0.29	172 / 94
[RuCl(^t Pr-pymox)(mes)] ⁺	2.45, R = ^t Pr	100 / 0.17	72 / 0.38	93 / 0.36	215 / 92
[RuCl(^t Bu-pymox)(mes)] ⁺	2.45, R = ^t Bu	100 / 0.17	77 / 0.38	93 / 0.36	217 / 91
[RuCl(Ph-pymox)(mes)] ⁺	2.45, R = Ph	70 / 0.12	59 / 0.26	65 / 0.25	163 / 95
[RuCl(Bn-pymox)(mes)] ⁺	2.45, R = Bn	100 / 0.17	90 / 0.38	93 / 0.36	228 / 91
[RuCl(Me ₂ -pymox)(mes)] ⁺	2.46	80 / 0.137	53 / 0.30	75 / 0.29	169 / 92
[RuCl(Indanyl-pymox)(mes)] ⁺	2.47	80 / 0.137	66 / 0.28	73 / 0.28	175 / 88
[RuCl(^t Pr-pymox)(C ₆ Me ₆)] ⁺	2.48	90 / 0.135	54 / 0.28	73 / 0.28	185 / 95

Table (2B.1) cont.

Compound	Code	Quantity of dimer (mg / mmol)	Quantity of ligand N-N (mg / mmol)	Quantity of NaSbF ₆ (mg / mmol)	Final Yield (mg / %)
[RhCl(Et-pymox)Cp*] ⁺	2.49, R = Et	85 / 0.14	52 / 0.30	72 / 0.28	150 / 79
[RhCl(ⁱ Pr-pymox)Cp*] ⁺	2.49, R = ⁱ Pr	85 / 0.14	53 / 0.30	72 / 0.28	166 / 86
[RhCl(^t Bu-pymox)Cp*] ⁺	2.49, R = ^t Bu	100 / 0.16	74 / 0.36	86 / 0.33	196 / 84
[RhCl(Ph-pymox)Cp*] ⁺	2.49, R = Ph	80 / 0.13	67 / 0.30	70 / 0.27	153 / 80
[RhCl(Bn-pymox)Cp*] ⁺	2.49, R = Bn	100 / 0.16	85 / 0.36	86 / 0.33	201 / 83
[RhCl(Me ₂ -pymox)Cp*] ⁺	2.50	105 / 0.17	62 / 0.35	90 / 0.35	210 / 90
[RhCl(Indanyl-pymox)Cp*] ⁺	2.51	84 / 0.136	66 / 0.28	72 / 0.28	194 / 96
[IrCl(ⁱ Pr-pymox)Cp*] ⁺	2.52	100 / 0.13	49 / 0.26	66 / 0.26	177 / 89
[RuCl(ⁱ Pr-animox)(mes)] ⁺	2.53	80 / 0.137	56 / 0.275	72 / 0.278	184 / 96
[RhCl(ⁱ Pr-animox)Cp*] ⁺	2.54	84 / 0.137	56 / 0.275	72 / 0.278	187 / 96

Table (2B.2): ¹H NMR spectroscopic data for complexes [RuCl(R-pymox)(C₆H₆)]SbF₆ (2.43) in d₆-acetone (δ / ppm)

Cation (Code)	$\eta^6\text{-C}_6\text{H}_6$	Pyridine ring	Oxazoline ring	Substituent
[RuCl(¹ Pr-pymox)(C ₆ H ₆)] ⁺ (2.43, R = ¹ Pr) (S _{Ru})	6.21	7.92 (m, 1H, pyH), 8.05 (m, 1H, pyH), 8.33 (m, 1H, py-H), 9.63 (d, 1H, <i>J</i> 3.5 Hz, py-6-H)	5.06 (m, 2H, 2 × OCH), 5.19 (m, 1H, NCH)	0.87 and 1.06 (d, 3H, <i>J</i> 7 Hz, CHMe ₂), 2.50 (m, 1H, CHMe ₂)
[RuCl(¹ Pr-pymox)(C ₆ H ₆)] ⁺ (2.43, R = ¹ Pr) (R _{Ru})	6.21	7.92 (m, 1H, pyH), 8.05 (m, 1H, pyH), 8.33 (m, 1H, py-H), 9.73 (d, 1H, <i>J</i> 3.5 Hz, py-6-H)	4.57 (ddd, 1H, <i>J</i> 10, 7, 3.5 Hz, NCH), 4.93 (t, 1H, <i>J</i> 10 Hz, OCH), 5.06 (m, 1H, OCH)	1.10 and 1.14 (d, 3H, <i>J</i> 7 Hz, CHMe ₂) 2.88 (m, 1H, CHMe ₂)
[RuCl(¹ Bu-pymox)(C ₆ H ₆)] ⁺ (2.43, R = ¹ Bu)	5.93	7.77 (m, 1H, py-5-H), 7.88 (d, 1H, <i>J</i> 7 Hz, py-3-H), 8.15 (t, 1H, <i>J</i> 7 Hz, py-4-H), 9.19 (d, 1H, <i>J</i> 5 Hz, py-6-H)	4.61 (dd, 1H, <i>J</i> 10, 7 Hz, NCH), 4.90 (dd, 1H, <i>J</i> 10, 7 Hz, OCH), 5.02 (t, 1H, <i>J</i> 10 Hz, OCH)	1.09 (CMe ₃)

Table (2B.3): ^1H NMR data for complexes $[\text{RuCl}(\text{R-pymox})(p\text{-Cy})]\text{SbF}_6$ (2.44) in CD_2Cl_2 (δ / ppm)

Cation (Code)	Arene signals	Pyridine ring	Oxazoline ring	Substituent
$[\text{RuCl}(\text{}^i\text{Pr-pymox})(p\text{-cy})]^+$ (2.44, R = ^iPr) (S)-isomer	1.07 and 1.16 (2 \times d, 3H, J 6 Hz, CHMe_2), 2.20 (s, 3H, ArMe), 2.77 (m, 1H, CHMe_2), 5.80 (m, 3H, ArH), 5.91 (d, 1H, J 6 Hz, ArH)	7.85 (m, 2H, py-H), 8.09 (m, 1H, py-H), 9.30 (d, 1H, J 5.5 Hz, py-6-H)	4.80 (m, 1H, OCH), 4.94 (m, 1H, NCH), 5.10 (t, 1H, J 9 Hz, OCH)	0.84 and 1.12 (2 \times d, 3H, J 7 Hz, CHMe_2), 2.29 (m, 1H, CHMe_2)
$[\text{RuCl}(\text{}^i\text{Pr-pymox})(p\text{-cy})]^+$ (2.44, R = ^iPr) (R)-isomer	1.07 and 1.16 (2 \times d, 3H, J 6 Hz, CHMe_2), 2.23 (s, 3H, ArMe), 2.77 (m, 1H, CHMe_2), 5.69 (m, 2H, ArH), 5.80 (m, 1H, ArH), 6.08 (d, 1H, J 6 Hz, ArH)	7.85 (m, 2H, py-H), 8.09 (m, 1H, py-H), 9.50 (d, 1H, J 5.5 Hz, py-6-H)	4.42 (m, 1H, NCH), 4.80 (m, 2H, NCH + OCH), 4.94 (m, 1H, NCH), 5.10 (t, 1H, J 9 Hz, OCH)	0.84 and 1.12 (2 \times d, 3H, J 7 Hz, CHMe_2), 2.29 (m, 1H, CHMe_2)
$[\text{RuCl}(\text{}^t\text{Bu-pymox})(p\text{-cy})]^+$ (2.44, R = ^tBu) Major isomer	1.06 (m, 6H, CHMe_2), 2.27 (s, 3H, ArMe), 2.65 (sept, 1H, CHMe_2), 5.56, 5.67, 5.77 and 5.97 (4 \times d, 1H, J 6 Hz, ArH),	7.84 (m, 2H, pyH), 8.11 (t, 1H, J 8 Hz, py-4-H), 9.27 (d, 1H, J 5 Hz, py-6-H)	4.70 (dd, 1H, J 8, 4 Hz, NCH), 4.95 (m, 2H, OCH_2)	1.08 (CMe_3)
$[\text{RuCl}(\text{}^t\text{Bu-pymox})(p\text{-cy})]^+$ (2.45, R = ^tBu) Minor isomer	1.07, 5.38	7.87 (m, py-3-H), 7.99 (m, 7.7 Hz, py-3-H), 8.12 (t, J 7 Hz, py-4-H), 9.29 (d, J 5.5 Hz, py-6-H)	4.84 (dd, J 8, 7.5 Hz, OCH), 5.20 (m, 1H, OCH), 5.39 (m, 1H, NCH)	7.44 (m, 1H, Py), 7.58 (m, 2H, Py)

Table (2B.4): ^1H NMR data for complexes $[\text{RuCl}(\text{R-pymox})(\text{mes})]\text{SbF}_6$ in CD_2Cl_2 (δ / ppm)

Cation (Code)	mes ring	Pyridine Ring	Oxazoline Ring	Substituent R
$[\text{RuCl}(\text{Et-pymox})(\text{mes})]^+$ (2.45, R = Et)	2.19, 5.54	7.81 (m, py-5-H), 7.91 (d, J 7 Hz, py-H-3), 8.19 (td, J 7, 1 Hz, py-H-4), 9.36 (d, J 5 Hz, py-6-H)	4.76 (dd, J 8.5, 5.5 Hz, OCH), 4.93 (m, NCH), 5.05 (t, J 8.5 Hz, OCH)	0.87 (t, 3H, J 7.5 Hz, CH_2Me), 1.47 (m, 1H, CHMe), 1.99 (m, 1H, CHMe)
$[\text{RuCl}(\text{}^i\text{Pr-pymox})(\text{mes})]^+$ (2.45, R = ^iPr)	2.25, 5.34	7.73 (m, py-5-H), 7.86 (d, J 7 Hz, py-3-H), 8.07 (dt, J 7.5, 1.5 Hz, py-4-H), 9.01 (d, J 5 Hz, py-6-H)	4.82 (m, 2H, NCH + OCH), 5.00 (t, J 11 Hz, OCH)	0.77 and 1.02 ($2 \times$ d, 3H, J 7 Hz, CHMe_2), 2.23 (m, 1H, CHMe_2)
$[\text{RuCl}(\text{}^t\text{Bu-pymox})(\text{mes})]^+$ (2.45, R = ^tBu)	2.19, 5.14	7.69 (m, py-5-H), 7.82 (d, J 8 Hz, py-3-H), 8.02 (td, J 8, 1 Hz, py-4-H), 8.92 (d, J 5 Hz, py-6-H)	4.47 (dd, J 10, 4 Hz, OCH), 4.85 (m, 2H, NCH + OCH)	0.99 (s, 9H, CMe_3)
$[\text{RuCl}(\text{Ph-pymox})(\text{mes})]^+$ (2.45, R = Ph) Major isomer	2.11, 5.22	7.78 (m, py-5-H), 7.93 (d, J 7 Hz, py-3-H), 8.08 (dt, J 7, 1 Hz, py-4-H), 9.11 (d, J 5.5 Hz, py-6-H)	4.55 (dd, J 11, 8.5 Hz, OCH), 5.49 (t, J 11, 8.5 Hz, OCH), 6.10 (t, J 11 Hz, NCH)	7.44 (m, 3H, Ph), 7.58 (m, 2H, Ph)
$[\text{RuCl}(\text{Ph-pymox})(\text{mes})]^+$ (2.45, R = Ph) Minor isomer	2.07, 5.38	7.87 (m, py-5-H), 7.99 (d, J 7 Hz, py-3-H), 8.12 (t, J 7 Hz, py-4-H), 9.29 (d, J 5.5 Hz, py-6-H)	4.84 (dd, J 8, 7.5 Hz, OCH), 5.20 (m, 1H, OCH), 5.39 (m, 1H, NCH)	7.44 (m, 3H, Ph), 7.58 (m, 2H, Ph)

Table (2B.5): ^1H NMR data for complexes $[\text{RuCl}(\text{R-pymox})(\text{arene})]\text{SbF}_6$ in CD_2Cl_2 (δ / ppm)

Cation (Code)	π -arene	Pyridine Ring	Oxazoline Ring	Substituent R
$[\text{RuCl}(\text{Bn-pymox})(\text{mes})]^+$ (2.45, R = Bn)	2.22, 5.28	7.70 (m, py-5-H), 7.83 (d, J 8 Hz, py-3-H), 8.04 (dt, J 8, 1.5 Hz, py-4-H), 9.02 (d, J 5.5 Hz, py-6-H)	4.55 (dd, J 9, 5.5 Hz, OCH), 4.84 (t, J 9 Hz, OCH), 5.10 (m, NCH)	2.63 (dd, 1H, J 14.5, 11 Hz, CH_2Ph), 3.40 (dd, 1H, J 14.5, 3.5 Hz, CH_2Ph), 7.38-7.11 (m, 5H, Ph)
$[\text{RuCl}(\text{Me}_2\text{-pymox})(\text{mes})]^+$ (2.46)	2.25, 5.70	7.72 (m, py-5-H), 7.83 (d, J 8 Hz, py-3-H), 8.05 (t, J 8 Hz, py-4-H), 9.05 (d, J 5 Hz, py-6-H)	4.44 (d, 1H, J 9 Hz, OCH) 4.61 (d, 1H, J 9 Hz, OCH)	1.42 (s, 3H, CMe_2), 1.73 (s, 3H, CMe_2),
$[\text{RuCl}(\text{Indanyl-pymox})(\text{mes})]^+$ (2.47)	2.23, 5.38	7.66 (m, 1H, py-5-H), 7.80 (d, 1H, J 9 Hz, py-3-H), 8.00 (td, 1H, J 8, 1 Hz, py-4-H), 8.96 (d, 1H, J 6 Hz, py-6-H)	6.13 (ddd, 1H, J 8, 6, 2 Hz, OCH), 6.20 (d, 1H, J 8 Hz, NCH)	3.54 (m, 2H, CH_2Ar), 7.27 (m, 3H, Ar-H), 7.53 (d, 1H, J 7 Hz, Ar-H)
$[\text{RuCl}(\text{}^i\text{Pr-pymox})(\text{C}_6\text{Me}_6)]^+$ (2.48)	2.18	7.77 (dd, 1H, J 7.5, 5.5 Hz, py-5-H), 7.88 (d, 1H, J 7.5 Hz, py-3-H), 8.06 (t, 1H, J 7.5 Hz, py-4-H), 8.84 (d, 1H, J 5.5 Hz, py-6-H)	4.71 (m, 1H, NCH), 4.81 (d, 1H, J 9, 4.5 Hz, OCH), 5.00 (t, 1H, J 9 Hz, OCH)	0.70 and 1.03 ($2 \times$ d, 3H, J 6.5 Hz, CHMe_2), 2.06 (m, 1H, CHMe_2)

Table (2B.6): ^1H NMR data for complexes $[\text{RhCl}(\text{R-pymox})\text{Cp}^*]\text{SbF}_6$ in CD_2Cl_2 (δ / ppm)

Complex (Code)	Cp*	Pyridine ring	Oxazoline ring	Substituent
$[\text{RhCl}(\text{Et-pymox})\text{Cp}^*]\text{SbF}_6$ (2.49, R = Et)	1.75	7.86 (m, py-5-H), 7.97 (dd, J 8, 1.5 Hz, py-3-H), 8.16 (td, J 8, 1.5 Hz, py-4-H), 8.78 (dd, J 5 Hz, py-6-H)	4.64 (m, 1H, NCH), 4.73 (m, 1H, OCH), 5.06 (t, 1H, J 9 Hz, OCH)	0.97 (t, 3H, J 7.5 Hz, CH_2Me), 1.60 (m, 1H, CHMe), 1.95 (m, 1H, CHMe)
$[\text{RhCl}(\text{}^i\text{Pr-pymox})\text{Cp}^*]\text{SbF}_6$ (2.49, R = ^iPr)	1.73	7.86 (m, py-5-H), 7.95 (d, J 8.5 Hz, py-3-H), 8.16 (t, J 8.5 Hz, py-4-H), 8.77 (d, J 6 Hz, py-6-H)	4.65 (m, 1H, NCH), 4.84 (dd, 1H, J 10, 5.5 Hz, $\text{OCH}_{\text{trans}}$), 4.94 (t, 1H, J 10 Hz, OCH_{cis})	0.79 (d, 3H, J 6.5 Hz, CHMe_2), 1.01 (d, 3H, J 7 Hz, CHMe_2), 2.15 (m, 1H, CHMe_2)
$[\text{RhCl}(\text{}^t\text{Bu-pymox})\text{Cp}^*]\text{SbF}_6$ (2.49, R = ^tBu)	1.59	7.79 (m, py-5-H), 7.88 (d, J 8 Hz, py-3-H), 8.10 (t, J 8, 1 Hz, py-4-H), 8.65 (d, J 5 Hz, py-6-H)	4.31 (dd, 1H, J 10, 4 Hz, OCH), 4.80 (m, 2H, OCH + NCH)	0.94 (s, 9H, CMe_3)
$[\text{RhCl}(\text{Ph-pymox})\text{Cp}^*]\text{SbF}_6$ (2.49, R = Ph)	1.45	7.84 (m, py-5-H), 7.97 (d, J 6.5 Hz, py-3-H), 8.13 (td, J 6.5, 1 Hz, py-4-H), 8.73 (d, J 5 Hz, py-6-H)	4.43 (dd, 1H, J 11, 9 Hz, OCH), 5.39 (dd, 1H, J 10.5, 10 Hz, OCH), 5.88 (t, 1H, 10.5 Hz, OCH)	7.37 (m, 3H, Ph), 7.53 (m, 2H, Ph)

Table (2B.7): ¹H NMR data for complexes [MCl(R,R'-pymox)Cp*]SbF₆ in CD₂Cl₂ (δ / ppm)

Complex (Code)	Cp*	Pyridine ring	Oxazoline ring	Substituent
[RhCl(Bn-pymox)Cp*]SbF ₆ (2.49, R = Bn)	1.74	7.82 (m, py-5-H), 7.92 (d, <i>J</i> 8 Hz, py-3-H), 8.11 (td, <i>J</i> 8, 1.5 Hz, py-4-H), 8.74 (d, <i>J</i> 5.5 Hz, py-6-H)	4.64 (dd, 1H, <i>J</i> 9, 5.5 Hz, OCH), 4.81 (t, 1H, <i>J</i> 9 Hz, OCH), 4.91 (m, 1H, NCH)	2.65 (dd, 1H, <i>J</i> 14, 11 Hz, CHPh), 3.33 (dd, 1H, <i>J</i> 14, 3.5 Hz, CHPh), 7.25 (m, 5H, Ph)
[RhCl(Me ₂ -pymox)Cp*]SbF ₆ (2.50)	1.77	7.89 (m, py-5-H), 7.98 (d, <i>J</i> 8 Hz, py-3-H), 8.17 (dt, <i>J</i> 8, 1 Hz, py-4-H), 8.81 (d, <i>J</i> 5 Hz, py-6-H)	4.51 (d, 1H, <i>J</i> 9 Hz, OCH), 4.66 (d, 1H, <i>J</i> 9 Hz, OCH)	1.52 (s, 3H, CMe ₂), 1.75 (s, 3H, CMe ₂)
[RhCl(Indanyl-pymox)Cp*]SbF ₆ (2.51)	1.93	7.97 (m, py-5-H), 8.05 (d, 1H, <i>J</i> 7 Hz, py-3-H), 8.30 (td, 1H, <i>J</i> 9, 1 Hz, py-4-H), 9.08 (d, 1H, <i>J</i> 6 Hz, py-6-H)	6.21 (m, 1H, OCH), 6.37 (d, 1H, <i>J</i> 7 Hz, NCH)	3.62 (m, 2H, CH ₂ Ar), 7.27 (m, 3H, Ar-H), 7.63 (m, 1H, Ar-H)
[IrCl(Pr-pymox)Cp*]SbF ₆ (2.52)	1.77	7.81 (m, py-5-H), 7.98 (d, <i>J</i> 8.5 Hz, py-3-H), 8.11 (t, <i>J</i> 8.5 Hz, py-4-H), 8.85 (d, <i>J</i> 6 Hz, py-6-H)	4.61 (m, 1H, NCH), 4.90 (dd, 1H, <i>J</i> 10, 5.5 Hz, OCH _{trans}), 5.08 (t, 1H, <i>J</i> 10 Hz, OCH _{cis})	0.87 and 1.02 (2 × d, 3H, <i>J</i> 7 Hz, CHMe ₂), 2.17 (m, 1H, CHMe ₂)

Table (2B.8): ^1H NMR data for $[\text{MCl}(\text{}^i\text{Pr-animox})(\text{ring})]^{n+}$ ($n = 0, 1$) in CD_2Cl_2 (δ / ppm)

Compound (Code)	π -ring	Aniline-group	Oxazoline ring	Substituent
$[\text{RuCl}(\text{}^i\text{Pr-animox})(\text{mes})]^+$ (2.53) Major Isomer	2.08, 4.82	7.43 (t, 1H, J 8 Hz, Ar-5-H), 7.66 (m, 2H, Ar-H), 7.89 (d, 1H, J 8 Hz, Ar-6-H), 4.99 (br d, 1H, NH), 6.13 (br d, 1H, NH)	4.39 (m, 1H, NCH), 4.63 (m, 2H, OCH)	0.51 and 0.88 ($2 \times$ d, 3H, J 6 Hz, CHMe_2), 2.80 (m, 1H, CHMe_2)
$[\text{RuCl}(\text{}^i\text{Pr-animox})(\text{mes})]^+$ Minor Isomer	1.99, 4.82	Obscured by major signals	Obscured by major signals	0.98 and 1.04 ($2 \times$ d, 3H, J 6 Hz, CHMe_2), 2.34 (m, 1H, CHMe_2)
$[\text{RuCl}(\text{}^i\text{Pr-animox}^-)(\text{mes})]$ (2.53D)	2.27, 5.55	7.26 (t, 1H, J 7 Hz, Ar-5-H), 7.49 (t, 1H, J 6 Hz, Ar-4-H), 7.75 (m, 2H, ArH)	4.71 (m, 2H, $2 \times$ OCH), 4.63 (m, 1H, NCH)	0.50 and 1.13 ($2 \times$ d, 3H, J 6 Hz, CHMe_2), 2.69 (m, 1H, CHMe_2)
$[\text{RhCl}(\text{}^i\text{Pr-animox})\text{Cp}^*]^+$ (2.54)	1.42	7.37 (t, 1H, J 8 Hz, Ar-5-H), 7.45 (d, 1H, Ar-3-H), 7.63 (td, 1H, Ar-4-H), 7.87 (dd, 1H, Ar-6-H), 4.93 (br d, 1H, NH), 5.36 (br d, 1H, NH)	4.31 (m, 1H, NCH), 4.57 (m, 2H, OCH)	0.62 and 0.88 ($2 \times$ d, 3H, J 6 Hz, CHMe_2), 2.81 (m, 1H, CHMe_2)
$[\text{RhCl}(\text{}^i\text{Pr-animox}^-)\text{Cp}^*]$ (2.54D)	1.57	7.20 (t, 1H, J 7 Hz, Ar-5-H), 7.41 (t, 1H, J 6 Hz, Ar-4-H), 7.68 (m, 2H, ArH)	4.62 (m, 2H, $2 \times$ OCH), 4.57 (m, 1H, NCH)	0.63 and 1.05 ($2 \times$ d, 3H, J 6 Hz, CHMe_2), 2.54 (m, 1H, CHMe_2)

Table (2B.9) - Mass Spectrometry Data and Elemental Analysis for complexes [MCl(N-N)(ring)]SbF₆ (N-N = pymox, animox) (2.43 - 2.54)

Complex	Code	Mass Spectrometry (m/z)		Elemental Analysis: Found (Calculated)		
		(M ⁺)	Other ion patterns	C %	H %	N %
[RuCl(^t Pr-pymox)(C ₆ H ₆)] ⁺	2.43, R = ^t Pr		406 (MH ⁺)	31.52 (31.87)	3.06 (3.15)	3.93 (4.37)
[RuCl(^t Bu-pymox)(C ₆ H ₆)] ⁺	2.43, R = ^t Bu		420 (MH ⁺)	33.35 (33.03)	3.52 (3.39)	4.15 (4.28)
[RuCl(^t Pr-pymox)(<i>p</i> -cy)] ⁺	2.44, R = ^t Pr		462 (MH ⁺)	36.59 (36.20)	4.19 (4.05)	3.91 (4.02)
[RuCl(^t Bu-pymox)(<i>p</i> -cy)] ⁺	2.44, R = ^t Bu		476 (MH ⁺)	37.41 (37.18)	4.35 (4.25)	3.83 (3.94)
[RuCl(Et-pymox)(mes)] ⁺	2.45, R = Et	433		34.82 (34.13)	3.66 (3.62)	4.47 (4.19)
[RuCl(^t Pr-pymox)(mes)] ⁺	2.45, R = ^t Pr	447	412 (M - Cl) ⁺	40.80 (40.58)*	4.18 (4.43)	3.94 (4.02)
[RuCl(^t Bu-pymox)(mes)] ⁺	2.45, R = ^t Bu	461		36.33 (36.20)	3.71 (4.05)	3.94 (4.02)
[RuCl(Ph-pymox)(mes)] ⁺	2.45, R = Ph	481		35.67 (35.98)	2.97 (3.27)	3.53 (3.50)
[RuCl(Bn-pymox)(mes)] ⁺	2.45, R = Bn	495		40.37 (40.31) [†]	3.90 (3.85)	3.58 (3.69)
[RuCl(Me ₂ -pymox)(mes)] ⁺	2.46	433		32.80(32.94) [†]	3.36(3.54)	3.44(3.94)
[RuCl(Indanyl-pymox)(mes)] ⁺	2.47	493		39.68 (39.56)	3.34 (3.32)	3.80 (3.84)
[RuCl(^t Pr-pymox)(C ₆ Me ₆)] ⁺	2.48	489		37.42 (38.12)	4.26 (4.45)	3.23 (3.87)

* PF₆⁻ salt

[‡] includes 0.5 equivalents acetone

[†] includes 0.5 equivalents CH₂Cl₂

Table (2B.9) cont.

Cation	Code	Mass Spectrometry (m/z)		Elemental Analysis: Found (Calculated)		
		(M ⁺)	Other ion patterns	C %	H %	N %
[RhCl(Et-pymox)Cp*] ⁺	2.49, R = Et	449		35.29 (35.04)	3.75 (3.97)	4.16 (4.09)
[RhCl(¹ Pr-pymox)Cp*] ⁺	2.49, R = ¹ Pr	463	427 (M - HCl) ⁺	41.81 (41.43)*	4.39 (4.80)	4.63 (4.60)
[RhCl(^t Bu-pymox)Cp*] ⁺	2.49, R = ^t Bu	477		36.32 (37.03)	3.93 (4.38)	3.67 (3.97)
[RhCl(Ph-pymox)Cp*] ⁺	2.49, R = Ph	497	461 (M - HCl) ⁺	44.51 (44.84)*	4.10 (4.23)	4.19 (4.36)
[RhCl(Bn-pymox)Cp*] ⁺	2.49, R = Bn	511	475 (M - HCl) ⁺	40.35 (40.16)	3.97 (3.91)	3.77 (3.75)
[RhCl(Me ₂ -pymox)Cp*] ⁺	2.50	449		34.90(35.04)	3.83 (3.97)	3.50 (4.09)
[RhCl(Indanyl-pymox)Cp*] ⁺	2.51	509	473 (M - HCl) ⁺	39.48 (39.32)	3.63 (3.83)	3.40 (3.76)
[IrCl(¹ Pr-pymox)Cp*] ⁺	2.52	553	518 (M - Cl) ⁺	36.62 (36.13)*	3.96 (4.19)	4.14 (4.01)
[RuCl(¹ Pr-animox)(mes)] ⁺	2.53	461	425 (M - HCl) ⁺	35.97 (36.20) [†]	3.86 (4.05)	3.80 (4.02)
[RhCl(¹ Pr-animox)Cp*] ⁺	2.54	477	441 (M - HCl) ⁺	36.81 (27.03)	4.33 (4.38)	3.75 (3.93)

* PF₆ salt † Calculated for monohydrate

Table (2C.1): Preparative details, Yields obtained and Mass spectrometry data for complexes (2.57 - 2.62)

Compound	(Code)	Quantity of dimer (mg / mmol)	Quantity of N-YH (mg / mmol)	Quantity of NaOMe (mg / mmol)	Yield (mg / %)	Molecular Ion (M ⁺) m/z	Other ion patterns m/z
RuCl(¹ Pr-NTs-animox)(mes)	(2.57)	80 / 0.14	100 / 0.28	17 / 0.32	122 / 71	614	579 (M - Cl) ⁺
RhCl(¹ Pr-NTs-animox)Cp*	(2.58)	84 / 0.14	100 / 0.28	17 / 0.32	129 / 73	630	595 (M - Cl) ⁺
RuCl(¹ Pr-phenmox)(<i>p</i> -cy)	(2.59)	80 / 0.13	56 / 0.27	15 / 0.28	98 / 79	475	
RuCl(¹ Pr-phenmox)(mes)	(2.60)	100 / 0.17	73 / 0.27	19 / 0.35	129 / 82	461	
RhCl(¹ Pr-phenmox)Cp*	(2.61)	80 / 0.13	55 / 0.27	15 / 0.28	103 / 84	477	
IrCl(¹ Pr-phenmox)Cp*	(2.62)	100 / 0.13	53 / 0.26	14 / 0.27	112 / 78	567	

Table (2C.2): Elemental microanalysis results for complexes (2.59 - 2.62)

Complex	Code	Found (Calculated)		
		C %	H %	N %
RuCl(¹ Pr-phenmox)(<i>p</i> -cy)	(2.59)	55.48 (55.63)	5.90 (5.94)	2.89 (2.95)
RuCl(¹ Pr-phenmox)(mes)	(2.60)	54.47 (54.72)	5.55 (5.68)	2.96 (3.04)
RhCl(¹ Pr-phenmox)Cp*	(2.61)	55.05 (55.30)	5.92 (6.12)	2.88 (2.93)
IrCl(¹ Pr-phenmox)Cp*	(2.62)	48.49 (48.65)*	5.63 (5.85)	2.00 (2.14)

* includes 1.5 equivalents of acetone

Table (2C.3): ^1H NMR data for complexes $[\text{MCl}(\text{}^1\text{Pr-NTs-animox})(\text{ring})]$ in CDCl_3 (δ / ppm)

Complex (Code)	π -ring	Tosyl group	Aniline ring	Oxazoline ring	CHMe_2 group ^a
$\text{RuCl}(\text{}^1\text{Pr-NTs-animox})(\text{mes})$ (2.57) Major isomer	2.02, 4.91	2.24 (s, 3H, Ar- <i>Me</i>); 6.92 and 7.33 both (d, 2H, J 7 Hz, Ar- <i>H</i>)	7.09 (t, 1H, J 7 Hz, Ar-4-H), 7.38 (dd, 1H, J 7, 1 Hz, Ar-3-H), 7.54 (m, 1H, Ar-5-H), 8.09 (d, 1H, J 7 Hz, Ar-6-H)	3.73 (dd, 1H, J 10, 8 Hz, OCH), 4.25 (m, 2H, OCH + NCH)	0.88 (d, 3H, J 6 Hz, <i>MeCHMe'</i>), 0.97 (d, 3H, J 6 Hz, <i>MeCHMe'</i>), 2.25 (m, 1H, <i>CHMe</i> ₂)
$\text{RuCl}(\text{}^1\text{Pr-NTs-animox})(\text{mes})$ (2.57) Minor isomer	2.11, 4.80	Obscured by signals of Major isomer	7.66 (m, 1H, Ar-5-H), 8.50 (d, 1H, J 7 Hz, Ar-6-H)	4.13 (m, 1H, OCH), 4.37 (m, 1H, OCH), 4.44 (m, 1H, NCH)	0.08 (d, 3H, J 6 Hz, <i>MeCHMe'</i>), 0.78 (d, 3H, J 6 Hz, <i>MeCHMe'</i>)
$\text{RhCl}(\text{}^1\text{Pr-NTs-animox})\text{Cp}^*$ (2.58) Major isomer	1.48	2.23 (s, 3H, Ar- <i>Me</i>); 6.96 and 7.52 both (d, 2H, J 7 Hz, Ar- <i>H</i>)	6.96 (m, 1H, Ar-4-H), 7.38 (m, 1H, Ar-3-H), 7.66 (dd, 1H, J 8, 2 Hz, Ar-5-H), 8.21 (d, 1H, J 8 Hz, Ar-6-H)	3.82 (dd, 1H, J 10, 8 Hz, OCH), 4.33 (dd, 1H, J 8, 5 Hz, OCH), 4.74 (ddd, 1H, J 10, 5, 3 Hz, NCH)	0.87 (d, 3H, J 6 Hz, <i>MeCHMe'</i>), 0.94 (d, 3H, J 6 Hz, <i>MeCHMe'</i>), 2.02 (m, 1H, <i>CHMe</i> ₂)
$\text{RhCl}(\text{}^1\text{Pr-NTs-animox})\text{Cp}^*$ (2.58) Minor isomer	1.48	2.21 (s, 3H, Ar- <i>Me</i>); 6.96 and 7.72 both (m, 2H, Ar- <i>H</i>)	6.85 (t, 1H, J 8 Hz, Ar-4-H), 7.38 (m, 2H, Ar- <i>H</i>), 8.60 (d, 1H, J 9 Hz, Ar-6-H)	4.02 (m, 1H, NCH), 4.24 (t, 1H, J 8 Hz, OCH), 4.45 (dd, 1H, J 8, 3 Hz, OCH)	0.18 (d, 3H, J 6 Hz, <i>MeCHMe'</i>), 0.80 (d, 3H, J 6 Hz, <i>MeCHMe'</i>), 3.32 (m, 1H, <i>CHMe</i> ₂)

Table (2C.4): ^1H NMR data for complexes $[\text{MCl}(\text{}^i\text{Pr-phenmox})(\text{ring})]$ in CDCl_3 (δ / ppm)

Complex (Code)	π -Ring signals	^iPr -group	Oxazoline ring	Phenol ring
RuCl($^i\text{Pr-Phenmox}$)(<i>p</i> -Cy) (2.59)	1.17 and 1.27 (2 \times d, 3H, J 6.5 Hz, CHMe_2), 2.26 (s, 3H, Ar-Me), 2.81 (sept, 1H, J 6.5 Hz, CHMe_2), 4.98 and 5.37 (2 \times d, 1H, J 6 Hz, Ar-H), 5.46 (m, 2H, Ar-H)	0.81 and 1.01 (2 \times d, 3H, J 7 Hz, CHMe_2), 2.70 (m, 1H, CHMe_2)	4.40 (m, 1H, NCH), 4.49 (m, 1H, 2 \times OCH)	6.38 (t, 1H, J 7Hz, py-5-H), 6.93 (d, 1H, J 8Hz, py-3-H), 7.12 (m, 1H, py-4-H), 7.40 (d, 1H, J 7 Hz, py-6-H)
RuCl($^i\text{Pr-Phenmox}$)(mes) (2.60)	2.19 (s, 9H, $\text{C}_6\text{H}_3\text{Me}_3$), 4.84 (s, 3H, $\text{C}_6\text{H}_3\text{Me}_3$)	0.74 and 0.97 (2 \times d, 3H, J 7 Hz, CHMe_2), 2.79 (m, 1H, CHMe_2)	4.37 (m, 2H, NCH + OCH), 4.49 (m, 1H, OCH)	6.38 (t, 1H, J 7Hz, py-5-H), 6.95 (d, 1H, J 8Hz, py-3-H), 7.14 (t, 1H, J 7Hz, py-4-H), 7.43 (d, 1H, J 8Hz, py-6-H)
RhCl($^i\text{Pr-Phenmox}$)Cp* (2.61)	1.59 (s, 15H, Cp*)	0.77 and 0.96 (2 \times d, 3H, J 7 Hz, CHMe_2), 2.80 (m, 1H, CHMe_2)	4.34 (m, 2H, NCH + OCH), 4.49 (m, 1H, OCH)	6.40 (t, 1H, J 7Hz, py-5-H), 6.97 (d, 1H, J 8Hz, py-3-H), 7.17 (t, 1H, J 7Hz, py-4-H), 7.46 (d, 1H, J 8Hz, py-6-H),
IrCl($^i\text{Pr-Phenmox}$)Cp* (2.62)	1.62 (s, 15H, Cp*)	0.87 and 0.95 (2 \times d, 3H, J 7 Hz), 2.68 (m, 1H, CHMe_2)	4.19 (m, 1H, NCH) 4.30 (t, 1H, J 8.5 Hz, OCH), 4.44 (dd, J 8.5, 4 Hz, 1H, OCH)	6.39 (t, 1H, J 7Hz, py-5-H), 6.90 (d, 1H, J 8Hz, py-3-H), 7.19 (t, 1H, J 7Hz, py-4-H), 7.52 (d, 1H, J 8Hz, py-6-H)

Table (2D.1): Preparative details and Yields obtained for complexes

[M(OH₂)(N-N)(ring)](SbF₆)_n (n = 1, 2) (N-N = box, bop, benbox, pymox, animox, NTs-animox)

Cation	Code	Precursor	Quantity of Precursor (mg / mmol)	Quantity of AgSbF ₆ (mg / mmol)	Yield (mg / %)
[Ru(OH ₂)(^t Pr-box)(mes)] ²⁺	2.30	2.20	50 / 0.070	25 / 0.073	63 / 97
[Rh(OH ₂)(^t Pr-box)Cp*] ²⁺	2.31	2.21	70 / 0.095	33 / 0.096	85 / 94
[Ru(OH ₂)(^t Pr-bop)(mes)] ²⁺	2.32	2.22	27 / 0.038	13 / 0.038	34 / 91
[Rh(OH ₂)(^t Pr-bop)Cp*] ²⁺	2.33	2.23	100 / 0.13	45 / 0.13	120 / 93
[Ru(OH ₂)(^t Pr-benbox)(C ₆ H ₆)] ²⁺	2.34	2.25	100 / 0.133	48 / 0.14	107 / 83
[Ru(OH ₂)(^t Pr-benbox)(<i>p</i> -Cy)] ²⁺	2.35	2.26, R = ^t Pr	60 / 0.074	26 / 0.076	67 / 88
[Ru(OH ₂)(Et-benbox)(mes)] ²⁺	2.36, R = Et	2.27, R = Et	113 / 0.15	53 / 0.15	119 / 82
[Ru(OH ₂)(^t Pr-benbox)(mes)] ²⁺	2.36, R = ^t Pr	2.27, R = ^t Pr	100 / 0.126	44 / 0.128	117 / 92
[Rh(OH ₂)(^t Pr-benbox)Cp*] ²⁺	2.37	2.28, R = ^t Pr	60 / 0.074	27 / 0.078	73 / 96
[Ru(OH ₂)(^t Pr-pymox)(C ₆ H ₆)] ²⁺	2.63, R = ^t Pr	2.43, R = ^t Pr	70 / 0.109	38 / 0.111	86 / 92
[Ru(OH ₂)(^t Bu-pymox)(C ₆ H ₆)] ²⁺	2.63, R = ^t Bu	2.43, R = ^t Bu	64 / 0.10	34 / 0.10	80 / 94
[Ru(OH ₂)(^t Pr-pymox)(<i>p</i> -Cy)] ²⁺	2.64, R = ^t Pr	2.44, R = ^t Pr	70 / 0.101	35 / 0.102	84 / 91
[Ru(OH ₂)(^t Bu-pymox)(<i>p</i> -Cy)] ²⁺	2.64, R = ^t Bu	2.44, R = ^t Bu	85 / 0.12	45 / 0.13	101 / 91
[Ru(OH ₂)(Et-pymox)(mes)] ²⁺	2.65, R = Et	2.45, R = Et	100 / 0.15	51 / 0.15	124 / 93
[Ru(OH ₂)(^t Pr-pymox)(mes)] ²⁺	2.65, R = ^t Pr	2.45, R = ^t Pr	100 / 0.147	52 / 0.15	121 / 92

Cation	Code	Precursor	Quantity of Precursor (mg / mmol)	Quantity of AgSbF ₆ (mg / mmol)	Yield (mg / %)
[Ru(OH ₂)(^t Bu-pymox)(mes)] ²⁺	2.65, R = ^t Bu	2.45, R = ^t Bu	100 / 0.144	50 / 0.146	117 / 89
[Ru(OH ₂)(Ph-pymox)(mes)] ²⁺	2.65, R = Ph	2.45, R = Ph	100 / 0.14	48 / 0.14	118 / 90
[Ru(OH ₂)(Bn-pymox)(mes)] ²⁺	2.65, R = Bn	2.45, R = Bn	100 / 0.137	47 / 0.137	113 / 87
[Ru(OH ₂)(Me ₂ -pymox)(mes)] ²⁺	2.66	2.46	100 / 0.15	52 / 0.15	112 / 84
[Ru(OH ₂)(Indanyl-pymox)(mes)] ²⁺	2.67	2.47	90 / 0.123	44 / 0.128	112 / 96
[Ru(OH ₂)(ⁱ Pr-pymox)(C ₆ Me ₆)] ²⁺	2.68	2.48	84 / 0.116	41 / 0.119	83 / 76
[Rh(OH ₂)(Et-pymox)Cp*] ²⁺	2.69, R = Et	2.49, R = Et	100 / 0.146	50 / 0.146	124 / 94
[Rh(OH ₂)(ⁱ Pr-pymox)Cp*] ²⁺	2.69, R = ⁱ Pr	2.49, R = ⁱ Pr	100 / 0.143	50 / 0.146	125 / 95
[Rh(OH ₂)(^t Bu-pymox)Cp*] ²⁺	2.69, R = ^t Bu	2.49, R = ^t Bu	100 / 0.14	48 / 0.14	122 / 94
[Rh(OH ₂)(Ph-pymox)Cp*] ²⁺	2.69, R = Ph	2.49, R = Ph	100 / 0.136	47 / 0.137	115 / 89
[Rh(OH ₂)(Bn-pymox)Cp*] ²⁺	2.69, R = Bn	2.49, R = Bn	100 / 0.134	46 / 0.134	119 / 92
[Rh(OH ₂)(Me ₂ -pymox)Cp*] ²⁺	2.70	2.50	100 / 0.146	50 / 0.146	120 / 91
[Rh(OH ₂)(Indanyl-pymox)Cp*] ²⁺	2.71	2.51	80 / 0.107	38 / 0.111	100 / 97
[Ir(OH ₂)(ⁱ Pr-pymox)Cp*] ²⁺	2.72	2.52	45 / 0.057	20 / 0.058	54 / 94
[Ru(OH ₂)(ⁱ Pr-animox)(mes)] ²⁺	2.73	2.53	70 / 0.101	35 / 0.102	73 / 79
[Ru(OH ₂)(ⁱ Pr-NTs-animox)(mes)] ⁺	2.74	2.57	80 / 0.13	45 / 0.131	97 / 90
[Rh(OH ₂)(ⁱ Pr-NTs-animox)Cp*] ⁺	2.75	2.58	80 / 0.127	44 / 0.128	99 / 92

Table (2D.2): ^1H NMR data for complexes $[\text{M}(\text{OH}_2)(^i\text{Pr-box})(\text{ring})](\text{SbF}_6)_2$ in d_6 -acetone (δ / ppm)

Cation (Code)	π -ring	Oxazoline ring	CHMe_2 group	H_2O ligand
$[\text{Ru}(\text{OH}_2)(^i\text{Pr-box})(\text{mes})]^{2+}$ (2.30)	2.42, 6.34	4.72 (m, 1H, NCH), 4.87 (t, 1H, J 10 Hz, OCH), 5.12 (m, 2H, OCH), 5.26 (m, 2H, OCH + NCH)	0.71, 1.05, 1.12 and 1.13 (4 \times d, 3H, J 7 Hz, CHMe_2), 2.46 (m, 1H, CHMe_2), 2.91 (m, 1H, CHMe_2)	7.15 (s, 2H)
$[\text{Rh}(\text{OH}_2)(^i\text{Pr-box})\text{Cp}^*]^{2+}$ (2.31) 223 K	1.94	4.70 (m, 1H, NCH), 4.85 (t, 1H, J 11 Hz, OCH), 4.94 (t, 1H, J 11 Hz, OCH), 5.10 (m, 1H, NCH), 5.24 (m, 2H, 2 \times OCH)	0.65, 0.99, 1.07, 1.08 all (d, 3H, J 6 Hz, CHMe_2), 2.30 (m, 1H, CHMe_2), 2.67 (m, 1H, CHMe_2)	7.00 (s, 2H)
$[\text{Rh}(\text{OH}_2)(^i\text{Pr-box})\text{Cp}^*]^{2+}$ (2.31) 300 K	1.94	4.95 (m, 4H, 2 \times NCH, 2 \times OCH), 5.18 (m, 2H, 2 \times OCH)	0.90 and 1.13 (2 \times d, 6H, J 6 Hz, CHMe_2), 2.57 (m, 2H, CHMe_2)	-

Table (2D.3): ^1H NMR data for complexes $[\text{M}(\text{OH}_2)(^i\text{Pr-bop})(\text{ring})](\text{SbF}_6)_2$ in d_6 -acetone (δ / ppm)

Cation (Code)	π -ring	Oxazoline ring	CMe_2	CHMe_2 group	H_2O ligand
$[\text{Ru}(\text{OH}_2)(^i\text{Pr-bop})(\text{mes})]^{2+}$ (2.32) 233 K	2.42, 6.41	4.36 (t, 1H, J 10 Hz, OCH), 4.52 (m, 1H, NCH), 4.88 (t, 1H, J 10 Hz, OCH), 4.94 (m, 2H, 2 \times OCH), 5.25 (m, 1H, NCH)	1.53 and 1.77 (2 \times s, 3H)	0.54, 1.06, 1.08, 1.12 (4 \times d, 3H, J 7 Hz, CHMe_2), 2.42 (m, 1H, CHMe_2), 2.96 (m, 1H, CHMe_2)	7.06 (s, 2H)
$[\text{Ru}(\text{OH}_2)(^i\text{Pr-bop})(\text{mes})]^{2+}$ (2.32) 300 K	2.47, 6.41	4.70 (br m, 2H, NCH + OCH), 4.93 (m, 4H, NCH + 3 \times OCH)	1.66 (s, 6H)	0.90 (br s, 6H, CHMe_2), 1.17 (d, 6H, J 7 Hz, CHMe_2)	-
$[\text{Rh}(\text{OH}_2)(^i\text{Pr-bop})\text{Cp}^*]^{2+}$ (2.33) 213 K	1.90	4.25, 4.53, 4.79, 4.89, 5.00 and 5.08 (6 \times br m, 4 \times OCH + 2 \times NCH)	1.55 and 1.77 (2 \times br s, 3H)	0.54 and 0.96 (2 \times br s, 3H, CHMe_2), 1.04 (m, 6H, CHMe_2), 2.30 and 2.61 (2 \times br m, 1H, CHMe_2)	6.55 (br s, 2H)
$[\text{Rh}(\text{OH}_2)(^i\text{Pr-bop})\text{Cp}^*]^{2+}$ (2.33) 300 K	1.88	4.61 (m, 2H), 4.88 (m, 4H)	1.71 (s, 6H)	0.85 and 1.12 (2 \times d, 6H, CHMe_2), 2.53 (m, 2H, CHMe_2)	-

Table (2D.4): ^1H NMR data for complexes $[\text{Ru}(\text{OH}_2)(\text{R-benbox})(\text{arene})](\text{SbF}_6)_2$ in d_6 -acetone (δ / ppm)

Cation (Code)	π -Arene ring	Benzene ring	Oxazoline ring	Substituent	H_2O Ligand
$[\text{Ru}(\text{OH}_2)(^i\text{Pr-benbox})(\text{C}_6\text{H}_6)]^{2+}$ (2.34)	6.02 (s, 6H, C_6H_6)	8.06 (m, 3H), 8.31 (m, 1H)	4.45 (ddd, 1H, J 10, 2, 3 Hz, NCH), 4.81 (t, 1H, J 10 Hz, OCH), 4.95 (m, 1H, NCH), 5.13 (m, 1H, OCH), 5.24 (m, 2H, OCH)	0.53, 0.84, 0.96, 1.16 all (d, 3H, J 7 Hz, CHMe_2), 2.00 (m, 1H, CHMe_2), 2.78 (m, 1H, CHMe_2)	7.65 (s, 2H)
$[\text{Ru}(\text{OH}_2)(^i\text{Pr-benbox})(p\text{-Cy})]^{2+}$ (2.35)	1.21 and 1.29 both (d, 3H, J 6.5 Hz, CHMe_2); 1.61 (s, 3H, ArMe), 2.72 (sept, 1H, J 6.5 Hz, CHMe_2); 5.08, 5.57, 5.72, 5.85 (4 \times d, 1H, J 5.5 Hz, Ar-H)	7.91 (m, 3H), 8.24 (m, 1H)	4.07 (m, 1H, NCH), 4.43 (t, 1H, J 10 Hz, OCH), 4.53 (dt, 1H, J 1, 8 Hz, NCH), 4.77 (m, 2H, OCH), 4.98 (t, 1H, J 10 Hz, OCH)	0.48, 0.84, 1.03, 1.33 (4 \times d, 3H, J 7 Hz, CHMe_2), 1.63 (m, 1H, CHMe_2), 2.72 (m, 1H, CHMe_2)	6.37 (s, 2H)

Table (2D.5): ^1H NMR data for complexes $[\text{M}(\text{OH}_2)(\text{R-benbox})(\text{ring})](\text{SbF}_6)_2$ in d_6 -acetone (δ / ppm)

Cation (Code)	π -ring	Benzene ring	Oxazoline ring	Substituent	H_2O Ligand
$[\text{Ru}(\text{OH}_2)(\text{Et-benbox})(\text{mes})]^{2+}$ (2.36, R = Et)	1.92, 5.16	8.10 (m, 1H), 8.21 (m, 1H), 8.37 (m, 2H)	4.38 (m, 1H, NCH), 4.58 (m, 1H, NCH), 4.82 (t, 1H, J 9 Hz, OCH), 4.98 (m, 3H, 3 \times OCH)	0.75 and 0.99 (2 \times t, 3H, J 7 Hz, CH_2Me), 1.63 (m, 2H, CH_2Me), 1.92 (m, 1H, CH_2Me), 2.54 (m, 1H, CH_2Me)	6.96 (s, 2H)
$[\text{Ru}(\text{OH}_2)(^i\text{Pr-benbox})(\text{mes})]^{2+}$ (2.36, R = ^iPr)	2.14, 5.30	8.12 (m, 2H), 8.18 (m, 1H), 8.43 (m, 1H)	4.23 (ddd, 1H, J 10, 5, 3 Hz, NCH), 4.65 (t, 1H, J 10 Hz, OCH), 4.83 (m, 1H, NCH), 5.08 (m, 3H, 3 \times OCH)	0.60, 0.93, 1.05 and 1.35 (4 \times d, 3H, J 7 Hz, CHMe_2), 2.1 (m, 1H, CHMe_2), 2.75 (m, 1H, CHMe_2)	7.23 (s, 2H)
$[\text{Rh}(\text{OH}_2)(^i\text{Pr-benbox})\text{Cp}^*]^{2+}$ (2.37)	1.46	8.13 (m, 3H), 8.38 (d, 1H, J 9 Hz)	4.46 (m, 1H, NCH), 4.60 (t, 1H, J 10 Hz, OCH), 4.71 (m, 1H, NCH), 5.07 (m, 3H, 3 \times OCH)	0.58, 0.85, 0.98 and 1.19 (4 \times d, 3H, J 7 Hz, CHMe_2), 2.10 (m, 1H, CHMe_2), 2.41 (m, 1H, CHMe_2)	7.47 (s, 2H)

Table (2D.6): ¹H NMR data for complexes [Ru(OH₂)(R -pymox)(arene)](SbF₆)₂ in d₆-acetone (δ / ppm)

Cation (Code)	Arene Ring	Pyridine ring	Oxazoline ring	Substituents	H ₂ O Ligand
[Ru(OH ₂)(^t Bu-pymox)(C ₆ H ₆)] ²⁺ (2.63, R = ^t Bu)	6.46	8.11 (m, 1H, pyH), 8.19 (d, 1H, <i>J</i> 7 Hz, pyH), 8.50 (t, 1H, <i>J</i> 7 Hz, pyH), 9.94 (d, 1H, <i>J</i> 5 Hz, py-6-H)	5.24 (m, 3H, OCH ₂ , NCH)	1.16 (s, 9H, CMe ₃)	7.33 (br. s)
[Ru(OH ₂)(ⁱ Pr-pymox)(C ₆ H ₆)] ²⁺ (2.63, R = ^t Bu)	6.47 (major) 6.53 (minor)	8.08 (m, 1H, py-5-H), 8.15 (d, 1H, <i>J</i> 7 Hz, py-3-H), 8.46 (dt, 1H, <i>J</i> 7, 1 Hz, py-4-H), 9.94 (d, 1H, <i>J</i> 5 Hz, py-6-H, major), 10.01 (d, <i>J</i> 5 Hz, py-6-H, minor)	5.16 (m, 2H, OCH ₂), 5.39 (ddd, 1H, <i>J</i> 10, 7, 3Hz, NCH)	0.83 and 1.13 (2 × d, 3H, <i>J</i> 7 Hz, CHMe ₂), 2.6 (m, 1H, CHMe ₂)	7.12 (br. s)
[Ru(OH ₂)(ⁱ Pr-pymox)(C ₆ Me ₆)] ²⁺ (2.68)	2.41	8.15 (m, 2H, py-H), 8.45 (td, 1H, <i>J</i> 7, 1 Hz, py-4-H), 9.51 (dd, 1H, <i>J</i> 6, 1 Hz, py-6-H)	5.19 (m, 2H, OCH), 5.28 (m, 1H, NCH)	0.68 and 1.17 (2 × d, 3H, <i>J</i> 6.5 Hz, CHMe ₂), 2.26 (m, 1H, CHMe ₂)	5.19 (s, 2H)

* other signals obscured by those of major isomer

Table (2D.7): ^1H NMR data for complexes $[\text{Ru}(\text{OH}_2)(\text{R-pymox})(p\text{-Cy})](\text{SbF}_6)_2$ in d_6 -acetone (δ / ppm)

Cation (Code)	Arene Ring	Pyridine ring	Oxazoline ring	Substituents	H_2O Ligand
$[\text{Ru}(\text{OH}_2)(^i\text{Pr-pymox})(p\text{-cy})]^{2+}$ (2.64, R = ^iPr) major isomer	1.22 and 1.25 (2 \times d, 3H, J 6.5 Hz, CHMe_2), 2.35 (s, 3H, Ar-Me), 6.60 and 6.85 (2 \times d, 2H, J 6 Hz, Ar-H)	8.25 (m, 1H, py-5-H), 8.31 (d, 1H, J 7.5 Hz, py-3-H), 8.60 (t, 1H, J 7.5 Hz, py-4-H), 10.03 (d, 1H, J 5 Hz, py-6-H)	5.22 (t, 1H, J 9 Hz, OCH), 5.28 (t, 1H, J 9 Hz, OCH), 5.40 (m, 1H, NCH)	0.88 and 1.19 (2 \times d, 3H, J 6.5 Hz, CHMe_2), 2.63 (m, 1H, CHMe_2)	6.43 (br. s)
$[\text{Ru}(\text{OH}_2)(^i\text{Pr-pymox})(p\text{-cy})]^{2+}$ (2.64, R = ^iPr) minor isomer*	2.33 (s, 3H, Ar-Me), 6.77 (m, Ar-H)	10.05 (d, 1H, J 5 Hz, py-6-H)	5.52 (m, 1H, NCH)	0.97 and 1.15 (2 \times d, 3H, J 6.5 Hz, CHMe_2), 2.82 (m, 1H, CHMe_2)	
$[\text{Ru}(\text{OH}_2)(^t\text{Bu-pymox})(p\text{-cy})]^{2+}$ (2.64, R = ^tBu)	1.03 and 1.09 (2 \times d, 3H, J 6.5 Hz, CHMe_2), 2.17 (s, 3H, Ar-Me), 5.93 (d, 1H, J 6 Hz, Ar-H), 6.08 (m, 3H, Ar-H)	7.98 (m, 2H, py-H), 8.27 (m, 1H, py-4-H), 9.53 (d, 1H, J 5 Hz, py-6-H)	4.88 (dd, J 8, 4 Hz, 1H, NCH), 5.08 (m, 2H, OCH_2)	1.06 (s, 9H, CMe_3)	6.23 (br. s)

* other signals obscured by those of major isomer

Table (2D.8): ^1H NMR spectroscopic data for complexes $[\text{Ru}(\text{OH}_2)(\text{R-pymox})(\text{mes})](\text{SbF}_6)_2$ (δ / ppm)

Cation (Code)	mes ring	Pyridine ring	Oxazoline ring	Substituents	H ₂ O Ligand
$[\text{Ru}(\text{OH}_2)(\text{Et-pymox})(\text{mes})]^{2+}$ (2.65, R = Et) in d_6 -acetone	2.28, 5.82	8.02 (m, 2H, pyH), 8.34 (m, 1H, pyH), 9.73 (d, 1H, J 5 Hz, py-6-H)	4.79 (t, 1H, J 8 Hz, OCH), 5.13 (m, 1H, NCH), 5.20 (m, 1H, OCH)	0.92 (t, 3H, J 7 Hz, CH_2Me), 1.51 and 2.19 ($2 \times$ m, 1H, CHMe)	6.33 (br s)
$[\text{Ru}(\text{OH}_2)(^i\text{Pr-pymox})(\text{mes})]^{2+}$ (2.65, R = ^iPr) in $\text{CD}_2\text{Cl}_2/d_6$ -acetone (10:1)	2.22, 5.55	7.87 (m, 2H, pyH), 8.15 (t, 1H, J 8 Hz, py-4-H), 9.40 (d, 1H, J 5 Hz, py-6-H)	4.78 (dd, 1H, J 8.5, 5 Hz, OCH), 4.92 (m, 1H, NCH), 5.03 (t, 1H, J 9 Hz, OCH)	0.57 and 1.01 ($2 \times$ d, 3H, J 7 Hz, CHMe_2), 2.20 (m, 1H, CHMe_2)	5.40 (br s)
$[\text{Ru}(\text{OH}_2)(^i\text{Pr-pymox})(\text{mes})]^{2+}$ (2.65, R = ^iPr) in d_6 -acetone	2.33, 5.97	8.13 (m, 2H, pyH), 8.46 (dt, 1H, J 1, 7.5 Hz, py-4-H), 9.88 (d, 1H, J 5.5 Hz, py-6-H)	5.15 (m, 2H, $2 \times$ OCH), 5.30 (dt, 1H, J 2.5, 8 Hz, NCH)	0.73 and 1.13 ($2 \times$ d, 3H, J 7 Hz, CHMe_2), 2.38 (m, 1H, CHMe_2)	6.68 (s, 2H)
$[\text{Ru}(\text{OH}_2)(^t\text{Bu-pymox})(\text{mes})]^{2+}$ (2.65, R = ^tBu) in $\text{CD}_2\text{Cl}_2/d_6$ -acetone (10:1)	2.31, 5.73	7.93 (m, 2H, pyH), 8.24 (t, 1H, J 7 Hz, py-4-H), 9.37 (d, 1H, J 5 Hz, py-6-H)	4.72 (m, 1H, NCH), 4.96 (m, 1H, OCH), 5.05 (t, 1H, J 9 Hz, OCH)	1.02 (s, 9H, CMe_3)	5.82 (br s)

Table (2D.9): ^1H NMR data for complexes $[\text{Ru}(\text{OH}_2)(\text{R,R}'\text{-pymox})(\text{mes})](\text{SbF}_6)_2$ in $\text{CD}_2\text{Cl}_2/\text{d}_6\text{-acetone}$ (10:1) (δ / ppm)

Cation (Code)	mes ring	Pyridine ring	Oxazoline ring	Substituents	H_2O Ligand
$[\text{Ru}(\text{OH}_2)(\text{Ph-pymox})(\text{mes})]^{2+}$ (2.65, R = Ph)	2.10, 5.29	7.88 (m, 1H, py-5-H), 7.99 (d, 1H, J 7 Hz, py-3-H), 8.18 (t, 1H, J 7 Hz, py-4-H), 9.32 (d, 1H, J 5 Hz, py-6-H)	4.68 (t, 1H, J 10 Hz, OCH), 5.50 (t, 1H, J 10 Hz, OCH), 6.01 (t, 1H, J 10 Hz, NCH)	7.29 (m, 2H, Ph), 7.43 (m, 3H, Ph)	5.00 (br s)
$[\text{Ru}(\text{OH}_2)(\text{Bn-pymox})(\text{mes})]^{2+}$ (2.65, R = Bn)	2.29, 5.56	7.92 (m, 2H, pyH), 8.19 (t, 1H, J 8 Hz, py-4-H), 9.47 (d, 1H, J 5.5 Hz, py-6-H)	4.68 (dd, 1H, J 9, 5.5 Hz, OCH) 5.04 (t, 1H, J 9 Hz, OCH), 5.33 (m, 1H, NCH)	2.67 (dd, 1H, J 14, 11 Hz, CH_2Ph), 3.46 (dd, 1H, J 14, 3.5 Hz, CH_2Ph), 7.27 (m, 2H, Ph), 7.37 (m, 3H, Ph)	5.45 (br s)
$[\text{Ru}(\text{OH}_2)(\text{Me}_2\text{-pymox})(\text{mes})]^{2+}$ (2.66)	2.35, 5.95	7.96 (m, 2H, pyH), 8.24 (t, 1H, J 8 Hz, py-4-H), 9.40 (d, 1H, J 5 Hz, py-6-H)	4.58 and 4.75 ($2 \times$ d, 1H, J 9 Hz, $2 \times$ OCH)	1.52 (s, 3H, MeCMe'), 1.90 (s, 3H, MeCMe'),	5.50 (s, 2H)
$[\text{Ru}(\text{OH}_2)(\text{Indanyl-pymox})(\text{mes})]^{2+}$ (2.67) in $\text{d}_6\text{-acetone}$	2.49, 6.08	8.07 (m, 1H, py-5-H), 8.16 (d, 1H, py-3-H), 8.41 (t, 1H, J 7 Hz, py-4-H), 9.79 (d, 1H, J 7 Hz, py-6-H)	6.36 (dd, 1H, J 8, 7 Hz, OCH), 6.71 (d, 1H, J 8 Hz, NCH)	3.49 (d, 1H, J 19 Hz, $\text{CHH}'\text{Ph}$), 3.75 (dd, 1H, J 19, 7 Hz, $\text{CHH}'\text{Ph}$), 7.35 (m, 3H, Ph), 7.82 (d, 1H, J 7 Hz, Ph)	6.11 (s, 2H)

Table (2D.10): ^1H NMR data for complexes $[\text{Rh}(\text{OH}_2)(\text{R-pymox})\text{Cp}^*](\text{SbF}_6)_2$ in d_6 -acetone (δ / ppm)*

Cation (Code)	Cp*	Pyridine ring	Oxazoline ring	Substituent
$[\text{Rh}(\text{OH}_2)(\text{Et-pymox})\text{Cp}^*]^{2+}$ (2.69, R = Et)	1.99	7.86 (m, py-5-H), 7.97 (dd, J 8, 1 Hz, py-3-H), 8.16 (td, J 8, 1 Hz, py-4-H), 8.78 (dd, J 5, 1 Hz, py-6-H)	4.64 (m, 1H, NCH), 4.73 (m, 1H, OCH), 5.06 (t, 1H, J 9 Hz, OCH)	0.97 (t, 3H, J 7 Hz, CH_2Me), 1.60 and 1.95 ($2 \times$ m, 1H, CHMe)
$[\text{Rh}(\text{OH}_2)(^i\text{Pr-pymox})\text{Cp}^*]^{2+}$ (2.69, R = ^iPr)	1.99	8.22 (m, 2H, pyH), 8.52 (dt, 1H, J 1.5, 8 Hz, py-4-H), 9.55 (d, 1H, J 4.5 Hz, py-6-H)	5.13 (dt, 1H, J 2.5, 11.5 Hz, NCH), 5.24 (m, 2H, $2 \times$ OCH)	0.84 and ($2 \times$ d, 3H, J 7 Hz, CHMe_2), 2.47 (m, 1H, CHMe_2)
$[\text{Rh}(\text{OH}_2)(^t\text{Bu-pymox})\text{Cp}^*]^{2+}$ (2.69, R = ^tBu)	1.96	8.26 (m, 2H, pyH), 8.57 (t, 1H, J 8 Hz, py-4-H), 9.55 (d, 1H, J 5 Hz, py-6-H)	5.04 (m, 1H, NCH), 5.14 (t, 1H, J 9 Hz, OCH), 5.35 (dd, 1H, J 9, 4 Hz, OCH)	1.18 (s, 9H, CMe_3)
$[\text{Rh}(\text{OH}_2)(\text{Ph-pymox})\text{Cp}^*]^{2+}$ (2.69, R = Ph)	1.70	8.18 (m, 1H, py-5-H), 8.29 (d, 1H, J 7 Hz, py-3-H), 8.50 (t, 1H, J 7 Hz, py-4-H), 9.43 (d, 1H, J 5 Hz, py-6-H)	4.81 (t, 1H, J 10 Hz, OCH), 5.57 (dd, 1H, J 10, 9 Hz, OCH), 6.28 (dd, 1H, J 10, 9 Hz, NCH)	7.50 (m, 3H, Ph), 7.59 (m, 2H, Ph)
$[\text{Rh}(\text{OH}_2)(\text{Bn-pymox})\text{Cp}^*]^{2+}$ (2.69, R = Bn)	1.98	8.20 (m, 2H, pyH), 8.50 (t, 1H, J 7 Hz, py-4-H), 9.49 (d, 1H, J 5 Hz, py-6-H)	4.91 (dd, 1H, J 10, 8 Hz, OCH), 5.09 (t, 1H, J 10 Hz, OCH), 5.48 (m, 1H, NCH)	2.83 (dd, 1H, J 14, 11 Hz, CHPh), 3.59 (dd, 1H, J 14, 3.5 Hz, CHPh), 7.38 (m, 5H, Ph)

* Signal for coordinated H_2O ligand not resolved at RT

Table (2D.11): ^1H NMR data for complexes $[\text{M}(\text{OH}_2)(\text{R,R}'\text{-pymox})\text{Cp}^*](\text{SbF}_6)_2$ in d_6 -acetone (δ / ppm)

Cation (Code)	Cp*	Pyridine ring	Oxazoline ring	Substituent	H ₂ O ligand
$[\text{Rh}(\text{OH}_2)(\text{Me}_2\text{-pymox})\text{Cp}^*]^{2+}$ (2.70) 300 K	1.96	8.21 (m, 2H, pyH), 8.50 (dt, 1H, J 8, 1 Hz, py-4-H), 9.54 (d, 1H, J 5 Hz, py-6-H)	4.83 (s, 2H, OCH ₂)	1.83 (s, 6H, CMe ₂)	-
$[\text{Rh}(\text{OH}_2)(\text{Me}_2\text{-pymox})\text{Cp}^*]^{2+}$ (2.70) 233 K	1.94	8.19 (m, 1H, py-5-H), 8.24 (dd, 1H, J 7.5, 1 Hz, py-3-H), 8.51 (dt, 1H, J 1, 8 Hz, py-4-H), 9.54 (d, 1H, J 5 Hz, py-6-H)	4.72 (d, 1H, J 9 Hz, OCH), 4.93 (d, 1H, J 9 Hz, OCH)	1.61 and 1.92 (2 \times s, 3H, CMe ₂)	6.70 (s, 2H)
$[\text{Rh}(\text{OH}_2)(\text{Indanyl-pymox})\text{Cp}^*]^{2+}$ (2.71)	2.06	8.17 (m, 1H, py-5-H), 8.24 (d, 1H, J 7.5 Hz, py-3-H), 8.48 (dt, 1H, J 1.5, 8 Hz, py-4-H), 9.46 (m, 1H, py-6-H)	6.37 (t, 1H, J 7 Hz, NCH), 6.63 (d, 1H, J 7 Hz, OCH)	3.60 (d, 1H, J 19 Hz, CHPh), 3.78 (dd, 1H, J 19, 7 Hz, CHPh), 7.41 (m, 3H, ArH), 7.66, d, 1H, J 7 Hz, ArH)	6.10 (br s)
$[\text{Ir}(\text{OH}_2)(^i\text{Pr-pymox})\text{Cp}^*]^{2+}$ (2.72) 243 K	1.91	8.20 (m, 2H, py-5-H), 8.35 (d, 1H, J 8 Hz, py-3-H), 8.56 (dt, 1H, J 1, 8 Hz, py-4-H), 9.55 (d, 1H, J 5 Hz, py-6-H)	5.10 (m, 1H, NCH), 5.16 (t, 1H, J 10 Hz, OCH), 5.40 (dd, 1H, J 10, 4 Hz, OCH)	0.79 and 1.13 (2 \times d, 3H, J 7 Hz, CHMe ₂), 2.31 (m, 1H, CHMe ₂)	7.84 (s, 2H)

Table (2D.12): ^1H NMR data for complex $[\text{M}(\text{OH}_2)(^i\text{Pr-NTs-animox})\text{Cp}^*](\text{SbF}_6)_2$ in d_6 -acetone (δ / ppm)

Complex (code)	π -ring	Tosyl group	Aniline ring	Oxazoline ring	CHMe_2 group	H_2O ligand
$[\text{Ru}(\text{OH}_2)(^i\text{Pr-NTs-animox})(\text{mes})]\text{SbF}_6$ (2.74) 253 K	2.24, 5.68	2.26 (s, 3H, Ar- <i>Me</i>); 6.92 (d, 2H, <i>J</i> 7 Hz, Ar-3,5- <i>H</i>), 7.33 (d, 2H, <i>J</i> 7 Hz, Ar-2,6- <i>H</i>)	6.94 (t, 1H, <i>J</i> 8 Hz, Ar-4-H), 7.38 (m, 1H, Ar-5-H), 7.67 (dd, 1H, <i>J</i> 7, 1 Hz, Ar-3-H), 8.08 (d, 1H, <i>J</i> 7 Hz, Ar-6-H)	4.84 (m, 2H, 2 \times OCH), 4.99 (m, 1H, NCH)	0.67 and 1.01 (2 \times d, 3H, <i>J</i> 8 Hz, CHMe_2), 2.29 (m, 1H, CHMe_2)	6.87 (s, 2H)
$[\text{Ru}(\text{OH}_2)(^i\text{Pr-NTs-animox})(\text{mes})]\text{SbF}_6$ 295 K	2.25, 5.68	2.42 (br m, 3H, Ar- <i>Me</i>); 8.10 - 7.20 (br m, 4H, Ar-H)	8.10 - 7.20 (br m, 4H, Ar-H)	4.86 and 4.94 (2 \times m, 1H, OCH), 5.08 (m, 1H, NCH)	0.76 and 1.09 (2 \times br s, 3H, CHMe_2), 2.40 (m, 1H, CHMe_2)	-
$\text{Rh}(\text{OH}_2)(^i\text{Pr-NTs-animox})\text{Cp}^*]\text{SbF}_6$ (2.75) 213 K	1.68	2.23 (s, 3H, Ar- <i>Me</i>); 7.21 (d, 2H, <i>J</i> 8 Hz, Ar-3,5- <i>H</i>), 7.56 (d, 2H, <i>J</i> 7 Hz, Ar-2,6- <i>H</i>)	6.97 (t, 1H, <i>J</i> 8 Hz, Ar-4-H), 7.47 (m, 1H, Ar-5-H), 7.69 (dd, 1H, <i>J</i> 8, 1.5 Hz, Ar-3-H), 8.26 (d, 1H, <i>J</i> 8.5 Hz, Ar-6-H)	4.77 (t, 1H, OCH), 4.86 (m, 2H, OCH + NCH)	0.73 and 0.99 (2 \times d, 3H, <i>J</i> 7 Hz, CHMe_2), 2.37 (m, 1H, CHMe_2)	6.79 (br s, 2H)

Table (2D.13) - Mass Spectrometry Data and Elemental Analysis results for complexes

$[M(OH_2)(N-N)(ring)](SbF_6)_2$ (N-N = ⁱPr-box, ⁱPr-bop, R-benbox) (2.20 - 2.29)

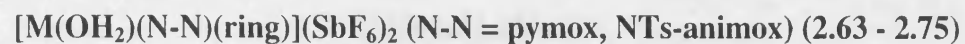
		Mass Spectrometry (m/z)	Elemental Analysis		
			Found (Calculated)		
Complex	Code	Major ion patterns	C %	H %	N %
$[Ru(OH_2)(^iPr\text{-}box)(mes)]^{2+}$	2.30	682 [$\{Ru(^iPr\text{-}box)(mes)\}+SbF_6\}^+$			
$[Rh(OH_2)(^iPr\text{-}box)Cp^*]^{2+}$	2.31	698 [$\{Rh(^iPr\text{-}box)Cp^*\}+SbF_6\}^+$	28.11 (27.76)	4.31 (3.92)	2.51 (2.94)
$[Ru(OH_2)(^iPr\text{-}bop)(mes)]^{2+}$	2.32	724 [$\{Ru(^iPr\text{-}bop)(mes)\}+SbF_6\}^+$	31.90 (31.99) [†]	4.74 (4.79)	2.61 (2.66)
$[Rh(OH_2)(^iPr\text{-}bop)Cp^*]^{2+}$	2.33	740 [$\{Rh(^iPr\text{-}bop)Cp^*\}+SbF_6\}^+$			
$[Ru(OH_2)(^iPr\text{-}benbox)(C_6H_6)]^{2+}$	2.34	716 [$\{Ru(^iPr\text{-}benbox)(C_6H_6)\}+SbF_6\}^+$	29.89 (29.75)	3.59 (3.33)	2.80 (2.59)
$[Ru(OH_2)(^iPr\text{-}benbox)(p\text{-}Cy)]^{2+}$	2.35	772 [$\{Ru(^iPr\text{-}benbox)(p\text{-}Cy)\}+SbF_6\}^+$			
$[Ru(OH_2)(Et\text{-}benbox)(mes)]^{2+}$	2.36, R = Et	730 [$\{Ru(Et\text{-}benbox)(mes)\}+SbF_6\}^+$	31.97 (32.30) [†]	3.35 (3.87)	3.58(2.85)
$[Ru(OH_2)(^iPr\text{-}benbox)(mes)]^{2+}$	2.36, R = ⁱ Pr	758 [$\{Ru(^iPr\text{-}benbox)(mes)\}+SbF_6\}^+$	29.73 (29.75)*	3.49 (3.48)	2.20 (2.48)
$[Rh(OH_2)(^iPr\text{-}benbox)Cp^*]^{2+}$	2.37	774 [$\{Rh(^iPr\text{-}benbox)Cp^*\}+SbF_6\}^+$	32.59 (32.71)	3.99 (4.02)	2.64 (2.72)

[†] includes one equivalent of diethyl ether

[‡] includes one equivalent of acetone

* includes one equivalent of CHCl₃

Table (2D.14) - Mass Spectrometry Data and Elemental results for complexes



Complex	Code	Mass Spectrometry (m/z)		Elemental Analysis: Found (Calculated)		
		$[M(OH_2) + SbF_6]^+$	$[M(OH)(Pymox)(arene)]^+$	C %	H %	N %
$[Ru(OH_2)(^iPr-pymox)(C_6H_6)]^{2+}$	2.63, R = ⁱ Pr	605	387			
$[Ru(OH_2)(^iBu-pymox)(C_6H_6)]^{2+}$	2.63, R = ⁱ Bu	619	401	24.11 (24.27)	2.89 (2.94)	3.05 (3.14)
$[Ru(OH_2)(^iPr-pymox)(p-cy)]^{2+}$	2.64, R = ⁱ Pr	661	443			
$[Ru(OH_2)(^iBu-pymox)(p-cy)]^{2+}$	2.64, R = ⁱ Bu	675	457			
$[Ru(OH_2)(Et-pymox)(mes)]^{2+}$	2.65, R = Et	633	415	25.08 (25.22)	3.09 (3.12)	3.03 (3.10)
$[Ru(OH_2)(^iPr-pymox)(mes)]^{2+}$	2.65, R = ⁱ Pr	647	429	26.37 (26.66)	2.87 (3.13)	3.04 (3.11)
$[Ru(OH_2)(^iBu-pymox)(mes)]^{2+}$	2.65, R = ⁱ Bu	661	443			
$[Ru(OH_2)(Ph-pymox)(mes)]^{2+}$	2.65, R = Ph	681	463			
$[Ru(OH_2)(Bn-pymox)(mes)]^{2+}$	2.65, R = Bn	695	477			
$[Ru(OH_2)(Me_2-pymox)(mes)]^{2+}$	2.66	633	415	25.44 (25.73)	2.85 (2.95)	3.02 (3.16)
$[Ru(OH_2)(Indanyl-pymox)(mes)]^{2+}$	2.67	693	475	30.29 (30.44)	2.82 (2.77)	2.69 (2.96)
$[Ru(OH_2)(^iPr-pymox)(C_6Me_6)]^{2+}$	2.68	689	471	29.03 (29.29)	3.51 (3.63)	2.84 (2.97)

Table (2D.14) cont.

Complex	Code	Mass Spectrometry (m/z)	Elemental Analysis: Found (Calculated)		
		Major Ion Patterns	C %	H %	N %
[Rh(OH ₂)(Et-pymox)Cp*] ²⁺	2.69, R = Et	649 [{M-OH ₂ }+SbF ₆] ⁺	28.15 (28.19*)	3.44 (3.81)	2.61 (2.86)
[Rh(OH ₂)(ⁱ Pr-pymox)Cp*] ²⁺	2.69, R = ⁱ Pr	663 [{M-OH ₂ }+SbF ₆] ⁺	27.95 (27.48)	3.38 (3.40)	3.23 (3.05)
[Rh(OH ₂)(^t Bu-pymox)Cp*] ²⁺	2.69, R = ^t Bu	677 [{M-OH ₂ }+SbF ₆] ⁺	28.27 (28.36)	3.49 (3.57)	2.95 (3.01)
[Rh(OH ₂)(Ph-pymox)Cp*] ²⁺	2.69, R = Ph	697 [{M-OH ₂ }+SbF ₆] ⁺			
[Rh(OH ₂)(Bn-pymox)Cp*] ²⁺	2.69, R = Bn	711 [{M-OH ₂ }+SbF ₆] ⁺			
[Rh(OH ₂)(Me ₂ -pymox)Cp*] ²⁺	2.70	649 [{M-OH ₂ }+SbF ₆] ⁺	26.29 (26.58)	3.18 (3.23)	3.01 (3.18)
[Rh(OH ₂)(Indanyl-pymox)Cp*] ²⁺	2.71	709 [{M-OH ₂ }+SbF ₆] ⁺	31.01 (31.15)	2.98 (3.03)	2.78 (2.91)
[Ir(OH ₂)(ⁱ Pr-pymox)Cp*] ²⁺	2.72	754 [{M-OH ₂ }+SbF ₆] ⁺	25.30 (25.04)	2.96 (3.10)	2.64 (2.78)
[Ru(OH ₂)(ⁱ Pr-animox)(mes)] ⁺	2.73	661 [{M-OH ₂ }+SbF ₆] ⁺			
[Ru(OH ₂)(ⁱ Pr-NTs-animox)(mes)] ⁺	2.74	579 [M-OH ₂] ⁺	40.27 (40.40)	4.27 (4.24)	3.01 (3.37)
[Rh(OH ₂)(ⁱ Pr-NTs-animox)Cp*] ⁺	2.75	595 [M-OH ₂] ⁺	40.87 (41.01)	4.47 (4.51)	3.15 (3.30)

* includes 1 equivalent of acetone +1 equivalent of H₂O

General Synthesis E: Complexes [MX(R-pymox)(ring)]SbF₆ (2.76 - 2.79)

To a solution of the corresponding aqua complex [M(OH₂)(R-pymox)(ring)](SbF₆)₂ (2.65, R = ⁱPr or Ph; 2.69, R = ⁱPr) (one equivalent) in MeOH (3 cm³) was added KBr or NaI (1, 1.5 or 2 equivalents) and the mixture was stirred at room temperature for 30 mins, during which time the solution colour changed from orange to red. The solvent was then removed *in vacuo* and the residue was dissolved in CH₂Cl₂. The resulting solution was then filtered through celite and evaporated to give the crude product. Recrystallisation from CH₂Cl₂/ether afforded pure samples of (2.76 - 2.79), as shown by ¹H NMR. Quantities of reagents used and yields obtained are given in Table (2E.1). ¹H NMR spectroscopic data are given in Tables (2E.2 - 2E.3), with Mass spectrometry data and elemental analysis results given in Table (2E.6).

Table (2E.1): Preparative details and yields for complexes (2.76 - 2.79)

Complex	Code	Precursor	Quantity of Precursor (mg / mmol)	Halide Salt	Quantity of Salt (mg / mmol)	Yield (mg / %)
[RuBr(ⁱ Pr-Pymox)(mes)]SbF ₆	2.76, R = ⁱ Pr	2.65, R = ⁱ Pr	90 / 0.10	KBr	18 / 0.15	70 / 96
[RuBr(Ph-Pymox)(mes)]SbF ₆	2.76, R = Ph	2.65, R = Ph	94 / 0.10	KBr	18 / 0.15	73 / 95
[RuI(ⁱ Pr-Pymox)(mes)]SbF ₆	2.77, R = ⁱ Pr	2.65, R = ⁱ Pr	90 / 0.10	NaI	24 / 0.20	75 / 97
[RuI(Ph-Pymox)(mes)]SbF ₆	2.77, R = Ph	2.65, R = Ph	105 / 0.11	NaI	26 / 0.17	87 / 97
[RhBr(ⁱ Pr-Pymox)Cp*]SbF ₆	2.78	2.69, R = ⁱ Pr	70 / 0.076	KBr	14 / 0.12	54 / 95
[RhI(ⁱ Pr-Pymox)Cp*]SbF ₆	2.79	2.69, R = ⁱ Pr	63 / 0.068	NaI	15 / 0.10	53 / 98

Table (2E.2): ^1H NMR data for complexes $[\text{MCl}(\text{}^i\text{Pr-pymox})(\text{ring})](\text{SbF}_6)$ in d_6 -acetone (δ / ppm)

Cation (Code)	π - Ring	Pyridine Ring	Oxazoline Ring	^iPr -group
$[\text{RuBr}(\text{}^i\text{Pr-pymox})(\text{mes})]^+$ (2.76, R = ^iPr) (S_{Ru})	2.40, 6.23	7.96 (m, py-5-H), 8.08 (m, py-3-H), 8.34 (m, py-4-H), 9.61 (d, 1H, J 5.5 Hz, py-6-H)	4.53 (ddd, 1H, NCH, J 10, 5, 3 Hz), 4.83 (t, 1H, J 10 Hz, OCH), 5.20 (dd, 1H, J 5 Hz, OCH)	1.06 and 1.22 ($2 \times$ d, 3H, J 7 Hz, CHMe_2), 2.89 (m, 1H, CHMe_2)
$[\text{RuBr}(\text{}^i\text{Pr-pymox})(\text{mes})]^+$ (2.76, R = ^iPr) (R_{Ru})	2.37, 5.78	7.96 (m, py-5-H), 8.08 (m, py-3-H), 8.34 (m, py-4-H), 9.51 (d, 1H, J 5.5 Hz, py-6-H)	5.09 (m, 3H, NCH + OCH_2)	0.83 and 1.09 ($2 \times$ d, 3H, J 7 Hz, CHMe_2), 2.37 (m, 1H, CHMe_2)
$[\text{RuI}(\text{}^i\text{Pr-pymox})(\text{mes})]^+$ (2.77, R = ^iPr) (S_{Ru})	2.42, 6.36	7.93 (m, py-5-H), 8.09 (m, py-3-H), 8.33 (m, py-4-H), 9.60 (d, 1H, J 6 Hz, py-6-H)	4.50 (ddd, 1H, NCH, J 10, 5, 3 Hz), 4.85 (t, 1H, J 10 Hz, OCH), 5.20 (dd, 1H, J 5 Hz, OCH)	1.09 and 1.21 ($2 \times$ d, 3H, J 7 Hz, CHMe_2), 2.89 (m, 1H, CHMe_2)
$[\text{RuI}(\text{}^i\text{Pr-pymox})(\text{mes})]^+$ (2.77, R = ^iPr) (R_{Ru})	2.42, 5.92	7.93 (m, py-5-H), 8.09 (m, py-3-H), 8.33 (m, py-4-H), 9.52 (d, 1H, J 6 Hz, py-6-H)	5.09 (m, 3H, NCH + OCH_2)	0.85 and 1.11 ($2 \times$ d, 3H, J 7 Hz, CHMe_2), 2.40 (m, 1H, CHMe_2)
$[\text{RhBr}(\text{}^i\text{Pr-pymox})\text{Cp}^*]^+$ (2.79) (in CD_2Cl_2)	1.79	7.85 (m, py-5-H), 7.96 (d, J 8 Hz, py-3-H), 8.16 (dt, 1H, J 7.5, 1 Hz, py-4-H), 8.75 (d, J 5.5 Hz, py-6-H)	4.61 (m, 1H, NCH), 4.87 (dd, 1H, J 9.5, 5 Hz, $\text{OCH}_{\text{trans}}$), 4.95 (t, 1H, J 9.5 Hz, OCH_{cis})	0.81 and 1.02 ($2 \times$ d, 3H, J 7 Hz, CHMe_2), 2.18 (m, 1H, CHMe_2)

Table (2E.3): ^1H NMR data for complexes $[\text{MCl}(\text{R-pymox})(\text{ring})](\text{SbF}_6)$ in CD_2Cl_2 (δ / ppm)

Cation (Code)	π - Ring	Pyridine Ring	Oxazoline Ring	Substituent
$[\text{RhI}(\text{}^i\text{Pr-pymox})\text{Cp}^*]^+$ (2.79)	1.93	7.85 (m, py-5-H), 8.01 (d, J 7.5 Hz, py-3-H), 8.19 (m, py-4-H), 8.80 (d, J 5 Hz, py-6-H)	4.62 (m, 1H, NCH), 4.93 (dd, 1H, J 10, 5 Hz, $\text{OCH}_{\text{trans}}$), 5.04 (t, 1H, J 10 Hz, OCH_{cis})	0.90 and 1.01 ($2 \times$ d, 3H, J 7 Hz, CHMe_2), 2.25 (m, 1H, CHMe_2)
$[\text{RuBr}(\text{Ph-pymox})(\text{mes})]^+$ (2.76, R = Ph) (S_{Ru})	2.08, 5.36	7.86 (m, py-5-H), 8.02 (dd, J 7.5, 1 Hz, py-3-H), 8.16 (td, J 7, 1 Hz, py-4-H), 9.20 (dd, 1H, J 5.5 Hz, py-6-H)	4.87 (dd, 1H, J 12, 10 Hz, OCH), 5.23 (dd, 1H, J 10.5, 10 Hz, OCH), 5.39 (dd, 1H, J 12, 10.5 Hz, NCH)	7.51 (m, 2H, Ph), 7.63 (m, 3H, Ph)
$[\text{RuBr}(\text{Ph-pymox})(\text{mes})]^+$ (2.76, R = Ph) (R_{Ru})	2.10, 5.31	7.79 (m, py-5-H), 7.91 (m, py-3-H), 8.06 (m, py-4-H), 9.11 (d, 1H, J 5.5 Hz, py-6-H)	4.52 (dd, 1H, J 12, 10 Hz, OCH), 5.48 (dd, 1H, J 10.5, 10 Hz, OCH), 6.04 (dd, 1H, J 12, 10.5 Hz, NCH)	7.42 (m, 2H, Ph), 7.57 (m, 3H, Ph)
$[\text{RuI}(\text{Ph-pymox})(\text{mes})]^+$ (2.77, R = Ph) (S_{Ru})	2.15, 5.61	7.97 (m, py-5-H), 8.02 (dd, J 7.5, 1 Hz, py-3-H), 8.13 (td, J 7, 1 Hz, py-4-H), 9.45 (dd, 1H, J 5.5 Hz, py-6-H)	4.86 (dd, 1H, J 12, 10 Hz, OCH), 5.20 (dd, 1H, J 10.5, 10 Hz, OCH), 5.37 (dd, 1H, J 12, 10.5 Hz, NCH)	7.55 (m, 2H, Ph), 7.62 (m, 3H, Ph)
$[\text{RuI}(\text{Ph-pymox})(\text{mes})]^+$ (2.77, R = Ph) (R_{Ru})	2.18, 5.64	7.78 (m, py-5-H), 7.9 (m, py-3-H), 8.1 (m, py-4-H), 9.16 (d, 1H, J 5.5 Hz, py-6-H)	4.57 (dd, 1H, J 12, 10 Hz, OCH), 5.65 (dd, 1H, J 10.5, 10 Hz, OCH), 6.22 (dd, 1H, J 12, 10.5 Hz, NCH)	7.39 (m, 2H, Ph), 7.63 (m, 3H, Ph)

Table (2E.4): ^1H NMR data for complex $[\text{M}(4\text{-Me-py})(^i\text{Pr-pymox})(\text{ring})](\text{SbF}_6)_2$ in d_6 -acetone (δ / ppm)

Cation (Code)	π - Ring	Pyridine Ring	Oxazoline Ring	^iPr -group	4-Me-py ligand
$[\text{Ru}(4\text{-Me-py})(^i\text{Pr-pymox})(\text{mes})]^+$ (2.82) (R_{Ru})	2.41, 6.37	8.10 (dd, 1H, J 7, 1 Hz, py-3-H), 8.26 (m, 1H, py-5-H), 8.49 (m, 1H, py-4-H), 10.04 (d, 1H, J 6 Hz, py-6-H)	4.81 (t, 1H, J 9 Hz, OCH), 5.23 (dt, 1H, J 3, 9 Hz, NCH), 5.35 (m, 1H, OCH)	1.01 and 1.28 ($2 \times$ d, 3H, J 7 Hz, CHMe_2), 2.97 (m, 1H, CHMe_2)	2.43 (s, 3H, py-Me), 7.40 (d, 2H, J 6.5 Hz, py-3,5-H), 8.32 (d, 2H, J 6.5 Hz, py-2,6-H)
$[\text{Ru}(4\text{-Me-py})(^i\text{Pr-pymox})(\text{mes})]^+$ (2.82) (S_{Ru})	2.25, 6.05	8.26 (m, 1H, py-5-H), 8.32 (m, 1H, py-3-H), 8.58 (m, 1H, py-4-H), 10.01 (d, 1H, J 5.5 Hz, py-6-H)	5.06 (dd, 1H, J 9, 7 Hz, OCH), 5.13 (t, 1H, J 10 Hz, OCH), 5.35 (m, 1H, NCH)	0.28 and 1.14 ($2 \times$ d, 3H, J 7 Hz, CHMe_2), 2.61 (m, 1H, CHMe_2)	2.46 (s, 3H, py-Me), 7.46 (d, 2H, J 6.5 Hz, py-3,5-H), 8.49 (d, 2H, J 6.5 Hz, py-2,6-H)
$[\text{Rh}(4\text{-Me-py})(^i\text{Pr-pymox})\text{Cp}^*]^+$ (2.83) (R_{Rh})	1.91	8.15 (d, 1H, J 9 Hz, py-3-H), 8.35 (m, 1H, py-5-H), 8.55 (t, 1H, J 9 Hz, py-4-H), 9.60 (d, 1H, J 7 Hz, py-6-H)	4.84 (t, 1H, J 9 Hz, OCH), 5.15 (m, 1H, NCH), 5.28 (m, 1H, OCH)	1.07 and 1.25 ($2 \times$ d, 3H, J 6 Hz, CHMe_2), 2.77 (m, 1H, CHMe_2)	2.45 (s, 3H, py-Me), 7.50 (d, 2H, J 6 Hz, py-3,5-H), 8.48 (d, 2H, J 6 Hz, py-2,6-H)
$[\text{Rh}(4\text{-Me-py})(^i\text{Pr-pymox})\text{Cp}^*]^+$ (2.83) (S_{Rh})	1.89	8.25 (d, 1H, J 9 Hz, py-5-H), 8.35 (m, 1H, py-3-H), 8.55 (t, 1H, J 9 Hz, py-4-H), 9.60 (d, 1H, J 7 Hz, py-6-H)	5.15 (m, 2H, $2 \times$ OCH), 5.28 (m, 1H, NCH)	0.47 and 1.18 ($2 \times$ d, 3H, J 6 Hz, CHMe_2), 2.57 (m, 1H, CHMe_2)	2.47 (s, 3H, py-Me), 7.53 (d, 2H, J 6 Hz, py-3,5-H), 8.46 (d, 2H, J 6.5 Hz, py-2,6-H)

Table (2E.5): ^1H NMR data for complex $[\text{ML}(\text{}^1\text{Pr-pymox})(\text{ring})](\text{SbF}_6)_2$ in d_6 -acetone (δ / ppm)

Cation (Code)	π - Ring	Pyridine Ring	Oxazoline Ring	^1Pr -group	Ligand L
$[\text{Ru}(\text{NCMe})(\text{}^1\text{Pr-pymox})(\text{mes})]^+$ (2.80)	2.23, 5.58	7.90 (m, 1H, py-5-H), 7.94 (d, 1H, J 7 Hz, py-3-H), 8.30 (t, 1H, J 7 Hz, py-4-H), 9.27 (d, 1H, J 5 Hz, py-6-H)	4.79 (m, 2H, NCH + OCH), 5.04 (t, 1H, J 9 Hz, OCH)	0.62 and 1.01 (2 \times d, 3H, J 7 Hz, CHMe_2), 2.20 (m, 1H, CHMe_2)	2.30 (s, 3H, MeCN)
$[\text{Rh}(\text{NCMe})(\text{}^1\text{Pr-pymox})\text{Cp}^*]^+$ (2.81)	1.98	8.16 (m, 1H, py-5-H), 8.26 (d, 1H, J 7 Hz, py-3-H), 8.50 (dt, 1H, J 1, 7 Hz, py-4-H), 9.36 (d, 1H, J 5 Hz, py-6-H)	5.06 (t, 1H, J 9 Hz, OCH), 5.14 (m, 1H, NCH), 5.29 (dd, 1H, J 9, 4 Hz, OCH)	0.82 and 1.10 (2 \times d, 3H, J 7 Hz, CHMe_2), 2.31 (m, 1H, CHMe_2)	2.44 (s, 3H, MeCN)
$[\text{Ru}(2\text{-Me-py})(\text{}^1\text{Pr-pymox})(\text{mes})]^+$ (2.84) Major isomer	2.35, 6.35	7.91 (t, 1H, J 7 Hz, py-4-H), 8.08 (d, 1H, J 7 Hz, py-3-H), 8.30 (m, 1H, py-5-H), 10.15 (d, 1H, J 5 Hz, py-6-H)	4.96 (t, 1H, J 9 Hz, OCH), 5.24 (m, 1H, NCH), 5.33 (dd, 1H, J 9, 1 Hz, OCH)	0.93 and 1.28 (2 \times d, 3H, J 7 Hz, CHMe_2), 2.95 (m, 1H, CHMe_2)	3.03 (s, 3H, py-Me), 7.21 (d, 2H, py-H), 7.65 (m, 1H, py-H), 8.11 (m, 1H, py-H), 8.77 (d, 1H, J 5 Hz, py-6-H)
$[\text{Ru}(2\text{-Me-py})(\text{}^1\text{Pr-pymox})(\text{mes})]^+$ Minor isomer*	2.30, 6.39	10.22 (d, 1H, J 5 Hz, py-6-H)	5.10 (t, 1H, J 9 Hz, OCH)	0.56 and 1.15 (2 \times d, 3H, J 7 Hz, CHMe_2)	

* Other signals obscured by those of major isomer

Table (2E.6): Mass Spectrometry data and Elemental Microanalysis results for complexes (2.76 - 2.84)

Complex	Code	Mass Spectrometry (m/z)	Elemental Analysis: Found (Calculated)		
		Major ion patterns	C %	H %	N %
[RuBr(¹ Pr-pymox)(mes)]SbF ₆	2.76, R = ¹ Pr	493 (M ⁺), 412 (M - Br)	33.20 (33.04)	3.38 (3.60)	3.66 (3.85)
[RuBr(Ph-pymox)(mes)]SbF ₆	2.76, R = Ph	528 (MH ⁺)	36.33 (36.29)	2.96 (3.18)	3.36 (3.68)
[RuI(¹ Pr-pymox)(mes)]SbF ₆	2.77, R = ¹ Pr	539 (M ⁺), 412 (M - I)	31.57 (31.03)	3.28 (3.39)	3.61 (3.62)
[RuI(Ph-pymox)(mes)]SbF ₆	2.77, R = Ph	573 (M ⁺), 446 (M - I)	34.44 (34.18)	3.02 (2.99)	3.40 (3.47)
[RhBr(¹ Pr-pymox)Cp*]SbF ₆	2.78	509 (M ⁺), 428 (M - Br)	33.77 (33.90)	3.82 (3.93)	3.40 (3.77)
[RhI(¹ Pr-pymox)Cp*]SbF ₆	2.79	555 (M ⁺), 428 (M - I)	33.68 (33.95)*	3.91 (4.15)	3.23 (3.30)
[Ru(NCMe)(¹ Pr-pymox)(mes)] ²⁺	2.80	688 [M+SbF ₆] ⁺ , 647 [(M-MeCN)+SbF ₆] ⁺	28.39 (28.60)	3.11 (3.16)	4.48 (4.55)
[Rh(NCMe)(¹ Pr-pymox)Cp*] ²⁺	2.81	663 [{Rh(pymox)Cp*}+SbF ₆] ⁺			
[Ru(4-Me-py)(¹ Pr-pymox)(mes)] ²⁺	2.82	740 [{Ru(4-pic)(pymox)(mes)}+SbF ₆] ⁺ 647 [{Ru(pymox)(mes)}+SbF ₆] ⁺	32.61 (32.86) [†]	3.54 (3.61)	4.40 (4.18)
[Rh(4-Me-py)(¹ Pr-pymox)Cp*] ²⁺	2.83	663 [{Rh(pymox)Cp*}+SbF ₆] ⁺	32.47 (32.66)	3.59 (3.65)	4.14 (4.23)
[Ru(2-Me-py)(¹ Pr-pymox)(mes)] ²⁺	2.84	740 [{Ru(2-pic)(pymox)(mes)}+SbF ₆] ⁺ 647 [{Ru(pymox)(mes)}+SbF ₆] ⁺			

* Calculated figures include one equivalent of acetone

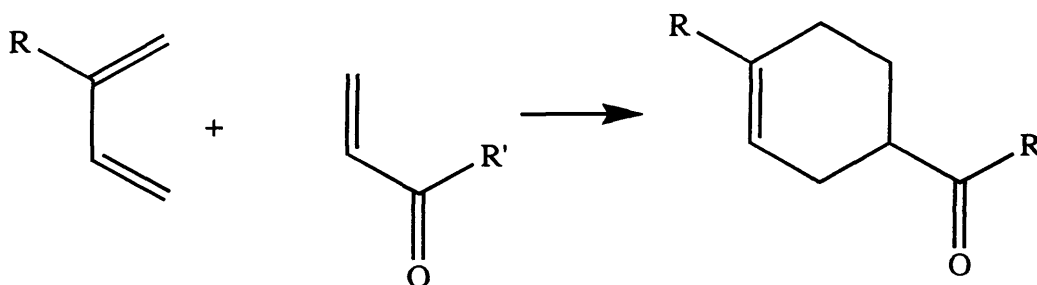
† Calculated figures include 0.5 equivalent of acetone

**Chapter Three:
Chiral Half-Sandwich
Complexes as
Lewis-Acid Catalysts**

Chapter Three - Chiral Half-sandwich Complexes as Lewis-acid Catalysts

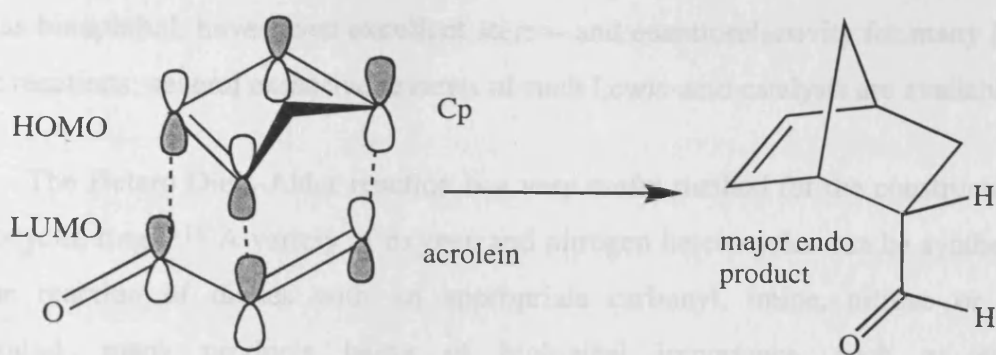
(3.1) - Introduction

For a Lewis acid to accelerate a reaction, it must coordinate to one of the reactants, often via a carbonyl group. This group will then either undergo a reaction itself, or an adjacent C=C bond will be activated. Activation of other groups (*e.g.* imines, sulfoxides) is also possible. The classical cycloaddition, Diels-Alder reaction (**Scheme 3.1**), is one of the most powerful synthetic methods in organic chemistry and is used for constructing large ring systems (*e.g.* terpenes, steroids), with control over regio-, diastereo- and enantioselectivity being possible.¹¹¹ Coordination of a Lewis acid to a carbonyl of the dienophile lowers the activation enthalpy (ΔH^\ddagger) of the reaction, thus increasing the rate. Detailed discussion of the molecular orbital theory of Diels-Alder reactions and Lewis acid catalysis can be found in various reviews.¹¹²



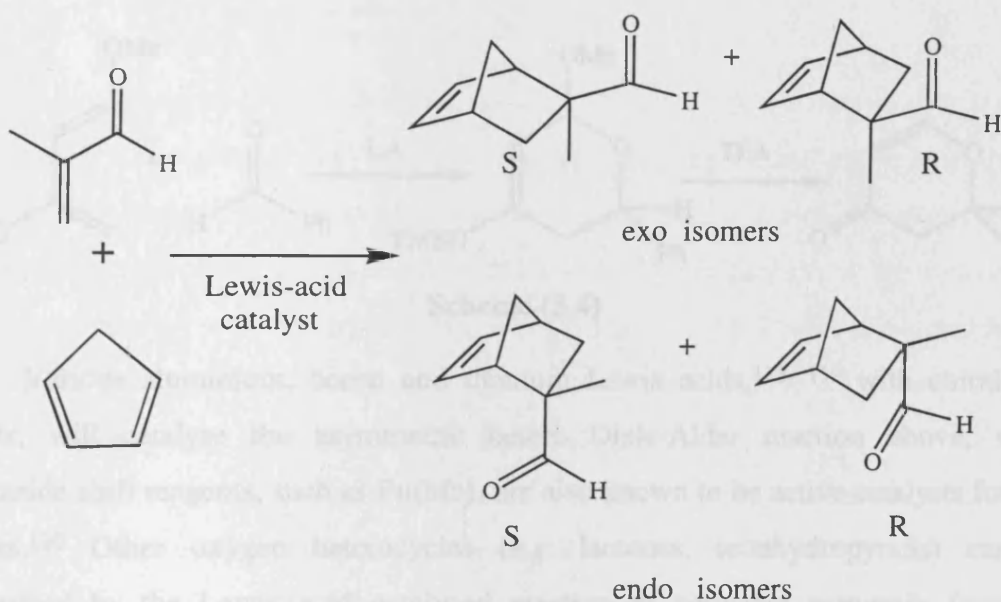
Scheme (3.1)

In the reaction of a diene with a dienophile, up to four chiral centres can be formed, the configuration about each being, in principle, controllable by the use of a chiral Lewis acid catalyst. In reactions where only one regioisomer is possible, there are still four possible products, depending on the orientation of the diene and dienophile in the transition state. In the reaction of acrolein ($\text{CH}_2=\text{CHCHO}$) with cyclopentadiene (Cp), the *endo* isomer (for which the carbonyl group is positioned underneath the diene in the transition state) is formed preferentially (although not exclusively), due to favourable interactions between the π -orbitals of the carbonyl group and those of the diene (**Scheme 3.2**). Coordination of a Lewis acid to the carbonyl group increases the favourable orbital interactions, thus dramatically improving the *endo* selectivity.



Scheme (3.2)

On the other hand, in the reaction of methacrolein with cyclopentadiene (**Scheme 3.3**), the *exo* products are favoured, due to the substitution of the carbon α - to the carbonyl. Thermally, the ratio of *exo:endo* is ~80:20, but with a Lewis acid catalyst, the ratio is often >95:5.¹¹³ The relative amounts of the R and S enantiomers will, of course, depend on whether a chiral Lewis acid catalyst is used.

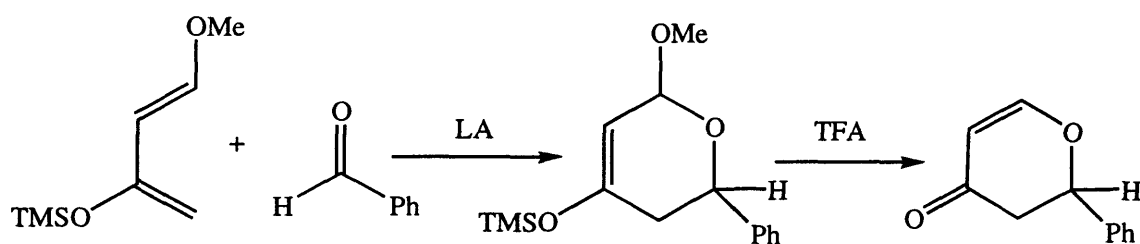


Scheme (3.3)

Initial attempts to catalyse Diels-Alder reactions used the halides of B(III), Al(III) and Ti(IV), which are strong Lewis-acids. These species, whilst being excellent catalysts for many reactions, were found to promote undesired polymerisations, or even decomposition, of more sensitive substrates. Subsequently, the catalysts were modified by replacing the halides with alkoxy or alkyl groups, and more importantly, the use of chiral chelating ligands, in order to control both the reactivity and the stereoselectivity of the Lewis acid. Combinations of $[\text{TiCl}_2(\text{OR})_2]$, RAlCl_2 , or BR_3 with chiral diols,

such as binaphthol, have given excellent stereo- and enantioselectivity for many Diels-Alder reactions; several extensive reviews of such Lewis-acid catalysts are available.^{114, 115}

The Hetero Diels-Alder reaction is a very useful method for the construction of heterocyclic rings.¹¹⁶ A variety of oxygen and nitrogen heterocycles can be synthesised by the reaction of dienes with an appropriate carbonyl, imine, nitroso or other compound, many products being of biological importance, such as sugars, oligosaccharides and alkaloids. The precursors to various carbohydrates are pyrone rings (six-membered unsaturated cyclic ethers), synthesised by the Lewis-acid catalysed reaction of aldehydes with siloxy-dienes. A common example is the reaction of benzaldehyde with 1-methoxy-3-trimethylsilyloxy-1,3-butadiene (Danishefsky's diene) (**Scheme 3.4**). The initially formed cycloadduct is usually converted *in situ* to the more stable pyrone product.¹¹⁷

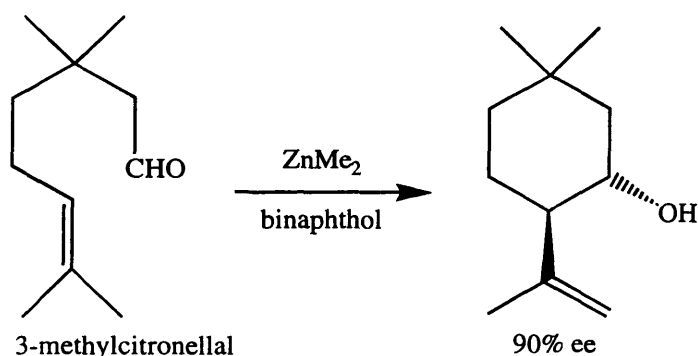


Scheme (3.4)

Various aluminium, boron and titanium Lewis acids,^{118, 119} with chiral diol ligands, will catalyse the asymmetric hetero Diels-Alder reaction above, while Lanthanide shift reagents, such as $\text{Eu}(\text{hfc})_3$ are also known to be active catalysts for this process.¹²⁰ Other oxygen heterocycles (*e.g.* lactones, tetrahydropyrans) can be synthesised by the Lewis acid catalysed reaction of activated carbonyls (such as glyoxylic esters) with common dienes; the products are useful intermediates in the synthesis of natural products. The reaction of Danishefsky's diene with imines leads to nitrogen heterocycles (*e.g.* pyridinones) that are useful intermediates in the synthesis of alkaloids (such as (S)-coniine and (S)-anabasine).^{121, 122}

The ene reaction is another useful Lewis acid-catalysed C-C bond forming process. It involves the reaction of an alkene having an allylic hydrogen (the "ene") with a compound containing a double or triple bond (enophile) to form a new bond with migration of the ene double bond and a 1,5-hydrogen shift.¹²³ The best substrates for

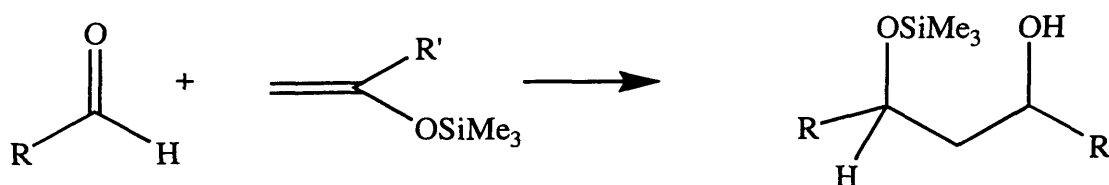
Lewis acid catalysed ene reactions are electron-deficient aldehydes (such as C_6F_5CHO , chloral and glyoxylates) and disubstituted alkenes (particularly thio-ethers). Some of the more useful reactions of this type are intramolecular cyclisations, where an aldehyde group from one end of a linear molecule undergoes an ene reaction with an alkene from the opposite end of the chain. An example of this is the reaction of 3-methylcitronellal, giving the terpene shown in **Scheme (3.5)**.¹²⁴



Scheme (3.5)

Aldol reactions involve the condensations of two carbonyl compounds to give a compound with a carbonyl and a hydroxyl group.¹²⁵ They can be either acid or base mediated, the intermediates being an enol or an enolate. When two different carbonyl compounds are involved, a mixture of products will often be formed, as the acid or base catalyst can interact with either substrate. It is often preferable if one of the reactants is a synthetic alternative to a carbonyl, *e.g.* an enol ether. Some of these reactions, however, are still slow, even with Lewis-acid catalysis.

A version of this reaction is the Mukaiyama aldol (**Scheme 3.6**);¹²⁶ the condensation of a carbonyl compound with a silyl enol ether, the TMS group moving from one oxygen atom to the other. The silyl enol ethers are much more reactive than alkyl enol ethers, due to the increased electropositive character of Si compared to C. The rate of this reaction can be dramatically enhanced by the use of Lewis acids.



Scheme (3.6)

The major advantages of using traditional Lewis acid catalysts are that they are active enough to catalyse a whole range of cycloadditions and other reactions, with good selectivity (when the appropriate ligand is used) and, importantly, the metals are fairly inexpensive, so do not need to be reclaimed after the reaction. Indeed, it is often the chiral auxiliary that must be recycled after the catalysis is complete as the complex ligands necessary to obtain high enantioselectivity are often difficult and expensive to synthesise.

However, there are several important disadvantages with the use of traditional Lewis acid catalysts. They are highly oxophilic, so both the reactants and products of catalysis bind very strongly to the Lewis-acid centre; hence the reaction is often inhibited by slow dissociation of products and slow turnover. In addition, the catalysts are often very water sensitive and as a result, the Lewis-acids are often employed at very high loadings (up to 20%). A further disadvantage is that some ligated Lewis-acids have a strong tendency to oligomerise and as most catalysts are generated *in situ*, the true nature of the active species has been the subject of much debate. For instance, identifying the active species from the combination of $[\text{TiCl}_2(\text{O}^i\text{Pr})_2]$ with binaphthol has proved very difficult.¹²⁷ Mikami has shown that non-activated 4Å Molecular Sieves (*i.e.* containing up to 5 % water) are essential to obtain very high yields and enantioselectivity for cycloadditions using the *in situ* catalyst formed from $[\text{TiCl}_2(\text{O}^i\text{Pr})_2]$ and binaphthol,¹²⁸ and that the proposed catalytic species cannot be a 1:1 adduct of titanium with the diol. The major species formed under catalytic-type conditions, using H_2^{17}O -doped molecular sieves, was a μ_3 -oxo species (Ti_3O), which was observed by ^{17}O NMR. The spectrum showed only peaks in the μ_3 -oxo (Ti_3O) region (δ 520 - 590), which indicated that this trimeric species could be the active catalyst and that the oxygen was derived from water in the molecular sieves. As a result of this type of complication, understanding the molecular basis of the enantioselectivity with traditional Lewis-acid catalysts (and hence how to fine tune the steric and electronic properties of the catalyst) is made difficult.

Because of the disadvantages of the traditional LA catalysts (see above), the use of an *appropriate* transition metal catalyst might be preferable. An ideal transition metal Lewis acid should:

- a) be Lewis acidic enough to accelerate the reaction so that there is no competing thermal reaction (usually at least 100 fold acceleration), but should not decompose

or polymerise the reactants. The complex should, therefore, have at least one overall positive charge, and/or electron withdrawing or π -acidic ligands.

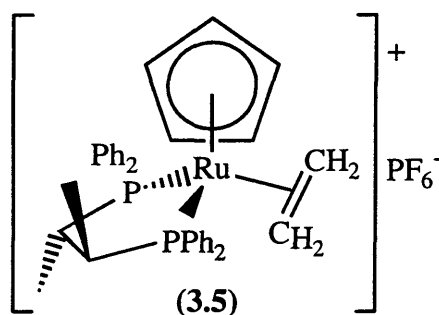
- b) not be air or oxygen sensitive and should not be dramatically affected by small amounts of water.
- c) have a stable, well-defined geometry with only one catalytically active species present in solution. Varying the steric and electronic environment about the metal centre, to improve rate and stereoselectivity, can then be attempted in a rational manner.
- d) bind in an σ -fashion to the oxygen of the carbonyl group in the substrate and should, ideally, not bind alkenes, which would inhibit catalysis. At the very least, binding to carbonyls should be strongly favoured over that of alkenes. The coordination of the carbonyls should be rapid and reversible, to allow rapid catalytic turnover.

Early work on transition metal Lewis acid catalysts involved low oxidation state metals from the centre of the transition series, notably Mo(0) and W(0). The Lewis acidity of the complexes was increased by incorporation of π -acidic ligands such as CO and the electron-withdrawing NO^+ , but was decreased by the use of electron-rich phosphines. Examples of some early catalysts for the Diels-Alder reaction were $[\text{W}(\text{CO})_3(\text{PR}_3)(\text{NO})(\text{SbF}_6)]$ (**3.1** - in which the SbF_6^- was replaced by dienophile)¹²⁹ and $[\text{M}(\text{HC}(\text{py})_3)(\text{NO})_2]^{2+}$ (**3.2**, $\text{M} = \text{Mo}, \text{W}$).¹³⁰ However these complexes were often too Lewis acidic and were capable of polymerising the diene and dienophiles.

A slightly less Lewis-acidic series of complexes, extensively investigated by Hersh *et al.*, were $[\text{Fe}(\text{CO})_2\text{LCp}]^+$ (**3.3**, $\text{L} = \text{THF}$ or acrolein).¹³¹ These complexes were found to catalyse the reaction of acrylic dienophiles with simple dienes, with *exo/endo* selectivities higher than those of the thermal reactions. A problem with catalysts (**3.1**) and (**3.3**) was ruling out the possibility that adventitious impurities or decomposition products were responsible for some, or even most, of the catalysis.¹³¹ It was found that the addition of a hindered (and hence non-coordinating) base, such as 2,6-di-*tert*-butyl pyridine, resulted in a significant lowering of the yield of cycloadduct in many cases. Identifying the actual species scavenged by the hindered base proved difficult; the most likely candidates were thought to be H^+ or BF_3 (derived from the BF_4^- counter-ion). As less than one equivalent of base was found to greatly inhibit the catalysis in many cases, the acidic impurity might only have been present in a low concentration, although the

source of protic acid was unclear. Kinetic studies on (3.3) indicated that the catalytic activity was greater than expected, based on stoichiometric rate constants, which cast doubt on the role of (3.3) as Lewis acid catalysts. It was concluded that the best way to demonstrate that the metal complex was acting as a catalyst would be to synthesise chiral analogues and use these in an asymmetric cycloaddition.

In complexes (3.3), the cationic charge and the presence of π -acidic CO ligands increase the Lewis acidity, but the cyclopentadienyl ligand results in a relatively mild Lewis-acid overall. Incorporation of phosphine ligands would be expected to reduce the Lewis-acidity still further. This was demonstrated, in 1989, by Faller *et al.*, who synthesised the complex $[\text{Ru}(\text{C}_2\text{H}_4)(\text{PPh}_3)_2\text{Cp}]\text{PF}_6$ (3.4), which is an efficient catalyst for the less Lewis-acid demanding hetero Diels-Alder reaction of benzaldehyde with Danishefsky's diene (the ethylene ligand being replaced by a carbonyl under reaction conditions).¹³² Complex (3.4), however, is not Lewis-acidic enough to catalyse the classical Diels-Alder reaction, which is also disfavoured due to the binding of the C=C of a dienophile being preferred to that of the carbonyl. Replacement of the two PPh_3 groups with a chiral phosphine, such as (S,S)-CHIRAPHOS giving the complex $[\text{Ru}(\text{C}_2\text{H}_4)(\text{CHIRAPHOS})\text{Cp}]\text{PF}_6$ (3.5), gave moderate enantioselectivity in the hetero Diels-Alder reaction (25% *ee*) (the first chiral half-sandwich complex to be used as an asymmetric Lewis-acid catalyst).



Although complex (3.5) preferentially binds the C=C bond of acrylic dienophiles over the carbonyl, coordination of benzaldehyde in the hetero Diels-Alder reaction presumably has to occur via an η^1 -interaction (*i.e.* σ -binding). Gladysz has reported that complexes $[\text{Re}(\text{NO})(\text{PPh}_3)(\text{OCHAr})\text{Cp}]\text{BF}_4$ exist as rapidly interconverting mixtures of σ/π isomers (Figure 3.1), the equilibrium ratios depending to a large extent on the nature of the Ar group on the aldehyde.¹³³ With electron-

withdrawing aryl groups, π -coordination of the aldehyde dominates, whilst with electron-donating substituents, σ -coordination is preferred.

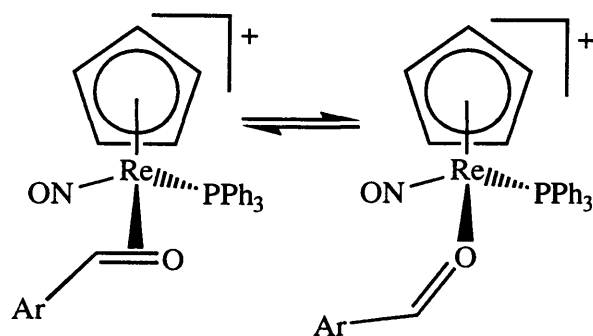
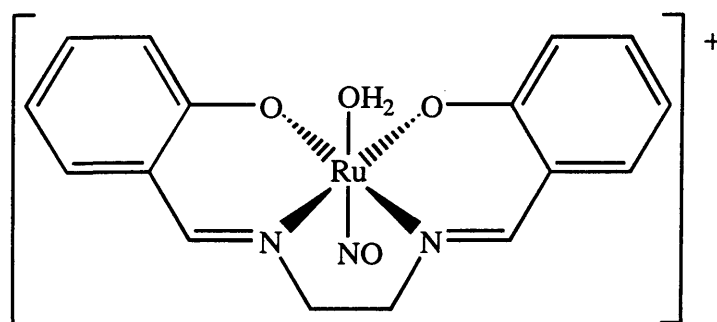


Figure (3.1)

Such π -coordination of aldehydes is only favoured with electron-rich half-sandwich complexes, usually containing phosphine ligands and/or cyclopentadienyl. With “arene-Ru” and “Cp*Rh” complexes, which are often rather Lewis-acidic, σ -aldehyde coordination is presumed to occur in the vast majority of cases.

A Lewis-acidic ruthenium complex that is a catalyst for the Diels-Alder reaction is [Ru(salen)(NO)(H₂O)]SbF₆ (**3.6**), developed by Bosnich *et al.* in 1992.¹³⁴ This catalyst has the advantage of being air and water stable and is particularly efficient for the reaction of acrylic dienophiles with simple dienes, in nitromethane solution, where the dienophiles are found to be better ligands than water. Complex (**3.6**) can also catalyse the Mukaiyama aldol reaction, but the catalyst tended to decompose due to reduction by the silyl enol ethers used.¹³⁵

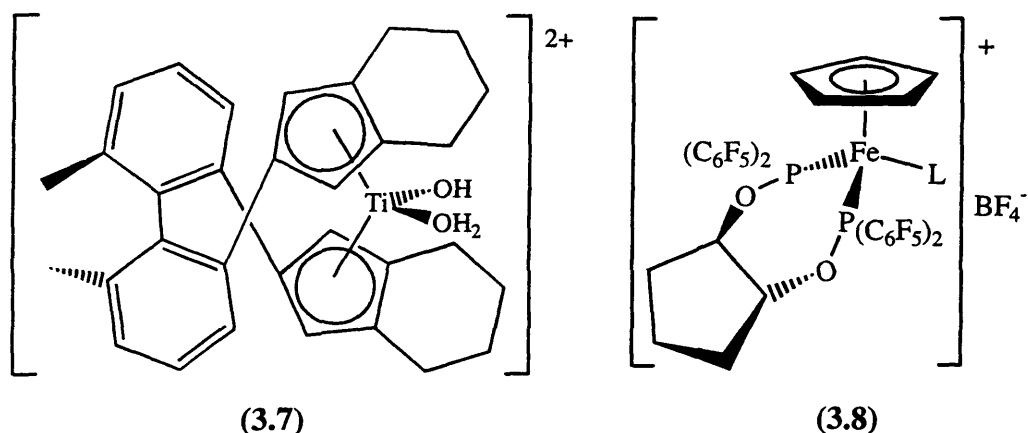


(3.6)

No chiral analogues of (**3.6**) have yet been used as catalysts, but one would anticipate that asymmetric Lewis-acid catalysis will be possible with such a complex. Recently, Jacobsen has reported that chiral “(salen)Cr(III)” complexes are efficient and highly enantioselective catalysts for the asymmetric ring-opening of epoxides¹³⁶ and the hetero

Diels-Alder reaction of aldehydes with Danishefsky's diene (*ees* of up to 85 % obtained),¹³⁷ both processes requiring relatively mild Lewis-acids.

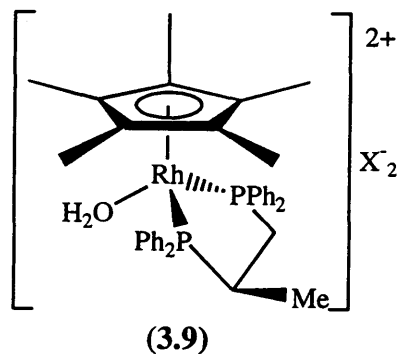
On screening a variety of transition metal complexes for use as Lewis acid catalysts, Bosnich *et al.* discovered that metallocenes such as $[\text{Ti}(\text{Cp}^*)_2(\text{H}_2\text{O})_2](\text{OTf})_2$ were efficient catalysts for the Diels-Alder reaction, good *exo:endo* selectivity being achieved.¹³⁵ Interestingly, the catalysts were not significantly water sensitive, unlike the majority of titanium-based Lewis acid catalysts. The chiral titanocene derivative $[\text{Ti}\{(\text{S})\text{-biphenacene}\}(\text{H}_2\text{O})_2](\text{OTf})_2$ (**3.7**) was found to catalyse the reaction of acrylic dienophiles with cyclopentadiene, with *ees* of up to 75%.¹³⁸



The first examples of chiral half-sandwich complexes as highly enantioselective catalysts for the Diels-Alder reaction were $[\text{Fe}(\text{L})\{(\text{C}_6\text{F}_5)_2\text{POC}_5\text{H}_8\text{OP}(\text{C}_6\text{F}_5)_2\}\text{Cp}]\text{BF}_4$ (**3.8**, L = dienophile, MeCN) reported by Kundig *et al.* in 1994.¹¹⁰ The chiral bisphosphinite ligand is electronically similar to CO (due to the electron-withdrawing C_6F_5 substituents reducing the σ -donor ability of the ligand) and the complexes are thus chiral analogues of complexes (**3.3**). Very high enantioselectivity was obtained for the Diels-Alder reaction of acrylic dienophiles with simple dienes; *e.g.* an *ee* of 99 % is obtained for the reaction of bromoacrolein and cyclohexadiene. The use of complexes (**3.8**), however, is limited by their low thermal stability, reactions generally carried out at -20°C or below.

The first enantioselective rhodium catalysts for the Diels-Alder reaction were reported in 1996, by Carmona *et al.*, who synthesised the complexes $[\text{Rh}(\text{H}_2\text{O})(\text{R-Prophos})\text{Cp}^*]\text{X}_2$ (**3.9**, X = BF_4^- , SbF_6^-), the Lewis-acidity presumably being due to the dicationic charge.¹³⁹ Complexes (**3.9**) catalyse the reaction of methacrolein and cyclopentadiene with up to 71 % *ee*. When SbF_6^- was used as anion, both the rate and enantioselectivity of catalysis were found to increase significantly over that with BF_4^- ,

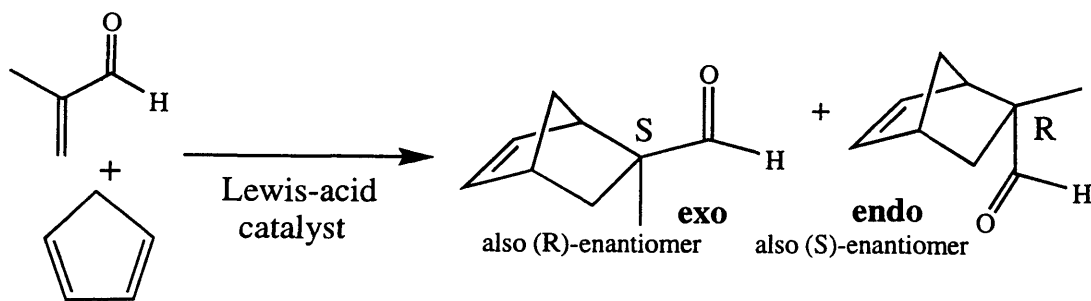
because of the different degree of interaction of the anions with the metal centre, as found previously for copper complexes (see Chapter One).⁴²



As of 1996, the half-sandwich complexes that had been used as Diels-Alder catalysts had all contained P-donor chiral ligands. With Kundig's "Fe-Cp" catalyst (3.8),¹¹⁰ the ligand has π -acceptor characteristics, so is ideally suited for use in Lewis-acid catalysis. With the phosphine complex (3.9),¹³⁹ however, the Lewis-acidity observed most likely derives from the overall dicationic charge, so it is reasonable that dicationic half-sandwich complexes containing less electron-rich ligands than phosphines might result in even more active Lewis-acid catalysts. Thus, "Cp*Rh" and "(arene)Ru" aqua complexes containing chiral oxazoline ligands (many of which will have considerable π -accepting abilities) are strong candidates for use as asymmetric Lewis-acid catalysts.

(3.2) -Results and Discussion

The Diels-Alder reaction of methacrolein and cyclopentadiene (Scheme 3.7) was chosen as a model catalytic reaction with which to test the efficiency of the aqua complexes (2.63 - 2.75) as asymmetric Lewis acid catalysts. This reaction can often be catalysed by mild Lewis acids and standard methods exist to determine the *exo:endo* ratio and enantioselectivity. In addition, the reaction has been catalysed by most of the known transition metal catalysts, so comparison of the relative reactivities and selectivities can be made.



Scheme (3.7)

In the general procedure, one equivalent of dienophile and two equivalents of diene were reacted, with 0.5 - 5 mol% of catalyst (using either the pre-formed or *in-situ* formed water complex) in CH_2Cl_2 in the presence of the hindered base 2,6-di-*tert*-butylpyridine (equimolar with catalyst) used to mop up protons, which may also catalyse the Diels-Alder reaction.¹³¹

In an initial screening, a series of complexes $[\text{M}(\text{OH}_2)(\text{N-N})(\text{ring})](\text{SbF}_6)_2$ ($\text{M} = \text{Ru}$, ring = mes; $\text{M} = \text{Rh}$, ring = Cp^* ; N-N = ⁱPr-box, ⁱPr-bop, ⁱPr-benbox, ⁱPr-pymox, ⁱPr-animox) and $[\text{M}(\text{OH}_2)(\text{N-Y})(\text{ring})]\text{SbF}_6$ ($\text{M} = \text{Ru}$, ring = mes; $\text{M} = \text{Rh}$, ring = Cp^* ; N-Y = ⁱPr-NTs-animox or ⁱPr-phenmox) were tested as catalysts for the Diels-Alder reaction above, with 5 mol % catalyst loading at room temperature (all other conditions as described above) (**Table 3.1**).

Table (3.1) - Diels-Alder catalysis with 5 mol% $[\text{M}(\text{OH}_2)(\text{L-L})(\text{ring})]^{n+}$

Entry	Metal	Ligand	Yield %	Time / h	<i>exo:endo</i>	<i>Ee</i> %
1	Ru	ⁱ Pr-box	47	24	94:6	10
2	Rh	ⁱ Pr-box	5	48	85:15	0
3	Ru	ⁱ Pr-bop	0	48	-	-
4	Rh	ⁱ Pr-bop	62	24	95:5	29
5	Ru	ⁱ Pr-benbox	> 95	0.5	94:6	66
6	Rh	ⁱ Pr-benbox	10	48	88:12	2
7	Ru	ⁱ Pr-pymox	> 95	0.5	94:6	72
8	Rh	ⁱ Pr-pymox	57	24	95:5	53
9	Ru	ⁱ Pr-animox	60	6	90:10	13
10	Ru	ⁱ Pr-NTs-animox	90	72	92:8	16
11	Ru	ⁱ Pr-phenmox	95	24	95:5	40
12	Rh	ⁱ Pr-phenmox	0	48	-	-

Using (S)-configured ligands, the major product was identified as (1R,2S,4R)-2-methylbicyclo[2.2.1]hept-5-ene-2-carbaldehyde, by comparison of the sign of the optical rotation $[\alpha]$, and the GC behaviour of the acetal formed from (2R,4R)-pentanediol with literature values.¹⁴⁰

There are three main conclusions that can be drawn from **Table (3.1)** -

1. Ruthenium complexes are, in general, considerably more active for this reaction than their rhodium analogues
2. Dications are more catalytically active than monocations
3. C₂-symmetry is not required to obtain optimum selectivity

There are three main systems, shown in the table, that give promising activity and enantioselectivity for the Diels-Alder reaction- the Ru/benbox, Ru/pymox and Rh/pymox catalysts (entries 5, 7 and 8 respectively). The two ruthenium catalysts perform similarly under the chosen conditions; in both cases, > 80 % Diels-Alder product formation was observed after 15 minutes, the reaction going essentially to completion after 30 minutes (the reactions were performed in an NMR tube in CD₂Cl₂, spectra obtained at 5 minute intervals). For the pymox catalyst (**2.65**, R = ⁱPr), an *ee* of 72% was obtained, whilst for the benbox catalyst, the *ee* was 66% (the limited solubility of the latter complex with 5 Mol% catalyst loading may limit the observed selectivity). For both catalysts, the *exo:endo* ratio was 94:6, considerably better than the thermal ratio. The rhodium/pymox complex (**2.69**, R = ⁱPr) was found to be considerably less active than the ruthenium analogue, a 57% yield of adduct obtained after one day, the rate much slower after this point. Good *exo:endo* selectivity (95:5), but moderate enantioselectivity (*ee* 53%) were obtained with this catalyst. Further discussion of the three best catalysts will follow shortly.

Of the other rhodium complexes tested, only that with ⁱPr-bop as ligand showed any significant catalytic activity, a 62% yield of product obtained after one day, with an *exo:endo* ratio of 95:5. The enantioselectivity, however, was rather low (*ee* 29%) and it should be noted that the catalyst was formed *in situ*; use of the pre-formed aqua complex gave almost no product at all. The rhodium box and benbox complexes showed almost no activity at all, due partly to their very low solubility under catalytic conditions, whilst the monocationic rhodium/phenmox complex (formed *in situ*) was presumably insufficiently Lewis-acidic to promote the Diels-Alder reaction. The

ruthenium/phenmox complex was, in contrast, a reasonably active catalyst, a 95% yield of adduct obtained after one day but gave moderate enantioselectivity (*ee* 40%), which may be associated with the six-membered chelate ring. The animox and NTs-animox complexes (both with six-membered chelate rings) gave poorer enantioselectivity.

As mentioned above, the ruthenium pymox and benbox catalysts have been studied in more detail, varying catalyst loading, reaction temperature, R-substituent and arene-ligand; similar trends are observed with both ligand classes. Firstly, the effects of loading and temperature were studied for the standard catalysts (**2.65**, R = ⁱPr) (Table 3.2) and (**2.36**, R = ⁱPr) (Table 3.3), again with one equivalent methacrolein, two equivalents Cp and hindered base in dichloromethane.

Table (3.2): [Ru(OH₂)(ⁱPr-pymox)(mes)](SbF₆)₂ (2.65**, R = ⁱPr) catalyst**

Entry	Catalyst (mol %)	T/°c	t/h	Yield (%)	Isomer Ratio (<i>exo:endo</i>)	<i>Ee</i> (%)
1	0.5	RT	0.25	> 95	95:5	70
2	1	RT	0.2	> 95	95:5	70
3	1	0	3	72	96:4	76
4	1	-20	24	30	96:4	78
5	2	RT	0.33	> 95	95:5	71
6	2	0	4	72	95:5	75
7	5	RT	0.5	> 95	94:6	72
8	5	0	6	53	95:5	75
9	5	-20	72	90	96:4	81

Table (3.3): [Ru(OH₂)(ⁱPr-benbox)(mes)](SbF₆)₂ (2.36**, R = ⁱPr) catalyst**

Entry	Catalyst (mol %)	T/°c	t/h	Yield (%)	Isomer Ratio (<i>exo:endo</i>)	<i>Ee</i> (%)
1	1	RT	0.5	> 95	94:6	64
2	2	RT	0.5	> 95	94:6	65
3	5	RT	0.5	> 95	94:6	66
4	5	0	6	92	94:6	68
5	5	-20	48	71	95:5	70

With either of (2.65, R = ⁱPr) and (2.36, R = ⁱPr) as catalyst, the reactions proceeded rapidly at room temperature, essentially going to completion in < 30 min, as monitored by ¹H NMR. The rate did not greatly alter when using 0.5, 1, 2 or 5 mol% catalyst, although for the pymox catalyst, the optimum rate was surprisingly obtained with 1 mol %. With (2.65), good *exo:endo* selectivity (95:5) and enantioselectivity (*ee* 70 %) were obtained, even with 0.5 mol% catalyst (Table 3.2, entry 1). Increasing the catalyst ratio (entries 2, 5 and 7), had little effect on the *exo:endo* or enantioselectivity, but lowering the temperature of the reaction to 0 and -20°C led to improvements in the enantioselectivity (entries 3, 4, 6, 8 and 9), an *ee* of 81% being obtained at -20°C, with 5 mol% catalyst. Use of the complex formed from (R)-ⁱPr-pymox lead to the opposite configuration of the DA adduct, with the same *ees*. With the benbox complex (2.36), increasing the catalyst loading only gave slight improvements in *ee* (up to 66% with 5 mol%), whilst lowering the reaction temperature to -20°C (Table 3.3, entry 5) increased the *ee* to 70% (some 11% lower than 2.65, R = ⁱPr under the same conditions).

The reaction of methacrolein and cyclopentadiene was catalysed by a series of complexes (2.36), (2.65) and the indanyl-pymox complex (2.67) varying the R-substituents (Table 3.4), all reactions being carried out at 0°C with 2 mol% catalyst.

Table (3.4) -Variation of R-substituent *

Entry	Catalyst	R-Group	t/h	Yield (%)	Isomer Ratio (<i>exo:endo</i>)	<i>Ee</i> (%) (abs. config.)
1	2.65	(R)-Et	4	61	95:5	54 (R)
2	2.65	(S)- ⁱ Pr	4	72	95:5	75 (S)
3	2.65	(S)- ^t Bu	5	94	96:4	83 (S)
4	2.65	(S)-Ph	7	30	94:6	58 (S)
5	2.65	(S)-Bn	6	31	95:5	70 (S)
6	2.67	indanyl	72	23	93:7	6 (S)
7	2.36	(R)-Et	24	94	94:6	45 (R)
8	2.36	(S)- ⁱ Pr	7	88	94:6	67 (S)
9	2.36	(S)-Ph	48	13	88:12	5 (S)

* All reactions carried out at 0°C, with 2 mol% catalyst.

The expected trend of increasing enantioselectivity with size of R-group was found. With the purely alkyl substituents, a significant change in *ee* was observed. For pymox

complexes (**2.65**), going from R = Et to R = ⁱBu (entries 1 - 3) the *ee* improved from 54% to 83%, although the rates and *exo* : *endo* selectivity were similar. Similarly, with complexes (**2.36**), 67% *ee* was observed with ⁱPr-benbox, whilst the *ee* with Et-benbox was 44%. For (**2.65**), an increase in *ee* was observed by replacing R = Ph with the more bulky R = Bn, but the rates of reaction (entries 4 and 5) were noticeably slower than those with R = alkyl (entries 1-3) and the enantioselectivity was lower than for R = ⁱPr or ⁱBu. The indanyl-pymox complex (**2.67**) was a very poor catalyst, only 23% yield being obtained after 3 days. With (**2.36**, R = Ph) (entry 9), low catalytic activity and enantioselectivity (*ee* 5%) were observed.

It is not entirely clear why slow rates are obtained with aryl-substituted catalysts. One explanation might be that the phenyl rings are *too* bulky, inhibiting the approach of substrate to complex, allowing alternative proton-catalysed Diels-Alder reactions to become more competitive, thus reducing the enantioselectivity. Alternatively, the slow rates might be due to the phenyl-containing substituents being somewhat more electron-withdrawing than the alkyl groups, affecting the electronic properties of the Lewis acid. However, there is no evidence for large electronic differences in the X-ray crystal structures of the Ph- and Bn-pymox complexes compared to their ⁱPr-Pymox analogues (see Chapter Two).

It can be seen that changing the R-group of the bidentate ligand and lowering the temperature of reaction have a significant effect on the enantioselectivity of the reaction of methacrolein and cyclopentadiene catalysed by $[\text{Ru}(\text{OH}_2)(\text{N-N})(\text{arene})]^{2+}$ (N-N = pymox, benbox). In contrast, the catalyst loading has a much smaller effect. A possible explanation is that the ratio of methacrolein to free water in solution has to be large, in order to give a high proportion of methacrolein-coordinated species (the presumed active intermediate). At 5 mol% loading, therefore, the relative proportion of the active species may only be slightly greater than that at 2 mol%, hence the marginally better selectivity.

The solvent used in all catalytic reactions described above was dichloromethane, which is just polar enough to dissolve most of the catalysts (particularly in the presence of dienophile), but does not coordinate to the metal centre. A series of other solvents were used for the reaction of methacrolein and Cp, in the presence of 2 mol% (**2.65**, R = ⁱPr) catalyst. In d₆-acetone (at room temperature), the reaction proceeded steadily, such that 80% conversion was observed after one day, as shown by ¹H NMR. An

exo:endo ratio of 95:5 and *ee* of 70% were obtained, indicating that only the rate is reduced when using acetone as solvent; the reduction in rate is presumably due to competing acetone coordination and possibly to the slightly higher water content of the solvent. Use of the solvent mixture CH₂Cl₂/acetone (10:1) gave a 92% yield of Diels-Alder product in 3 hours at room temperature, with similar selectivity to that described above. Thus, the use of acetone might help dissolve some of the more insoluble catalysts, but is only practical with the most active species. Use of either THF or nitromethane as solvent gave none of the desired product after one day at room temperature, suggesting that they coordinate to the ruthenium centre. However, attempts to isolate, or observe by NMR, species [RuL(pymox)(mes)]²⁺ (L = MeNO₂ or THF) failed; only the aqua complexes were found in each case.

The nature of the η⁶-arene ligand in the catalysts [Ru(OH₂)(ⁱPr-pymox)(arene)]²⁺ (**2.63-2.65**, **2.68**) and [Ru(OH₂)(ⁱPr-benbox)(arene)]²⁺ (**2.34-2.36**) was found to have a significant effect on the rate and selectivity of the Diels-Alder reaction of methacrolein and cyclopentadiene (**Table 3.5**) (all reactions at room temperature, with 2 mol% catalyst).

Table (3.5): Variation in η⁶-arene

Entry	Catalyst	Arene	t/h	Yield (%)	Isomer Ratio (<i>exo:endo</i>)	<i>Ee</i> (%)
1	2.63	C ₆ H ₆	24	73	90:10	18
2	2.64	<i>p</i> -cy	24	91	93:7	45
3	2.65	mes	0.33	> 95	95:5	71
4	2.68	C ₆ Me ₆	24	93	94:6	66
5	2.34	C ₆ H ₆	2	90	88:12	31
6	2.35	<i>p</i> -cy	3	87	88:12	6
7	2.36	mes	0.5	> 95	94:6	65

Surprisingly, the mesitylene-containing catalysts (**2.65**) and (**2.36**) were found to be superior in terms of selectivity *and* rate to complexes with other arenes. The general increase in *ee* and *exo:endo* ratio with size of arene is reasonable, as rotation of the coordinated methacrolein in the presumed active intermediate, which would result in the C=C group, rather than the aldehyde-H, being oriented towards the η⁶-arene (see

later), might be less favoured with bulky arenes. Thus, with the benzene-containing complexes (2.63) and (2.34), enantiomeric excesses of 18% and 31%, respectively, were obtained, whilst with the corresponding mesitylene species (2.65) and (2.36), 71% and 65% ee were obtained. With the C₆Me₆-containing (2.68), the ee was 66% (lower than with the mesitylene analogue), but the rate was noticeably slower than that with (2.65), which might account for the slightly poorer selectivity (if a small amount of uncatalysed reaction occurred).

The reduced catalytic rate with the C₆Me₆-containing (2.68), compared to (2.65), may be due to the greater steric bulk of the arene ligand, hindering approach of diene to the coordinated methacrolein complex. Following this argument, one would expect the benzene-containing catalysts (which should also be more-Lewis acidic) to give higher rates than those with mesitylene, which is clearly not the case. For both the pymox and benbox complexes, the benzene-containing catalysts are significantly less active than their mesitylene analogues. With (2.34), a 90% conversion to Diels-Alder product was observed (by ¹H NMR) after 2 hours (the reaction proceeding reasonably steadily to this point), whilst with (2.36), a 90% yield was obtained after only 10 minutes. With ⁱPr-pymox as ligand, the rate with the benzene complex (2.63) was even slower than that with the benbox analogue, only 21% conversion found after 8 minutes, the rate then slowing considerably, such that 42% conversion was found after 95 minutes. After 24 hours, a yield of 73% was obtained, whilst with (2.65), a 90% yield was obtained after only 8 minutes.

A possible explanation for the lower catalytic rates observed with the benzene (and also *p*-cymene) complexes is they are rather more oxophilic, thus binding too strongly to either the water ligand or to the Diels-Alder product; in either case, catalytic turnover would be reduced. For a series of analogous complexes [Ru(OH₂)(bipy)(arene)]X₂, the rate of water exchange was found to increase only slightly with the degree of substitution of the arene ligand.¹⁰⁴ Thus, when arene = C₆H₆, $K_{\text{ex}} = 6.8 \times 10^{-2} \text{ s}^{-1}$, whilst with arene = C₆Me₆, $k_{\text{ex}} = 10.2 \times 10^{-2} \text{ s}^{-1}$, which indicates that the rate of *water* exchange is not the main factor in reducing the catalytic activity of the benzene-containing complexes relative to those of mesitylene. However, the rates of exchange of dienophile and Diels-Alder product for the different catalysts do not necessarily follow the same pattern as that for water exchange. Indeed, water exchange in the Ru/pymox system (the best Diels-Alder catalysts of those tested) is considerably

slower than that in the Rh/pymox system, for which significantly slower rates are observed (see below).

With pymox- and benbox-containing catalysts, selectivity and rate are considerably lower with arene = *p*-cymene than with arene = mes. With complexes [Ru(OH₂)(ⁱPr-phenmox)(arene)]SbF₆ (formed *in situ*), however, the *p*-cymene complexes were equally reactive but slightly more selective for the Diels-Alder reaction of methacrolein and Cp. Thus, when arene = *p*-cy, a 92% yield was obtained after 24 hours, with an *exo:endo* ratio of 95:5 and an *ee* of 45% (which is the same as that obtained with the analogous pymox catalyst **2.64**, R = ⁱPr). In comparison, the mesitylene analogue gave similar rates and *exo:endo* selectivity, but only 40% *ee*.

It is apparent that enantioselectivity in the reaction of methacrolein with Cp is greater with pymox complexes (which have a five-membered chelate ring) than with those of phenmox (six-membered chelate ring). Even poorer selectivity is obtained with the structurally similar animox and NTs-animox-containing catalysts. The catalytic activity and selectivity of [Ru(OH₂)(ⁱPr-animox)(mes)]²⁺ depends strongly on the quantity of hindered base used in the catalysis. With no base present, the complex is fairly active, a 60% yield of the methacrolein/Cp adduct found after 6 hours, but is poorly selective (13% *ee*). Addition of one equivalent of base renders the catalyst almost totally inactive, presumably due to deprotonation of the NH₂-group (*i.e.* giving a monocationic, less Lewis-acidic complex - see Chapter Two). With 0.5 equivalents of base, slightly reduced rate, but improved enantioselectivity are observed (*ee* 28%); however, the animox complexes are clearly not useful catalysts for the Diels-Alder reaction described.

Complexes [M(OH₂)(R-pymox)Cp*](SbF₆)₂ (**2.69**, M = Rh; **2.72**, R = Ir) were found to be slow Lewis-acid catalysts for the Diels-Alder reaction of methacrolein and cyclopentadiene. Reactions at room temperature gave ~ 50% yield after 1 day, with the reaction then becoming very slow, possibly due to competing water coordination. At RT, *ees* of ca. 53% and *exo:endo* ratios of 95:5 were obtained using 1 - 5 mol% of (**2.69**, R = ⁱPr). The catalyst loading had little effect on selectivity, partly due to the insolubility of the complexes in dichloromethane. Greater than 50 equivalents of methacrolein were required to keep the catalyst in solution during the reaction. Similar results were obtained with the corresponding iridium complex. The best results with these complexes were obtained by carrying out the reactions at 0°C, which slowed

down the reactions somewhat, but allowed better overall yields to be obtained in some cases, possibly due to reduced dicyclopentadiene formation. **Table (3.6)** shows a series of results for the reaction of methacrolein with cyclopentadiene, catalysed by $[M(OH_2)(R\text{-pymox})Cp^*]^{2+}$, all at 0°C with 2 mol% catalyst.

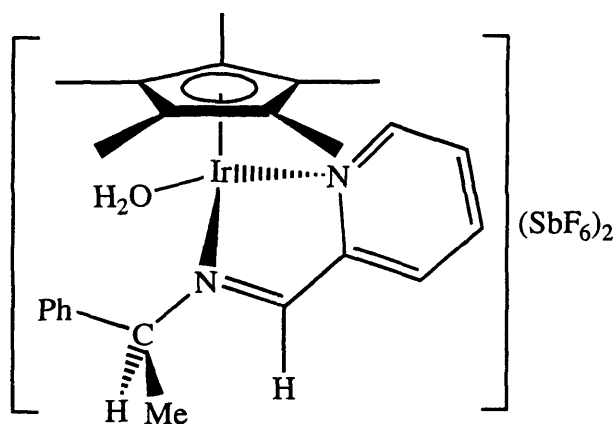
Table (3.6) - $[M(OH_2)(R\text{-pymox})Cp^*]^{2+}$ catalyst*

Entry	M	R	t/days	Yield (%)	exo:endo	Ee (%)
1	Rh	Et	7	28	93:7	5
2	Rh	^t Pr	3	81	95:5	68
3	Rh	^t Bu	3	85	95:5	52
4	Rh	Ph	3	56	94:6	44
5	Rh	Bn	3	71	93:7	3
6	Ir	^t Pr	3	51	95:5	57

* All reactions use 2 mol% catalyst at 0°C

The *ee* of the $[Rh(OH_2)(^t\text{Pr-pymox})Cp^*]^{2+}$ catalysed reaction was improved from 53% at RT to 68% at 0°C (entry 2). There is no uniform increase in enantioselectivity with increasing size of the R-group, as was found for the corresponding ruthenium catalysts; the complex where R = ^tBu gave a lower *ee* than that where R = ^tPr. The Et-pymox complex (entry 1) gave a low *ee*, but this could have been due to the low solubility of the complex, which also resulted in a low yield.

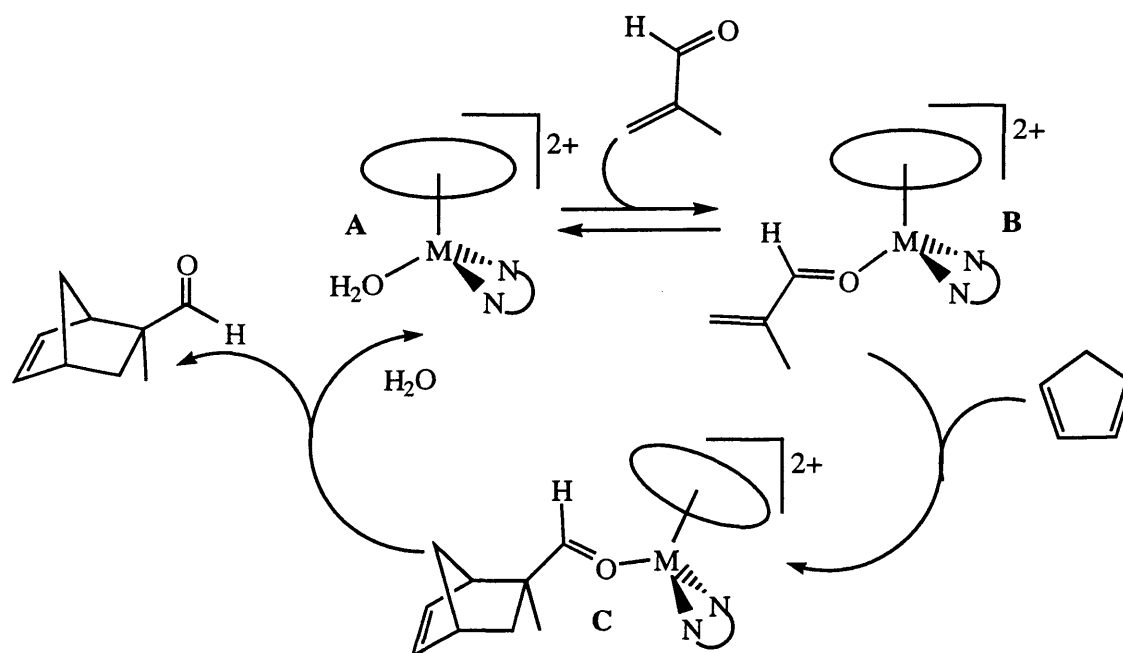
Recently, Carmona has reported that iridium complexes such as $[Ir(OH_2)(L)Cp^*](SbF_6)_2$ {**3.10**, L = *N*-(2-pyridylmethylene)-(*R*)-1-phenylethylamine},¹⁴¹ analogous to the pymox complex (**2.72**), are catalysts for the Diels-Alder reaction of methacrolein and cyclopentadiene.



(3.10)

Complex **(3.10)** (formed *in situ* from the chloro-analogue) is more catalytically active (94% yield after 1.5 hours, at RT) than **(2.72)** (for which only ca. 50% yield was achieved, after one day), but is rather less enantioselective (32% *ee* at -50°C, compared to 57% *ee* at 0°C with **(2.72)**). The lower selectivity with **(3.10)** might be attributed to epimerisation under catalytic conditions; the chloro-precursor was formed as a 78:22 mixture of diastereomers, the major crystallising selectively and being configurationally stable in dichloromethane. The aqua-complex **(3.10)**, however, is expected to be more configurationally labile (see Chapter Two), so epimerisation is a potential problem. Alternatively, **(3.10)** might just give inherently low enantioselectivity, due to the free rotation about the N–CH(Me)Ph bond.

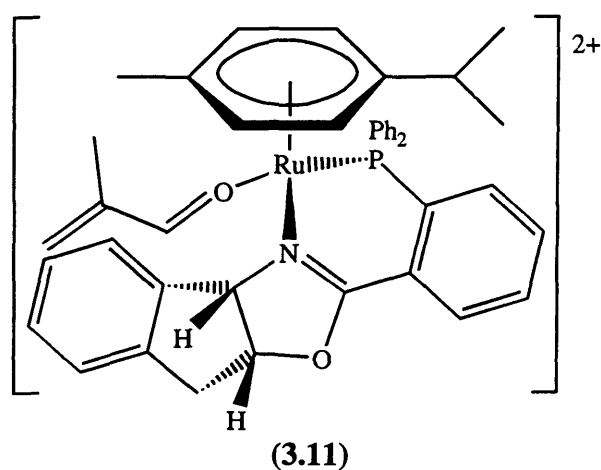
To rationalise the observed results for the catalysed reactions of methacrolein and cyclopentadiene, it is helpful to consider the likely reaction mechanism (**Scheme 3.8**). It is probable there is a different equilibrium mixture (**A** ⇌ **B**) of coordinated water and methacrolein for each catalyst, which may be the main reason for the varying catalytic activity. For “Cp*Rh” and “(C₆H₆)Ru” complexes, the equilibria appear to be largely over to the coordinated water complex **A**, except at very low catalyst loadings, whilst for **(2.36/2.65)**, significant methacrolein coordination (*i.e.* **B**) must occur, even at high loading.



Scheme (3.8)

As described in Chapter Two, addition of six equivalents of methacrolein to (**2.65**, $R = \text{Pr}$) in CD_2Cl_2 results in $\sim 50\%$ replacement of the water ligand by dienophile, as shown by ^1H NMR, which indicates that under catalytic conditions (20-100 equivalents), the methacrolein-coordinated species would dominate. However, in the NMR-tube Diels-Alder reactions, signals due to methacrolein or product-coordinated complexes (**B** and **C** respectively) are not readily observed.

With acrylic dienophiles, it is assumed that Lewis-acid catalysis occurs by η^1 -coordination of the carbonyl group to the Lewis-acid centre, but in many cases there is little direct evidence for this mechanism (although Kundig has shown that complexes **3.8**, $L = \text{acrolein}$ are active catalysts for the Diels-Alder¹¹⁰). During the course of this work, Carmona has reported an X-ray structure of a Lewis acid-Dienophile adduct, (**3.11**),¹⁴² formed by addition of methacrolein to a solution of the corresponding aqua complex. Complex (**3.11**) was formed as a 9:1 mixture of diastereomers, the major one being shown below. The methacrolein ligand was found to coordinate in the expected η^1 -fashion, adopting an *S-trans* configuration (such that the carbonyl and C=C bonds are parallel). Complex (**3.11**) and the precursor aqua-complex were both found to be active catalysts for the reaction of methacrolein and cyclopentadiene, with moderate enantioselectivity being observed (*ee* up to 48%).



Carmona has proposed a mechanism similar to that in **Scheme (3.7)** to explain the Diels-Alder catalysis with complex (**3.11**);¹⁴² the presence of the phosphino-oxazoline ligand allows the use of ^{31}P NMR to study the reaction mechanism. Thus, at 183 K, signals due to both diastereomers of (**3.11**) could be observed; subsequent addition of excess cyclopentadiene (to a solution containing 20 equivalents of free methacrolein) gave a new signal, assigned as a complex in which the Diels-Alder

adduct was still coordinated to the metal, with corresponding loss of the signal due to the major isomer of the methacrolein complex. On warming to 253 K, catalysis was observed, the only species observed by NMR being the aqua complex (*i.e.* the same situation that was found with **2.65**, **R** = ⁱPr).

With (*S*)-configured oxazoline ligands, catalysts (**2.36/2.65**) give primarily the (1*R*, 2*S*, 4*R*)-product from the methacrolein/Cp reaction, which indicates that a similar active intermediate is present in all cases; for complex (**2.65**, **R** = ⁱPr), the proposed active species is shown in **Figure (3.2)**. To account for the observed enantioselectivity, the most likely orientation of the methacrolein ligand will have the aldehyde-H (rather than MeC=CH₂) oriented towards the arene. In this conformation, the isopropyl group shields the *Si* face of the dienophile, leading to attack of the cyclopentadiene at the *Re* face, as shown.

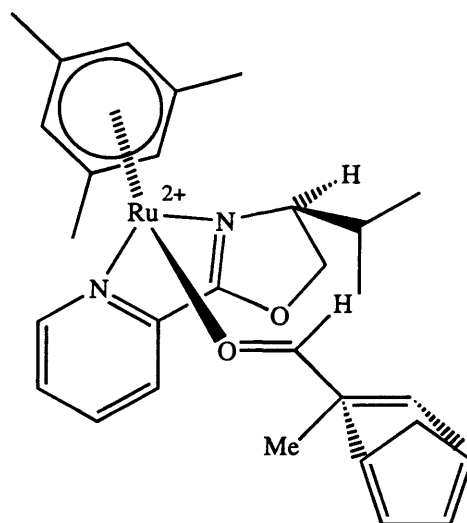


Figure (3.2)

It should be noted that the conformation of the coordinated methacrolein shown in **Figure (3.2)** is different to that in the X-ray structure of (**3.11**), in which the methacrolein is rotated through 180°, around the Ru—O bond. The solid-state conformation of (**3.11**) may not be the major under catalytic conditions, as equilibration of the two least hindered orientations of the methacrolein ligand (**Figure 3.3**) might occur fairly readily.

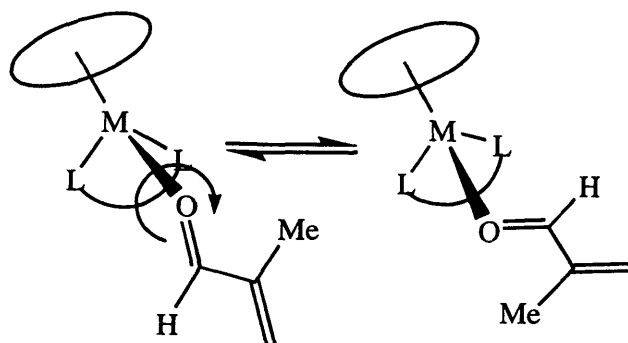


Figure (3.3)

As similar levels of enantioselectivity and rate are found for the Diels-Alder reaction with pymox catalysts (**2.65**) and benbox catalysts (**2.36**), it is reasonable to assume the ligand environment about the coordinated methacrolein is similar. Thus, in the benbox complexes, only one R-substituent would be close enough to the coordinated dienophile to effect the selectivity. This is observed in the X-ray structures of complexes (**2.26a/2.28a**, **R = Et**) (Chapter Two); the oxazoline rings of the benbox ligands are forced to rotate out of the plane of the benzene ring, in order to coordinate to the metal centre. For the ruthenium complex (**2.26a**, **R = Et**), the angles of rotation are 45.2° and 48.3° , the latter for the ring with the Et substituent oriented towards the arene ligand. As a result, one ethyl group in each case is brought closer to the chloride ligand than would be expected if the benbox ligand were planar, whilst the second ethyl group is moved further away. Thus, the benbox ligand coordinates in a significantly different manner to the other C_2 -symmetric ligands ⁱPr-box or ⁱPr-bop, which may explain the large differences in both rate and selectivity (for the Diels-Alder) between complexes of benbox and those of box/bop.

It is not entirely clear why poor results are obtained with ruthenium complexes of box and bop ligands. The box complex (**2.30**) shows lower catalytic activity and significantly lower enantioselectivity (*ee* 10%) than the analogous pymox complex (**2.65**, **R = ⁱPr**). This is surprising, as each ligand form a five-membered chelate ring with the ruthenium, so might be expected to give similar *selectivity* in the Diels-Alder reaction, whilst catalytic *activity* might vary because of electronic differences between pyridine and oxazoline rings. A possible explanation for the lower selectivity with box might be a difference in the angle between the bidentate ligand planes and the arene ring. Thus, with box, this angle might be greater, due to the steric interaction of one ⁱPr-

group with the mesitylene ring. As a result, the other ⁱPr might be further from the active site.

Another difference in steric environment for methacrolein molecules coordinated to the Ru/pymox and Ru/box systems is the presence of the extra chiral centre in the latter. In both systems, one face of the coordinated methacrolein is shielded by an isopropyl group. With pymox, the opposite face is unhindered because of the planar pyridine ring, but with ⁱPr-box, the hydrogen substituent at the second chiral centre will partially shield the second face of the coordinated methacrolein (**Figure 3.4**); thus, both faces will be hindered to some extent, which may reduce the enantioselectivity.

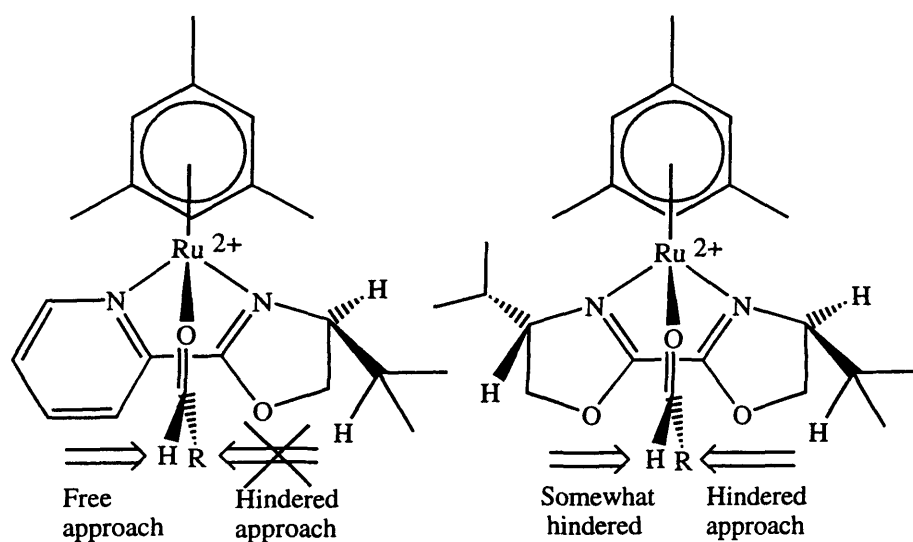


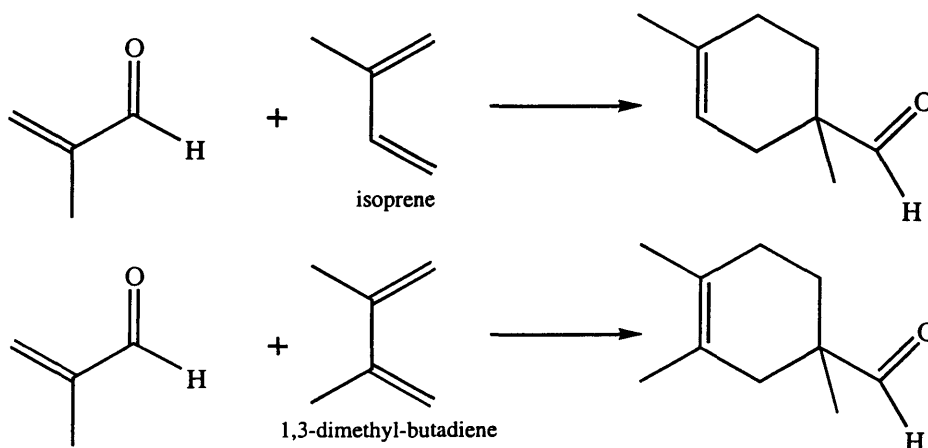
Figure (3.4)

Similar factors to those outlined above might explain the poor performance of the ⁱPr-bop complex (**2.32**) in the catalysis. In initial reactions with this complex, reasonable yields of racemic Diels-Alder product were obtained after 1 day (ca. 60%), which indicated either that the complex was active, but not selective, or that the catalysis was due to a species other than (**2.32**). When the reaction was repeated in the presence of six equivalents of the hindered base, no product formation was observed, which indicated that (**2.32**) is not a catalyst for this reaction. A possible explanation might be that the isopropyl and hydrogen substituents oriented closest to the potential active site completely hinder the approaching dienophile (the six-membered chelate ring might bring the substituents closer than in the box analogue). It should also be noted that no evidence of acetone coordination is found in the ¹H NMR spectra of

(2.32) in d_6 -acetone, unlike in the corresponding spectra of the box and benbox analogues (2.30/2.36, $R = {}^iPr$) (for which two distinct sets of complex signals are observed, due to water and acetone coordination). This indicates that coordination of carbonyl-species is generally disfavoured for (2.32).

With rhodium complexes of benbox and bop, the opposite relative reactivity is found to that with ruthenium; thus, the benbox complex (2.37) shows essentially no activity in the Diels-Alder reaction, whilst the bop complex (2.33) (when formed *in situ*) is fairly active, giving moderate enantioselectivity (*ee* 29%). The varying catalytic activity may be due to the relative preference for water and methacrolein coordination and/or the relative solubilities.

Complexes $[Ru(OH_2)(R-pymox)(arene)](SbF_6)_2$ were also used as catalysts for Diels-Alder reactions with other substrates. The reactions of methacrolein with isoprene or dimethylbutadiene (DMBD) (Scheme 3.9) both proceeded with high enantioselectivity, catalysed by (2.65, $R = {}^iPr, {}^tBu$).



Scheme (3.9)

The isoprene adduct was obtained as >98% 1,4-regioisomer, with an *ee* of 90%, for (2.65, $R = {}^iPr$) (the reaction taking ~ 13 hr with 2 mol% catalyst at RT). The DMBD adduct was obtained in 74% *ee* with (2.65, $R = {}^iPr$), the reaction taking 5 hr at RT, with 2 mol% catalyst, whilst with (2.65, $R = {}^tBu$), an *ee* of 84% was obtained under the same conditions. For other Lewis acid catalysts (*e.g.* alkoxy boranes¹⁴³), the DMBD-methacrolein adduct is obtained in higher *ee* than the corresponding isoprene adduct; it is not clear why complexes (2.65) give a smaller *ee* with DMBD. With cyclohexadiene, no reaction with methacrolein was observed under the conditions described above, possibly due to steric factors.

Complexes (**2.65**, $R = \text{}^i\text{Pr}$, $\text{}^t\text{Bu}$) and the indanyl-pymox complex (**2.67**) were also used as catalysts (2 mol%) for the Diels-Alder reactions of Cp and DMBD with acrolein, (Table 3.7). The reaction of acrolein with Cp is faster than methacrolein, being complete after two hours at 0°C with catalysts (**2.65**). The selectivity, however, is considerably reduced with acrolein; the *exo:endo* ratios obtained were all 1:2, with the highest *ee* obtained (for major *endo* product) being 46% (entry 2). Interestingly, the indanyl-pymox complex (**2.67**) proved to be a reasonably selective catalyst, an *ee* of 44% being obtained (entry 3), which is considerably higher than that for the reaction of methacrolein with Cp under the same conditions (*ee* 6%). This indicates that the steric environment at the active site of (**2.67**) is too crowded to allow efficient Diels-Alder reactions with methacrolein, but allows reactions with the smaller acrolein. The reaction of acrolein with DMBD (entry 4), catalysed by (**2.65**, $R = \text{}^i\text{Pr}$), proceeds more slowly than that with Cp, but gives higher enantioselectivity (*ee* 50 %).

Table (3.7)

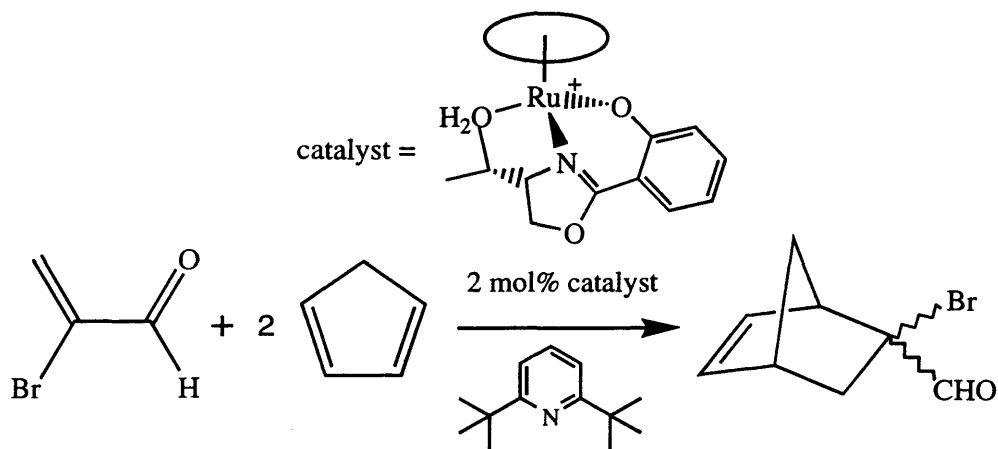
Entry	Diene	Catalyst	T/°c	t/h	Yield (%)	<i>exo:endo</i>	<i>Ee</i> (%)
1	Cp	2.65, $R = \text{}^i\text{Pr}$	0	2	98	1:2	36
2	Cp	2.65, $R = \text{}^t\text{Bu}$	0	2	96	1:2	46
3	Cp	2.67	0	5	93	1:2	44
4	DMBD	2.65, $R = \text{}^i\text{Pr}$	RT	24	54	-	50

The use of a dienophile with a larger α -substituent than methyl is expected to increase the selectivity, over that found with methacrolein. The reaction of α -bromoacrolein ($\text{H}_2\text{C}=\text{C}(\text{Br})\text{CHO}$) with cyclopentadiene has previously been shown to proceed with high enantioselectivity, with a number of chiral catalysts.^{110, 144} Bromoacrolein is a very reactive dienophile, the reaction with Cp proceeding rapidly at room temperature (> 90% after 2 hours in CD_2Cl_2 solution, with an *exo:endo* ratio of 78:22), so to minimise competing thermal reaction, fairly reactive Lewis acid catalysts are required. In addition, low temperatures are usually employed to obtain the optimum selectivity in catalysed reactions.

Surprisingly, cations $[\text{Ru}(\text{OH}_2)(\text{R-pymox})(\text{arene})]^{2+}$ were found to be poor catalysts for the reaction of bromoacrolein with Cp. Only a 20% yield of product was

obtained with 2 mol% (**2.65**, $R = \text{}^i\text{Pr}$) after 90 mins at 0°C with an *exo:endo* ratio of 80:20, indicative of thermal reaction. The observed rate is considerably slower than that for the analogous reaction of Cp with the less reactive dienophiles acrolein and methacrolein, which indicates that coordination of bromoacrolein to the Ru/pymox complexes is disfavoured. However, with 2 mol% of the rhodium analogue (**2.69**, $R = \text{}^i\text{Pr}$), the reaction of bromoacrolein and Cp (2 equivs.) proceeded rapidly at room temperature, an 83% yield being obtained after 8 mins, increasing to 90% after 15 mins. The rate is clearly faster than that of the uncatalysed reaction, with an improved *exo:endo* ratio (91:9), but the *ee* was only 33%. Carrying out the reaction at 0°C gave the same *exo:endo* ratio, but slightly improved enantioselectivity (*ee* 38%).

The best catalysts for the reaction of bromoacrolein with Cp were found to be $[\text{Ru}(\text{OH}_2)(\text{}^i\text{Pr-phenmox})(\text{arene})]\text{SbF}_6$ (arene = *p*-cymene, mes; formed in situ from the corresponding chloride complexes), as shown in **Table (3.8)**. All reactions use 2 mol% of catalyst and hindered base, with two equivalents of Cp for each bromoacrolein, in dichloromethane (**Scheme 3.10**).



Scheme (3.10)

Table (3.8): $[\text{Ru}(\text{OH}_2)(\text{}^i\text{Pr-phenmox})(\text{arene})]\text{SbF}_6$ (*in situ*) catalyst

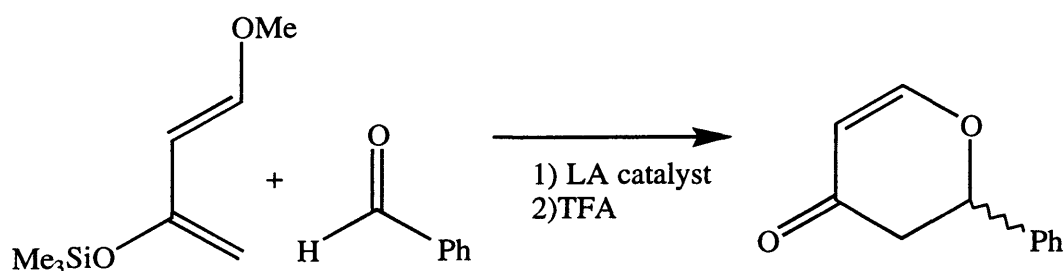
Entry	Arene	Temp/°C	t/h	yield (%)	<i>Exo:endo</i>	<i>Ee</i> (%)
1	<i>p</i> -cy	0	18	97	96:4	48
2	<i>p</i> -cy	-20	72	84	97:3	53
3	mes	0	24	90	95:5	44
4	mes	-20	72	94	97:3	49

In general, there is relatively little difference between the enantioselectivities observed for any of the reactions shown above, which is somewhat surprising. Increasing the size of the α -substituent from Me to Br increases the observed *ee* slightly (by 3-4%), with both catalysts used, but the fact that the bromoacrolein reactions were carried out at lower temperatures than those with methacrolein may also be important. As expected, decreasing the reaction temperature to -20°C (entries 2 and 4) improved the *ee* of the bromoacrolein adduct by 5% in each case, but only to a maximum of 53%.

The much greater activity for the bromoacrolein/Cp reaction shown by the rhodium/pymox catalyst, compared to the ruthenium analogue, is somewhat surprising. Sterically, one would anticipate that the two systems would be similar, so the most important factor may be an electronic effect, *i.e.* binding of the electron-withdrawing dienophile to the more electron-rich “Cp*Rh” system is favoured over that to “(mes)Ru”. This may also explain why the monocationic Ru/phenmox system (which should be even more electron-rich) is the most efficient catalyst for Diels-Alder reactions of bromoacrolein.

Of the aqua cations used, the Ru/pymox complexes (**2.65**, $\text{R} = \text{}^i\text{Pr}$ or $\text{}^t\text{Bu}$) gave the highest activity and enantioselectivity for most of the Diels-Alder reactions performed. The less expensive catalyst (**2.65**, $\text{R} = \text{}^i\text{Pr}$) was chosen to test a series of other Lewis-acid catalysed reactions; in particular, hetero Diels-Alder, inverse electron-demand hetero Diels-Alder, and Mukaiyama aldol reactions.

The Hetero Diels-Alder reaction of benzaldehyde with Danishefsky's diene (**Scheme 3.11**) was performed with various Lewis acidic aqua complexes, in particular the ruthenium and rhodium pymox complexes (**2.65/2.69**, $\text{R} = \text{}^i\text{Pr}$) and $[\text{Ru}(\text{OH}_2)(\text{}^i\text{Pr-phenmox})(\text{mes})]\text{SbF}_6$. In each case, the diene was added, under N_2 , to a solution of PhCHO, hindered base and aqua cation in CH_2Cl_2 , the mixture stirred for 1-2 days, before addition of a catalytic quantity of trifluoroacetic acid (TFA), potentially to hydrolyse the presumed intermediate silyl species to the desired pyrone.¹³⁷



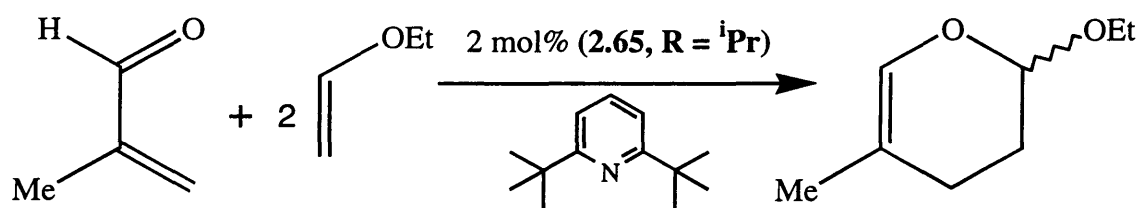
Scheme (3.11)

None of the complexes tested were found to catalyse the Hetero Diels-Alder reaction; in each case, the ^1H NMR of the reaction products showed a large proportion of unreacted benzaldehyde and none of the desired pyrone; other signals were due to hydrolysed silyloxy-diene. There are several possible reasons for the failure of any of the aqua cations tested to catalyse the hetero Diels-Alder reaction:

1. The environment about the active site is too sterically crowded for the diene to approach the coordinated aldehyde (coordination of the aldehyde is presumed, as addition of PhCHO to a suspension of catalyst in CH_2Cl_2 gives a yellow solution).
2. Deactivation of catalyst occurs, possibly by product inhibition or by reaction with the silyl species. A colour change from yellow/orange to dark red/brown is observed during the catalysis, suggesting a change in the nature of the metal complex.

A more reactive aldehyde than PhCHO might be needed (*e.g.* glyoxylates)

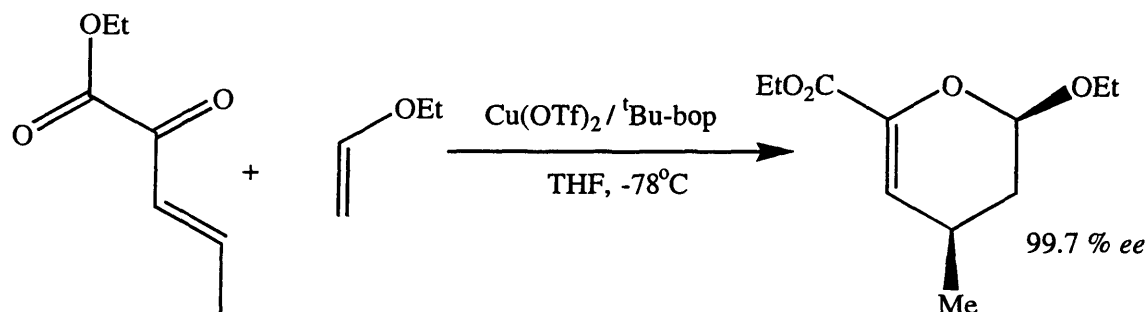
In the inverse electron-demand hetero Diels-Alder reaction of methacrolein and ethyl vinyl ether, the latter acts as “dienophile”, with the former as “diene”. The reaction was catalysed by (**2.65**, $\text{R} = \text{}^i\text{Pr}$), under similar conditions to those described earlier (one equivalent of methacrolein, two equivalents vinyl ether and 2 mol% catalyst and 2,6-di-tert butyl pyridine in CH_2Cl_2), giving a 77% yield of adduct after 48 hours at room temperature (**Scheme 3.12**). The adduct was identified as 2-ethoxy-5-methyl-3,4-dihydro-2H-pyran, by comparison of the ^1H NMR spectrum with that for similar known compounds.



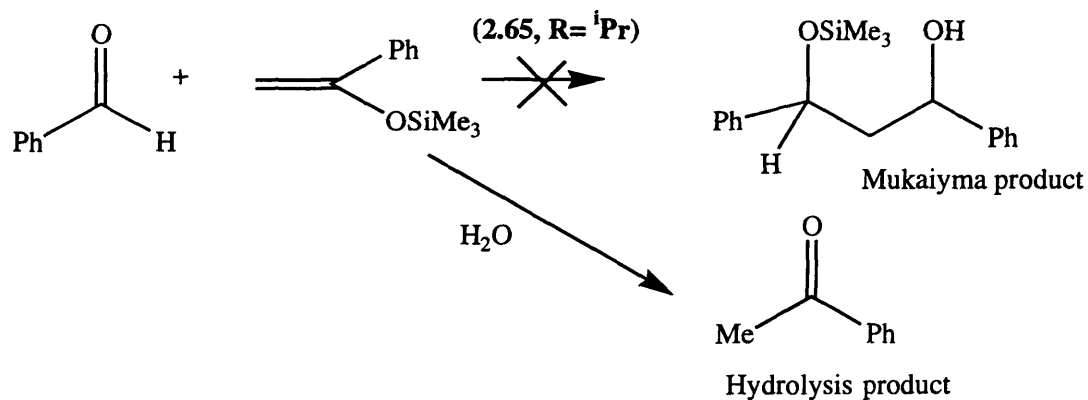
Scheme (3.12)

To discover if the reaction had been performed asymmetrically, an optical rotation measurement was obtained ($[\text{S}_{\text{rot}}]^{25} = -24.6$). This indicates that some asymmetric induction had occurred, but no literature value could be found for comparison, as the reaction has only been studied with achiral Lewis-acid catalysts.¹⁴⁵ As such, the reaction apparently represented the first example of an asymmetric Inverse-electron demand Hetero Diels-Alder reaction with a simple acrylic hetero-diene. There have, recently, however, been several reports of reactions of vinyl ethers with hetero-dienes

activated by phosphonate and oxylate-type groups, catalysed by $\text{Cu(II)}/^t\text{Bu-bop}$.^{146, 147} An example is shown in **Scheme (3.13)**, from a recent paper by Jorgensen, the dihydropyran product being obtained in 99.7 % *ee*.¹⁴⁷ The pyran products are useful in the synthesis of carbohydrates, so catalysts for the inverse-electron demand hetero Diels-Alder reaction are of particular interest.



Another Lewis-acid reaction investigated was the Mukaiyama aldol reaction of benzaldehyde with 1-phenyl-1-trimethylsilyloxy-ethylene (**Scheme 3.14**). Bosnich has shown that the (salen)Ru complex (**3.6**) is a very efficient catalyst for this reaction, a 90% yield of Mukaiyama product observed after only 6 minutes.



Thus, it seemed reasonable that similar activity might be found with ruthenium complexes such as (**2.65**, $\text{R} = ^i\text{Pr}$). However, on performing the reaction in CD_2Cl_2 (with 2 mol% of **2.65**, $\text{R} = ^i\text{Pr}$ and hindered base present), no aldol reaction was observed by ^1H NMR, with slow hydrolysis of the silyl reagent (giving acetophenone) occurring over several hours. Similar results were obtained with the rhodium analogue (**2.69**, $\text{R} = ^i\text{Pr}$) and the in situ-formed Ru/phenmox aqua complex. Although hydrolysis of the silyl reagent was observed, the complexes tested were clearly not active catalysts

for the Mukaiyama aldol reaction (certainly in comparison with catalyst 3.6), which may again be due to steric factors.

(3.3) - Experimental

Diels-Alder substrates were dried/distilled from the following reagents:

1. Acrolein from CaSO_4
2. Methacrolein from CaH_2
3. Isoprene from 4Å Molecular Sieves

Bromoacrolein was prepared by the literature method¹⁴⁸ and cyclopentadiene was freshly cracked prior to use. All other reagents were used as received and other solvents were purified as described in Chapter Two.

Diels-Alder Reactions

NMR tube experiments (in air): Dienophile[†] (ca. 0.25 mmol) was added to a suspension of catalyst (1.25, 2.5, 5 or 12.5 μmol) in CD_2Cl_2 (0.5 cm^3) which lead to rapid dissolution of catalyst to give a yellow/orange solution. The solution was transferred to an NMR tube and 2,6-di-*tert*-butylpyridine (1 equivalent/mol of catalyst) and diene[†] (0.5 mmol) were added. The ^1H NMR spectrum was recorded immediately and then repeated after suitable time intervals.

Schlenk reactions (under N_2): Dienophile[†] (1 mmol) and 2,6-di-*tert*-butylpyridine (1 equivalent/mol of catalyst) were added to a suspension of catalyst (0.01, 0.02 or 0.05 mmol) in CH_2Cl_2 (2 cm^3). The resulting solution was cooled to the appropriate temperature before addition of diene[†] (2 mmol). At the end of the reactions, the mixture was passed through a silica plug (to remove catalyst), the solvent was removed and the product was obtained as a colourless oil. The *exo:endo* ratio (where appropriate) was determined by NMR spectroscopy. The catalysts could also be prepared *in situ*, from the corresponding chloride complex and one equivalent of AgSbF_6 in CH_2Cl_2 , filtration through celite to remove AgCl and then addition of the reagents as described above.

[†]Dienophile = Acrolein, methacrolein or bromoacrolein

[†]Diene = Cyclopentadiene, isoprene, 1,3-dimethylbutadiene or cyclohexadiene

The enantiomeric excesses were determined by several routes:

1. The *ees* of adducts from acrolein/methacrolein with cyclopentadiene were determined by GC after conversion to the acetal with (2R,4R)-pentanediol, according to the method of Evans.⁴²
2. The *ees* of adducts from acrolein/methacrolein with isoprene/1,3-dimethylbutadiene were determined by GC after conversion to the acetal with (2R,4R)-pentanediol and by ¹H NMR {by integration of the singlets due to RCH(OR')₂}.
3. The *ees* of adducts from bromoacrolein with cyclopentadiene were determined by ¹H NMR {by integration of the singlets due to RCH(OR')₂}, after conversion to the acetal with (2R,4R)-pentanediol (a reaction time of 4 days was required to synthesise the acetal).

Inverse-electron demand Diels-Alder reaction

To a degassed solution of (**2.65**, R = ⁱPr) (9 mg, 10 μmol) and 2,6-di-tert-butylpyridine (2.3 μl, 10.3 μmol) in CH₂Cl₂ (2 cm³), was added methacrolein (41 μl, 0.50 mmol) and ethyl vinyl ether (96 μl, 1 mmol) by syringe. The solution was stirred at room temperature for 2 days, then filtered through a plug of silica, to remove the catalyst. The resulting colourless solution was evaporated and dried *in vacuo* to afford a colourless oil (55 mg, 77%), identified as 2-ethoxy-5-methyl-3,4-dihydro-2H-pyran, by comparison of the ¹H NMR spectrum with that for similar known compounds.

Hetero Diels-Alder reaction

To a degassed solution of catalyst (11 μmol), 2,6-di-tert-butyl-pyridine (2.6 μl, 11 μmol) and PhCHO (22.5 μl, 0.22 mmol) in CH₂Cl₂ (2 cm³) was added 1-methoxy-3-trimethylsilyloxy-1,3-butadiene (50 μl, 0.23 mmol) via syringe. The resulting solution was stirred for 2 days at room temperature under N₂, before addition of a drop of trifluoroacetic acid, giving a brown-coloured solution. The mixture was evaporated and a crude ¹H NMR spectrum obtained.

Conclusions and Further Work

In Section (2.2.1), a series of half-sandwich complexes containing C_2 -symmetric bis-oxazoline ligands were prepared. X-ray crystallography and 1H NMR were used to confirm the expected pseudo-octahedral structure and the loss of C_2 -symmetry on complexation. Replacement of the chloride ligand with water gave dications that were shown to undergo exchange processes in solution. For aqua complexes of box and bop ligands, exchange of water and time-averaging of ligand signals in the NMR, due to exchange of its environment, were observed, both processes being slowed at low temperature. With benbox, no exchange process involving the chiral ligand was observed (at least, not on the NMR timescale), possibly due to the mode of coordination of the ligand. Further work on these systems might entail a detailed kinetic study of the various exchange processes involved.

In section (2.2.2), diastereomeric half-sandwich complexes of the unsymmetrical oxazoline-containing ligands pymox, animox, NTs-animox and phenmox were prepared. In general, complex formation was highly diastereoselective. With bulky η -rings and/or large R-substituents, complexes $[MCl(R\text{-pymox})(ring)]SbF_6$ were formed as single isomers, except where $M = Ru$, $R = Ph$. Similarly, all phenmox complexes were formed highly diastereoselectivity. With both pymox and phenmox complexes, no epimerisation was observed on the NMR timescale. With complexes of animox and NTs-animox, equilibrium mixtures of diastereomers are observed at room temperature. Chemical exchange of isomers is slow on the NMR timescale in each case, but could be observed by use of phase-sensitive NOESY experiments. Unusually, the major isomers in the complexes $[MCl(^iPr\text{-NTs-animox})(ring)]$ have the iPr -substituents oriented towards the η -ring, rather than towards the chloride, which is attributed to the steric effect of the tosyl group.

The corresponding aqua cations $[M(OH_2)(N\text{-}N')(ring)]^{n+}$ ($N\text{-}N' = \text{pymox}$ or NTs-animox) were formed highly diastereoselectively, with only a maximum of 10% of the isomer with the R-substituent oriented towards the η -ring. The aqua ligands readily undergo exchange with deuterium in solution, particularly in d_6 -acetone solution, where evidence of replacement of water by acetone is also found, for $M = Ru$. As expected, water exchange is faster for rhodium/iridium than for ruthenium.

The aqua ligands are readily displaced by addition of halides or small N-donor ligands. Increasing the size of the halide ligand (from Cl to Br to I) greatly influences the observed diastereoselectivity in the resultant complex; the iodide complex (**2.77**, **R** = ⁱPr), for example, is formed with the major isomer having the ⁱPr-group oriented towards the η^6 -mesitylene, rather than towards the iodide. With iodide as the halide, slow epimerisation is observed in MeOH solution, unlike for the corresponding chlorides. With N-donors replacing the water, diastereoselectivity again depends on the steric bulk of the ligand. Further work in this area might again involve a kinetic study of water exchange and a detailed investigation of the mechanism of the ligand substitution reactions.

Many of the half-sandwich aqua complexes synthesised were found to be catalysts for the asymmetric Diels-Alder reaction (Chapter Three). The best systems (in terms of activity and enantioselectivity) were found to be dicationic ruthenium complexes, containing pymox or benbox as the chiral ligand, *ees* of up to 90% observed (for the reaction of methacrolein with isoprene). In general, ruthenium complexes are more active than their rhodium analogues (which is somewhat surprising as the rhodium aqua complexes undergo considerably faster exchange reactions than their ruthenium analogues). The selectivity of the catalysis was found to increase with decreasing temperature, whilst raising the catalyst loading had a fairly small effect. With ruthenium catalysts, the choice of η^6 -arene is important. Mesitylene was found to be the optimum arene; the use of η^6 -C₆H₆ led to considerable reductions in enantioselectivity and, surprisingly, rate.

The Ru/pymox complex (**2.65**, **R** = ⁱPr) was used in screening reactions for a selection of other Lewis-acid catalysed processes, with varying success. For the Hetero Diels-Alder reaction of PhCHO with Danishefsky's diene, none of the desired product was observed. Future work in this area might require the use of a more reactive aldehyde, such as glyoxylate. A reaction that was successful was the inverse-electron demand hetero Diels-Alder reaction of methacrolein with ethyl vinyl ether. Optical rotation studies indicated that some enantioselectivity had been obtained, but no *ee* was calculated. Further investigation of this reaction is clearly warranted, as is identification of other reactions that can be catalysed by the chiral half-sandwich complexes synthesised.

References

- 1 R. McCague and A. Richards, *Chemistry & Industry*, 1997, 422.
- 2 J. B. H. Warneck and R. A. Wisdom; International Patent application WO 9420634; 1994
- 3 R. Noyori and H. Takaya, *Acc. Chem. Res.*, 1990, **23**, 345.
- 4 W. S. Knowles, M. J. Sabacky, B. D. Vineyard, and D. J. Weinkauff, *J. Am. Chem. Soc.*, 1975, **97**, 2567.
- 5 A. Togni and L. M. Venanzi, *Angew. Chem., Int. Ed. Engl.*, 1994, **33**, 497.
- 6 E. N. Jacobsen in *Comprehensive Organometallic Chemistry 2*, ed. G. Wilkinson, F. G. A. Stone, and E. W. Abel; Pergamon Press, Oxford; 1995; 12; 1097.
- 7 J. T. Groves, G. N. Thomas, and R. S. Myers, *J. Am. Chem. Soc.*, 1979, **101**, 1032.
- 8 W. Zhang, J. L. Loebach, S. R. Wilson, and E. N. Jacobsen, *J. Am. Chem. Soc.*, 1990, **112**, 2801.
- 9 R. Irie, K. Noda, Y. Ito, N. Matsumoto, and T. Katsuki, *Tetrahedron-Asymmetry*, 1991, **2**, 481.
- 10 E. N. Jacobsen, W. Zhang, A. R. Muci, J. R. Ecker, and L. Deng, *J. Am. Chem. Soc.*, 1991, **113**, 7063.
- 11 A. Pfaltz, *Acc. Chem. Res.*, 1993, **26**, 339.
- 12 H. Fritschi, U. Leutenegger, and A. Pfaltz, *Angew. Chem., Int. Ed. Engl.*, 1986, **98**, 1028.
- 13 M. P. Doyle in *Comprehensive Organometallic Chemistry 2*, ed. G. Wilkinson, F. G. A. Stone, and E. W. Abel; Pergamon Press, Oxford; 1995; 12; 387.
- 14 A. K. Ghosh, P. Mathivanan, and J. Cappiello, *Tetrahedron-Asymmetry*, 1998, **9**, 1.
- 15 G. Helmchen, A. Krotz, K.-T. Ganz, and D. Hansen, *Synlett*, 1991, 257.
- 16 M. J. McKennon, A. I. Meyers, K. Drauz, and M. Scharm, *J. Org. Chem.*, 1993, **58**, 3568.
- 17 F. G. Schaefer and G. A. Peters, *J. Org. Chem.*, 1961, **26**, 412.
- 18 J. Hall, J. Lehn, A. DeCian, and J. Fischer, *Helvetica Chimica Acta*, 1991, **74**, 1.
- 19 C. Bolm, K. Weickharott, M. Zender, and T. Ranff, *Chem. Ber.*, 1991, **124**, 1173.

- 20 M. Peer, J. C. d. Jong, M. Kiefer, T. Langer, h. Rieck, H. P. Sennhenn, J. Sprinz,
H. Steinhagen, B. Wiese, and G. Helmchen, *Tetrahedron*, 1996, **52**, 7547.
- 21 S. E. Denmark, N. Nakajima, O. J.-C. Nicaise, A.-M. Faucher, and J. P. Edwards,
J. Org. Chem., 1995, **60**, 4884.
- 22 A. I. Meyers and E. D. Mihelich, *J. Am. Chem. Soc.*, 1975, **97**, 7383.
- 23 A. I. Meyers, G. Knaus, K. Kamata, and M. E. Ford, *J. Am. Chem. Soc.*, 1976, **98**,
567.
- 24 A. I. Meyers, *Acc. Chem. Res.*, 1978, **11**.
- 25 H. Brunner, U. Obermann, and P. Wimmer, *J. Organomet. Chem.*, 1986, **316**, C1.
- 26 H. Brunner and U. Obermann, *Chem. Ber.*, 1989, **122**, 499.
- 27 H. Nishiyama, H. Sakaguchi, T. Nakamura, M. Horihata, M. Kondo, and K. Itoh,
Organomet., 1989, **8**, 846.
- 28 H. Nishiyama, M. Kondo, T. Nakamura, and K. Itoh, *Organomet.*, 1991, **10**, 500.
- 29 H. Nishiyama, Y. Itoh, Y. Sugawara, H. Matsumoto, K. Aoki, and K. Itoh, *Bull.*
Chem. Soc. Jpn., 1995, **68**, 1247.
- 30 R. E. Lowenthal, A. Abiko, and S. Masamune, *Tetrahedron Lett.*, 1990, **31**, 6005.
- 31 D. A. Evans, K. A. Woerpel, M. M. Hinman, and M. M. Faul, *J. Am. Chem. Soc.*,
1991, **113**, 726.
- 32 D. A. Evans, M. M. Faul, M. T. Bilodeau, B. A. Anderson, and D. M. Barnes, *J.*
Am. Chem. Soc., 1993, **115**, 5328.
- 33 A. Pfaltz, A. S. Gokhale, and A. B. E. Minidis, *Tetrahedron Lett.*, 1995, **36**,
1831.
- 34 D. Muller, G. Umbricht, B. Weber, and A. Pfaltz, *Helvetica Chimica Acta*, 1991,
74, 232.
- 35 P. von Matt, G. C. Lloyd-Jones, A. B. E. Minidis, A. Pfaltz, L. Macko, M.
Neuberger, M. Zehnder, H. Reugger, and P. S. Pregosin, *Helvetica Chimica Acta*,
1995, **78**, 265.
- 36 A. Pfaltz, *Acta Chem. Scand.*, 1996, **50**, 189.
- 37 E. J. Corey and K. Ishihara, *Tetrahedron Lett.*, 1992, **33**, 6807.
- 38 E. J. Corey, N. Imai, and H.-Y. Zhang, *J. Am. Chem. Soc.*, 1991, **113**, 728.
- 39 D. A. Evans, S. J. Miller, and T. Lectka, *J. Am. Chem. Soc.*, 1993, **115**, 6460.
- 40 M. Johannsen and K. A. Jorgensen, *J. Org. Chem.*, 1995, **60**, 5757.

- 41 D. A. Evans, C. S. Burgey, N. A. Paras, T. Vojkovsy, and S. W. Tregay, *J. Am. Chem. Soc.*, 1998, **120**, 5824.
- 42 D. A. Evans, J. A. Murry, P. v. Matt, R. D. Norcross, and S. J. Miller, *Angew. Chem., Int. Ed. Engl.*, 1995, **34**, 798.
- 43 E. J. Corey and Z. Wang, *Tetrahedron Lett.*, 1993, **34**, 4001.
- 44 A. V. Bedekar, E. B. Koroleva, and P. G. Andersson, *J. Org. Chem.*, 1997, **62**, 2518.
- 45 J. M. Takacs, E. C. Lawson, M. J. Reno, M. A. Youngman, and D. A. Quincy, *Tetrahedron-Asymmetry*, 1997, **8**, 3073.
- 46 I. W. Davies, L. Gerena, D. Cai, R. D. Larsen, T. R. Verhoeven, and P. J. Reider, *Tetrahedron Lett.*, 1997, **38**, 1145.
- 47 T. Ichiyonagi, M. Shimizu, and T. Fujisawa, *J. Org. Chem.*, 1997, **62**, 7937.
- 48 M. B. Andrus, D. Asgari, and J. A. Sclafani, *J. Org. Chem.*, 1997, **62**, 9365.
- 49 A. I. Meyers and A. Price, *J. Org. Chem.*, 1998, **63**, 412.
- 50 S. Bennett, S. M. Brown, G. Conole, M. Kessler, S. Rowling, E. Sinn, and S. Woodward, *J. Chem. Soc., Dalton Trans.*, 1995, 367.
- 51 C. Bolm, K. Weickharott, M. Zender, and D. Glasmacher, *Helvetica Chimica Acta*, 1991, **74**, 717.
- 52 C. Bolm, G. Schlingloff, and K. Weickhardt, *Angew. Chem., Int. Ed. Engl.*, 1994, **33**, 1848.
- 53 G. Natta, R. Ercoli, and F. Calderazzo, *Chimica Industria*, 1958, **40**, 287.
- 54 E. P. Kundig, A. Quattropiani, M. Inage, A. Ripa, C. Dupré, A. F. J. Cunningham, and B. Bourdin, *Pure Appl. Chem.*, 1996, **68**, 97.
- 55 G. Winkaus and H. Singer, *J. Organomet. Chem.*, 1967, **7**, 487.
- 56 M. A. Bennett, K. Khan, and E. Wenger in *Comprehensive Organometallic Chemistry 2*, ed. G. Wilkinson, F. G. A. Stone, and E. W. Abel; Pergamon Press, Oxford, 1995; **7**; 476.
- 57 F. Morandini, G. Consiglio, B. Straub, G. Ciani, and A. Sironi, *J. Chem. Soc., Dalton Trans.*, 1983, 2293.
- 58 P. R. Sharp in *Comprehensive Organometallic Chemistry 2*, ed. G. Wilkinson, F. G. A. Stone, and E. W. Abel; Pergamon Press, Oxford; 1995; **8**; 167.
- 59 M. A. Bennett, T. Huang, T. W. Matheson, and A. K. Smith, *Inorganic Synthesis*, 1982, **21**, 75.

- 60 C. White, A. Yates, and P. M. Maitlis, *Inorganic Synthesis*, 1992, **29**, 228.
- 61 M. R. Churchill and S. A. Julis, *Inorg. Chem.*, 1977, **16**, 1488.
- 62 J. W. Hull, Jr. and W. L. Gladfelter, *Organomet.*, 1984, **3**, 605.
- 63 M. A. Bennett in *Comprehensive Organometallic Chemistry 2*, ed. G. Wilkinson, F. G. A. Stone, and E. W. Abel; Pergamon Press, Oxford; 1995; **7**; 556.
- 64 P. M. Maitlis, *Acc. Chem. Res.*, 1978, **11**, 301.
- 65 L. Carter, D. L. Davies, J. Fawcett, and D. R. Russell, *Polyhedron*, 1993, **12**, 1599.
- 66 W. Rigby, H. Lee, P. M. Bailey, and J. A. McCleverty, *J. Chem. Soc., Dalton Trans.*, 1979, 387.
- 67 L. C. Carter, PhD Thesis, University of Leicester, 1994.
- 68 D. F. Dersnah and M. C. Baird, *J. Organomet. Chem.*, 1977, **127**, C55.
- 69 S. G. Davies, *Pure Appl. Chem.*, 1988, **60**, 13.
- 70 J. H. Merrifield, C. E. Strouse, and J. A. Gladysz, *Organomet.*, 1982, **1**, 1204.
- 71 J. H. Merrifield, M. Fernandez, W. E. Buhro, and J. A. Gladysz, *Inorg. Chem.*, 1984, **23**, 4022.
- 72 J. Fernandez and J. A. Gladysz, *Inorg. Chem.*, 1986, **25**, 2672.
- 73 T. R. Ward, O. Schafer, C. Daul, and P. Hofmann, *Organomet.*, 1997, **16**, 3207.
- 74 M. A. Dewey, Y. Zhou, Y. Liu, and J. A. Gladysz, *Organomet.*, 1993, **12**, 3924.
- 75 G. Consiglio, F. Morandini, and F. Bangerter, *Inorg. Chem.*, 1982, **21**, 455.
- 76 E. Cesarotti, G. Ciani, and A. Sironi, *J. Organomet. Chem.*, 1981, 87.
- 77 K. Mashima, K. Kusano, T. Ohta, R. Noyori, and H. J. Takaya, *Chem. Commun.*, 1989, 1208.
- 78 S. G. Davies, *Chem. Ind.*, 1986, 506.
- 79 M. Uemura, T. Kobayashi, K. Isobe, T. Minami, and Y. Hayashi, *J. Am. Chem. Soc.*, 1987, **109**.
- 80 P. Pertici, F. Borgherini, G. Uitulli, P. Salvadori, C. Rosini, C. Moise, and J. Besancon, *Inorg. Chim. Acta*, 1998, **268**, 323.
- 81 G. Consiglio and F. Morandini, *Chem. Rev.*, 1987, **87**, 761.
- 82 M. I. Bruce, M. G. Humphrey, A. G. Swincer, and R. G. Wallis, *Aust. J. Chem.*, 1984, **37**, 1747.
- 83 F. Morandini, G. Consiglio, and V. Lucchini, *Organomet.*, 1985, **4**, 1202.

- 84 D. Carmona, F. J. Lahoz, L. A. Oro, M. P. Lamata, F. Viguri, and E. San Jose, *Organomet.*, 1996, **15**, 2961.
- 85 K. Severin, R. Bergs, and W. Beck, *Angew. Chem., Int. Ed. Engl.*, 1998, **37**, 1635.
- 86 K. Stanley and M. C. Baird, *J. Am. Chem. Soc.*, 1975, **97**, 6598.
- 87 T. E. Sloan, *Top. Stereochem.*, 1981, **12**, 1.
- 88 R. Kramer, K. Polborn, H. Wanjek, I. Zahn, and W. Beck, *Chem. Ber.*, 1990, **123**, 767.
- 89 W. S. Sheldrick and S. Heeb, *Inorg. Chim. Acta*, 1990, **168**, 93.
- 90 L. C. Carter, D. L. Davies, K. T. Duffy, J. Fawcett, and D. R. Russell, *Acta Crystallogr., Sect. C*, 1994, **50**, 1559.
- 91 G. Capper, PhD Thesis, University of Leicester, 1995.
- 92 D. Carmona, A. Medoza, F. J. Lahoz, L. A. Oro, M. P. Lamata, and E. San Jose, *J. Organomet. Chem.*, 1990, **396**, C17.
- 93 D. Carmona; Unpublished Work
- 94 H. Brunner, R. Oeschey, and B. Nuber, *J. Chem. Soc., Dalton Trans.*, 1996, 1499.
- 95 H. Brunner, R. Oeschey, and B. Nuber, *Inorg. Chem.*, 1995, **34**, 3349.
- 96 S. K. Mandal and A. R. Chakravarty, *J. Chem. Soc., Dalton Trans.*, 1992, 1627.
- 97 S. K. Mandal and A. R. Chakravarty, *Inorg. Chem.*, 1993, **32**, 3851.
- 98 M. L. Loza, J. Parr, and A. M. Z. Slawin, *Polyhedron*, 1997, **16**, 2321.
- 99 H. Brunner, R. Oeschey, and B. Nuber, *Organomet.*, 1996, **15**, 3616.
- 100 D. L. Davies, J. Fawcett, R. Krafczyk, and D. R. Russell, *J. Organomet. Chem.*, 1997, **545-546**, 581.
- 101 R. Noyori and S. Hashiguchi, *Acc. Chem. Res.*, 1997, **30**, 97.
- 102 K.-J. Haack, S. Hashiguchi, A. Fujii, T. Ikariya, and R. Noyori, *Angew. Chem., Int. Ed. Engl.*, 1997, **36**, 285.
- 103 H. Asano, K. Katayama, and H. Kurosawa, *Inorg. Chem.*, 1996, **35**, 5760.
- 104 L. Dadci, H. Elias, U. Frey, A. Hornig, U. Koelle, A. E. Merbach, H. Paulus, and J. S. Schneider, *Inorg. Chem.*, 1995, **34**, 306.
- 105 P. E. Hansen, *Prog. NMR Spectrosc.*, 1988, **20**, 207.
- 106 W. Arias and J. M. Risley, *J. Org. Chem.*, 1991, **56**, 4741.
- 107 J. C. Christofides and D. B. Davies, *Chem. Commun.*, 1982, 560.

- 108 P. E. Hansen, F. M. Nicolaisen, and K. Schaumberg, *J. Am. Chem. Soc.*, 1986, **108**, 625.
- 109 A. J. Davenport and D. L. Davies; Unpublished Work
- 110 E. P. Kundig, B. Bourdin, and G. Bernardinelli, *Angew. Chem., Int. Ed. Engl.*, 1994, **33**, 1856.
- 111 W. Oppolzer in *Comprehensive Organic Synthesis*, vol.5, Chapter 4.1, ed. B. Trost; Pergamon Press, Oxford; 1991; 315.
- 112 J. Sauer and R. Sustmann, *Angew. Chem., Int. Ed. Engl.*, 1980, **19**, 779.
- 113 D. Kaufmann and R. Boese, *Angew. Chem., Int. Ed. Engl.*, 1990, **29**, 545.
- 114 H. B. Kagan and O. Riant, *Chem. Rev.*, 1992, **92**, 1007.
- 115 K. Narasaka, *Synthesis*, 1991, 1.
- 116 H. Waldmann, *Synthesis*, 1994, 535.
- 117 T. Kitehara in ; 1995; 3395.
- 118 K. Maruoka, T. Itoh, T. Shirasaka, and H. Yamamoto, *J. Am. Chem. Soc.*, 1988, **110**, 310.
- 119 M. Terada, K. Mikami, and T. Nakai, *Tetrahedron Lett.*, 1991, **32**.
- 120 S. J. Danishefsky and M. P. DeNinno, *Angew. Chem., Int. Ed. Engl.*, 1987, **26**, 15.
- 121 H. Waldmann and M. Braun, *J. Org. Chem.*, 1992, **57**, 4444.
- 122 K. Hattori and H. Yamamoto, *Tetrahedron*, 1993, **49**, 1749.
- 123 K. Mikami, M. Terada, S. Narisawa, and T. Nakai, *Synlett*, 1992, 255.
- 124 S. Sakane, K. Maruoka, and H. Yamamoto, *Tetrahedron Lett.*, 1985, **26**, 5535.
- 125 C. H. Heathcock in *Comprehensive Organic Synthesis*, vol.2, Chapter 1.6, ed. B. Trost; Pergamon Press, Oxford; 1991; 133.
- 126 T. Mukaiyama, K. Narasaka, and K. Bunno, *Chem. Lett.*, 1973, 1011.
- 127 K. Mikami, Y. Motoyama, and M. Terada, *J. Am. Chem. Soc.*, 1994, **116**, 2812.
- 128 M. Terada, Y. Matsumoto, Y. Nakamura, and K. Mikami, *Chem. Commun.*, 1997, 281.
- 129 W. H. Hersh, *J. Am. Chem. Soc.*, 1985, **107**, 4599.
- 130 J. W. Faller and Y. Ma, *J. Am. Chem. Soc.*, 1991, **113**, 1579.
- 131 P. V. Bonnesen, C. L. Puckett, R. V. Honeychuck, and W. H. Hersh, *J. Am. Chem. Soc.*, 1989, **111**, 6070.
- 132 J. W. Faller and C. J. Smart, *Tetrahedron Lett.*, 1989, **30**, 1189.

- 133 N. Quiros-Mendez, A. M. Arif, and J. A. Gladysz, *Angew. Chem., Int. Ed. Engl.*, 1990, **29**, 1473.
- 134 W. Odenkirk and B. Bosnich, *J. Am. Chem. Soc.*, 1992, **114**, 6392.
- 135 T. K. Hollis, W. Odenkirk, N. P. Robinson, J. Whelan, and B. Bosnich, *Tetrahedron*, 1993, **49**, 5415.
- 136 L. E. Martinez, J. L. Leighton, D. H. Carsten, and E. N. Jacobsen, *J. Am. Chem. Soc.*, 1995, **117**.
- 137 S. E. Schaus, J. Branalt, and E. N. Jacobsen, *J. Org. Chem.*, 1998, **63**, 403.
- 138 W. Odenkirk and B. Bosnich, *J. Chem. Soc., Chem. Commun.*, 1995, 1181.
- 139 D. Carmona, C. Cativiela, R. Garcia-Correas, F. J. Lahoz, M. P. Lamata, J. A. Lopez, M. P. Lopez-Ram de Viu, L. A. Oro, E. San Jose, and F. Viguri, *Chem. Commun.*, 1996, 1247.
- 140 D. A. Evans, J. A. Murry, and M. C. Kozlowski, *J. Am. Chem. Soc.*, 1996, **118**, 5814.
- 141 D. Carmona, F. J. Lahoz, S. Elipe, L. A. Oro, M. P. Lamata, F. Viguri, C. Mir, C. Cativiela, and M. P. Lopez-Ram de Viu, *Organomet.*, 1998, **17**, 2986.
- 142 D. Carmona, C. Cativiela, S. Elipe, F. J. Lahoz, M. P. Lamata, M. P. Lopez-Ram de Viu, L. A. Oro, C. Vega, and F. Viguri, *Chem. Commun.*, 1997, 2351.
- 143 K. Furuta, S. Shimizu, Y. Miwa, and H. Yamamoto, *J. Org. Chem.*, 1989, **54**, 1481.
- 144 K. Ishihara, Q. Gao, and H. Yamamoto, *J. Org. Chem.*, 1993, **58**, 6917.
- 145 S. Danishefsky and M. Bednarski, *Tetrahedron Lett.*, 1984, **25**, 721.
- 146 D. A. Evans and J. S. Johnson, *J. Am. Chem. Soc.*, 1998, **120**, 4895.
- 147 J. Thorhauge, M. Johannsen, and K. A. Jorgensen, *Angew. Chem., Int. Ed. Engl.*, 1998, **37**, 2404.
- 148 R. H. Baker, S. W. Tinsley, D. Butler, and B. Riegel, *J. Am. Chem. Soc.*, 1950, **72**, 393.